

Doctorate Program in Molecular  
Oncology and Endocrinology

XVIII cycle - 2002–2006

Coordinator: Professor Giancarlo Vecchio

**Characterization of the oncogenic  
activity of NF- $\kappa$ B in thyroid and  
identification of a novel inhibitory  
mechanism of NF- $\kappa$ B activation**

Claudio Mauro

University of Naples Federico II  
Dipartimento di Biologia e Patologia  
Cellulare e Molecolare  
“L. Califano”

## **Administrative Location**

Dipartimento di Biologia e Patologia Cellulare e Molecolare “L. Califano”,  
Università degli Studi di Napoli Federico II

## **Partner Institutions**

### **Italian Institutions**

Università di Napoli Federico II, Naples, Italy

Istituto di Endocrinologia ed Oncologia Sperimentale “G. Salvatore”, CNR,  
Naples, Italy

Seconda Università di Napoli, Naples, Italy

Università del Sannio, Benevento, Italy

Università di Genova, Genoa, Italy

Università di Padova, Padua, Italy

### **Foreign Institutions**

Johns Hopkins University, Baltimore, MD, USA

National Institutes of Health, Bethesda, MD, USA

Ohio State University, Columbus, OH, USA

Université Paris Sud XI, Paris, France

### **Supporting Institutions**

Università di Napoli Federico II

Ministero dell’Istruzione, dell’Università e della Ricerca

Istituto Superiore di Oncologia (ISO)

Polo delle Scienze e delle Tecnologie per la Vita, Università di Napoli  
Federico II

Polo delle Scienze e delle Tecnologie, Università di Napoli Federico II

Terry Fox Foundation

Istituto di Endocrinologia ed Oncologia Sperimentale “G. Salvatore”, CNR,  
Naples, Italy

Centro Regionale di Competenza in Genomica (GEAR)

## Faculty

### **Italian Faculty**

Giancarlo Vecchio, MD, Co-ordinator

Francesco Beguinot, MD

Angelo Raffaele Bianco, MD

Francesca Carlomagno, MD

Gabriella Castoria, MD

Angela Celetti, MD

Fortunato Ciardiello, MD

Sabino De Placido, MD

Pietro Formisano, MD

Massimo Imbriaco, MD

Paolo Laccetti, MD

Antonio Leonardi, MD

Barbara Majello, PhD

Rosa Marina Melillo, MD

Claudia Miele, PhD

Pacelli Roberto, MD

Giuseppe Palumbo, PhD

Silvio Parodi, MD

Renata Piccoli, PhD

Giuseppe Portella, MD

Antonio Rosato, MD

Massimo Santoro, MD

Giampaolo Tortora, MD

Donatella Tramontano, PhD

Giancarlo Troncone, MD

Bianca Maria Veneziani, MD

### **Foreign Faculty**

#### *National Institutes of Health (USA)*

Michael M. Gottesman, MD

Silvio Gutkind, PhD

Derek LeRoith, MD

Stephen Marx, MD

Ira Pastan, MD

#### *Johns Hopkins University (USA)*

Vincenzo Casolaro, MD

Pierre Coulombe, PhD

James G. Herman MD

Robert Schleimer, PhD

#### *Ohio State University, Columbus (USA)*

Carlo M. Croce, MD

#### *Université Paris Sud XI, Paris, Francia*

Martin Schlumberger, MD

**Characterization of the oncogenic  
activity of NF- $\kappa$ B in thyroid and  
identification of a novel inhibitory  
mechanism of NF- $\kappa$ B activation**

# TABLE OF CONTENTS

<b>LIST OF PUBLICATIONS</b>	<b>7</b>
<b>ABSTRACT</b>	<b>8</b>
<b>BACKGROUND</b>	<b>10</b>
I – Introduction	10
II – The family of NF- $\kappa$ B transcription factors	10
III – The classical pathway of NF- $\kappa$ B activation	11
IV – Ubiquitination and NF- $\kappa$ B signaling pathway	12
V – The role of NF- $\kappa$ B in oncogenesis	13
VI – Thyroid carcinomas and NF- $\kappa$ B	14
VII – The control of programmed cell death by NF- $\kappa$ B	14
VIII – JNK signaling in programmed cell death	15
IX – NF- $\kappa$ B as target for cancer therapies	16
<b>AIM OF THE STUDY</b>	<b>20</b>
<b>MATERIALS AND METHODS</b>	<b>21</b>
I – Cell cultures and biological reagents	21
II – Immunohistochemical analysis	21
III – Electro-Mobility Shift Assay (EMSA)	22
IV – In vitro and in vivo tumorigenicity assays	22
V – Cytotoxic treatments and measurements of apoptosis	23
VI – [ <sup>3</sup> H]-thymidine DNA incorporation	23
VII – CFSE cell proliferation assay	23
VIII – Gel filtration of cellular extracts	23
IX – In vitro translation and GST pull-down assays	23
X – Transfection, immunoprecipitation and luciferase assay	24
XI – In vivo ubiquitination and de-ubiquitination assays	24
XII – ABIN-1 and A20 siRNA expression vectors	24
<b>RESULTS AND DISCUSSION</b>	<b>26</b>
I – Basal NF- $\kappa$ B activity in human thyroid carcinomas	26
II – NF- $\kappa$ B transcriptional activity in human thyroid transformed cells	27
III – NF- $\kappa$ B activity is essential to confer resistance to drug-induced apoptosis in thyroid carcinoma cell lines	27
IV – Inhibition of FRO transforming potential by NF- $\kappa$ B inactivation	30
V – The anti-apoptotic activity of NF- $\kappa$ B is mediated by down-regulation of JNK activity	30
VI – ABIN-1 is an inhibitor of NF- $\kappa$ B and an interactor of NEMO/IKK $\gamma$	31
VII – Mapping of the NEMO/IKK $\gamma$ and the A20 binding domains on ABIN-1	34

VIII – ABIN-1 and A20 inhibit NF- $\kappa$ B at the level of the IKK-complex by associating with NEMO/IKK $\gamma$	35
IX – A20 inhibits NF- $\kappa$ B by de-ubiquitinating NEMO/IKK $\gamma$	37
X – ABIN-1 mediates the de-ubiquitinating activity of A20 on NEMO/IKK $\gamma$	39
<b>CONCLUSIONS</b>	<b>42</b>
<b>ACKNOWLEDGEMENTS</b>	<b>43</b>
<b>REFERENCES</b>	<b>44</b>
<b>APPENDIX: ORIGINAL PAPERS</b>	<b>50</b>

## List of Publications

- Leonardi A, Vito P, **Mauro C**, Pacifico F, Ulianich L, Consiglio E, Formisano S, Di Jeso B. Endoplasmic reticulum stress causes Thyroglobulin retention in this organelle and triggers activation of NF- $\kappa$ B via TNF-Receptor Associated Factor 2 (TRAF2). *Endocrinology* 2002; 143:2169–77.
- Mauro C**, Vito P, Mellone S, Pacifico F, Chariot A, Formisano S, Leonardi A. Role of the adaptor protein CIKS in the activation of the IKK-complex. *B.B.R.C.* 2003; 309:84–90.
- Spagnuolo G, **Mauro C**, Leonardi A, Santillo M, Paternò R, Schweikl H, Avvedimento EV, Rengo S. NF- $\kappa$ B protection against apoptosis induced by HEMA. *J. Dent. Res.* 2004; 83:837–42.
- Pacifico F, **Mauro C**<sup>#</sup>, Barone C, Crescenzi E, Mellone S, Monaco M, Chiappetta G, Terrazzano G, Liguoro D, Vito P, Consiglio E, Formisano S, Leonardi A. Oncogenic and anti-apoptotic activity of NF- $\kappa$ B in human thyroid carcinomas. *J. Biol. Chem.* 2004; 279:54610–19. <sup>#</sup>**Mauro C. is joint first author.**
- Mauro C**, Crescenzi E, De Mattia R, Pacifico F, Mellone S, Salzano S, De Luca C, D'Adamio L, Palumbo G, Formisano S, Vito P, Leonardi A. Central role of the scaffold protein TNF-Receptor associated factor 2 in regulating endoplasmic reticulum stress-induced apoptosis. *J. Biol. Chem.* 2006; 281:2631–8.
- Mauro C**, Pacifico F, Lavorgna A, Mellone S, Iannetti A, Vito P, Formisano S, Leonardi A. ABIN-1 binds to NEMO/IKK $\gamma$  and co-operates with A20 in inhibiting NF- $\kappa$ B. *J. Biol. Chem.* 2006; 281:18482–8.
- Cirillo P, Pacileo M, De Rosa S, Calabrò P, Gargiulo A, Angri V, Granato Corigliano F, Fiorentino I, Prevete N, De Palma R, **Mauro C**, Leonardi A, Chiariello M. Neopterin induces pro-atherothrombotic phenotype in human coronary endothelial cells. *J. Thromb. Haemost.* 2006; 4:2248–55.

## Abstract

Constitutive activation of NF- $\kappa$ B is a common feature of many human tumors. In fact, it predisposes normal cells to neoplastic transformation. Mainly by inhibiting apoptosis, NF- $\kappa$ B overturns the balance between proliferation and apoptosis towards malignant growth. Therefore, targeting NF- $\kappa$ B for cancer therapy is one of the new challenges of modern tumor biology.

Since very little was known about the role of NF- $\kappa$ B in thyroid oncogenesis, we focused on the model of thyroid carcinomas. We showed that NF- $\kappa$ B is strongly activated in human thyroid neoplasias, particularly in anaplastic carcinomas. To investigate the oncogenic activity of NF- $\kappa$ B in thyroid, we analyzed its activity in thyroid transformed cell lines, recapitulating different steps in thyroid oncogenesis. In this experimental system we showed a constitutive NF- $\kappa$ B activity, even though at different levels, and a different resistance to drug-induced apoptosis, which directly correlated with levels of NF- $\kappa$ B activation. The stable expression of a super-repressor form of I $\kappa$ B $\alpha$  (I $\kappa$ B $\alpha$ M), blocking NF- $\kappa$ B activity, in the human anaplastic thyroid carcinoma cell line FRO (FRO-I $\kappa$ B $\alpha$ M), led to an enhanced sensitivity to drug-induced apoptosis. Moreover, while FRO parental cells (FRO-Neo) were able to form colonies in soft-agar and to induce tumor growth in nude mice, FRO-I $\kappa$ B $\alpha$ M cells lost both these properties. To obtain insights into mechanisms sustaining the anti-apoptotic effect of NF- $\kappa$ B, we analyzed JNK activity in FRO and FRO-I $\kappa$ B $\alpha$ M clones. FRO cells showed a barely detectable JNK activity, whereas JNK activation was completely restored in FRO-I $\kappa$ B $\alpha$ M clones. In addition, FRO-I $\kappa$ B $\alpha$ M clones treated with a specific JNK inhibitor, SP600125, rescued their resistance to apoptosis induced by chemotherapeutic agents. These results provide evidence that NF- $\kappa$ B plays a pivotal role in thyroid carcinogenesis, maintaining the transformed phenotype and inducing resistance to drug-induced apoptosis, at least partially through the inhibition of JNK.

Because of the importance of sustained activation of NF- $\kappa$ B in oncogenesis, we then focused our efforts on the molecular mechanisms down-regulating NF- $\kappa$ B activation. Classical activation of NF- $\kappa$ B is dependent on the phosphorylation of the inhibitory sub-unit I $\kappa$ B $\alpha$  by a multimeric-, high molecular weight-complex, called I $\kappa$ B kinase (IKK)-complex. This is composed of two catalytic sub-units, IKK $\alpha$  and IKK $\beta$ , and a regulatory sub-unit, NEMO/IKK $\gamma$ , that is essential for activation of IKKs and NF- $\kappa$ B. The mechanisms regulating activation of the IKK-complex are not fully understood so far. In the last few years, we isolated novel interactors of the IKK-complex, by using a combined genetic and biochemical approach. Here, we studied the mechanism of NF- $\kappa$ B inhibition by ABIN-1 (A20 Binding Inhibitor of NF- $\kappa$ B), a known interactor of the NF- $\kappa$ B inhibitor A20. We found that both ABIN-1 and A20 inhibit NF- $\kappa$ B at level of the IKK-complex and that A20 blocks activation of NF- $\kappa$ B by de-ubiquitinating NEMO/IKK $\gamma$ . Importantly, by

using RNA-interference technology, we showed that ABIN-1 and A20 cooperate in inhibiting NF- $\kappa$ B at level of NEMO/IKK $\gamma$ . Altogether these data indicate that ABIN-1 physically links A20 to NEMO/IKK $\gamma$  and promotes the A20-mediated de-ubiquitination of NEMO/IKK $\gamma$ , thus resulting in inhibition of NF- $\kappa$ B.

The strong constitutive NF- $\kappa$ B activity in anaplastic thyroid carcinomas, besides to represent a novel diagnostic tool, makes it a molecular target for developing novel therapeutic strategies which, interfering with NF- $\kappa$ B activity, could potentiate the effects of well-established chemotherapeutic agents. In this scenario, ABIN-1 and A20 represent examples of signal-specific mediators of NF- $\kappa$ B activation, which could be targeted for therapeutic strategies intended to interfere with sustained activation of NF- $\kappa$ B in tumor progression.

# Background

## *I – Introduction*

In addition to marshalling immunity and inflammation, NF- $\kappa$ B controls cell survival. Activation of NF- $\kappa$ B antagonizes apoptosis or programmed cell death (PCD) and the anti-apoptotic activity of NF- $\kappa$ B plays a pivotal role in various aspects of oncogenesis, including transformation, proliferation, invasiveness, metastasis formation and angiogenesis (Kucharczak et al. 2003). Actually, NF- $\kappa$ B activity has been found altered in many types of human tumors from either haematological or solid origin, such as melanomas (Amiri and Richmond 2005), and breast (Kalaitzidis and Gilmore 2005), prostate (Sweeney et al. 2004), ovarian (Mabuchi et al. 2004), pancreatic (Sclabas et al. 2005), colon (Kojima et al. 2004) and thyroid carcinomas (Visconti et al. 1997). The role of NF- $\kappa$ B in solid tumors has been well documented in several studies performed on primary tumors and neoplastic cell lines derived from different human tissues (Pacifico and Leonardi 2006). These studies show that the inhibition of constitutive NF- $\kappa$ B activity blocks the oncogenic potential of neoplastic cells by sensitizing tumor cells to chemotherapeutic drug-induced apoptosis, decreasing the highly proliferative rate which characterizes transformed cells, and inhibiting tissue invasiveness and metastatic potential of highly malignant cells (Karin et al. 2002).

Genes encoding NF- $\kappa$ B-family members are frequently rearranged, amplified or mutated in human cancers, and most oncogene products are capable of activating NF- $\kappa$ B. These alterations deregulate the ability of NF- $\kappa$ B to control both expression and function of a wide spectrum of genes involved in the control of cell cycle, apoptosis, cell growth, and tissue invasiveness. Further, since it is generally accepted that chronic inflammation contributes to the genesis of many solid tumors, it has been recently shown that activation of NF- $\kappa$ B is a crucial mediator of inflammation-induced tumor growth and progression in animal models of inflammation-associated cancer (Greten et al. 2004, Pikarsky et al. 2004). Thus, all these evidences show that the control of apoptosis by NF- $\kappa$ B is central to oncogenesis.

## *II – The family of NF- $\kappa$ B transcription factors*

NF- $\kappa$ B is an ubiquitously expressed family of transcription factors that control the expression of numerous genes involved in immune and inflammatory responses. NF- $\kappa$ B also regulates the expression of genes outside of the immune system and, hence, can influence multiple aspects of normal and disease physiology. In mammals, the NF- $\kappa$ B family consists of five members: p65 (RelA), RelB, c-Rel, p50/p105 (NF- $\kappa$ B1), and p52/p100 (NF- $\kappa$ B2). NF- $\kappa$ B1 and NF- $\kappa$ B2 are synthesized as large precursors, p105 and p100, that are post-translationally processed to the DNA-binding sub-units p50 and p52, respectively. All NF- $\kappa$ B proteins carry a N-terminus conserved 300-amino acid Rel-homology domain (RHD) that contains a nuclear localization sequence (NLS) and is responsible for dimerization, interaction with I $\kappa$ Bs, and binding

to DNA. Although p50 and p52 lack a transcription activation domain, such a domain is present in RelA, RelB and c-Rel. The NF- $\kappa$ B proteins form numerous homo- and heterodimers that are associated with specific biological responses, depending on their ability to regulate target gene transcription differentially. For instance, p50 and p52 homodimers function as repressors, whereas dimers that contain RelA or c-Rel are transcriptional activators. RelB can be both an activator and a repressor, forming only hetero-dimers with either p50 or p52 (Hayden and Ghosh 2004; Fig.1).

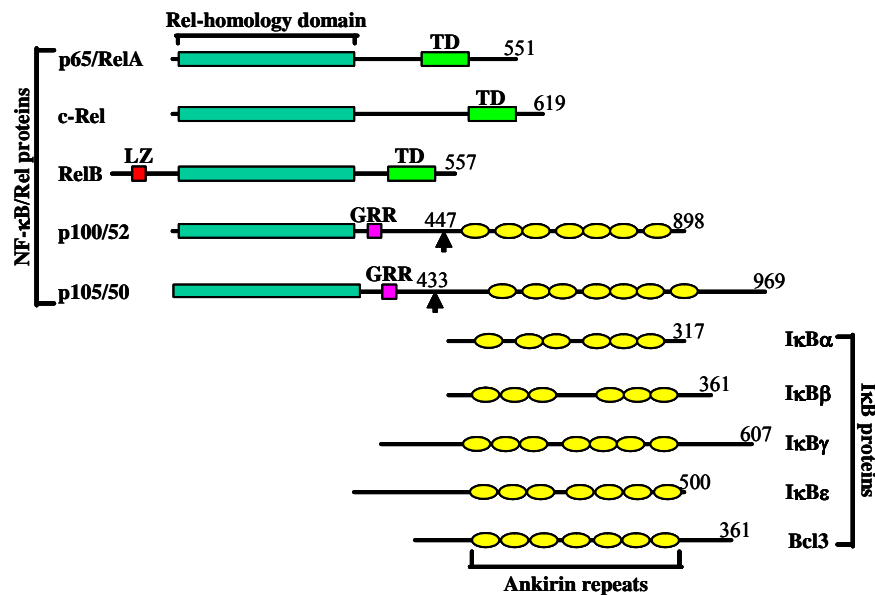


**Figure 1.** The family of NF- $\kappa$ B transcription factors.

In most cell types, NF- $\kappa$ B homo- or heterodimers are retained in the cytoplasm by I $\kappa$ Bs, which are a specific family of inhibitors binding to the RHD and interfering with NF- $\kappa$ B NLS function. These proteins contain 6–7 ankyrin repeats that mediate binding to the RHD. Binding of NF- $\kappa$ B to I $\kappa$ B results in constant shuttling of I $\kappa$ B:NF- $\kappa$ B complexes between the nucleus and the cytoplasm, although the steady-state localization of these complexes is in the cytosol, thereby maintaining NF- $\kappa$ B in an inactive state. The dynamic balance between cytosolic and nuclear localization is altered upon I $\kappa$ B degradation, because it exposes the previously masked NLS, resulting in predominantly nuclear localization of NF- $\kappa$ B (Hayden and Ghosh 2004; Fig.1).

### III – The classical pathway of NF- $\kappa$ B activation

Two major signaling pathways lead to translocation of NF- $\kappa$ B dimers from the cytoplasm to the nucleus: the classical and the alternative pathways. It is well established that the former pathway is essential for innate immunity, whereas the latter has been uncovered more recently and has been shown to play a crucial role in lymphoid organ development and adaptive immunity (Bonizzi and Karin 2004).

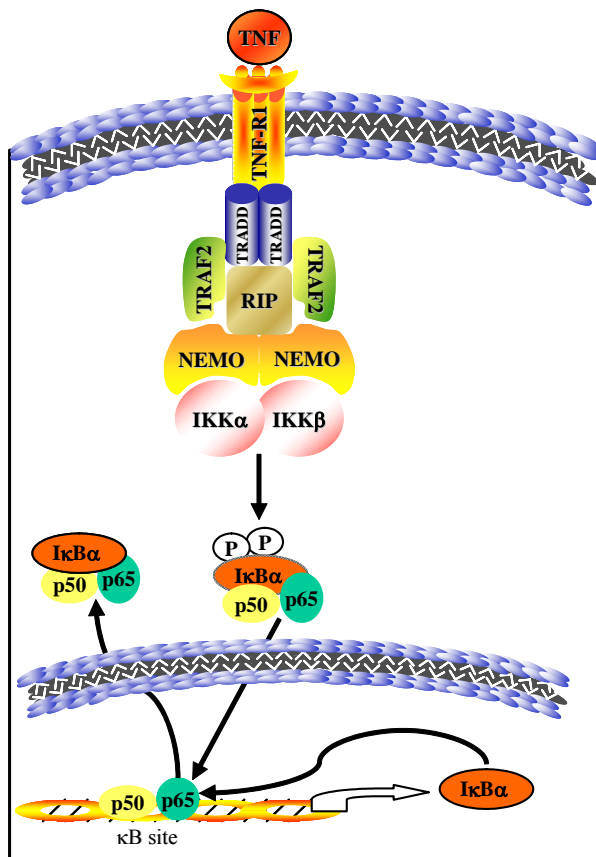


**Figure 2.** The classical pathway of NF-κB activation.

In the classical pathway, proinflammatory cytokines, such as tumor necrosis factor  $\alpha$  (TNF- $\alpha$ ) and pathogen-associated molecular patterns (PAMPs), working through different receptors belonging to the TNF receptor (TNFR) and Toll-like receptor (TLR)-interleukin-1 (IL-1) receptor (IL-1R) superfamilies, cause activation of the I $\kappa$ B kinase (IKK) complex. In cells the IKK activity can be purified as a 700–900-kDa complex, and has been shown to contain two kinase subunits, IKK $\alpha$  (IKK1) and IKK $\beta$  (IKK2), and a regulatory subunit, NEMO (NF- $\kappa$ B essential modifier) or IKK $\gamma$  (Ghosh and Karin 2002). The activated IKK complex, acting predominantly through IKK $\beta$  in a NEMO/IKK $\gamma$ -

dependent manner, catalyzes the phosphorylation of the inhibitory sub-unit I $\kappa$ B on specific serine residues (e.g. Ser32 and 36 of I $\kappa$ B $\alpha$ ). Phosphorylated I $\kappa$ Bs are recognized by the ubiquitin ligase machinery, leading to their lysine (K)-48-linked polyubiquitination (e.g. Lys21 and 22 of I $\kappa$ B $\alpha$ ) and subsequent degradation by the proteasome. The freed NF- $\kappa$ B dimers (in this pathway most commonly the p50-RelA dimer) translocate to the nucleus, where they bind to specific sequences in the promoter or enhancer regions of target genes and activate transcription. NF- $\kappa$ B can then be down-regulated through a feedback pathway whereby newly synthesized I $\kappa$ Bs proteins bind to nuclear NF- $\kappa$ B and export it out to the cytosol (Karin and Ben-Neriah 2000; Fig.2).

#### IV – Ubiquitination and NF- $\kappa$ B signaling pathway

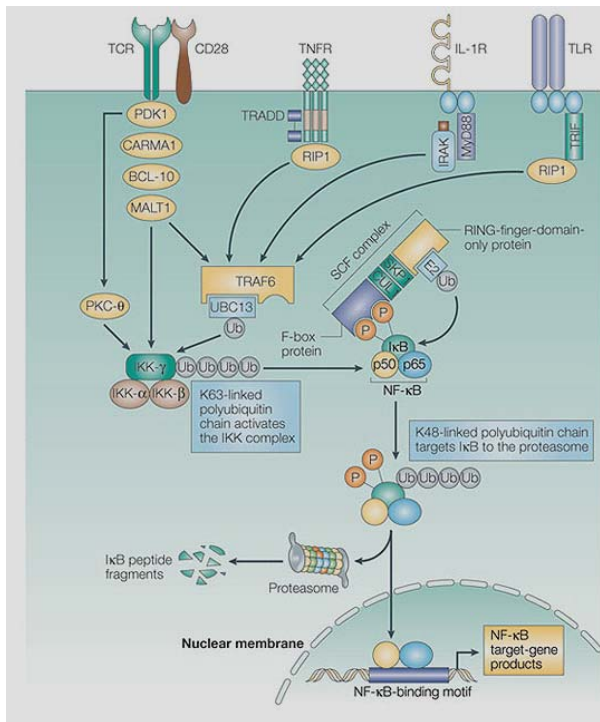


**Figure 3.** K-63-linked ubiquitination regulates NF- $\kappa$ B activation (Liu et al. 2005).

important mediators of signal transduction through TNFRs (Hsu et al. 1996). One TRAF-family member, TRAF6, promotes ubiquitin conjugation to itself and NEMO/IKK $\gamma$  through its RING-finger domain. However, instead of inducing conventional K-48-linked polyubiquitination, TRAF6 induces the formation of a K-63-linked polyubiquitin chain (Sun et al. 2004). Importantly, K-63-linked polyubiquitination of NEMO/IKK $\gamma$  does not lead to its degradation through a proteasome dependent pathway, rather it results in activation of the IKK complex, and the subsequent phosphorylation and degradation of I $\kappa$ B (Zhou et al. 2004). Thus, K-63-linked ubiquitination of NEMO/IKK $\gamma$  is an important step for the activation of IKKs and NF- $\kappa$ B following various receptors, such as TCR, TNFR, IL-1R and TLR (Boone et al. 2004, Tang et al. 2003, Zhou et al. 2004; Fig.3).

The key feature of the ubiquitination system is that ubiquitin can be rapidly removed by deubiquitinating enzymes (DUBs), which serve to switch off the ubiquitin signal. Notably, ubiquitination shares this feature with protein phosphorylation: both modifications are recognized by specific protein domains, providing a mechanism for translation of the ubiquitin- or phospho-specific signal to down-stream effectors (Hicke et al. 2005). Two DUBs have recently been shown to be important in suppressing NF- $\kappa$ B activation at a step upstream of IKK. One of these DUBs is the cylindromatosis tumor suppressor CYLD, which inhibits IKK and NF- $\kappa$ B activation by cleaving K-63-linked polyubiquitin chains on several proteins, such as TRAF2, TRAF6 and NEMO/IKK $\gamma$  (Kovalenko et al. 2003). Another DUB that acts in the NF- $\kappa$ B

Ubiquitin conjugation has been most prominently associated with protein degradation through a proteasome-dependent pathway, but it is becoming increasingly evident that ubiquitination plays a key role in the signal transduction pathway leading to activation of NF- $\kappa$ B (Chen 2005, Liu et al. 2005). Recent reports have shown that ubiquitination is crucial for activation of the IKK complex. Studies of TNFR and IL-1R signaling led to the discovery that TRAFs, a family of proteins characterized by the presence of a RING-finger domain and coiled-coil domain, are

pathway is A20, an NF- $\kappa$ B-induced protein that inhibits NF- $\kappa$ B in a negative-feedback loop. The central role played by A20 in terminating NF- $\kappa$ B activation is demonstrated by the evidence that A20<sup>-/-</sup> mice develop severe inflammation and cachexia, are hyper-sensitive to both LPS and TNF, and consequently die

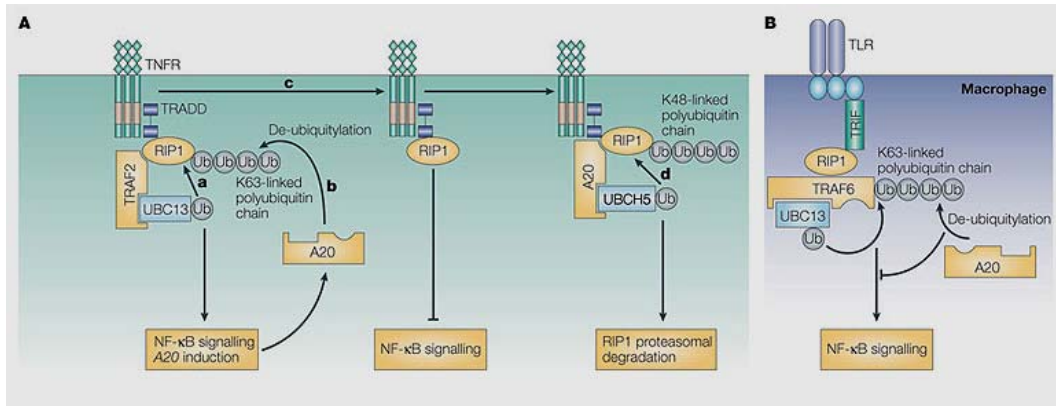


**Figure 4.** The deubiquitinating and E3 ubiquitin ligase activities of A20 in terminating NF- $\kappa$ B signaling (Liu et al. 2005).

prematurely (Lee et al. 2000). A20 contains a novel ovarian tumor (OTU)-type DUB domain at the N-terminus, and several zinc-finger in the remainder of the protein. The OTU domain disassembles K-63-linked ubiquitin chains from RIP, an essential mediator of the proximal TNFR-1 signaling complex, thereby suppressing IKK activation. Moreover, after K-63 chains are removed, A20 functions as an ubiquitin ligase through its zinc-finger domains to assemble K-48-linked polyubiquitin chains on RIP, targeting it for proteasomal degradation (Wertz et al. 2004). Furthermore, A20 terminates TLR-induced NF- $\kappa$ B signaling, by cleaving ubiquitin chains from TRAF6 (Boone et al. 2004; Fig.4).

#### V – The role of NF- $\kappa$ B in oncogenesis

According to Hanahan and Weinberg (2000), six essential alterations in cell physiology characterize a tumor cell: self-sufficiency in growth, insensitivity to growth-inhibitory signals, evasion of apoptosis, limitless replicative potential, sustained angiogenesis and metastasis. Many of the genes able to mediate such effects are under transcriptional control of NF- $\kappa$ B (Aggarwal 2004). Activity and expression of Cyclin D1 (Guttridge et al. 1999), CDK2 kinase (Perkins et al. 1997), and c-myc (Kim et al. 2000), which are involved in the control of cell cycle and are altered in several types of cancer are under control of NF- $\kappa$ B. Expression and function of numerous cytokines, that function as growth factors for tumor cells, are NF- $\kappa$ B-dependent. Among them are: IL-1 $\beta$ , a growth factor for acute myeloid leukemia (AML); TNF, a growth factor for Hodgkin's lymphoma, cutaneous T cell lymphoma and gliomas; interleukin (IL)-6, a growth factor for multiple myeloma (Pahl 1999). Some growth factors, such as epidermal growth factor (EGF), or growth factor receptors, such as HER2, able to promote growth of solid tumors, activate NF- $\kappa$ B (Biswas et al. 2000). Tissue invasion and metastasis, two crucial events of

tumor progression, are caused by NF- $\kappa$ B-dependent genes, including matrix metalloproteinases (MMPs; Farina et al. 1999), urokinase type of plasminogen activator (uPA; Novak et al. 1991), IL-8 (Kunsch and Rosen 1993), the adhesion molecules VCAM-1, ICAM-1 and ELAM-1 (Van de Stolpe et al. 1994) and chemokine receptors such as CXCR4 (Helbig et al. 2003). NF- $\kappa$ B activity is also involved in the regulation of angiogenesis, an essential step for tumor growth and invasiveness. For instance, vascular endothelial growth factor (VEGF), which is the main member of angiogenic factor family, is under transcriptional control of NF- $\kappa$ B (Kiriakidis et al. 2003). Finally, altered expression of genes involved in regulation of apoptosis, which is a feature of neoplastic cells, is often due to deregulated NF- $\kappa$ B activity. By promoting cell survival, these genes lead to the maintaining of cell transformed state and are responsible for the resistance to chemotherapeutic drugs. All these evidences highlight the crucial role of altered NF- $\kappa$ B in promoting neoplastic transformation. As a consequence, inactivation of NF- $\kappa$ B in different cell lines derived from tumors displaying high constitutive NF- $\kappa$ B activity leads to the loss of their tumorigenic potential due to either an increased susceptibility to drug-induced apoptosis and/or a decrease of their proliferative rate. Moreover, in some cases, blocking NF- $\kappa$ B activity inhibits the metastatic potential of cancer cells or reduces the tumor size.

#### *VI – Thyroid carcinomas and NF- $\kappa$ B*

Thyroid carcinomas are the most common neoplasias of endocrine system (Figge 1999). Four types of thyroid cancer comprise more than 98% of all thyroid tumors: papillary thyroid carcinoma (PTC), follicular thyroid carcinoma (FTC), both of which may be summarized as differentiated thyroid carcinoma, medullary thyroid carcinoma (MTC) and undifferentiated anaplastic thyroid carcinoma (ATC; Sherman 2003). PTC, FTC and ATC derive from the thyroid follicular epithelial cells, while MTC derives from the parafollicular C-cells (Gimm 2001). PTC is the most common malignant thyroid neoplasm in countries with sufficient iodine diets and comprises up to 80% of all thyroid malignancies. FTC is more common in regions with insufficient iodine diets and represents approximately 10-20% of all thyroid malignancies. The overall 5-10 year survival rate of patients with PTC is about 80-95%, while that of patients with FTC is about 70-95%. The incidence of MTC is not well known because epidemiologic studies are rare. Generally, it is believed that MTC comprises about 5-10% of all thyroid malignancies (Ball et al. 1996, Gimm 2001, Sherman 2003). ATC is one of the most aggressive human malignancies, with a very poor prognosis. Although rare, accounting for up to 10% of clinically recognized thyroid cancers, the overall median survival is limited to months (Gimm 2001, McIver et al. 2001, Sherman 2003). Surgery, radiotherapy and chemotherapy, based primarily on doxorubicin and cisplatin treatment, do not meaningfully improve survival of ATC patients (McIver et al. 2001, Tennvall et al. 1994). Novel therapeutic approaches are therefore needed.

Very little is known about the role that NF- $\kappa$ B plays in thyroid physiology. On the other hand, there is weak evidence that NF- $\kappa$ B may be important in RET-mediated carcinogenesis, by maintaining the transformed phenotype of thyroid cell lines (Visconti et al. 1997). However, the role that NF- $\kappa$ B plays “in vivo” in human thyroid neoplasia has not been fully investigated.

#### *VII – The control of programmed cell death by NF- $\kappa$ B*

Apoptosis is critical for maintenance of normal homeostasis together with other important processes such as proliferation and differentiation. Defects in apoptosis contribute to tumor pathogenesis and progression in several ways, such as allowing neoplastic cells to survive beyond their normal lifespan, providing protection against hypoxia as tumor mass expands, promoting angiogenesis and invasiveness during tumor progression, and allowing tumor cells to become resistant to radio- and chemotherapy. They also promote resistance to immune system, given that many of the weapons used by cytolytic T-cells and NK cells for killing tumor cells depend on the integrity of the apoptotic machinery. Thus, de-regulated apoptosis is a fundamental aspect of the biology of cancer.

The first indication that suppression of apoptosis is an important NF- $\kappa$ B function came from the evidence that *relA*<sup>-/-</sup> mice died during embryonic development as a result of massive liver apoptosis. The massive liver apoptosis, which is also displayed by mice lacking IKK $\beta$  or NEMO/IKK $\gamma$ , is mediated by TNF- $\alpha$  and is completely suppressed in TNF- $\alpha$  or TNFR1 knockout mice (Li and Verma 2002). Further experiments showed that NF- $\kappa$ B is a critical regulator of apoptotic response in different physiological and pathological contexts. The survival of peripheral B cells in response to antigen depends on B-cell receptor (BCR)-mediated activation of NF- $\kappa$ B and the induction of anti-apoptotic target genes (Bendall et al. 1999). The full activation of naïve T cells *via* T-cell receptor (TCR) leads to NF- $\kappa$ B activation and consequent cell survival *via* induction of anti-apoptotic genes (Jamieson et al. 1991). A link between NF- $\kappa$ B and apoptosis has also been demonstrated in the regulation of innate immune response, which plays a fundamental role in the detection and elimination of pathogens (Naumann 2000). The inhibition of NF- $\kappa$ B activity in mouse xenograft models of chemo-resistant tumors provokes tumor regression by sensitizing them to chemotherapeutic drug treatments (Greten and Karin 2004). Consistent with this work, NF- $\kappa$ B inhibition in many human tumor-derived cell lines induces spontaneous apoptosis and/or sensitizes them to killing by TNF- $\alpha$ , TRAIL or anti-cancer drugs.

Mechanisms for NF- $\kappa$ B-mediated protection from apoptosis are essentially based on its ability to activate the transcription of a number of genes capable of suppressing cell death (Kucharczak et al. 2003, Pacifico and Leonardi 2006; Fig.5). Among them are: 1) pro-survival members of the mammalian Bcl-2 gene family, Bcl-xL and Bfl-1/A1, which suppress the release of pro-apoptotic cytochrome c and Smac/Diablo from mitochondria,

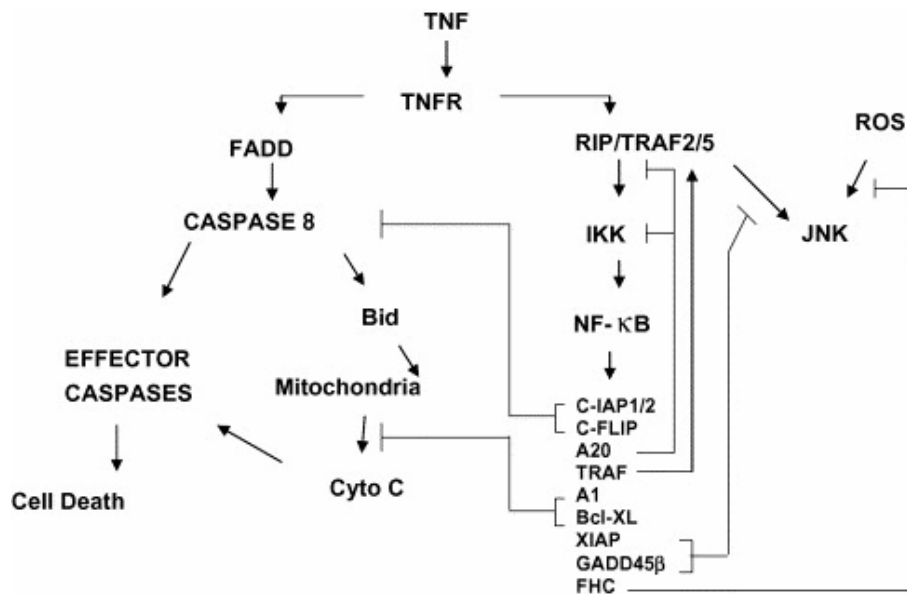


**Figure 5.** *NF-κB controls the transcription of a number of genes interfering with different steps in the apoptotic process (Pacifico and Leonardi 2006).*

thereby blocking programmed cell death in response to TNF- $\alpha$  and chemotherapeutic drugs (Boise et al. 1993, Wang et al. 1999); 2) the cellular inhibitors of apoptosis c-IAP1, c-IAP2, TRAF1 and TRAF2, the zinc-finger protein A20, and c-FLIP, all of them able to suppress cell death induced by TNF- $\alpha$ , death receptors or anti-cancer drugs (Deveraux et al. 1998, Yeh et al. 2000, Wang et al. 1998); 3) the anti-apoptotic protein XIAP, that inhibits the processing of procaspase-9 and the activities of caspase-7 and -3 (Tang et al. 2001), and GADD45 $\beta$ , belonging to the GADD45 family of factors involved in cell cycle control and DNA repair (De Smaele et al. 2001), both of them implicated in NF- $\kappa$ B-mediated suppression of pro-apoptotic JNK signaling in response to TNF- $\alpha$ . A similar mechanism of action is displayed by Ferritin Heavy Chain (FHC) that controls ROS production, responsible, in turn, to mediate the sustained activation of JNK and, thus, its pro-apoptotic activity (Pham et al. 2004). All these anti-apoptotic proteins may work in a coordinated manner to interfere with apoptosis at multiple steps along with the apoptotic signaling cascade, thus promoting tumor progression.

#### VIII – JNK signaling in programmed cell death

JNK1/2/3 are the downstream components of one of the major mitogen-activated protein kinase (MAPK) cascades, also comprising the extracellular signal-regulated kinase (ERK1/2) and p38( $\alpha/\beta/\gamma/\delta$ ) cascades (Chang and Karin 2001, Davis 2000, Johnson and Lapadat 2002). By and large, activation of JNK (and p38) is associated with the induction of apoptosis. In contrast, activation of ERK is linked to cell growth and survival (Chang and Karin 2001, Davis 2000, Johnson and Lapadat 2002, Tournier et al. 2000). Actually, *jnk1*<sup>-/-</sup> and *jnk2*<sup>-/-</sup> mouse embryonic fibroblasts (MEFs) exhibit a severe defect in the apoptotic response to stress (Tournier et al. 2000). JNK is

also required for TNFR-induced killing (De Smaele et al. 2001, Javelaud et al. 2001, Tang et al. 2001), as the JNK1 and JNK2 double deletion virtually abrogates this killing (Deng et al. 2003). Yet, precisely how JNKs activate the apoptotic signaling is unknown. However, from different experimental evidences it seems clear that the duration of JNK activation affects its role in apoptosis. Interestingly, it is the sustained (and not the acute) induction of JNK that has been linked to PCD. This has been recently demonstrated by different groups showing that NF- $\kappa$ B is able to inhibit TNF- $\alpha$ -induced apoptosis by negatively regulating the sustained activation of the JNK pathway. They have also shown that the negative regulation of JNK activity exerted by NF- $\kappa$ B is mediated by GADD45 $\beta$ , XIAP, and FHC, all of them under the transcriptional control of NF- $\kappa$ B (De Smaele et al. 2001, Pham et al. 2004, Tang et al. 2001). However, the prolonged JNK activation alone may not be sufficient to induce apoptosis (Tang et al. 2001). In contrast, some studies have indicated that JNK may also contribute to cell survival (Davis 2000). Thus, the dual role of JNK in both apoptotic and anti-apoptotic signaling pathways suggests that the function of JNK is complex and that the physiological response most likely reflects a balance between the ability of JNK to signal both apoptosis and cell survival.

#### *IX – NF- $\kappa$ B as target for cancer therapies*

All the evidences reported above clearly show that NF- $\kappa$ B is a key player in cancer. Thus, researchers have focused their efforts in looking for drugs able to suppress NF- $\kappa$ B activity in malignant cells. NF- $\kappa$ B activation could be blocked at different levels targeting various components of its signaling cascade, such as the IKK complex, the I $\kappa$ B inhibitory proteins, the p65 subunit of the transcriptionally active heterodimer, and/or the proteasome. Therefore, an increasing number of compounds able to block NF- $\kappa$ B, by inhibiting one or more molecules involved in its signaling pathway, have been tested and have shown to suppress the growth of those cancer cells whose tumorigenicity depends on NF- $\kappa$ B activity (Karin et al. 2002). Many of these drugs have given promising results in preclinical models for NF- $\kappa$ B-dependent solid tumors (breast, lung, colon, bladder, ovary, pancreas and prostate cancers), but their clinical efficacy has shown to be poorly appreciable. At present, the only pharmacological inhibitors of NF- $\kappa$ B activation approved for clinical use are represented by proteasome inhibitors for treatment of some haematological malignancies, such as multiple myeloma, or adult T-cell leukemia, for whose pathogenesis it has been clearly demonstrated the key role of NF- $\kappa$ B (Nasr et al. 2005, Richardson et al. 2004).

One of the most problematic aspects of a cancer therapy based on inhibition of NF- $\kappa$ B activity is represented by the difficulty to find compounds which block the oncogenic activity of NF- $\kappa$ B without interfering with its physiological roles in immunity, inflammation and cellular homeostasis. Unfortunately, most of the drugs analyzed so far also affect other cellular signaling pathways involved in the regulation of apoptosis and proliferation other than inflammatory and immunological response, thereby determining a

number of highly toxic side effects. To this end, all the efforts are now concentrated on the ability to identify novel NF- $\kappa$ B targets specifically activated in tumors, but not in normal cells, or agents that block the prosurvival effectors of NF- $\kappa$ B, rather than NF- $\kappa$ B itself.

## **Aims of the Study**

NF- $\kappa$ B family of transcription factors is deeply involved in the control of cell survival. Activation of NF- $\kappa$ B antagonizes apoptosis or programmed cell death and the anti-apoptotic activity of NF- $\kappa$ B plays a pivotal role in various aspects of oncogenesis, including transformation, proliferation, invasiveness, metastasis formation and angiogenesis.

Very little is known about the role of NF- $\kappa$ B in thyroid oncogenesis. It has been shown that NF- $\kappa$ B may be important in RET-mediated carcinogenesis, by maintaining the transformed phenotype of thyroid cell lines (Visconti et al. 1997). Thus, the first aim of this study has been to analyze the oncogenic activity of NF- $\kappa$ B in specimens from human thyroid carcinomas and in thyroid transformed cell lines reproducing *in vitro* the human thyroid neoplasias. Further, our efforts have focused on gaining an understanding of the precise mechanism(s) by which NF- $\kappa$ B promotes thyroid transformed cell survival and chemoresistance.

Because of the importance of sustained activation of NF- $\kappa$ B in promoting neoplastic transformation, the second aim of the present study has been to identify novel molecules involved in switching off NF- $\kappa$ B signaling pathways and dissect their inhibitory mechanisms.

However, our ultimate aim has been to uncover unknown pieces in the NF- $\kappa$ B puzzle that can be exploited as molecular targets for developing novel therapeutic strategies, which, interfering with NF- $\kappa$ B activity, could potentiate our weapons against tumors.

## Materials and Methods

### *I – Cell cultures and biological reagents*

NPA is a cell line derived from human papillary thyroid carcinoma (Ludwig et al. 2001), FRO is derived from human anaplastic thyroid carcinoma (Fagin et al. 1993), and WRO is derived from human follicular thyroid carcinoma (Estour et al. 1989). These cells were grown in Dulbecco's Modified Eagle's Medium (DMEM, Sigma) supplemented with 10% fetal bovine serum, 100 units/ml penicillin, 100 µg/ml streptomycin, and 1% glutamine. FRO cells were transfected with the empty expression vector pcDNA3.1-FLAG (Invitrogen; FRO-Neo) or with pcDNA3.1-FLAG encoding a mutant form (S32A/S36A) of IκBα (FRO-IκBαM; De Smaele et al. 2001). NPA cells were transfected with the empty expression vector pcDNA3.1-FLAG (NPA-Neo) or with pcDNA3.1-FLAG vector encoding human IKKβ (NPA-IKKβ; Leonardi et al. 2000a). Stable transfected clones were selected and maintained in the presence of 200 µg/ml geneticin (Sigma). HEK293 cells were maintained as described above.

Anti-ABIN-1 polyclonal antibodies were generated in rabbits, by using a recombinant peptide encompassing amino acids 380-636 of human ABIN-1. Other antibodies used for this study were: FLAG epitope (Sigma), p65 and A20 (BD Pharmingen), JNK1/2 and p-JNK1/2 (Cell Signaling), HA epitope, p65, NEMO/IKKγ, IKKβ, IκBα and Tubulin (Santa Cruz Biotechnologies). The following reagents were also used: cisplatin and doxorubicin (kindly provided by S. Pepe) used at different concentrations as indicated in the experiments; anisomycin (Sigma) 10 µg/ml; SP600125 (Biomol Research Laboratories) 10 µM; human TNF-α (Peprotech) 2,000 units/ml.

Human ABIN-1 was amplified by PCR from a human liver c-DNA library (BD Clontech) and cloned into pcDNA3.1-HA, -FLAG, and -His vectors (Invitrogen) for expression in mammalian cells. A20, TAX, and Ubiquitin expression vectors were gifts from G. Natoli, T. K. Jeang and G. Courtois, respectively. NEMO/IKKγ, IKKβ, CIKS and TRAF2 expression vectors were previously described (Leonardi et al. 2000a-b). All deletion mutants were prepared by conventional PCR and cloned into pcDNA3.1-HA or -FLAG vectors. Point mutants of A20 (C103S and D100A/C103S) were generated by the Quickchange Site-Directed Mutagenesis Kit (Stratagene), according to the manufacturer's protocol.

### *II – Immunohistochemical analysis*

Specimens from normal and pathological human thyroids were isolated, rinsed with PBS, fixed in 4% buffered neutral formalin and embedded in paraffin. 5-6 µm thick paraffin sections were deparaffinized, placed in a solution of absolute methanol and 0.3% hydrogen peroxide for 30 min, and washed in PBS before immunoperoxidase staining. Slides were incubated overnight at 4°C in a humidified chamber with antibody anti-p65 diluted 1:100 in PBS and subsequently incubated, first with biotinylated goat anti-rabbit IgG

for 20 min and then with pre-mixed reagent ABC for 20 min (Vectostain ABC kits, Vector Laboratories). The immunostaining was performed by incubating slides in diaminobenzidine (DAB-DAKO) solution containing 0.06 mM DAB and 2 mM hydrogen peroxide in 0.05% PBS pH 7.6 for 5 min. After chromogen development, slides were washed, dehydrated with alcohol and xylene, and mounted on coverslips using a permanent mounting medium (Permount).

### *III – Electro-Mobility Shift Assay (EMSA)*

To analyze NF- $\kappa$ B DNA binding activity, total cell extracts were prepared using a detergent lysis buffer [50 mM Tris pH 7.4, 250 mM NaCl, 50 mM NaF, 1 mM Na<sub>3</sub>VO<sub>4</sub>, 0.5% Nonidet P-40, 0.5 mM dithiothreitol and Complete Protease Inhibitor Mixture (Roche)]. Cells were harvested by centrifugation, washed once in cold PBS and resuspended in detergent lysis buffer (30  $\mu$ l/5x10<sup>6</sup> cells). The cell lysate was incubated on ice for 30 min, and then centrifuged for 5 min at 14,000 rpm 4°C. The protein content of the supernatant was determined, and equal amounts of protein (10  $\mu$ g) were added to a reaction mixture containing 20  $\mu$ g BSA, 2  $\mu$ g poly(dI-dC), 10  $\mu$ l binding buffer (20 mM HEPES pH 7.9, 10 mM MgCl<sub>2</sub>, 20% Glycerol, 100 mM KCl, 0.2 mM EDTA, 0.5 mM DTT and 0.5 mM PMSF) and 100,000 cpm of a <sup>32</sup>P-labeled oligonucleotide containing specific binding sites for NF- $\kappa$ B, in a final volume of 20  $\mu$ l. Samples were incubated at room temperature for 30 min and then run on a 4% acrylamide gel.

To analyze AP-1 DNA binding activity, nuclear extracts were prepared as follows: cells were harvested by centrifugation, washed once in cold PBS and resuspended in buffer A (10 mM HEPES pH 7.9, 10 mM KCl, 1.5 mM MgCl<sub>2</sub> and 0.1 mM EGTA). Then, cells were centrifuged for 5 min at 2,000 rpm and resuspended in cold buffer C (20 mM HEPES pH 7.9, 400 mM NaCl, 1.5 mM MgCl<sub>2</sub>, 0.1 mM EGTA and 25% Glycerol). The cell resuspension was subjected to strong shaking for 30 min at 4°C and then centrifuged for 15 min at 2,000 rpm. EMSA was performed as above, using <sup>32</sup>P-labeled AP-1 oligonucleotide.

### *IV – In vitro and in vivo tumorigenicity assays*

To analyze the ability of various FRO clones to form colonies in soft agar, 1x10<sup>4</sup> cells were seeded in 60 mm dishes onto 0.3% Noble Agar (DIFCO) on top of a 0.6% bottom layer. Colonies larger than 50 cells were scored after 2 weeks incubation at 37°C (Macpherson and Montagnier 1964).

To analyze the ability of various FRO clones to induce tumor growth in nude mice, 2x10<sup>7</sup> cells were injected sub-cutaneously on a flank of each 6-week-old nude mouse (Charles River). Thirty days later, mice were killed and tumors were excised. Weight of tumors was determined and their diameters were measured with calipers. Volumes were calculated by the formula:  $a^2 \times b \times 0.4$ , where  $a$  is the smallest diameter and  $b$  is the diameter perpendicular to  $a$ . None mouse showed signs of wasting or other visible indications of toxicity. Mice were maintained at the DBPCM animal facility, and experiments were

conducted in accordance with standards of animal care and Italian regulations for the welfare of animals used in studies of experimental neoplasia. Further, the study was approved by our institutional committee on animal care.

#### *V – Cytotoxic treatments and measurements of apoptosis*

$1 \times 10^3$  cells/well were seeded in 96-well culture plates, and incubated for 48 h at 37°C with different concentrations of cisplatin or doxorubicin and w/wo the specific JNK inhibitor, SP600125. Cell survival was examined by using 3-(4,5-dimethylthiazol-2-yl)-5-(3-carboxymethoxyphenyl)-2-(4-sulfophenyl)-2H-tetrazolium, inner salt (MTS) and an electron coupling reagent (phenazine methosulfate, PMS), according to manufacturer's instructions (Promega). Cell death was assessed by staining of exposed phosphatidylserine on cell membranes with fluorescein isothiocyanate (FITC)-conjugated annexin V (BD Pharmingen) or by propidium iodide staining according to Nicoletti et al. (1991). Samples were analyzed by flow cytometry using a FACScalibur (Beckman Coulter), equipped with ModFit Software. Results were mean  $\pm$ SD of at least three independent experiments.

#### *VI – [<sup>3</sup>H]-thymidine DNA incorporation*

$5 \times 10^4$  cells/well were seeded in 12-well culture plates and incubated for 4 h at 37°C with 0.5  $\mu$ Ci/well of [<sup>3</sup>H]-thymidine (Amersham). After three washings with cold PBS, cells were incubated for 10 min at 4°C with 0.5 ml of 20% TCA. Then, cells were lysed with gentle shaking for 30 min at 37°C in the presence of 1 N NaOH (0.5 ml/well). An aliquot of lysate (0.1 ml) was used to evaluate the protein content by colorimetric assay (BioRad), while the remainder was analyzed at the  $\beta$ -counter (Beckman Coulter).

#### *VII – CFSE cell proliferation assay*

The analysis of cell proliferation was performed by labelling cells with CFSE (Molecular Probes) according to Lyons (1999). Flow cytometry and data analysis were performed by using a two laser equipped FACScalibur apparatus and the CellQuest analysis software (Becton Dickinson).

#### *VIII – Gel filtration of cellular extracts*

Gel filtration procedures were performed as previously described (Mauro et al. 2003). Fractions were analyzed by Western blotting for ABIN-1, NEMO/IKK $\gamma$  and IKK $\beta$ .

#### *IX – In vitro translation and GST pull-down assays*

*In vitro* transcription and translation were carried out with 1  $\mu$ g of ABIN-1 constructs according to the TNT Quick Coupled Transcription/Translation System protocol (Promega) in the presence of <sup>35</sup>S methionine. GST-NEMO/IKK $\gamma$  fusion protein was produced and purified as described by Chariot et al. (1999). GST pull-down assays were performed by incubating an aliquot of GST-NEMO/IKK $\gamma$  bound to glutathion-sepharose beads (Amersham Biosciences) together with 10  $\mu$ l of *in vitro* translated ABIN-1 proteins in PBS-1% Triton X-100 buffer (including Complete Protease Inhibitor mixture) for 2 h at 4°C. Beads were then washed five times with the

same buffer, resuspended in Laemmli buffer and run on a SDS-polyacrylamide gel before autoradiography.

#### *X – Transfection, immunoprecipitation and luciferase assay*

Lipofect-AMINE-mediated transfections were performed according to the manufacturer's instructions (Invitrogen). All transfections included extra empty vector to ensure that total amount of transfected DNA was kept constant in each culture dish.

For immunoprecipitation of transfected proteins, HEK293 cells ( $3 \times 10^6$ ) were transiently transfected and 24 h after transfection cells were lysed in Triton X-100 lysis buffer (20 mM HEPES pH 7.4, 150 mM NaCl, 10% Glycerol, 1% Triton X-100, and Complete Protease Inhibitor mixture). After an additional 15 min on ice, cell extracts were centrifuged for 10 min at 14,000 rpm  $4^\circ\text{C}$ , and supernatants were incubated for 4 h at  $4^\circ\text{C}$  with anti-FLAG antibodies bound to agarose beads (M2, Sigma). The immunoprecipitates were washed five times with Triton X-100 lysis buffer and subjected to SDS-PAGE.

For luciferase assay, HEK293 cells ( $4 \times 10^5$ ) were seeded in six-well-plates. After 12 h cells were transfected with 0.5  $\mu\text{g}$  of Ig- $\kappa\text{B}$ -luciferase reporter plasmid and various combinations of expression plasmids, as indicated in the experiments. 24 h after transfection, cells were stimulated with TNF- $\alpha$  for 3 h or left untreated. Cell extracts were prepared and reporter gene activity was determined via the luciferase assay system (Promega). Expression of the pRSV- $\beta\text{Gal}$  vector (0.2  $\mu\text{g}$ ) was used to normalize transfection efficiencies.

#### *XI – In vivo ubiquitination and de-ubiquitination assays*

HEK293 cells ( $3 \times 10^6$ ) were co-transfected with expression vectors containing epitope-tagged Ubiquitin (1  $\mu\text{g}$ ) and NEMO/IKK $\gamma$  (200 ng), plus various constructs encoding A20 or ABIN-1 proteins. 24 h after transfection, cell lysates were prepared as above and analyzed for poly-ubiquitination of NEMO/IKK $\gamma$ , either by Western blot anti-NEMO/IKK $\gamma$  (-FLAG) on total extracts or by immunoprecipitating FLAG-NEMO/IKK $\gamma$  with anti-FLAG beads followed by Western blot anti HA-Ubiquitin.

#### *XII – ABIN-1 and A20 siRNA expression vectors*

To knock-down ABIN-1 expression, we designed double-stranded oligo-nucleotides containing sequences derived from the human ABIN-1 ORF (nucleotides 1136-1156 and 1685-1705), in forward and reverse orientation, separated by a 7-base-pair spacer region (caagaga), to allow the formation of the hairpin structure in the expressed siRNAs. ABINi-370: sense strand, 5'-aattcGAGGAGACCGACAAGGAGCAGcaagagaCTGCTCCTTGTCGGTCTCCTcttttc; anti-sense strand, 5'-tcgagaaaaGAGGAGACCGACAAGGAGCAGtctcttgCTGCTCCTTGTCGGTCTCCTCg. ABINi-560: sense strand, 5'-aattcCCACACCATGGCTTCGAGGACcaagagaGTCCTCGAAGCCATGGTGTGGtttttc; anti-sense strand, 5'-tcgagaaaaCCACACCATGGCTTCGAGGACtctcttgGTCCTCGAAGCCATG

GTGTGGg. The resulting double-stranded oligo-nucleotides were cloned into the pcRNAi vector that we derived from the pcDNA3.1 vector (Invitrogen) by replacing the viral promoter-cassette with the H1 gene promoter that is specifically recognized by RNA polymerase III.

Plasmids used to knock-down A20 expression (pU6-A20i and the pU6) were kindly provided from S. Yamaoka (Saitoh et al. 2005).

## Results and Discussion

### *I – Basal NF- $\kappa$ B activity in human thyroid carcinomas*

To determine the activation state of NF- $\kappa$ B in primary thyroid cancer tissues, human specimens from normal thyroid and papillary, follicular, and anaplastic thyroid carcinomas were collected and stained with anti-p65 (RelA) antibodies. Results are summarized in Table 1. No nuclear staining for RelA

Histological type of thyroid samples	N° positive cases/N° total cases analyzed by immunohistochemistry	NF- $\kappa$ B staining score
Normal thyroid	0/4	0
Papillary carcinoma	6/6	1+
Follicular carcinoma	5/5	2+
Anaplastic carcinoma	4/4	3+

**Table 1.** NF- $\kappa$ B nuclear localization in normal and pathological human thyroid tissues. The percentage of cells with nuclear staining for NF- $\kappa$ B was scored from 0 to 3: 0, no positive cells; 1+, <10% of positive cells; 2+, 11-50% of positive cells; 3+, 76-100% of positive cells.

was detected in normal thyroid follicular cells (Fig. 6A), while few nuclei from papillary carcinoma cells were positive for RelA. Follicular carcinoma cells showed ~50% of their nuclei stained for NF- $\kappa$ B, while anaplastic carcinoma cells showed almost 100%

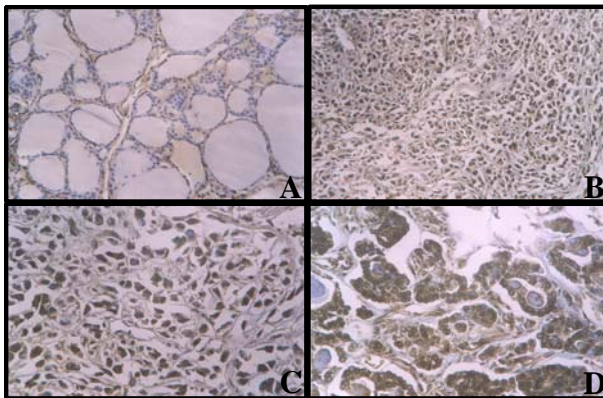


**Figure 6.** Immunohistochemical analysis of NF- $\kappa$ B activity in normal human thyroid and anaplastic human thyroid carcinomas. Localization of RelA (p65) in situ was determined by immunohistochemistry in sections from normal thyroid tissue (A) and 3 different anaplastic thyroid carcinomas (B, C, D).

feature of human anaplastic thyroid carcinomas, and suggest a role for NF- $\kappa$ B in human thyroid oncogenesis.

of their nuclei strongly positive for NF- $\kappa$ B (Fig. 6B, C, D and Tab. 1). Interestingly, the increased nuclear localization of NF- $\kappa$ B correlates with the increased malignant phenotype of thyroid carcinomas, suggesting that sustained activation of NF- $\kappa$ B confers an advantage for thyroid carcinoma progression.

These results indicate that the nuclear localization of p65 is a

## II – NF-κB transcriptional activity in human thyroid transformed cells

The high levels of basal NF-κB activity in human thyroid carcinomas prompted us to investigate the role of NF-κB in thyroid neoplastic transformation. To this aim, we used three different cell lines which resembled the features of thyroid tumors: WRO, FRO and NPA (see Materials and Methods). In these cells we analyzed, by EMSA, the nuclear localization of NF-κB. FRO cells showed the highest NF-κB DNA binding activity, while it was barely detectable in NPA cells (Fig. 7A). Then, to demonstrate that nuclear NF-κB was transcriptionally active, we performed reporter gene assays. Consistent with EMSA assays, FRO cells showed the highest NF-κB transcriptional activity, while NPA cells showed an almost undetectable activity (Fig. 7B).

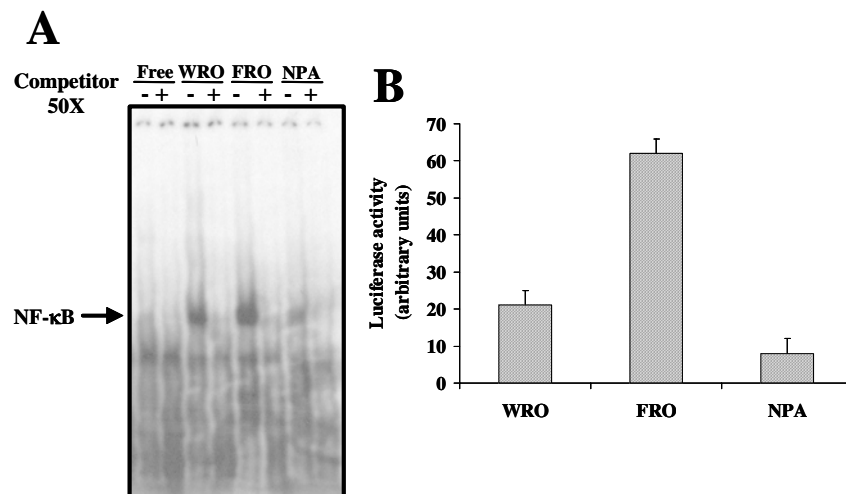


**Figure 7.** NF-κB activity in human thyroid carcinoma cell lines. **A)** EMSA on total cell extracts from human thyroid carcinoma cell lines WRO, FRO and NPA in the presence of a <sup>32</sup>P-labeled NF-κB oligonucleotide alone (*lanes -*) or with a 50-fold molar excess of an analogous unlabeled oligonucleotide (*lanes +*), as competitor. **B)** Relative reporter activity was evaluated in the same human thyroid carcinoma cell lines transfected with Ig-κB-luciferase plasmid. Values shown in arbitrary units represent the means  $\pm$  SD of three experiments done in triplicate, normalized for  $\beta$ -galactosidase expression of a co-transfected pRSV- $\beta$ gal plasmid.

Taken together, these data show that NF-κB is transcriptionally active in thyroid carcinoma cell lines, particularly in the human anaplastic thyroid cell line FRO.

## III – NF-κB activity is essential to confer resistance to drug-induced apoptosis in thyroid carcinoma cell lines

In order to determine a correlation between NF-κB activity and cell sensitivity to drug-induced apoptosis, we tested the ability of cisplatin and doxorubicin to promote cell death in WRO, FRO and NPA cells. As shown in Fig. 8A-B, both drugs induced cell death in all three cell lines, at an extent which correlated with the levels of basal NF-κB activity.

To causally link NF-κB activity to protection of neoplastic thyroid cells

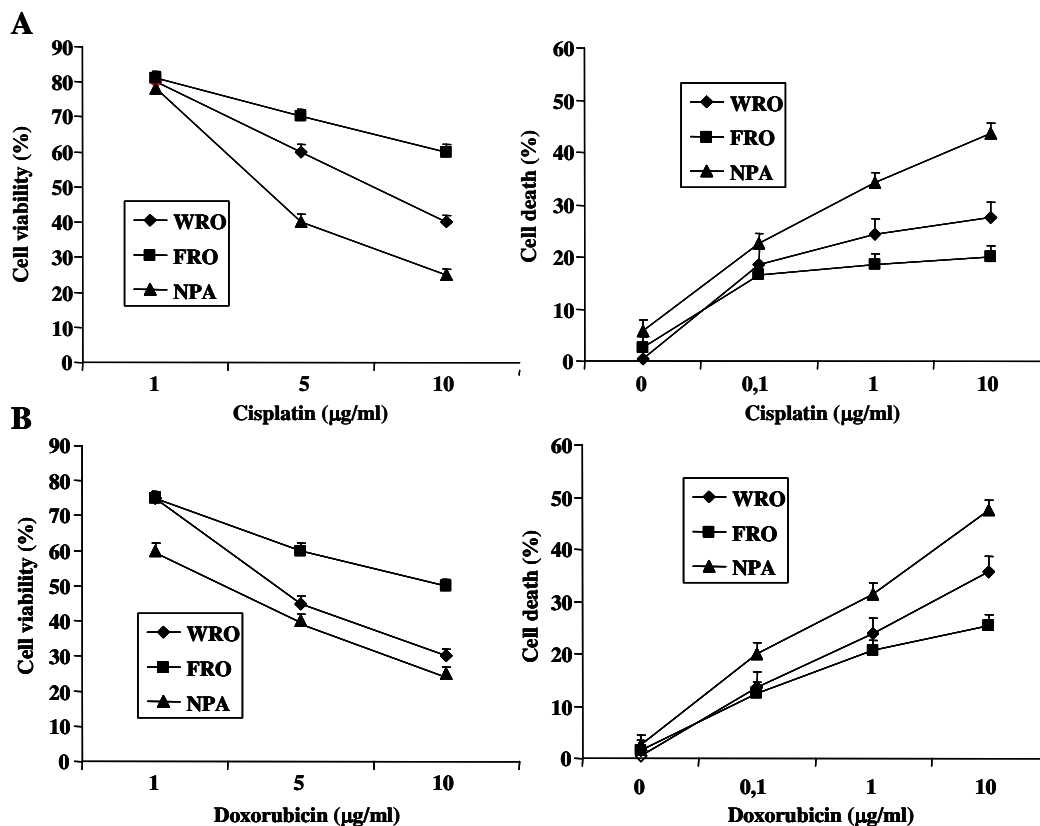


**Figure 8.** Cytotoxic effects of chemotherapeutic drugs on human thyroid carcinoma cell lines.  $1 \times 10^3$  cells/well were seeded in 96-well culture plates and incubated for 48 h with different concentrations of cisplatin (A) or doxorubicin (B). Cell survival was examined by MTS assay. Cell death was assessed by annexin V staining. Results were mean  $\pm$ SD of at least three separate experiments.

from apoptosis induced by chemotherapeutic drugs, we stably transfected NPA cells with an expression vector encoding IKK $\beta$ , to induce constitutive NF- $\kappa$ B activity, and FRO cells with a super-repressor form of I $\kappa$ B $\alpha$  (I $\kappa$ B $\alpha$ M), to suppress basal NF- $\kappa$ B activity. Two NPA clones, +7 and +18, as well as two FRO clones, +14 and +16, were analysed, because they expressed different levels of IKK $\beta$  or I $\kappa$ B $\alpha$ M and were differentially able to activate NF- $\kappa$ B (data not shown). Stably transfected cells were treated with increasing amounts of cisplatin or doxorubicin for 48 h, and cell survival and death were measured. While NPA-Neo clones were sensitive to cell death induced by chemotherapeutic drugs, NPA-IKK $\beta$  clones became resistant to apoptosis induced by either cisplatin or doxorubicin (Fig. 9A-B). On the other hand, FRO-Neo clones were resistant to drug-induced cell death, while FRO-I $\kappa$ B $\alpha$ M clones underwent apoptosis after treatment, even at low dosage, of either cisplatin or doxorubicin (Fig. 9C-D).

Since NF- $\kappa$ B controls cell proliferation, the inhibition of NF- $\kappa$ B activity in FRO cells could affect proliferation other than apoptosis. To test this hypothesis, we analyzed the proliferation rate of parental and transfected FRO cells by [ $^3$ H]-thymidine DNA incorporation and CFSE assay (data not shown). No significant differences in the rate of [ $^3$ H]-thymidine DNA incorporation

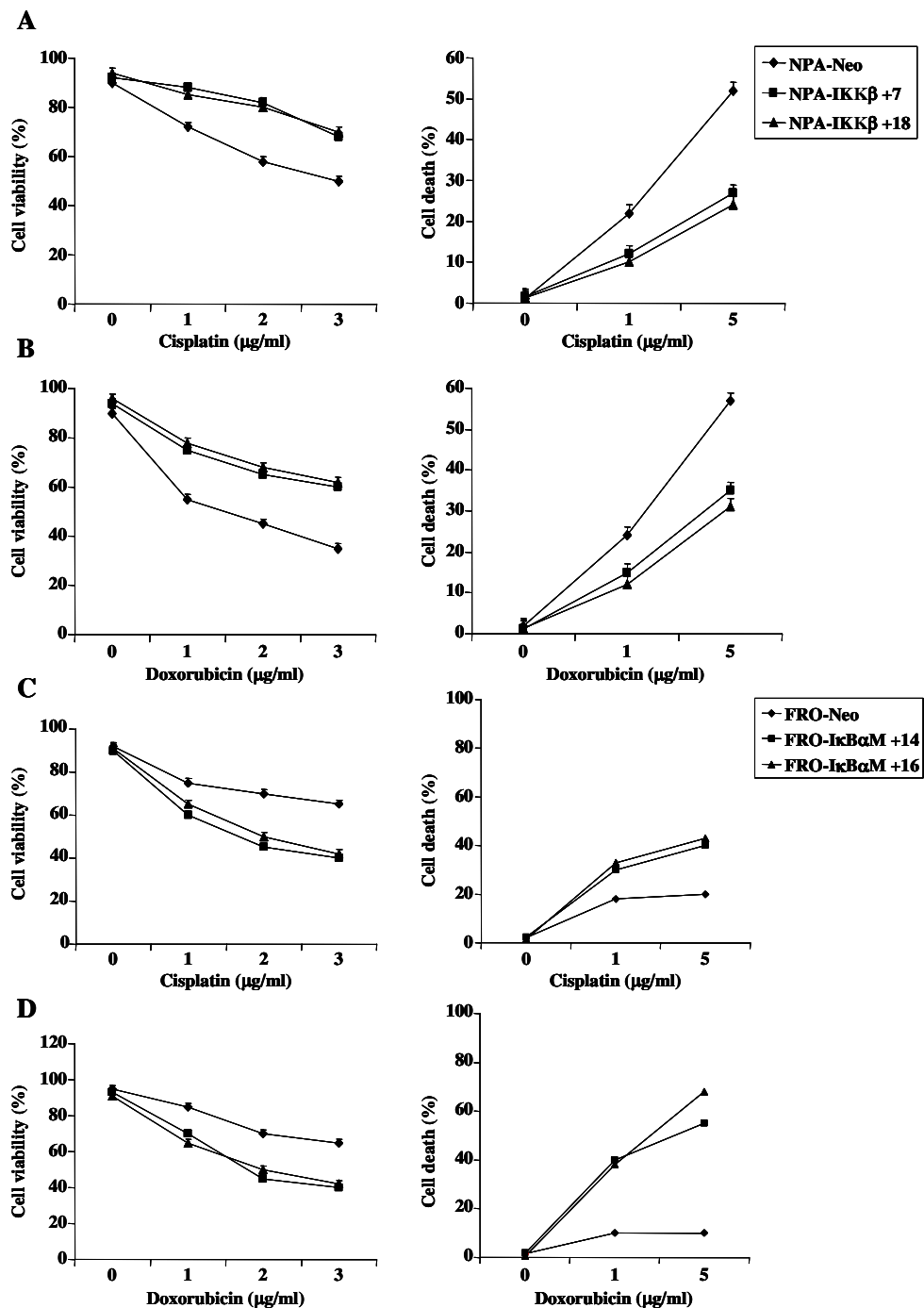


**Figure 9.** Cytotoxic effects of chemotherapeutic drugs on parental and transfected thyroid carcinoma cells.  $1 \times 10^3$  cells/well were seeded in 96-well culture plates and incubated for 48 h with different concentrations of cisplatin or doxorubicin. Cell survival was examined by MTS assay. Cell death was assessed by annexin V staining. A representative experiment out of three is shown. **A-B)** NPA-Neo and -IKK $\beta$  clones; **C-D)** FRO-Neo and -I $\kappa$ B $\alpha$ M clones.

were appreciable between FRO-Neo and -I $\kappa$ B $\alpha$ M clones, and a very similar doubling time was detected after 12 and 24 h of CFSE treatment, indicating that NF- $\kappa$ B activation is not required to control proliferation of FRO cells.

These results indicate that NF- $\kappa$ B activity confers resistance to drug-induced apoptosis in neoplastic thyroid cells.

#### IV – Inhibition of FRO transforming potential by NF-κB inactivation

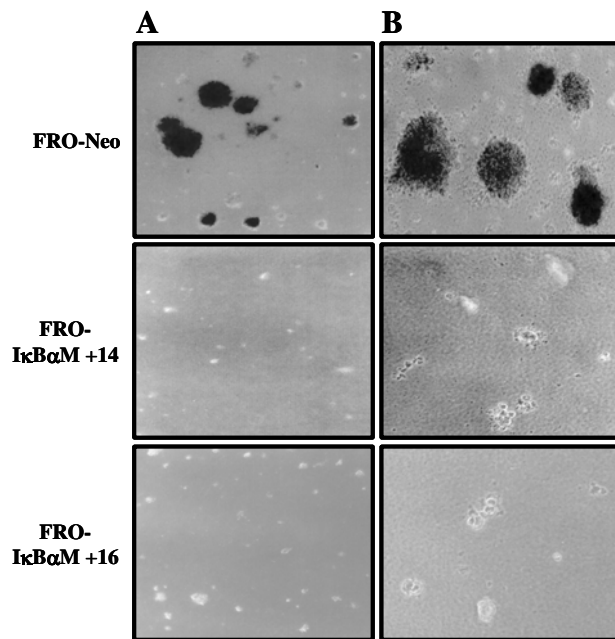


**Figure 10.** In vitro oncogenic potential of FRO-Neo and -IκBαM clones.  $1 \times 10^4$  cells were seeded in 60 mm dishes onto 0.3% Noble Agar on top of a 0.6% bottom layer. Colonies larger than 50 cells were scored after 2 weeks. FRO-Neo >50 colonies/plate; FRO-IκBαM +14 =0 colonies/plate; FRO IκBαM +16 <5 colonies/plate. A) 100 x magnification. B) 200 x magnification.

We next analyzed the *in vitro* and *in vivo* transforming potential of FRO-Neo and -IκBαM cells. The *in vitro* assay was performed by analyzing the ability of transformed cells to form colonies in soft agar. As shown in Fig. 10, while FRO-Neo gave rise to numerous and large colonies in soft agar (upper panels), -IκBαM +14 and +16 clones lost this property (middle and lower panels). These results were also confirmed by *in vivo* assays. Table 2 shows that injection in nude mice of FRO-Neo cells induced tumor formation in 6 out of 6 nude mice. Injection of FRO-IκBαM +14 and +16 cells induced tumor formation in 0 out of 6 and 2 out of 6 mice, respectively.

Cell type	Tumor incidence	Tumor volume average (cm <sup>3</sup> )	Tumor weight average (g)
<i>Parental cells</i>			
FRO Neo	6/6	1.48±0.4	0.146±0.04
<i>Transfected cells</i>			
FRO IκBαM +14	0/6	-	-
FRO IκBαM +16	2/6	0.27±0.06	0.029±0.002

**Table 2.** In vivo tumor growth induced by FRO-Neo and -IκBαM clones.  $2 \times 10^7$  cells were injected s.c. on a flank of each 6-week-old nude mouse. Thirty days later, mice were killed and tumors were excised. Tumor weight was determined and their diameters were measured with calipers. Tumor volumes were calculated by the formula:  $a^2 \times b \times 0.4$ , where  $a$  is the smallest diameter and  $b$  is the diameter perpendicular to  $a$ .

In addition, the two tumors developed from FRO-IκBαM +16 cells were about 5-fold smaller than those derived from injection of parental cells (Table 2).

Thus, inhibition of NF-κB activity led to a strong decrease of

FRO transforming potential.

#### V – The anti-apoptotic activity of NF-κB is mediated by down-regulation of JNK activity

It has been shown that NF-κB inhibits TNF-α-induced apoptosis by

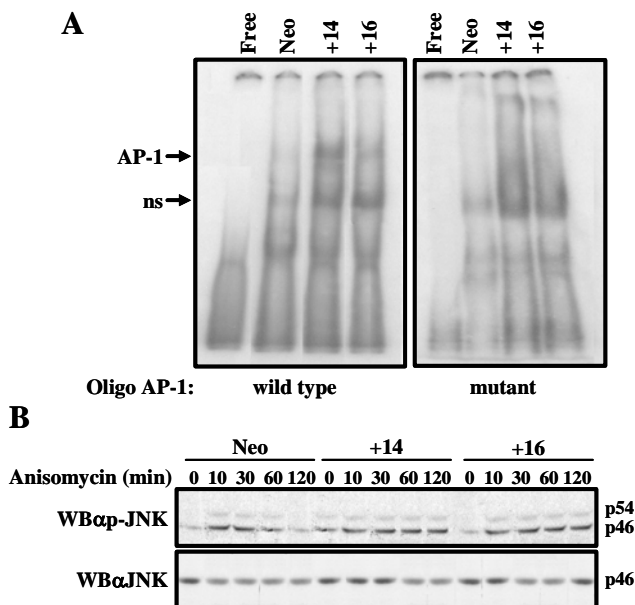


**Figure 11.** JNK activity in FRO-Neo and -IκBαM clones. **A**) EMSA on nuclear extracts from human thyroid carcinoma cell lines FRO-Neo, -IκBαM +14 and -IκBαM +16 in the presence of <sup>32</sup>P-labeled wild type (left panel) or mutant (right panel) AP-1 oligonucleotide. ns= nonspecific. **B**) 5x10<sup>5</sup> cells/well were seeded in six-well plates and incubated for different time with 10 μg/ml anisomycin. Cell lysates were analyzed by Western blot anti-p-JNK1/2 (upper panel) or total JNK1/2 (lower panel).

in FRO-Neo and -IκBαM clones, by analyzing its phosphorylation status following anisomycin stimulation (Fig. 11B, upper panel). Anisomycin induced JNK phosphorylation as early as 10 minutes of treatment in all cell lines. However, while p-JNK level in FRO-Neo cells decreased with time, it remained sustained in -IκBαM clones. Anisomycin treatment had no effect on total JNK levels, as assessed by Western blot analysis.

These data suggest that sensitivity of FRO-IκBαM clones to apoptosis induced by chemotherapeutic agents could be due to restoration of JNK activity. To investigate this hypothesis, we analyzed the apoptosis rate in FRO-Neo and -IκBαM +14 clones after treatment with cisplatin or doxorubicin in the presence of SP600125, a specific inhibitor of JNK activity (Bennett et al. 2001). Cell death was assessed by propidium iodide staining and was represented by the fraction of cells in sub-G1 phase (Fig. 12). The inhibition of JNK activity by SP600125 rendered FRO-IκBαM resistant to apoptosis induced by cisplatin (Fig. 12B) and doxorubicin (data not shown).

These results demonstrate that NF-κB inhibits chemotherapeutic drug-induced apoptosis in FRO cells by, at least partially, negatively regulating JNK signaling.

#### VI – ABIN-1 is an inhibitor of NF-κB and an interactor of NEMO/IKKγ

Our data together with many reports already present in literature (Aggarwal 2004) strongly support the idea that sustained activation of NF-κB is deeply involved in oncogenesis. Thus, we focused our efforts on the

repressing the JNK pathway (De Smaele et al. 2001, Pham et al. 2004, Tang et al. 2001). Therefore, we investigated if inhibition of NF-κB activity in FRO-IκBαM clones affects JNK activation. To this aim, we first analyzed transcriptional activity of AP-1, a target of JNK activity, by EMSA, on nuclear extracts from FRO-Neo and -IκBαM clones. As shown in Fig. 11A, AP-1 DNA binding activity, almost undetectable in FRO-Neo cells, was partially restored in FRO-IκBαM clones. Next, we investigated JNK activity

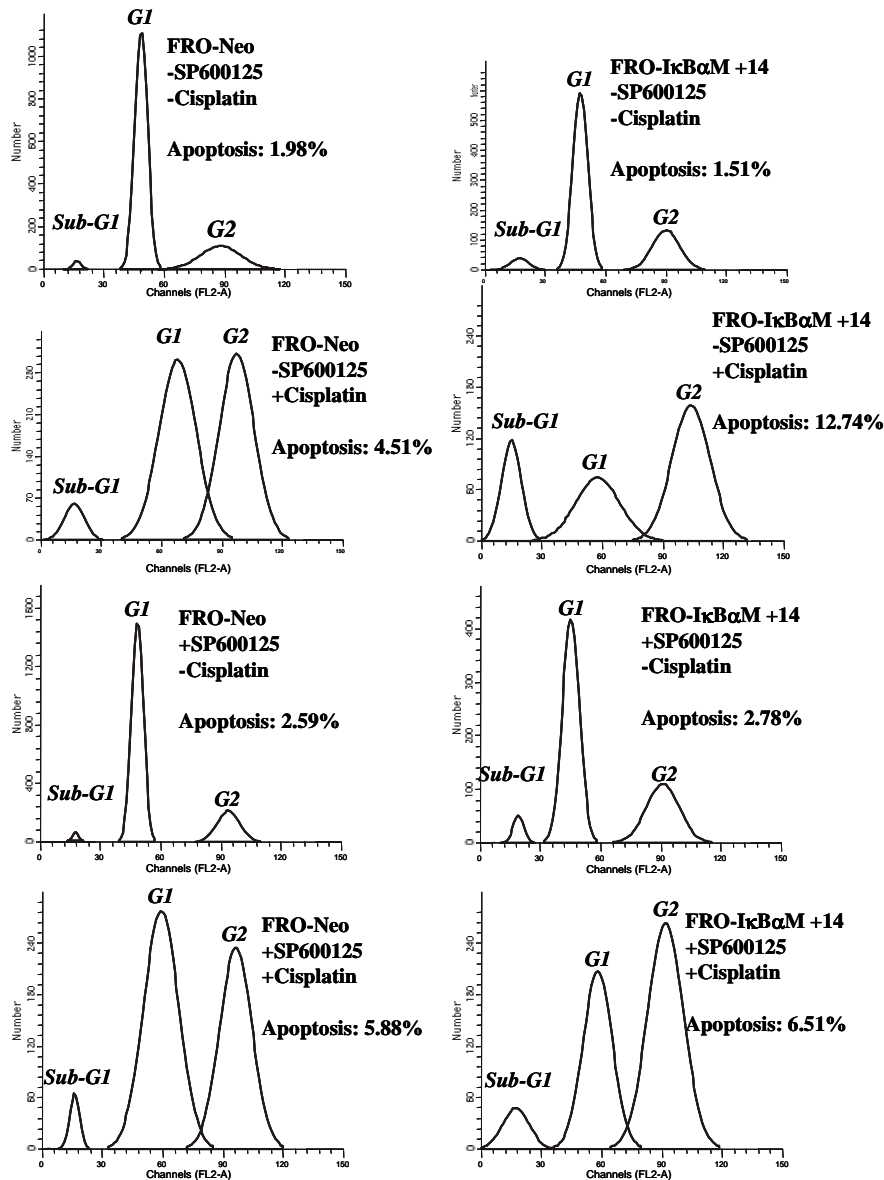


**Figure 12.** Inhibition of JNK activity restored cell death resistance in FRO-IκBαM clones.  $1 \times 10^5$  cells/well were seeded in six-well culture plates and incubated for 48 h with 5  $\mu\text{g/ml}$  cisplatin, in the presence of 10  $\mu\text{M}$  JNK inhibitor SP600125. Cell death was assessed by propidium iodide staining. A representative experiment out of two done in triplicate is shown.

identification of molecular mechanisms involved in switching off NF- $\kappa$ B activity. In the last few years, our group has largely used biochemical and genetic approaches to isolate critical interactors of the IKK-complex, the kinase complex controlling NF- $\kappa$ B activation (Leonardi et al. 2000a, Chariot et al. 2000, Mauro et al. 2003, Stilo et al. 2004). Thus, we have access to a collection of promising candidate genes in regulating NF- $\kappa$ B signal transduction. Following a careful analysis, we decided to study ABIN-1 to gain an understanding into the basis for its inhibition of NF- $\kappa$ B. In fact, ABIN-1

(A20 binding inhibitor of NF- $\kappa$ B) was identified as an interactor of A20, able to mimic the NF- $\kappa$ B inhibiting effects of A20 (Heyninck et al. 1999). We identified ABIN-1 in a yeast two-hybrid screening of a human liver c-DNA library, as an interactor of NEMO/IKK $\gamma$ , the regulatory subunit of the IKK-

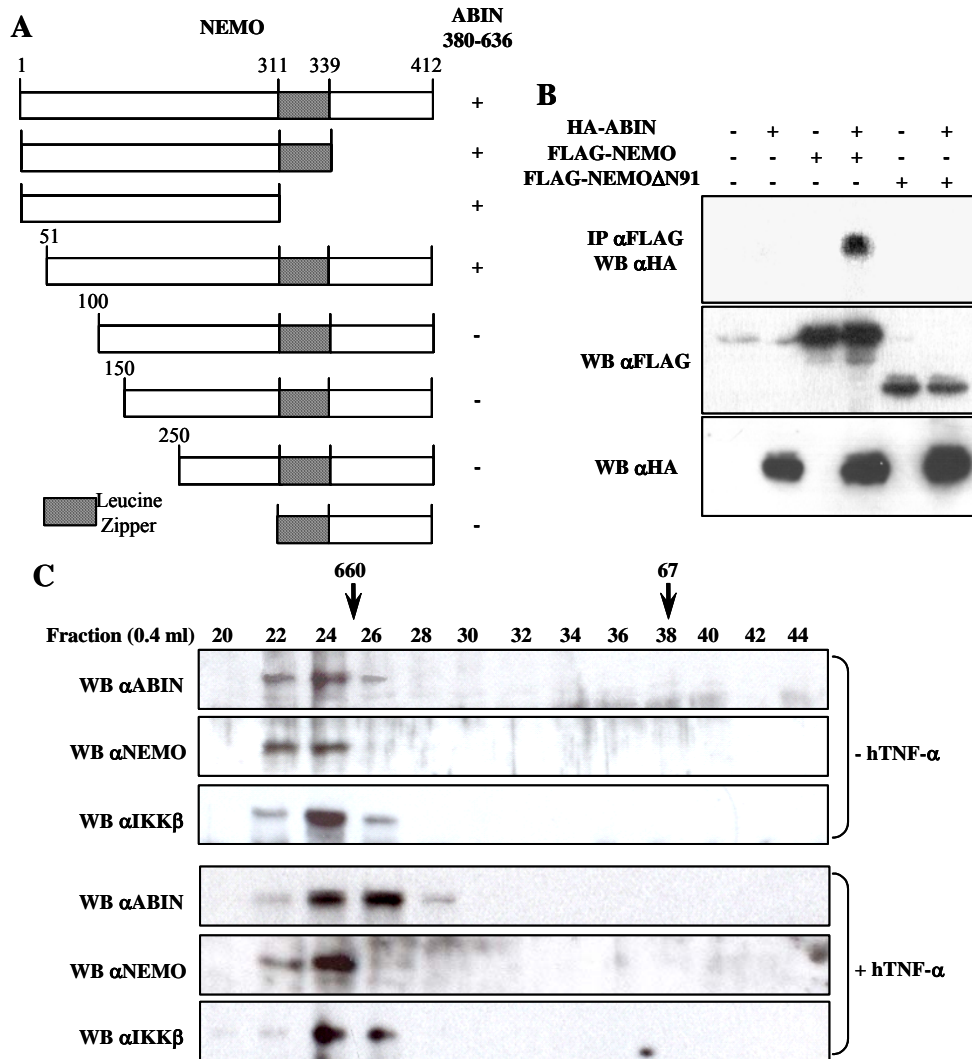


**Figure 13.** Mapping of the ABIN-1 interaction domain on NEMO/IKK $\gamma$ . **A)** Mapping of the NEMO-ABIN interaction by yeast-two hybrid experiments. **B)** In vivo mapping of the NEMO-ABIN interaction. HEK293 cells were transfected with the indicated combinations of expression constructs encoding HA-ABIN and either FLAG-NEMO or FLAG-NEMO $\Delta$ N91. Cell extracts were analyzed by immuno-blotting either directly or after immuno-precipitation with anti-FLAG antibodies. **C)** Chromatographic distribution of endogenous ABIN-1, NEMO and IKK $\beta$ . Cytoplasmic extracts were prepared from HEK293 treated with TNF for 120 min or left unstimulated, and subjected to chromatography on a Superdex S-200 column. Fractions were analyzed by Western blot by using the indicated antibodies. Molecular weight markers are indicated at the top of the figure.

complex.

To define the region of NEMO/IKK $\gamma$  required for its interaction with ABIN-1, we tested various deletion mutants of NEMO/IKK $\gamma$  for binding to ABIN-1 fragment (AA 380-636) in yeast. Data shown in Fig. 13A indicate that

the region between amino acids 50 and 100 of NEMO/IKK $\gamma$  is required for interaction with ABIN-1. The binding was confirmed in mammalian cells (Fig. 13B). HA-ABIN-1 was transiently co-expressed in HEK293 cells together with FLAG-NEMO/IKK $\gamma$  or a NEMO/IKK $\gamma$  mutant lacking the first 91 amino acids (FLAG-NEMO $\Delta$ N91). Immunoprecipitates of FLAG-NEMO/IKK $\gamma$  contained HA-ABIN-1 only if both proteins were co-expressed. In agreement with data obtained in yeast, ABIN-1 did not co-immunoprecipitate with NEMO $\Delta$ N91. We were unable to detect the association between endogenous NEMO/IKK $\gamma$  and ABIN-1, probably because of the transient nature of the association and/or the high stringent conditions we used to perform co-immunoprecipitation experiments. However, gel filtration experiments showed that endogenous ABIN-1 was eluted from the column in the same fractions containing endogenous NEMO/IKK $\gamma$  and other components of IKK-complex (Fig 13C).

#### VII – Mapping of the NEMO/IKK $\gamma$ and the A20 binding domains on ABIN-1

To define the domain of ABIN-1 required for its interaction with NEMO/IKK $\gamma$ , we performed pull-down assays by using recombinant GST-NEMO/IKK $\gamma$  and *in vitro* translated [<sup>35</sup>S]ABIN-1 (Fig. 14A). ABIN-1 bound to GST-NEMO/IKK $\gamma$ , indicating a direct interaction between the two proteins. Furthermore, amino acids 500-588 of ABIN-1 represent the minimal region that binds to NEMO/IKK $\gamma$  (Fig. 14A, upper panel). To confirm that the region between amino acids 500 and 588 of ABIN-1 was responsible for the interaction with NEMO/IKK $\gamma$ , we generated an internal deletion mutant of ABIN-1 ( $\Delta$ 500-588) and evaluated its ability to interact with NEMO/IKK $\gamma$ . As

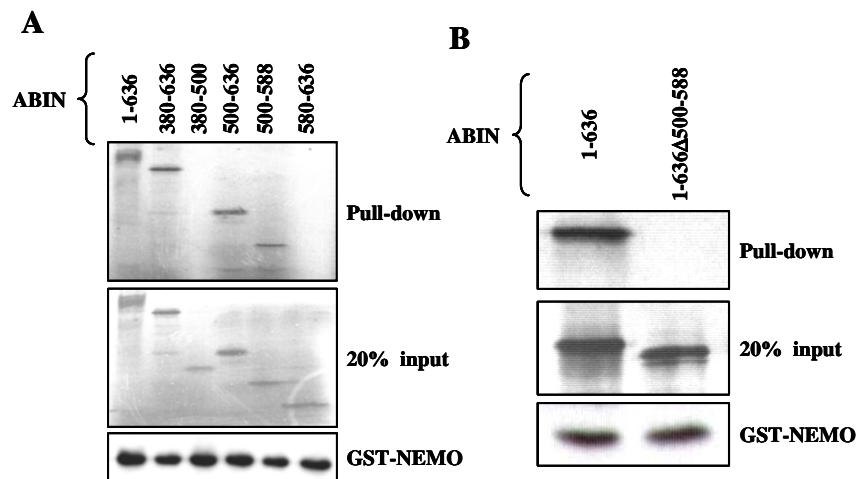


**Figure 14.** Mapping of the NEMO/IKK $\gamma$  and the A20 binding domains on ABIN-1. **A, B)** GST pull-down assays: GST-NEMO was incubated with *in vitro* translated full-length (FL) or deletion mutants of ABIN. Aliquots of *in vitro* translated constructs and GST-NEMO stained by Coomassie Blue are shown.

expected, the internal deletion of 89 amino acids from ABIN-1 abolished the interaction with NEMO/IKK $\gamma$  (Fig. 14B).

Because ABIN-1 was identified as an A20-interacting protein (Heyninck et al. 2003), we also confirmed that the region between amino acids 407-431 of ABIN-1 is responsible for interaction with A20 (data not shown).

*VIII – ABIN-1 and A20 inhibit NF- $\kappa$ B at level of the IKK-complex by associating with NEMO/IKK $\gamma$*

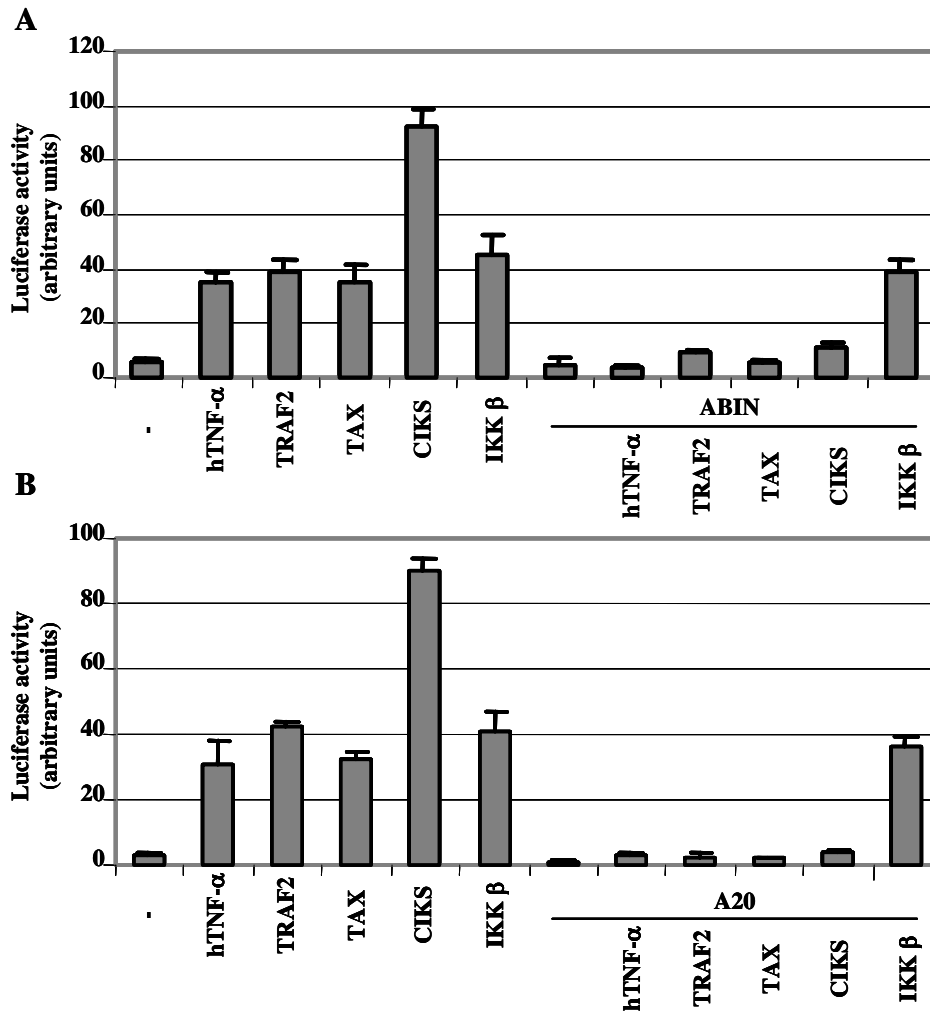


**Figure 15.** *ABIN-1 and A20 are inhibitors of NF- $\kappa$ B.* **A, B)** ABIN-1 and A20 inhibit NF- $\kappa$ B at level of the IKK-complex. Relative reporter activity was evaluated in HEK293 cells co-transfected with Ig- $\kappa$ B-luciferase plasmid and the indicated expression vectors. 24 h after transfection cells were stimulated with TNF for 3 h or left untreated, as indicated. Values shown in arbitrary units represent the means  $\pm$  SD of three experiments done in triplicate, normalized for  $\beta$ -galactosidase expression of a co-transfected pRSV- $\beta$ gal plasmid.

Both ABIN-1 and A20 are inhibitors of NF- $\kappa$ B. It has been proposed that they interfere with a RIP and TRAF2-mediated trans-activating signal (Heyninck et al. 1999). The identification of the interaction between ABIN-1 and NEMO/IKK $\gamma$  prompted us to investigate if ABIN-1 was involved in controlling NF- $\kappa$ B activation not only upstream but also at the level of the IKK-complex. To this aim, we performed reporter assays by transfecting

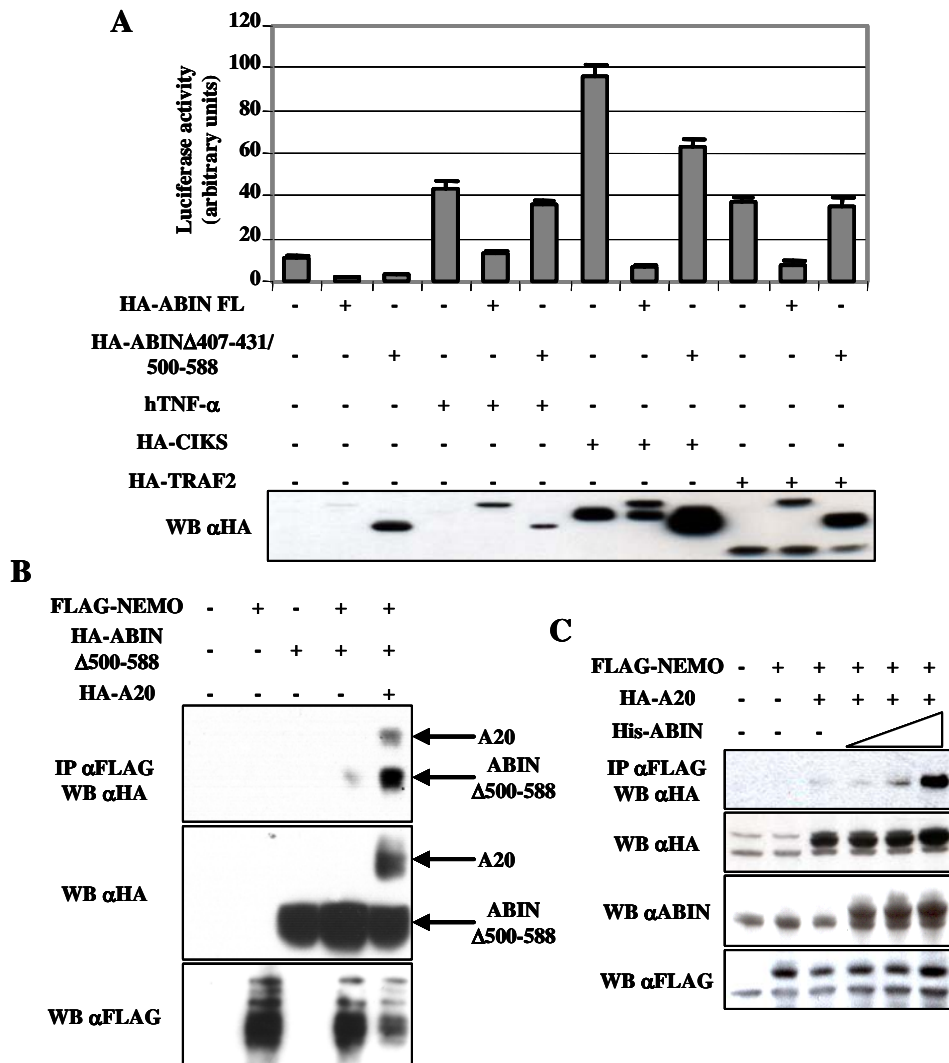


**Figure 16.** *ABIN-1* interacts with *NEMO/IKK $\gamma$*  and *A20* to inhibit *NF- $\kappa$ B* activity. **A**) The deletion mutant of *ABIN-1* lacking both *NEMO*- and *A20*-binding domains (*ABIN* $\Delta$ 407-431/ $\Delta$ 500-588) does not block *NF- $\kappa$ B* activation. HEK293 cells were co-transfected with *Ig- $\kappa$ B*-luciferase reporter plasmid and the indicated combinations of expression plasmids. 24 h after transfection cells were stimulated with *TNF* for 3 h or left untreated, as indicated. Analysis was done as in Fig. 15. Lower panel show the relative expression levels of transfected proteins. **B**) *ABIN-1* forms a complex with *NEMO* and *A20*. HEK293 cells were transfected with constructs encoding *NEMO*, *A20* and a deletion mutant of *ABIN* lacking the *NEMO* binding domain (*ABIN* $\Delta$ 500-588). Cell extracts were immunoprecipitated with anti-FLAG antibodies (*NEMO*) and Western blotted anti-HA to reveal the co-precipitation of *A20* and *ABIN*. The presence of -HA and -FLAG proteins in total extracts is shown. **C**) *ABIN-1* promotes association of *A20* with *NEMO*. HEK293 cells were transiently transfected with constructs encoding FLAG-*NEMO*, HA-*A20* and increasing amount of His-*ABIN*. Cell extracts were immunoprecipitated with anti-FLAG antibodies (*NEMO*) and Western blotted anti-HA to reveal the co-precipitation of *A20*. The presence of *ABIN*, *NEMO* and *A20* in the whole cell lysate is shown.

HEK293 cells with *Ig- $\kappa$ B*-luciferase plasmid in the presence of *ABIN-1* and various activators of *NF- $\kappa$ B*. *ABIN-1* efficiently inhibited *TNF- $\alpha$* - and *TRAF2*-dependent activation of *NF- $\kappa$ B* (Fig 15A). It also blocked *NF- $\kappa$ B*

activation induced by proteins acting at level of the IKK-complex, such as CIKS and TAX (Chu et al. 1999, Harhaj and Sun 1999, Jin et al. 1999, Leonardi et al. 2000a). In contrast, ABIN-1 was not able to inhibit the IKK $\beta$ -mediated activation of NF- $\kappa$ B (Fig. 15A). Similarly, A20 inhibits NF- $\kappa$ B activation mediated by TNF- $\alpha$  or ectopic expression of TRAF2, CIKS and TAX but not IKK $\beta$  (Fig. 15B). These results indicate that both ABIN-1 and A20 interfere with activation of NF- $\kappa$ B at level of the IKK-complex, suggesting that the association of ABIN-1 with NEMO/IKK $\gamma$  plays an important role in the inhibition of NF- $\kappa$ B.

Because ABIN-1 interacts with both NEMO/IKK $\gamma$  and A20, we tested whether the NEMO/IKK $\gamma$ - and A20-binding domains of ABIN-1 were required for inhibition of NF- $\kappa$ B. ABIN-1 deletion mutants lacking either the NEMO/IKK $\gamma$  binding domain (ABIN $\Delta$ 500-588) or the A20 binding domain (ABIN $\Delta$ 407-431) were still able to inhibit the activity of a NF- $\kappa$ B-driven luciferase reporter following different stimuli (data not shown). In contrast, a mutant of ABIN-1 in which both the NEMO/IKK $\gamma$ - and the A20-binding domains were deleted (ABIN $\Delta$ 407-431/ $\Delta$ 500-588) lost the ability to block activation of NF- $\kappa$ B (Fig. 16A). These data were consistent with the hypothesis that ABIN-1 forms a complex with both NEMO/IKK $\gamma$  and A20. To address this hypothesis, we immunoprecipitated FLAG-NEMO/IKK $\gamma$  and monitored the co-precipitation of the ABIN-1 mutant lacking the NEMO/IKK $\gamma$  binding domain (HA-ABIN $\Delta$ 500-588) either in the presence or absence of A20 (Fig. 16B). ABIN $\Delta$ 500-588 co-immunoprecipitated with NEMO/IKK $\gamma$  only in the presence of A20. To further support the idea that ABIN-1 promotes association of A20 with NEMO/IKK $\gamma$ , we transfected A20 and NEMO/IKK $\gamma$  in the presence of increasing amount of overexpressed ABIN-1. As expected, the amount of A20 co-immunoprecipitating with NEMO/IKK $\gamma$  increased in the presence of ABIN-1 (Fig. 16C). Taken together, these data indicated that ABIN-1 interferes with activation of NF- $\kappa$ B at level of the IKK-complex, and support the idea that ABIN-1 promotes association of A20 with NEMO/IKK $\gamma$ .

#### *IX – A20 inhibits NF- $\kappa$ B by de-ubiquitinating NEMO/IKK $\gamma$*

To explore the mechanism by which the interactions of both A20 and ABIN-1 with NEMO/IKK $\gamma$  down-regulate the NF- $\kappa$ B signaling, we assessed the effect of either A20 or ABIN-1 on NEMO/IKK $\gamma$  ubiquitination. Transfection of FLAG-NEMO/IKK $\gamma$  in the presence of HA-Ubiquitin resulted in the poly-ubiquitination of NEMO/IKK $\gamma$  (Fig. 17A, lane 3). Co-transfection of A20 and NEMO/IKK $\gamma$  resulted in a dose-dependent disappearance of the ubiquitinated forms of NEMO/IKK $\gamma$  (Fig. 17A, lanes 4 and 5). In contrast, co-transfection of ABIN-1 did not affect NEMO/IKK $\gamma$  ubiquitination (Fig. 17A, lanes 6 and 7). We did not observe reduction in the overall level of ubiquitinated cellular proteins in the presence of A20, indicating that A20 does not have a global de-ubiquitinating activity. Importantly, A20 also blocks I $\kappa$ B $\alpha$

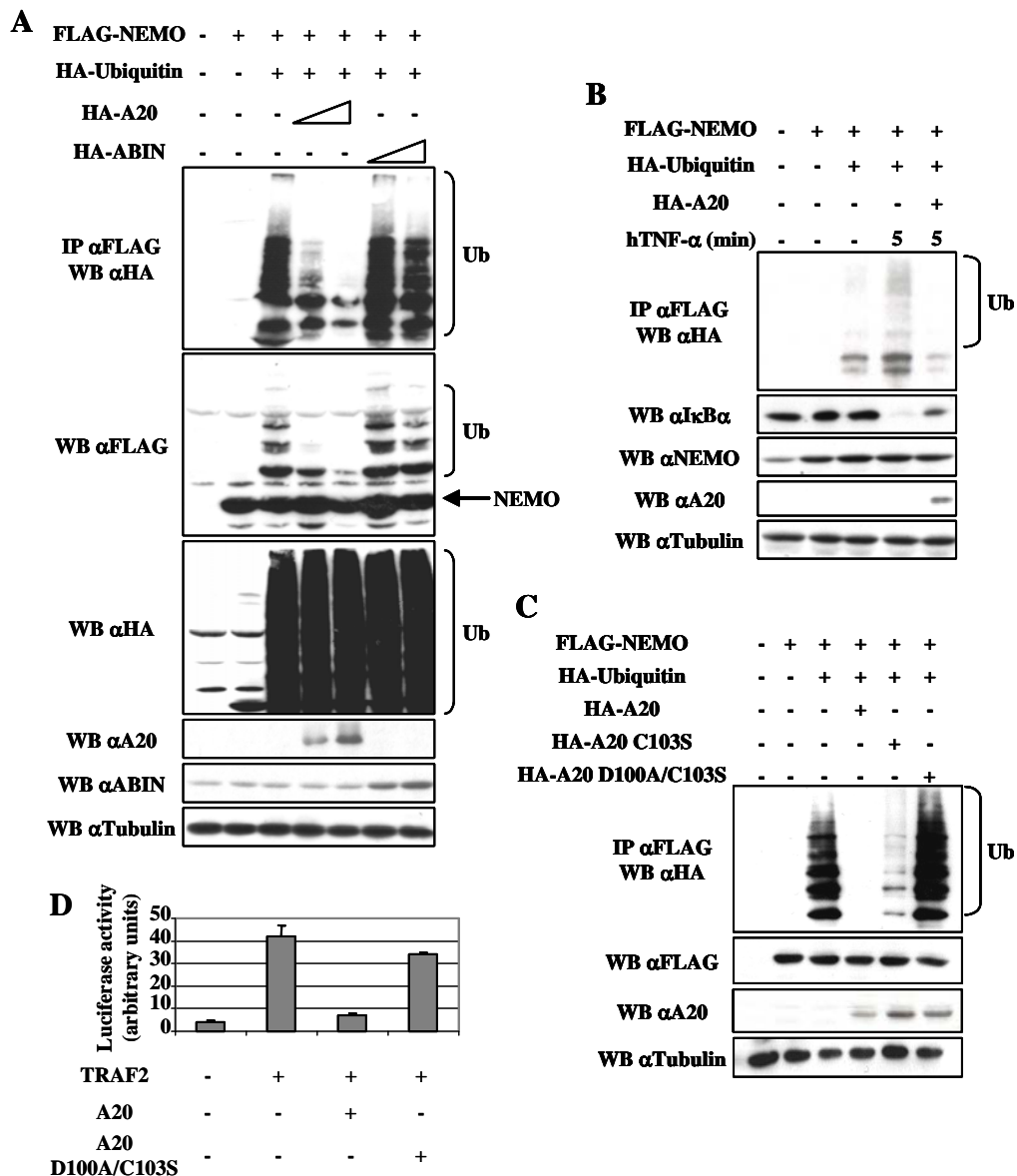


**Figure 17.** *A20* inhibits  $NF-\kappa B$  by de-ubiquitinating  $NEMO/IKK\gamma$ . **A)** *A20* but not *ABIN-1* de-ubiquitinates  $NEMO$ . HEK293 cells were transfected with FLAG- $NEMO$  and HA-Ubiquitin, plus increasing amounts of either HA-*A20* or HA-*ABIN*. Cell extracts were immunoprecipitated with anti-FLAG antibodies ( $NEMO$ ) followed by Western blot anti-HA. Western blot analyses against FLAG, HA, *A20*, *ABIN*, and Tubulin were performed on total extracts. **B)** *A20* blocks the ubiquitination of  $NEMO$  and the degradation of  $I\kappa B\alpha$  induced by TNF. HEK293 cells were transfected with FLAG- $NEMO$ , HA-Ubiquitin and HA-*A20*. 24 h after transfection cells were stimulated with TNF for 5 min or left untreated, as indicated. Cell extracts were immunoprecipitated with anti-FLAG antibodies ( $NEMO$ ) and Western blotted anti-HA. Western blots anti- $NEMO$ ,  $I\kappa B\alpha$ , *A20*, and *Tubulin* are shown. **C)** A catalytically inactive form of *A20* (D100A/C103S) does not de-ubiquitinate  $NEMO$ . Conditions were similar to those in **A**, except for the plasmids encoding HA-*A20* C103S, or D100A/C103S. **D)** *A20* D100A/C103S does not inhibit  $NF-\kappa B$  activation dependent on TRAF2 in contrast to wild type *A20*. Reporter assay was performed as above.

degradation and  $NEMO/IKK\gamma$  ubiquitination induced by TNF- $\alpha$  (Fig. 17B). To demonstrate that the de-ubiquitinating activity of *A20* was required for the

observed reduction in NEMO/IKK $\gamma$  ubiquitination, we generated two mutants in the OTU domain of A20, which is the domain responsible for the de-ubiquitinating activity of A20 (Evans et al. 2003). We replaced the cysteine residue of the DXXC motif with serine (C103S), or both the aspartic acid and the cysteine residues (D100A/C103S) with alanine and serine. The mutation C103S affected the ability of A20 to de-ubiquitinate NEMO/IKK $\gamma$  compared to wild type A20, whereas the double mutant D100A/C103S resulted in the complete loss of the de-ubiquitinating activity of A20 on NEMO/IKK $\gamma$  (Fig. 17C). As expected, the D100A/C103S mutant was not able to block the NF- $\kappa$ B activity induced by different stimuli, such as TRAF2 (Fig. 17D and data not shown).

These findings strongly suggest that NEMO/IKK $\gamma$  is a target for the de-ubiquitinating activity of A20 and confirmed that the ubiquitination of NEMO/IKK $\gamma$  is a crucial step in the mechanisms of NF- $\kappa$ B activation.

#### *X – ABIN-1 mediates the de-ubiquitinating activity of A20 on NEMO/IKK $\gamma$*

Next, we explored whether ABIN-1 was involved in the A20-dependent de-ubiquitination of NEMO/IKK $\gamma$ . To this purpose, we transfected HEK293 cells with sub-optimal amount of A20 and increasing amount of ABIN-1 and checked for NEMO/IKK $\gamma$  ubiquitination. We found that ABIN-1 increases the ability of A20 to de-ubiquitinate NEMO/IKK $\gamma$  (Fig. 18A). To demonstrate a role for ABIN-1 in the A20-mediated de-ubiquitination of NEMO/IKK $\gamma$ , we generated small interfering RNA constructs (siRNAs) targeting ABIN-1 (ABIN-i-370 and i-560; data not shown). Then, we evaluated whether RNA-interference of ABIN-1 impairs the de-ubiquitinating activity of A20 on NEMO/IKK $\gamma$ . We co-transfected HEK293 cells with FLAG-NEMO/IKK $\gamma$  and HA-Ubiquitin and we assessed the de-ubiquitinating activity of A20 alone or in the presence of either i-370 or i-560 constructs. The A20-dependent de-ubiquitination of NEMO/IKK $\gamma$  decreased only in the presence of i-370 construct (Fig. 18B). The i-370 construct led to a two fold increase of both basal and induced (TRAF2 and CIKS) NF- $\kappa$ B activity compared to the empty vector or the i-560 construct, that we used as controls (Fig. 18C). Accordingly with the data showed in Fig. 15A, interference of ABIN-1 did not influence the activation of NF- $\kappa$ B dependent on transfected IKK $\beta$ . Also in this case, the NF- $\kappa$ B activity correlated with the levels of NEMO/IKK $\gamma$  ubiquitination. In fact, transfected i-370 increased the ubiquitination of NEMO/IKK $\gamma$  respect to both empty vector and i-560 (data not shown). From these experiments, we concluded that reduced levels of ABIN-1 affect the ability of A20 to de-ubiquitinate NEMO/IKK $\gamma$  and, consequently the A20-mediated inhibition of NF- $\kappa$ B. To further support the functional interplay between ABIN-1 and A20, we knocked-down A20 (Saitoh et al. 2005) and evaluated the ability of ABIN-1 to interfere with NF- $\kappa$ B activation. As shown in Fig. 18D, ABIN-1 requires A20 to efficiently block NF- $\kappa$ B activation induced by TNF and TRAF2.

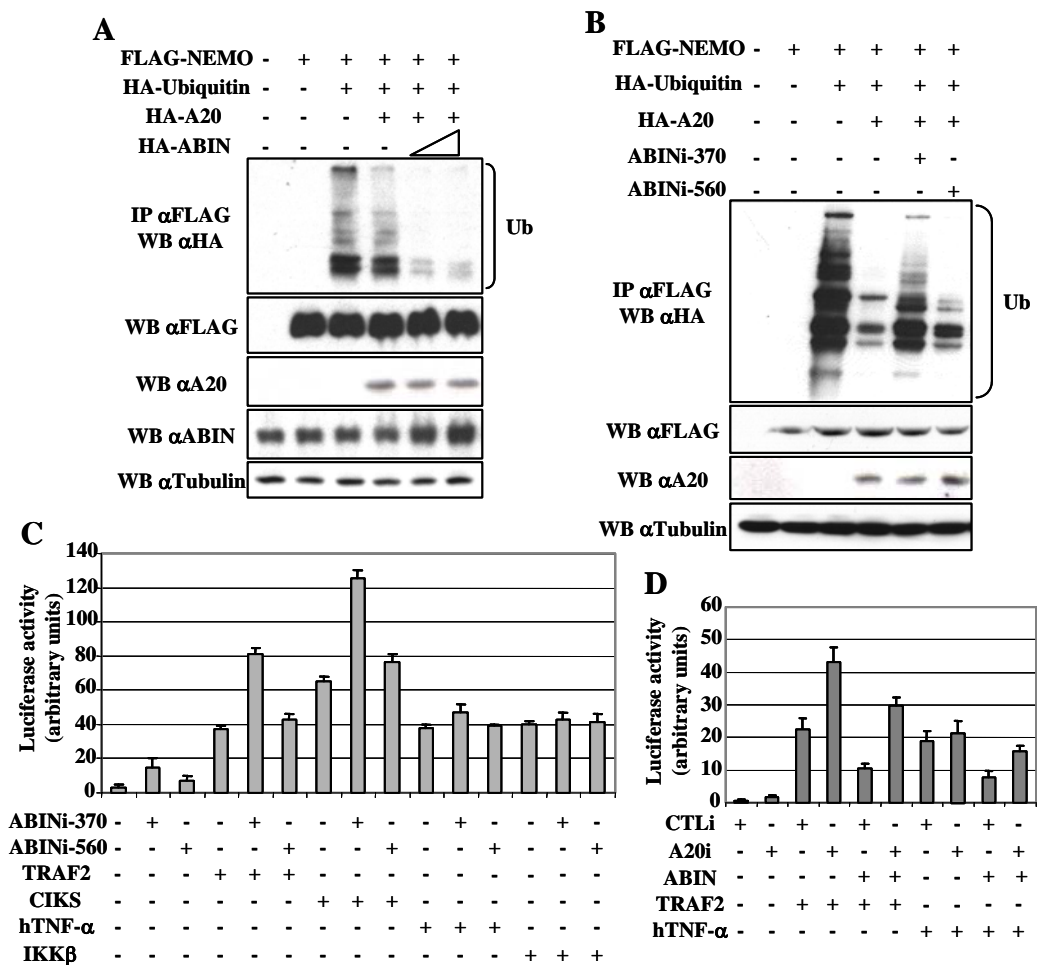


**Figure 18.** *ABIN-1* participates to the A20-dependent de-ubiquitination of NEMO/IKK $\gamma$ . **A**) *ABIN-1* increases the effects of A20 on NEMO ubiquitination. HEK293 cells were transfected with FLAG-NEMO, HA-Ubiquitin, sub-optimal amount of HA-A20 and increasing amount of HA-ABIN. Cell extracts were immunoprecipitated with anti-FLAG antibodies (NEMO) and Western blotted anti-HA. Western blots anti-FLAG, -A20, -ABIN and -Tubulin are shown. **B**) *ABIN-1* siRNAs impairs the A20-dependent de-ubiquitination of NEMO. HEK293 cells were co-transfected with FLAG-NEMO, HA-Ubiquitin and -A20, plus either ABINi-370 or -560. Cell extracts were immunoprecipitated with anti-FLAG antibodies and Western blotted anti-HA. Western blots anti-FLAG, -A20 and -Tubulin were performed on total extracts. **C**) *ABIN-1* siRNAs increase NF- $\kappa$ B activation by TRAF2 and CIKS. HEK293 cells were co-transfected with TRAF2, CIKS, or IKK $\beta$ , plus Ig- $\kappa$ B-luciferase reporter and either ABINi-370 or -570. 24 hours after transfection cells were stimulated with TNF for 3 h or left untreated. Analysis of reporter activity was done as above. **D**) RNA-interference of A20 impairs the *ABIN-1*-mediated inhibition of NF- $\kappa$ B. Relative reporter activity was evaluated in HEK293 cells co-transfected with Ig- $\kappa$ B-luciferase reporter, TRAF2 and either A20i or CTLi plasmids. 24 h after transfection cells were stimulated with TNF for 3 h or left untreated, as indicated. Analysis of reporter activity was done as above.

Taken together, these results support a model whereby *ABIN-1* and A20 co-operate in inhibiting NF- $\kappa$ B activation, by inducing de-ubiquitination of NEMO/IKK $\gamma$  (Fig. 19). In conclusion, blocking the inflammatory processes dependent on NF- $\kappa$ B activation, A20 and *ABIN-1* represent candidate targets for developing innovative anti-cancer therapies.

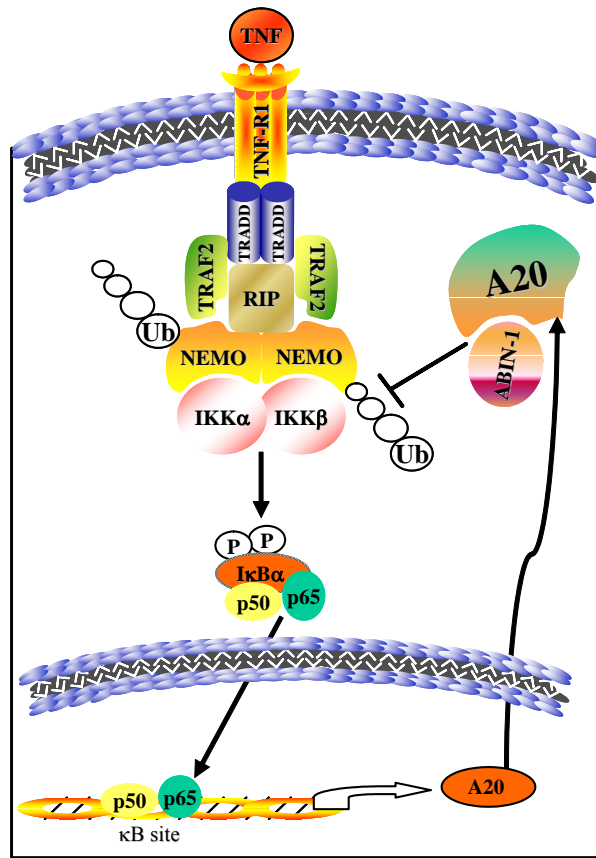


**Figure 19.** The model of ABIN-1/A20-mediated inhibition of NF- $\kappa$ B.

## Conclusions

NF- $\kappa$ B is a master regulator of cell survival and its anti-apoptotic activity plays a key role in oncogenesis. However, very little was known on the oncogenic potential of NF- $\kappa$ B in thyroid.

In the present study, we have shown that the activity of NF- $\kappa$ B is constitutively elevated in primary human thyroid carcinomas and correlates with malignant phenotype. In particular, anaplastic thyroid carcinoma cells display almost 100% of their nuclei positively stained for NF- $\kappa$ B. Activated NF- $\kappa$ B is also detected in an *in vitro* model of human thyroid cancer which resembles the *in vivo* differentiated and undifferentiated thyroid tumors. In these cell lines we have demonstrated that persistent NF- $\kappa$ B activity is progressively increasing from papillary thyroid carcinoma cells (NPA) to follicular carcinoma cells (WRO) until to reach the highest levels in anaplastic carcinoma cells (FRO), suggesting that sustained activation of NF- $\kappa$ B confers an advantage for malignant thyroid oncogenesis.

NF- $\kappa$ B inhibition in FRO cells strongly enhances their sensitivity to undergo drug-induced apoptosis, and causes a dramatic decrease of their transforming potential. These *in vitro* functions of NF- $\kappa$ B are consistent with its role in tumor growth *in vivo*. In fact, FRO-I $\kappa$ B $\alpha$ M cells fail to form tumor in nude mice. The increased susceptibility to apoptosis of FRO-I $\kappa$ B $\alpha$ M and the evidence that constitutive activation of the NF- $\kappa$ B pathway renders NPA cells resistant to drug-induced apoptosis extend the idea that protection from apoptosis represents the major mechanism through which NF- $\kappa$ B enhances neoplastic transformation.

Our data also suggest that the anti-apoptotic function of NF- $\kappa$ B is mediated by the inhibition of JNK signaling. We have shown that JNK activity is restored in FRO-I $\kappa$ B $\alpha$ M cells, where its duration is sustained after treatment with anisomycin. In addition, incubation of FRO-I $\kappa$ B $\alpha$ M cells with the specific JNK inhibitor SP600125 restores their resistance to chemotherapeutic drug-induced apoptosis.

Taken together, these data clearly substantiate the fundamental role of sustained activation of NF- $\kappa$ B in thyroid oncogenesis and open new perspectives for diagnosis and therapy of anaplastic thyroid carcinoma.

To come through our idea to identify molecular targets of NF- $\kappa$ B potentially druggable against cancer, we have focused our efforts on studying mechanisms to switch off NF- $\kappa$ B activation. We have identified a previously not reported association between ABIN-1 and NEMO/IKK $\gamma$ , the regulatory sub-unit of the IKK-complex. Further, we have provided evidence that ABIN-1 targets A20 on NEMO/IKK $\gamma$ . This trimeric association interferes with NEMO/IKK $\gamma$  ubiquitination, thus resulting in down-regulation of NF- $\kappa$ B activation.

## **Acknowledgements**

I dedicate my PhD thesis to the memory of my father. His thought has alleviated all my efforts to achieve these results.

Thanks to my family (my wife Valeria, mum, Enrico, Pierluigi, Marinella and Gabriele) for the help and the love daily received.

Thanks to all the members of the Formisano's Lab. They gave me teaching in sciences and daily life. After seven years passed together, they represent my second family.

Thanks to Dr Francesco Pacifico and Dr. Pasquale Vito for the daily hints received to develop my PhD project.

Thanks to Dr. Guido Franzoso for giving me the opportunity to continue my scientific career as a post-doc in his laboratory at the Ben May Institute for Cancer Research, the University of Chicago.

Thanks to Dr. Antonio Leonardi, my scientific supervisor, who spent a lot of time with me, giving me the great opportunity to learn, work and publish in sciences.

Thanks to Professor Silvestro Formisano, who allowed me to join his group in October 1999 and from then grow up as a scientist and as a man.

Thanks to Professor Giancarlo Vecchio, who coordinated at best the PhD program in Molecular Oncology and Endocrinology.

This work was supported by Associazione Italiana Ricerca sul Cancro (AIRC) and MIUR-PRIN 2005051307.

## References

- Aggarwal BB. Nuclear factor- $\kappa$ B: the enemy within. *Cancer Cell* 2004; 6:203–8.
- Amiri KI, Richmond A. Role of nuclear factor- $\kappa$ B in melanoma. *Cancer Metastasis Rev.* 2005; 24:301–13.
- Ball DW, Baylin SB, de Bustros AC. *The thyroid*. Werner and Ingbars 7th edn, Philadelphia: Lippincott-Raven; 1996.
- Bendall HH, Sikes ML, Ballard DW, Oltz EM. An intact NF-kappa B signaling pathway is required for maintenance of mature B cell subsets. *Mol. Immunol.* 1999; 36:187–95.
- Bennett BL, Sasaki DT, Murray BW, O'Leary EC, Sakata ST, Xu W, Leisten JC, Motiwala A, Pierce S, Satoh Y, Bhagwat SS, Manning AM, Anderson DW. SP600125, an anthrapyrazolone inhibitor of Jun N-terminal kinase. *Proc. Natl. Acad. Sci. USA* 2001; 98:13681–6.
- Biswas DK, Cruz AP, Gansberger E, Pardee AB. Epidermal growth factor-induced nuclear factor kappa B activation: a major pathway of cell-cycle progression in estrogen-receptor negative breast cancer cells. *Proc. Natl. Acad. Sci. USA* 2000; 97:8542–7.
- Boise LH, Gonzalez-Garcia M, Postema CE, Ding L, Lindsten T, Turka LA et al. Bcl-x, a bcl-2-related gene that functions as a dominant regulator of apoptotic cell death. *Cell* 1993; 74:597–608.
- Bonizzi G, Karin M. The two NF- $\kappa$ B activation pathways and their role in innate and adaptive immunity. *Trends Immunol.* 2004; 25:280–8.
- Boone DL, Turer EE, Lee EG, Ahmad RC, Wheeler MT, Tsui C, Hurley P, Chien M, Chai S, Hitotsumatsu O, McNally E, Pickart C, Ma A. The ubiquitin-modifying enzyme A20 is required for termination of Toll-like receptor responses. *Nat. Immunol.* 2004; 5:1052–60.
- Chang L, Karin M. Mammalian MAP kinase signaling cascades. *Nature* 2001; 410: 37–40.
- Chariot A, Leonardi A, Muller J, Bonif M, Brown K, Siebenlist U. Association of the adaptor TANK with the I kappa B kinase (IKK) regulator NEMO connects IKK complexes with IKK epsilon and TBK1 kinases. *J. Biol. Chem.* 2002; 277:37029–36.
- Chariot A, Princen F, Gielen J, Merville MP, Franzoso G, Brown K, Siebenlist U, Bours V. IkappaB-alpha enhances transactivation by the HOXB7 homeodomain-containing protein. *J. Biol. Chem.* 1999; 274:5318–25.
- Chen ZJ. Ubiquitin signaling in the NF- $\kappa$ B pathway. *Nat. Cell Biol.* 2005; 7:758–65.
- Chu ZL, Shin YA, Yang JM, Di Donato JA., Ballard DW. IKKgamma mediates the interaction of cellular IkappaB kinases with the tax transforming protein of human T cell leukemia virus type 1. *J. Biol. Chem.* 1999; 274:15297–300.
- Davis RJ. Signal transduction by the JNK group of MAP kinases. *Cell* 2000; 103: 239–52.

- Deng Y, Ren X, Yang L, Lin Y, Wu X. A JNK-dependent pathway is required for TNF $\alpha$ -induced apoptosis. *Cell* 2003; 115:61–70.
- De Smaele E, Zazzeroni F, Papa S, Nguyen DU, Jin R, Jones J, Cong R, Franzoso G. Induction of gadd45beta by NF-kappaB downregulates pro-apoptotic JNK signaling. *Nature* 2001; 414:308–13.
- Deveraux QL, Roy N, Stennicke HR, Van Arsdale T, Zhou Q, Srinivasula SM et al. IAPs block apoptotic events induced by caspase-8 and cytochrome c by direct inhibition of distinct caspases. *EMBO J.* 1998; 17:2215–23.
- Estour B, Van Herle AJ, Juillard GJ, Totanes TL, Sparkes RS, Giuliano AE, Klandorf H. Characterization of a human follicular thyroid carcinoma cell line (UCLA RO 82 W-1). *Virchows Arch. B. Cell. Pathol. Incl. Mol. Pathol.* 1989; 57:167–74.
- Evans PC, Smith TS, Lai MJ, Williams MG, Burke DF, Heyninck K, Kreike MM, Beyaert R, Blundell TL, Kilshaw PJ. A novel type of deubiquitinating enzyme. *J. Biol. Chem.* 2003; 278:23180–6.
- Fagin JA, Matsuo K, Karmakar A, Chen DL, Tang SH, Koeffler HP. High prevalence of mutations of the p53 gene in poorly differentiated human thyroid carcinomas. *J. Clin. Invest.* 1993; 91:179–84.
- Farina AR, Tacconelli A, Vacca A, Maroder M, Gulino A, Mackay AR. Transcriptional up-regulation of matrix metalloproteinase-9 expression during spontaneous epithelial to neuroblast phenotype conversion by SK-N-SH neuroblastoma cells, involved in enhanced invasivity, depends upon GT-box and nuclear factor kappaB elements. *Cell Growth Differ.* 1999; 10:353–67.
- Figge J. *Thyroid cancer: a comprehensive guide to clinical management*, Wartofsky L. edn., Totowa: Humana Pres. 1999.
- Ghosh S, Karin M. Missing pieces in the NF- $\kappa$ B puzzle. *Cell* 2002; 109 Suppl:S81–S96.
- Gimm O. Thyroid cancer. *Cancer Lett.* 2001; 163:143–56.
- Greten FR, Eckmann L, Greten FT et al. IKK $\beta$  links inflammation and tumorigenesis in a mouse model of colitis-associated cancer. *Cell* 2004; 118:285–96.
- Greten FR, Karin M. The IKK/NF-kappaB activation pathway-a target for prevention and treatment of cancer. *Cancer Lett.* 2004; 206:193–9.
- Guttridge DC, Albanese C, Reuther JY, Pestell RG, Baldwin AS Jr. NF-kappaB controls cell growth and differentiation through transcriptional regulation of cyclin D1. *Mol. Cell. Biol.* 1999; 19:5785–99.
- Hanahan D, Weinberg RA. The hallmarks of cancer. *Cell* 2000; 100:57–70.
- Harhaj EW, Sun SC. IKKgamma serves as a docking subunit of the IkappaB kinase (IKK) and mediates interaction of IKK with the human T-cell leukemia virus Tax protein. *J. Biol. Chem.* 1999; 274:22911–4.
- Hayden MS, Ghosh S. Signaling to NF- $\kappa$ B. *Genes Dev.* 2004; 18:2195–24.
- Helbig G, Christopherson KW 2nd, Bhat-Nakshatri P, Kumar S, Kishimoto H, Miller KD et al. NF-kappaB promotes breast cancer cell migration and

- metastasis by inducing the expression of the chemokine receptor CXCR4. *J. Biol. Chem.* 2003; 278:21631–8.
- Heyninck K, De Valck D, Vanden Berghe W, Van Criekinge W, Contreras R, Fierz W, Haegeman G, Beyaert R. The zinc finger protein A20 inhibits TNF-induced NF-kappaB-dependent gene expression by interfering with an RIP- or TRAF2-mediated transactivation signal and directly binds to a novel NF-kappaB-inhibiting protein ABIN. *J. Cell Biol.* 1999; 145:1471–8.
- Heyninck K, Kreike MM, Beyaert R. Structure-function analysis of the A20-binding inhibitor of NF-kappa B activation, ABIN-1. *FEBS Lett.* 2003; 536:135–40.
- Hicke L, Schubert HL, Hill CP. Ubiquitin-binding domains. *Nat. Rev. Mol. Cell. Biol.* 2005; 6:610–21.
- Hsu H, Shu HB, Pan MG, Goeddel DV. TRADD-TRAF2 and TRADD-FADD interactions define two distinct TNF receptor 1 signal transduction pathways. *Cell* 1996; 84:299–308.
- Jamieson C, McCaffrey PG, Rao A, Sen R. Physiologic activation of T cells via the T cell receptor induces NF-kappa B. *J. Immunol.* 1991; 147:416–20.
- Javelaud D, Besancon F. NF- $\kappa$ B activation results in rapid inactivation of JNK in TNF-treated Ewing sarcoma cells: a mechanism for the anti-apoptotic effect of NF- $\kappa$ B. *Oncogene* 2001; 20:4365–72.
- Jin DY, Giordano V, Kibler KV, Nakano H, Jeang KT. Role of adapter function in oncoprotein-mediated activation of NF-kappaB. Human T-cell leukemia virus type I Tax interacts directly with IkappaB kinase gamma. *J. Biol. Chem.* 1999; 274:17402–5.
- Johnson GL, Lapadat R. Mitogen-activated protein kinase pathways mediated by ERK, JNK, and p38 protein kinases. *Science* 2002; 298: 1911–2.
- Kalaitzidis D, Gilmore TD. Transcription factor cross-talk: the estrogen receptor and NF- $\kappa$ B. *Trends Endocrinol. Metab.* 2005; 16:46–52.
- Karin M, Ben-Neriah Y. Phosphorylation meets ubiquitination: the control of NF- $\kappa$ B activity. *Annu. Rev. Immunol.* 2000; 18:621–63.
- Karin M, Cao Y, Greten FR et al. NF- $\kappa$ B in cancer: from innocent bystander to major culprit. *Nature Rev. Cancer* 2002; 2:301–10.
- Kim DW, Gazourian L, Quadri SA, Romieu-Mourez R, Sherr DH, Sonenshein GE. The RelA NF-kappaB subunit and the aryl hydrocarbon receptor (AhR) cooperate to transactivate the c-myc promoter in mammary cells. *Oncogene* 2000; 19:5498–506.
- Kiriakidis S, Andreacos E, Monaco C, Foxwell B, Feldmann M, Paleolog E. VEGF expression in human macrophages is NF-kappaB-dependent: studies using adenoviruses expressing the endogenous NF-kappaB inhibitor IkappaBalpha and a kinase-defective form of the IkappaB kinase 2. *J. Cell. Sci.* 2003; 116:665–74.
- Kojima M, Morisaki T, Sasaki N, Nakano K, Mibu R, Tanaka M et al. Increased nuclear factor- $\kappa$ B activation in human colorectal carcinoma and its correlation with tumor progression. *Anticancer Res.* 2004; 24:675–81.

- Kovalenko A, Chable-Bessia C, Cantarella G, Israel A, Wallach D, Courtois G. The tumor suppressor CYLD negatively regulates NF- $\kappa$ B signaling by deubiquitination. *Nature* 2003; 424:801–5.
- Kucharczak J, Simmons MJ, Fan Y, Gelinas C. To be, or not to be: NF- $\kappa$ B is the answer - role of Rel/NF- $\kappa$ B in the regulation of apoptosis. *Oncogene*. 2003; 22:8961–82.
- Kunsch C, Rosen CA. NF-kappa B subunit-specific regulation of the interleukin-8 promoter. *Mol. Cell. Biol.* 1993; 13:6137–46.
- Lee EG, Boone DL, Chai S, Libby SL, Chien M, Lodolce GP, Ma A. Failure to regulate TNF-induced NF- $\kappa$ B and cell death responses in A20-deficient mice. *Science* 2000; 289:2350–4.
- Leonardi A, Chariot A, Claudio E, Cunningham K, Siebenlist U. CIKS, a connection to Ikappa B kinase and stress-activated protein kinase. *Proc. Natl. Acad. Sci. USA* 2000a; 97:10494–9.
- Leonardi A, Ellinger-Ziegelbauer H, Franzoso G, Brown K, Siebenlist U. Physical and functional interaction of filamin (actin-binding protein-280) and tumor necrosis factor receptor-associated factor 2. *J. Biol. Chem.* 2000b; 275:271–8.
- Li Q, Verma IM. NF-kappaB regulation in the immune system. *Nat. Rev. Immunol.* 2002; 2:725–34.
- Liu Y-C, Penninger J, Karin M. Immunity by ubiquitylation: a reversible process of modification. *Nature* 2005; 5:941–52.
- Ludwig L, Kessler H, Wagner M, Hoang-Vu C, Dralle H, Adler G, Böhm BO Schmid RM. Nuclear factor-kappaB is constitutively active in C-cell carcinoma and required for RET-induced transformation. *Cancer Res.* 2001; 61:4526–35.
- Lyons AB. Divided we stand: tracking cell proliferation with carboxyfluorescein diacetate succinimidyl ester. *Immunol. Cell. Biol.* 1999; 77:516–8.
- Mabuchi S, Ohmichi M, Nishio Y, Hayasaka T, Kimura A, Ohta T et al. Inhibition of NF- $\kappa$ B increases the efficacy of cisplatin in *in vitro* and *in vivo* ovarian cancer models. *J. Biol. Chem.* 2004; 279:23477–85.
- Macpherson I, Montagnier I. Agar suspension culture for the selective assay of cells transformed by polyoma virus. *Virology* 1964; 23:291–4.
- Mauro C, Vito P, Mellone S, Pacifico F, Chariot A, Formisano S, Leonardi A. Role of the adaptor protein CIKS in the activation of the IKK complex. *Biochem. Biophys. Res. Commun.* 2003; 309:84–90.
- McIver B, Hay ID, Giuffrida DF, Dvorak CE, Grant CS, Thompson GB, van Heerden JA, Goellner JR. Anaplastic thyroid carcinoma: a 50-year experience at a single institution. *Surgery* 2001; 130:1028–34.
- Nasr R, El-Sabban ME, Karam JA, Dbaiho G, Kfoury Y, Arnulf B et al. Efficacy and mechanism of action of the proteasome inhibitor PS-341 in T-cell lymphomas and HTLV-I associated adult T-cell leukemia/lymphoma. *Oncogene* 2005; 24:419–30.

- Naumann M. Nuclear factor-kappa B activation and innate immune response in microbial pathogen infection. *Biochem. Pharmacol.* 2000; 60:1109–14.
- Nicoletti I, Migliorati G, Pagliacci MC, Grignani F, Riccardi C. A rapid and simple method for measuring thymocyte apoptosis by propidium iodide staining and flow cytometry. *J. Immunol. Methods* 1991; 139:271–9.
- Novak U, Cocks BG, Hamilton JA. A labile repressor acts through the NF- $\kappa$ B-like binding sites of the human urokinase gene. *Nucleic Acids Res.* 1991; 19:3389–93.
- Pacifico F, Leonardi A. NF-kappaB in solid tumors. *Biochem. Pharmacol.* 2006; 72:1142–52.
- Pahl HL. Activators and target genes of Rel/NF- $\kappa$ B transcription factors. *Oncogene* 1999; 18:6853–66.
- Perkins ND, Felzien LK, Betts JC, Leung K, Beach DH, Nabel GJ. Regulation of NF-kappaB by cyclin-dependent kinases associated with the p300 coactivator. *Science* 1997; 275:523–7.
- Pham CG, Bubici C, Zazzeroni F, Papa S, Jones J, Alvarez K et al. Ferritin heavy chain upregulation by NF-kappaB inhibits TNFalpha-induced apoptosis by suppressing reactive oxygen species. *Cell* 2004; 119:529–42.
- Pikarsky E, Porat RM, Stein I et al. NF- $\kappa$ B functions as a tumor promoter in inflammation-associated cancer. *Nature* 2004; 431:461–66.
- Richardson PG, Hideshima T, Mitsiades C, Anderson K. Proteasome inhibition in hematologic malignancies. *Ann. Med.* 2004; 36:304–14.
- Saitoh T, Yamamoto M, Miyagishi M, Taira K, Nakanishi M, Fujita T, Akira S, Yamamoto N, Yamaoka S. A20 is a negative regulator of IFN regulatory factor 3 signaling. *J. Immunol.* 2005; 174:1507–12.
- Sclabas GM, Uwagawa T, Schmidt C, Hess KR, Evans DB, Abbruzzese JL et al. Nuclear factor- $\kappa$ B activation is a potential target for preventing pancreatic carcinoma by aspirin. *Cancer* 2005; 103:2485–90.
- Sherman SI. Thyroid carcinoma. *The Lancet* 2003; 361:501–11.
- Stilo R, Liguoro D, Di Jeso B, Formisano S, Consiglio E, Leonardi A, Vito P. Physical and functional interaction of CARMA1 and CARMA3 with Ikappa kinase gamma-NFkappaB essential modulator. *J. Biol. Chem.* 2004; 279:34323–31.
- Sun L, Deng L, Ea CK, Xia ZP, Chen ZJ. The TRAF6 ubiquitin ligase and TAK1 kinase mediate IKK activation by Bcl10 and MALT1 in T lymphocytes. *Mol. Cell* 2004; 14:289–301.
- Sweeney C, Li L, Shanmugam R, Bhat-Nakshatri P, Jayaprakasan V, Baldrige LA et al. Nuclear factor- $\kappa$ B is constitutively activated in prostate cancer *in vitro* and is overexpressed in prostatic intraepithelial neoplasia and adenocarcinoma of the prostate. *Clin. Cancer Res.* 2004; 10:5501–7.
- Tang ED, Wang CY, Xiong Y, Guan KL. J. A role for NF-kappaB essential modifier/IkappaB kinase-gamma (NEMO/IKKgamma) ubiquitination in the activation of the IkappaB kinase complex by tumor necrosis factor-alpha. *Biol. Chem.* 2003; 278:37297–305.
- Tang G, Minemoto Y, Dibling B, Purcell NH, Li Z, Karin M, Lin A. Inhibition

- of JNK activation through NF-kappaB target genes. *Nature* 2001; 414:313–7.
- Tennvall J, Lundell G, Hallquist A, Wahlberg P, Wallin G, Tibblin S. Combined doxorubicin, hyperfractionated radiotherapy, and surgery in anaplastic thyroid carcinoma. Report on two protocols. The Swedish Anaplastic Thyroid Cancer Group. *Cancer* 1994; 74:1348–54.
- Tournier C, Hess P, Yang DD, Xu J, Turner TK, Nimnual A, Bar-Sagi D, Jones SN, Flavell RA, Davis RJ. Requirement of JNK for stress-induced activation of the Cytochrome *c*-mediated death pathway. *Science* 2000; 288:870–4.
- Van de Stolpe A, Caldenhoven E, Stade BG, Koenderman L, Raaijmakers JA, Johnson JP et al. 12-O-tetradecanoylphorbol-13-acetate- and tumor necrosis factor alpha-mediated induction of intercellular adhesion molecule-1 is inhibited by dexamethasone. Functional analysis of the human intercellular adhesion molecular-1 promoter. *J. Biol. Chem.* 1994; 269:6185–92.
- Visconti R, Cerutti J, Battista S, Fedele M, Trapasso F, Zeki K et al. Expression of the neoplastic phenotype by human thyroid carcinoma cell lines requires NF-κB p65 protein expression. *Oncogene* 1997; 15:1987–94.
- Wang CY, Guttridge DC, Mayo MW, Baldwin AS Jr. NF-kappaB induces expression of the Bcl-2 homologue A1/Bfl-1 to preferentially suppress chemotherapy-induced apoptosis. *Mol. Cell. Biol.* 1999; 19:5923–9.
- Wang CY, Mayo MW, Korneluk RG, Goeddel DV, Baldwin AS Jr. NF-kappaB antiapoptosis: induction of TRAF1 and TRAF2 and c-IAP1 and c-IAP2 to suppress caspase-8 activation. *Science* 1998; 281:1680–3.
- Wertz IE, O'Rourke KM, Zhou H, Eby M, Aravind L, Seshgiri S, Wu P, Wlesmann C, Baker R, Boone DL, Ma A, Koonin EV, Dixit VM. Deubiquitination and ubiquitin ligase domains of A20 downregulate NF-κB signaling. *Nature* 2004; 430:694–99.
- Yeh WC, Itie A, Elia AJ, Ng M, Shu HB, Wakeham A et al. Requirement for Casper (c-FLIP) in regulation of death receptor-induced apoptosis and embryonic development. *Immunity* 2000; 12:633–42.
- Zhou H., Wertz IE, O'Rourke KM, Ultsch M, Seshgiri S, Eby M, Xiao W, Dixit VM. Bcl10 activates the NF-κB pathway through ubiquitination of NEMO. *Nature* 2004; 427:167–71.

## **Appendix: Original papers**

# Endoplasmic Reticulum Stress Causes Thyroglobulin Retention in this Organelle and Triggers Activation of Nuclear Factor- $\kappa$ B Via Tumor Necrosis Factor Receptor-Associated Factor 2

ANTONIO LEONARDI, PASQUALE VITO, CLAUDIO MAURO, FRANCESCO PACIFICO, LUCA ULIANICH, EDUARDO CONSIGLIO, SILVESTRO FORMISANO, AND BRUNO DI JESO

*Dipartimento di Biologia e Patologia Cellulare e Molecolare (A.L., C.M., L.U., S.F.), BioGem Consortium (P.V.), Centro di Endocrinologia e Oncologia Sperimentale (F.P., E.C.), Federico II, University of Naples, 80100 Naples, Italy; and Laboratorio di Patologia Generale, Dipartimento di Scienze e Tecnologie Biologiche ed Ambientali, University of Lecce (B.D.J.), 73100 Lecce, Italy*

Perturbing the endoplasmic reticulum homeostasis of thyroid cell lines with thapsigargin, a specific inhibitor of the sarcoplasmic reticulum  $\text{Ca}^{2+}$  adenosine triphosphatases, and tunicamycin, an inhibitor of the N-linked glycosylation, blocked Tg in the endoplasmic reticulum. This event was signaled outside the endoplasmic reticulum and resulted in activation of the c-Jun N-terminal kinase (JNK)/stress-activated protein kinase and nuclear factor- $\kappa$ B (NF- $\kappa$ B) stress response pathways. Activation of the JNK/stress-activated protein kinase signaling pathway was assessed by measuring the amount of phospho-JNK and the activity of JNK by kinase assays. Activation of the NF- $\kappa$ B signaling pathway was assessed by measuring the level of inhibitory subunit I $\kappa$ B $\alpha$ , DNA binding, and transcriptional activity of NF- $\kappa$ B. Cycloheximide treatment, at a dose able to profoundly inhibit protein synthesis in FRTL-5 cells, obliterated the decrease in the level of

the inhibitory subunit I $\kappa$ B $\alpha$  produced by thapsigargin and tunicamycin. Therefore, protein synthesis was required to generate a signal from stressed endoplasmic reticulum. This substantiates the hypothesis that endoplasmic reticulum retention of newly synthesized Tg and other cargo (secretory and membrane) proteins functions upstream of signal activation. Dominant negative TNF receptor-associated factor 2 (TRAF2) inhibited activation of NF- $\kappa$ B, which was also inhibited in embryonic fibroblasts derived from TRAF2<sup>-/-</sup> mice, respect to their normal counterpart. These data extend the recent demonstration that TRAF2 mediated JNK activation in response to endoplasmic reticulum stress and strongly strengthened the idea that endogenous stress signals initiated in the endoplasmic reticulum proceed by a pathway similar to that initiated by plasma membrane receptors in response to extracellular signals. (*Endocrinology* 143: 2169–2177, 2002)

**M**EMBRANE AND SECRETORY proteins are cotranslationally translocated in the lumen of the endoplasmic reticulum where addition of N-linked oligosaccharide chains, folding, and assembly occur. Protein folding and processing within the lumen of the endoplasmic reticulum are dependent upon the maintenance of a oxidizing environment, a high  $\text{Ca}^{2+}$  concentration, and a battery of endoplasmic reticulum-resident enzymes and chaperones. Alterations in the endoplasmic reticulum redox potential, glycosylation machinery, or  $\text{Ca}^{2+}$  levels of the endoplasmic reticulum secondary to various pathophysiological conditions or pharmacological manipulations, as well as many diseases, such as cystic fibrosis, Alzheimer's disease, and primary congenital hypothyroidism, cause misfolded proteins to accumulate in the endoplasmic reticulum lumen. These retained proteins, which are eventually degraded, trigger a complex chains of events termed the unfolded protein response (UPR) (1). Activation of mammalian UPR is char-

acterized in part by increased transcription of several genes encoding endoplasmic reticulum molecular chaperones, as well as induction of CHOP/GADD153, a transcription factor that regulates growth arrest and apoptosis (2). These changes occur concomitantly with a marked decrease in the rate of protein synthesis (3). Stress of the endoplasmic reticulum induced by agents that cause accumulation of misfolded proteins in that compartment also activates c-Jun N-terminal kinases (JNKs)/stress-activated protein kinases (SAPKs) (4). In mammals it has been shown that an overload of the endoplasmic reticulum by protein overexpression (major histocompatibility complex class I, adenovirus E3/19K) activates nuclear factor- $\kappa$ B (NF- $\kappa$ B), and this phenomenon has been termed the endoplasmic reticulum overload response (EOR) (5). However, many stimuli, such as tunicamycin, thapsigargin, and brefeldin A, trigger both the UPR and the EOR (6).

The signal transmission pathways that mediate the different responses in the UPR and EOR have been extensively studied over the past several years. Mammalian cells contain at least three endoplasmic reticulum signaling proteins. Inositol requiring (IRE) 1 $\alpha$  and IRE1 $\beta$ , encoded by different genes, are transmembrane proteins that act as folding sensors with their luminal domain and initiate the signal transmission with their cytosolic domain containing both an essential

Abbreviations: EndoH, Endo- $\beta$ -N-acetylglucosaminidase H; EOR, endoplasmic reticulum overload response; IRE, inositol requiring; JNK, c-Jun N-terminal kinase; MEF, mouse embryonic fibroblast; NF- $\kappa$ B, nuclear factor- $\kappa$ B; PERK, PKR-ER-related kinase; PNGase F, Peptide N-glycosylase F; SAPK, stress-activated protein kinase; THAPS, thapsigargin; TRAF, TNF receptor-associated factor; Tun, tunicamycin; UPR, unfolded protein response.

serine/threonine kinase and a ribonuclease module (7, 8). The induction of both endoplasmic reticulum chaperone genes and CHOP/GADD153 involves IRE1 activation (7, 8). The third identified endoplasmic reticulum signaling protein is PERK (PKR-ER-related kinase), which shows a luminal domain and a cytosolic domain homologous to the cytosolic RNA-dependent protein kinase (9). PERK mediates the repression of protein synthesis through phosphorylation of eIF-2 $\alpha$  (9). Finally, the pathway that leads to NF- $\kappa$ B involves, in sequence, Ca<sup>2+</sup> loss from the endoplasmic reticulum lumen, increased production of reactive oxygen intermediates, and activation of NF- $\kappa$ B (10). Very recently, the pathway that leads to JNK activation has been elucidated. After an endoplasmic reticulum stress, IRE1 becomes oligomerized and activated, and this causes the clustering of TRAF2 to the cytoplasmic portion of IRE1 and JNK activation (11). It appears, therefore, that the activation of JNK by endoplasmic reticulum stress proceeds by a pathway similar to that used by cells to respond to extracellular signals such as TNF $\alpha$ . In fact, TNF $\alpha$ -induced receptor trimerization results in recruitment of adapter proteins to their cytosolic side, among which are the TRAF proteins, in particular TRAF2 (12, 13). The TRAFs activate proximal kinases to initiate a kinase cascade, causing JNK activation (14, 15). Notably, TRAF recruitment to TNF receptors activates not only JNK, but also NF- $\kappa$ B (12, 16). Therefore, we reasoned that if TRAF2 recruitment by TNF receptors causes both JNK and NF- $\kappa$ B activation, perhaps TRAF2 recruitment by IRE1 after an endoplasmic reticulum stress activates not only JNK, but also NF- $\kappa$ B.

We have been studying a cellular system of fully differentiated thyroid cells in continuous culture, the FRTL-5 and PC-C13 cell lines. These cell lines synthesize and secrete very large amounts of Tg, a high molecular weight glycoprotein that constitutes the molecular site of synthesis and storage of thyroid hormones. We have shown that treatment of FRTL-5 cells with thapsigargin in a low Ca<sup>2+</sup> medium (0.1 mM) dramatically inhibits the secretion of Tg that is trapped in the endoplasmic reticulum and alters its folding and oligomerization (17). Moreover, we directly tested the action of thapsigargin on the endoplasmic reticulum Ca<sup>2+</sup> stores of FRTL-5 cells (17). Therefore, we decided to use this cellular system to test the hypothesis that an endoplasmic reticulum stress, chiefly a Ca<sup>2+</sup> loss from the endoplasmic reticulum lumen caused by thapsigargin, activates through TRAF2 not only JNK, but also NF- $\kappa$ B.

## Materials and Methods

### Cell culture and biological reagents

FRTL-5 cells (CRL 8305, American Type Culture Collection, Manassas, VA) are a continuous cloned line of thyroid differentiated cells (18). These cells were maintained as previously described (19). WT and TRAF2<sup>-/-</sup> mouse embryonic fibroblast (MEF) were provided by Drs. T. W. Mak and W. C. Yeh (20). These cells were cultured in MEM-Glutamax (Life Technologies, Inc., Gaithersburg, MD) supplemented with 10% FCS and 0.1 mM sodium pyruvate. Polyclonal anti-Tg rabbit antibodies were raised against rat Tg as previously described (21). All other antibodies were purchased from Santa Cruz Biotechnology, Inc. (Santa Cruz, CA). Thapsigargin was obtained from Calbiochem (La Jolla, CA); tunicamycin was purchased from Roche (Indianapolis, IN). The dominant negative form of TRAF6  $\Delta$ N275 was generated by PCR. The dominant negative form of TRAF2  $\Delta$ N105 was previously described (22).

### Metabolic labeling and immunoprecipitation

FRTL-5 cells ( $2 \times 10^6$ ) were labeled for 5 min at 37 C in medium without cysteine and methionine containing [<sup>35</sup>S]cysteine and [<sup>35</sup>S]methionine (50  $\mu$ Ci L-<sup>35</sup>S *in vitro* cell labeling mix/ml; Amersham Pharmacia Biotech, Piscataway, NJ). The labeled cells were washed with cold PBS and lysed in 1 ml 1% Triton X-100 lysis buffer [25 mM HEPES (pH 7.4), 150 mM NaCl, 10% glycerol, 5 mM EDTA, 2 mM dithiothreitol, and Complete protease inhibitor mixture (Roche)]. Nuclear and cellular debris were removed by centrifugation at  $10,000 \times g$  for 10 min at 4 C. The lysate was incubated for 2 h at 4 C with 2  $\mu$ l anti-Tg polyclonal antibodies and was collected with 20  $\mu$ l protein G-Sepharose beads (Amersham Pharmacia Biotech). Beads were washed extensively with lysis buffer and boiled in SDS sample buffer, and the supernatant was subjected to 5% SDS-PAGE and autoradiography.

### Kinase assay

Anti-JNK immunoprecipitates were used for the immune complex kinase assay that was performed at 30 C for 10 min with 2  $\mu$ g substrate, 10  $\mu$ Ci [ $\gamma$ -<sup>32</sup>P]ATP, and 50  $\mu$ M ATP in a total of 20  $\mu$ l kinase buffer [20 mM HEPES (pH 7.4), 10 mM MgCl<sub>2</sub>, 25 mM  $\beta$ -glycerophosphate, 50  $\mu$ M Na<sub>3</sub>VO<sub>4</sub>, and 50  $\mu$ M dithiothreitol]. The substrate was GST-c-Jun (amino acids 1–79). The reactions were terminated by boiling in SDS sample buffer, and the products were resolved by 12% SDS-PAGE. Phosphorylated proteins were detected by autoradiography.

### Reporter assay

FRTL-5 cells ( $4 \times 10^5$  cells/well) were seeded in six-well (35-mm) plates. After 12 h cells were transfected with 0.5  $\mu$ g Ig- $\kappa$ B-luciferase reporter gene plasmid and various amount of each expression plasmid. Lipofectamine-mediated transfections were performed according to the manufacturer's instructions (Life Technologies, Inc.). Total amounts of transfected DNA were kept constant by supplementing empty expression vector plasmids as needed. Twenty-four hours after transfection cells were stimulated with thapsigargin or tunicamycin for 8 h, cell extracts were prepared, and reporter gene activity was determined via the luciferase assay system (Promega Corp.). Expression of the Rous sarcoma virus promoter- $\beta$ -galactosidase vector (0.2  $\mu$ g) was used to normalize transfection efficiencies.

### EMSA

Total cell extracts were prepared using a detergent lysis buffer [50 mM Tris (pH 7.4), 250 mM NaCl, 50 mM NaF, 1 mM Na<sub>3</sub>VO<sub>4</sub>, 0.5% Nonidet P-40, 0.5 mM dithiothreitol, and Complete protease inhibitor mixture (Roche)]. Cells were harvested by centrifugation, washed once in cold PBS, and resuspended in detergent lysis buffer (30  $\mu$ l/ $5 \times 10^6$  cells). The cell lysate was incubated on ice for 30 min, then centrifuged for 5 min at  $10,000 \times g$  at 4 C. The protein content of the supernatant was determined, and equal amounts of protein (10  $\mu$ g) were added to a reaction mixture containing 20  $\mu$ g BSA, 2  $\mu$ g poly(dI-dC), 10  $\mu$ l binding buffer [20 mM HEPES (pH 7.9), 10 mM MgCl<sub>2</sub>, 20% glycerol, 100 mM KCl, 0.2 mM EDTA, 0.5 mM dithiothreitol, and 0.5 mM phenylmethylsulfonyl fluoride] and 100,000 cpm of a <sup>32</sup>P-labeled oligonucleotide in a final volume of 20  $\mu$ l. Samples were incubated at room temperature for 30 min and run on a 4% acrylamide gel.

### Other procedures

Endo- $\beta$ -N-acetylglucosaminidase H (EndoH) and peptide N-glycosylase F (PNGase F) digestions were performed as previously reported (19).

## Results

### Thapsigargin and tunicamycin caused retention of Tg in the endoplasmic reticulum

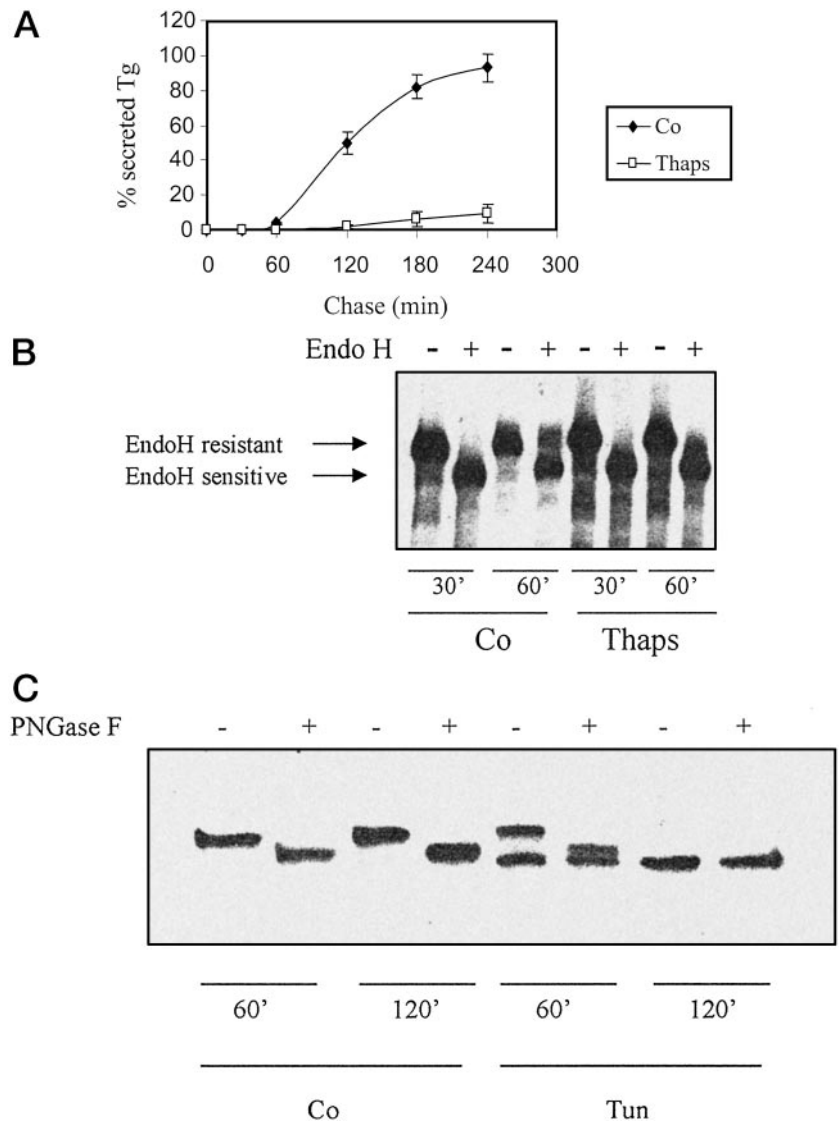
The ability of TRAF2 to transduce signals from both the plasma membrane and the endoplasmic reticulum prompted us to investigate its role in mediating NF- $\kappa$ B activation after

an endoplasmic reticulum stress. To this end we used a thyroid cell line system in which an endoplasmic reticulum stress was evaluated by monitoring the intracellular fate of newly synthesized Tg. Treatment of FRTL-5 cells with thapsigargin, a specific inhibitor of the sarco-endoplasmic reticulum  $\text{Ca}^{2+}$ -adenosine triphosphatases, in medium containing 0.1 mM  $\text{Ca}^{2+}$  led to depletion of  $\text{Ca}^{2+}$  from endoplasmic reticulum stores and dramatically inhibited the secretion of Tg. Tg was trapped in the endoplasmic reticulum and showed alteration in its folding and oligomerization (17). To improve the endoplasmic reticulum-stressing effect of thapsigargin, we decided to perform the thapsigargin treatments in a nominally  $\text{Ca}^{2+}$ -free medium instead of a 0.1 mM  $\text{Ca}^{2+}$  medium. FRTL-5 cells were pulse-labeled with [ $^{35}\text{S}$ ]methionine and chased in a nominally  $\text{Ca}^{2+}$ -free medium in the absence or presence of thapsigargin. At the indicated time of chase, the amounts of secreted and intracellular Tg were evaluated by immunoprecipitation and SDS-PAGE. As shown in Fig. 1A, treatment with thapsigargin dramatically inhibited Tg secretion in the culture medium. This suggested

that depletion of  $\text{Ca}^{2+}$  from the endoplasmic reticulum caused intracellular retention of Tg. As there were no differences between the total Tg (secreted plus retained) immunoprecipitated from cells incubated with or without thapsigargin in either media (not shown), the differences observed were due to inhibition of secretion and not to intracellular degradation. This effect was not specific for thapsigargin, as a 2-h treatment of cells with 10  $\mu\text{g}/\text{ml}$  tunicamycin, an inhibitor of protein glycosylation, caused Tg to be retained in FRTL-5 cells, as well (data not shown).

To confirm that thapsigargin also blocked Tg in the endoplasmic reticulum in a nominally  $\text{Ca}^{2+}$ -free medium, we decided to repeat in this condition the experiment exploring the EndoH sensitivity of the retained Tg. Newly synthesized Tg is *N*-linked glycosylated in the endoplasmic reticulum, where high mannose chains are attached to the protein. The carbohydrate chains are then processed, and they become EndoH resistant upon transport of the protein to the medial Golgi (23). FRTL-5 cells were pulse-labeled with [ $^{35}\text{S}$ ]methionine and chased for different times in a nominally  $\text{Ca}^{2+}$ -free

**FIG. 1.** A, Inhibition of Tg secretion by thapsigargin in FRTL-5 cells cultured in a nominally  $\text{Ca}^{2+}$ -free medium. B, Thapsigargin blocks the processing of Tg high mannose oligosaccharides into complex carbohydrates. C, Tunicamycin profoundly inhibits the *N*-linked glycosylation of Tg. A, FRTL-5 cells were labeled with [ $^{35}\text{S}$ ]cysteine and [ $^{35}\text{S}$ ]methionine as outlined in *Materials and Methods* and chased in a nominally  $\text{Ca}^{2+}$ -free medium in the absence (Co) or presence (Thaps) of 5  $\mu\text{M}$  thapsigargin for the indicated times. Secreted and intracellular Tg were immunoprecipitated, resolved by SDS-PAGE, and quantified by scanning densitometry. The mean labeled secreted Tg in three independent experiments ( $\pm\text{SD}$ ) is plotted against the time of chase. B, FRTL-5 cells were labeled with [ $^{35}\text{S}$ ]cysteine and [ $^{35}\text{S}$ ]methionine as outlined in *Materials and Methods* and chased in a nominally  $\text{Ca}^{2+}$ -free medium in the absence (Co) or presence (Thaps) of 5  $\mu\text{M}$  thapsigargin for the indicated times. Cells were lysed, and intracellular Tg was immunoprecipitated, divided in two aliquots, digested with or without EndoH, and resolved by SDS-PAGE. C, FRTL-5 cells were mock-treated or treated with 10  $\mu\text{g}/\text{ml}$  tunicamycin for 60 or 120 min in a nominally  $\text{Ca}^{2+}$ -free medium and labeled with [ $^{35}\text{S}$ ]cysteine and [ $^{35}\text{S}$ ]methionine as outlined in *Materials and Methods*. Intracellular Tg was immunoprecipitated, digested or mock-digested with PNGase F as outlined in *Materials and Methods*, and resolved by SDS-PAGE.



medium in the absence or presence of thapsigargin. Cells were lysed, and intracellular Tg was immunoprecipitated and digested with EndoH. The appearance of a slowly migrating, EndoH-resistant Tg species in untreated cells indicated that Tg moved from the endoplasmic reticulum to the medial Golgi (Fig. 1B). Tg immunoprecipitated from FRTL-5 cells treated with thapsigargin did not show any slowly migrating, EndoH-resistant form, thus demonstrating that a loss of  $\text{Ca}^{2+}$  from the endoplasmic reticulum caused Tg to be retained at a point before the medial Golgi (Fig. 1B). To show that 10  $\mu\text{g}/\text{ml}$  tunicamycin inhibited *N*-linked glycosylation of Tg we explored the sensitivity of Tg, after tunicamycin treatments, to PNGase F, which cleaves all *N*-linked chains. As shown in Fig. 1C, treatment of FRTL-5 cells with 10  $\mu\text{g}/\text{ml}$  tunicamycin for 1 h inhibited the *N*-linked glycosylation of the newly synthesized Tg by 50%, and treatment for 2 h almost completely inhibited the *N*-linked glycosylation of newly synthesized Tg. These data demonstrated that thapsigargin had a similar, perhaps more pronounced, effect on FRTL-5 cells in a nominally  $\text{Ca}^{2+}$ -free medium compared with a 0.1 mM  $\text{Ca}^{2+}$  medium and that tunicamycin, in our experimental conditions, strongly inhibited the *N*-linked glycosylation of newly synthesized Tg. We conclude, therefore, that both agents caused a block of Tg in the endoplasmic reticulum very likely because of a folding defect (17), probably causing an endoplasmic reticulum stress.

#### Endoplasmic reticulum stress causes activation of the JNK signaling pathway

It is well known that accumulation of proteins in the lumen of the endoplasmic reticulum initiates a stress response known as UPR/EOR. One of the pathways activated after endoplasmic reticulum stress is the SAPK/JNK pathway (11). To investigate whether the endoplasmic reticulum stress triggered by thapsigargin and tunicamycin was able to activate the SAPK/JNK pathway in FRTL-5 cells, we measured the levels of phospho-JNK, which is the active form of JNK, in cells treated with tunicamycin or thapsigargin. FRTL-5 cells were treated with tunicamycin for 60 and 120 min or with thapsigargin for 30 and 60 min. Cells were lysed, and the amount of phospho-JNK was measured by Western blot using phospho-specific anti-JNK antibodies. Both tunicamycin and thapsigargin increased the amount of phosphorylated JNK (Fig. 2A). Treatment of FRTL-5 cells with thapsigargin consistently caused activation of JNK within 60 min, whereas the effect of tunicamycin was clearly visible only after 120 min of treatment. Although it is possible that a higher dose of tunicamycin would shorten the signaling time, it is important to note that the time required for tunicamycin to activate JNK correlated well with the time required for tunicamycin to inhibit the *N*-linked glycosylation of newly synthesized Tg, which is complete after 120 min (Fig. 1C). To further demonstrate that the activity of JNK was increased after induction of endoplasmic reticulum stress, we also measured the relative levels of JNK kinase activity in cells treated with thapsigargin or tunicamycin by using an immune complex kinase assay. FRTL-5 cells were treated with tunicamycin for 120 min or with thapsigargin for 60 min. The cell lysates were immunoprecipitated with anti-

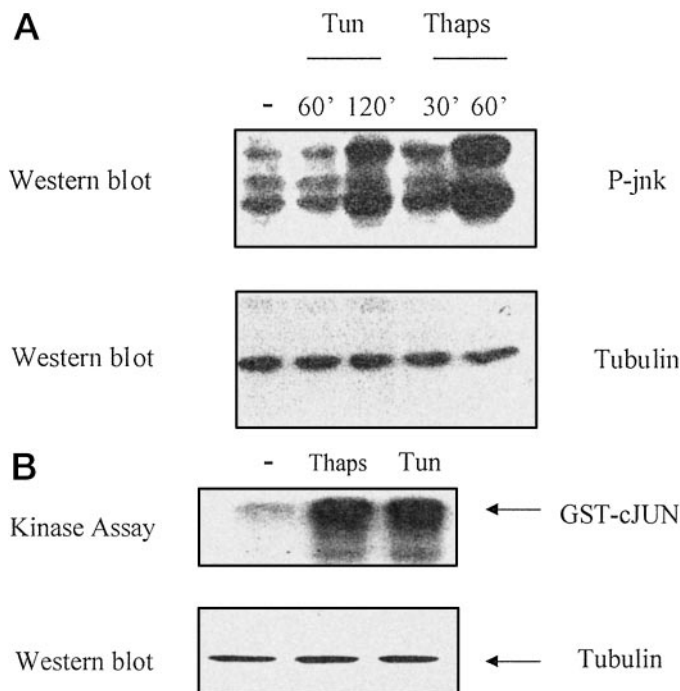


FIG. 2. Thapsigargin and tunicamycin activate the JNK signaling pathway. A, FRTL-5 cells were treated with thapsigargin (Thaps; 5  $\mu\text{M}$ ) for 30 and 60 min and with tunicamycin (Tun; 10  $\mu\text{g}/\text{ml}$ ) for 60 and 120 min in a nominally  $\text{Ca}^{2+}$ -free medium. Cells were lysed, and the amount of phospho-JNK was measured by Western blot using phospho-specific anti-JNK antibodies. The amounts of cell lysate loaded were normalized using polyclonal antitubulin antibodies. B, FRTL-5 cells were treated with tunicamycin (10  $\mu\text{g}/\text{ml}$ ) for 120 min or thapsigargin (5  $\mu\text{M}$ ) for 60 min in a nominally  $\text{Ca}^{2+}$ -free medium. Cell lysates were immunoprecipitated with anti-JNK antibodies, and the activity of endogenous JNK was measured by using GST-c-Jun (amino acids 1–79). To normalize the amounts of cell lysate used in the kinase assay, one tenth of each cell lysate was separately analyzed for tubulin content by Western blot.

JNK antibodies, and the activity of endogenous JNK was measured in an *in vitro* kinase assay using GST-c-Jun as substrate. Lysate from endoplasmic reticulum-stressed FRTL-5 cells all exhibited increased JNK kinase activity (Fig. 2B).

#### Endoplasmic reticulum stress causes activation of NF- $\kappa\text{B}$

NF- $\kappa\text{B}$  is a ubiquitously expressed family of transcription factors controlling the expression of numerous genes involved in inflammation, immune responses, and protection from apoptosis (24, 25). In most cell types NF- $\kappa\text{B}$  is present in an inactive form bound to its inhibitory subunit, I $\kappa\text{B}$ . Upon stimulation of cells with a variety of agents, such as inflammatory cytokines, UV irradiation, as well as bacterial and viral infection, I $\kappa\text{B}$  is phosphorylated on specific serine residues and degraded through a proteasome-dependent pathway (26). The released NF- $\kappa\text{B}$  dimer rapidly translocates to the nucleus, where it activates transcription of target genes.

To investigate whether the endoplasmic reticulum stress triggered by thapsigargin and tunicamycin was able to activate NF- $\kappa\text{B}$  in FRTL-5 cells, we treated cells with thapsigargin and tunicamycin and monitored the level of the inhibitory subunit I $\kappa\text{B}\alpha$  by Western blot. As shown in Fig. 3A,

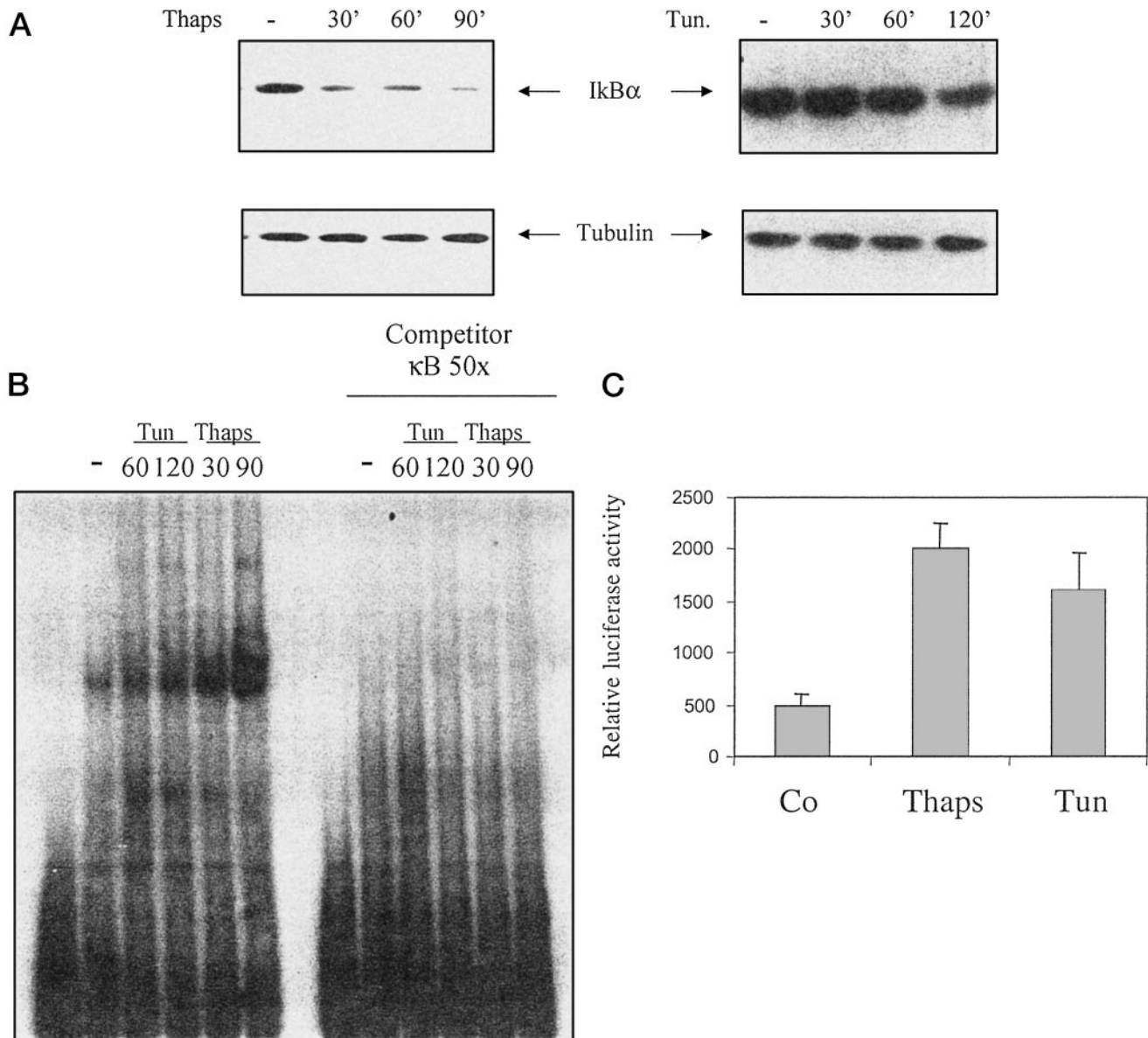


**FIG. 3.** Thapsigargin and tunicamycin activate NF- $\kappa$ B. **A**, FRTL-5 cells were treated with thapsigargin (Thaps; 5  $\mu$ M) and tunicamycin (Tun; 10  $\mu$ g/ml) for the indicated period of time. Cell extracts were Western blotted with anti-I $\kappa$ B $\alpha$  antibodies. The lower panel shows a Western blot antitubulin as control for protein loading. **B**, FRTL-5 cells were treated with thapsigargin (Thaps; 5  $\mu$ M) and tunicamycin (Tun; 10  $\mu$ g/ml) for the indicated period of time. Total cell extracts were prepared and analyzed by EMSA using a  $^{32}$ P-labeled oligonucleotide probe containing an NF- $\kappa$ B-binding site. The right part of the autoradiograph shows the same cell extracts incubated with a 50-fold molar excess of unlabeled NF- $\kappa$ B oligonucleotide. **C**, Relative luciferase activity observed in FRTL-5 cells transfected in triplicate with 0.5  $\mu$ g Ig- $\kappa$ B luciferase reporter plasmid. Twenty-four hours after transfection cells were stimulated with thapsigargin (Thaps; 5  $\mu$ M) or tunicamycin (Tun; 10  $\mu$ g/ml) for 12 h or were left untreated (Co) and then harvested. Measurements were normalized for  $\beta$ -galactosidase of a cotransfected Rous sarcoma virus- $\beta$ -galactosidase plasmid. Values shown (in arbitrary units) represent the mean ( $\pm$ SD) of at least three independent experiments.

the level of I $\kappa$ B $\alpha$  in the whole cell lysate was decreased after treatment with thapsigargin and tunicamycin. As for JNK activation, in the NF- $\kappa$ B activation there was a striking correlation between the time required to inhibit glycosylation of Tg and the time required to signal outside the endoplasmic reticulum. To further demonstrate the activation of NF- $\kappa$ B after endoplasmic reticulum stress, we performed an EMSA on nuclear extract from FRTL-5 cells treated in the same way. Both drugs caused the nuclear translocation of NF- $\kappa$ B and induced its DNA-binding activity (Fig. 3B). The specificity of

the protein-DNA complex was confirmed by a competition assay. Binding was competed by the addition of nonradioactive  $\kappa$ B oligonucleotide (Fig. 3B).

We subsequently tested whether the NF- $\kappa$ B activated by treatment with thapsigargin and tunicamycin was transcriptionally active. FRTL-5 cells were transfected with an Ig- $\kappa$ B luciferase reporter plasmid and 24 h after transfection were treated with thapsigargin and tunicamycin for 8 h. Both thapsigargin and tunicamycin activated the NF- $\kappa$ B-driven luciferase activity (Fig. 3C).

Thus, endoplasmic reticulum stress after a luminal  $\text{Ca}^{2+}$  loss or a block of glycosylation activated a functional NF- $\kappa\text{B}$  complex.

*Protein synthesis is required to activate NF- $\kappa\text{B}$  from the endoplasmic reticulum*

Our data suggest that the stressing effect of thapsigargin and tunicamycin is linked to the retention in the endoplasmic reticulum of Tg and other cargo proteins. To further support this contention we tested whether a block of protein synthesis by decreasing the level of newly synthesized Tg and other cargo (membrane and secretory) proteins was able to inhibit generation of the signal from the endoplasmic reticulum. We monitored the activation of NF- $\kappa\text{B}$  by assaying the level of I $\kappa\text{B}\alpha$  by Western blot after cycloheximide treatment. Preliminary experiments showed that in FRTL-5 cells, cycloheximide (0.5  $\mu\text{g}/\text{ml}$  for 1 h) was the optimal treatment, because in these conditions protein synthesis was inhibited by 70–80%, and a higher concentration did not give any significant additional inhibition (not shown). Cells were treated with cycloheximide (0.5  $\mu\text{g}/\text{ml}$  for 1 h), then with thapsigargin for 60 and 90 min and with tunicamycin for 60 and 120 min, in the presence of cycloheximide, and the levels of I $\kappa\text{B}\alpha$  were assayed by Western blot. As shown in Fig. 4, A and B, under control conditions thapsigargin and tunicamycin decreased I $\kappa\text{B}\alpha$  by about 50%; in presence of cycloheximide there was no reduction in I $\kappa\text{B}\alpha$ . In addition, the TNF-induced inhibition of I $\kappa\text{B}\alpha$  was cycloheximide insensi-

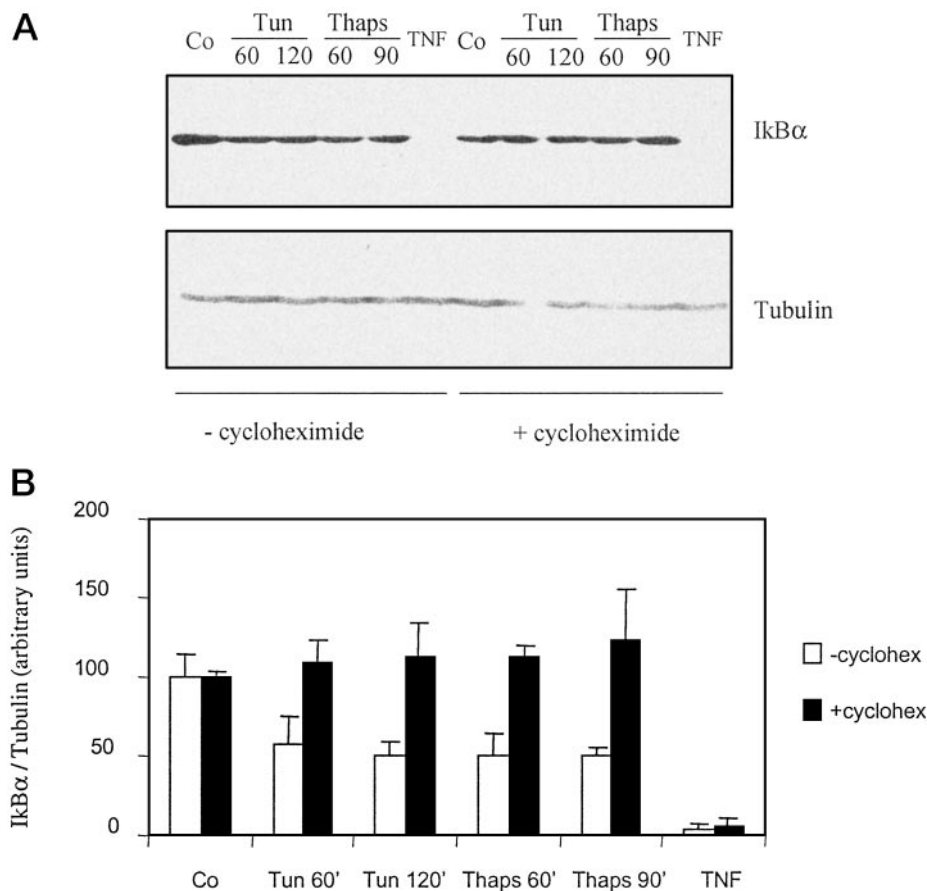
tive. In these experiments we observed a reduction in I $\kappa\text{B}\alpha$  in the controls in the presence of cycloheximide compared with the control level in the absence of cycloheximide. This was probably caused by the action of cycloheximide to decrease the steady state levels of I $\kappa\text{B}\alpha$ .

We concluded, therefore, that protein synthesis is specifically required to generate a signal from the endoplasmic reticulum, thus suggesting that signaling is a downstream event of endoplasmic reticulum retention of newly synthesized Tg and other cargo proteins.

*TRAF2 mediates the endoplasmic reticulum stress-induced activation of NF- $\kappa\text{B}$*

Recently, it has been demonstrated that endoplasmic reticulum stress activates JNK via the IRE1/TRAF2 complex (11). Given the central role of TRAF2 in mediating endoplasmic reticulum responses, we investigated whether TRAF2 was able to also mediate the endoplasmic reticulum stress-induced NF- $\kappa\text{B}$  activation. We tested the effect of an N-terminal deletion mutant of TRAF2, which acts as a dominant negative form of TRAF2 (22), on thapsigargin-induced  $\kappa\text{B}$  reporter expression using a transient transfection assay in FRTL5 cells. FRTL5 cells were transiently transfected with a NF- $\kappa\text{B}$ -driven luciferase reporter plasmid in the presence of increasing amount of TRAF2  $\Delta\text{N}105$ . This dominant negative form of TRAF2 was able to block the activation of NF- $\kappa\text{B}$  after thapsigargin treatment in a dose-dependent manner (Fig. 5). Overexpression of a dominant negative form of another

FIG. 4. Protein synthesis is required to activate NF- $\kappa\text{B}$  from the endoplasmic reticulum. A, FRTL-5 cells were treated with or without 0.5  $\mu\text{g}/\text{ml}$  cycloheximide for 1 h then with thapsigargin (Thaps; 5  $\mu\text{M}$ ) and tunicamycin (Tun; 10  $\mu\text{g}/\text{ml}$ ) for the indicated period of time in the presence or absence of 0.5  $\mu\text{g}/\text{ml}$  cycloheximide. Cell extracts were Western blotted with anti-I $\kappa\text{B}\alpha$  antibodies. The lower panel shows a Western blot antitubulin as a control for protein loading. B, I $\kappa\text{B}\alpha$ /tubulin ratios from two different experiments were plotted as a percentage of the control in the absence ( $\square$ ) and in the presence ( $\blacksquare$ ) of cycloheximide.



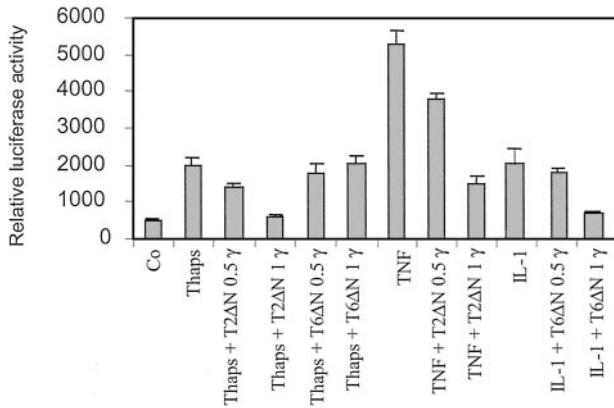


FIG. 5. Dominant negative TRAF2 blocks thapsigargin-dependent NF- $\kappa$ B activation. FRTL-5 cells ( $4 \times 10^5$ ) were transfected in triplicate with 0.5 mg Ig- $\kappa$ B luciferase reporter plasmid together with increasing amounts of dominant negative forms of TRAF2 (T2ΔN) or TRAF6 (T6ΔN). Twenty-four hours after transfection cells were either stimulated with thapsigargin (THAPS; 5  $\mu$ M) for 8 h or were left untreated (Co) and then harvested. Measurement were normalized for  $\beta$ -galactosidase activity, and data ( $\pm$ SD) are shown as arbitrary units.

member of the TRAF family, TRAF6  $\Delta$ N275, did not affect the NF- $\kappa$ B activation after thapsigargin treatment (Fig. 5). The dominant negative effect of TRAF2  $\Delta$ N105 on TRAF2-mediated signal transmission and that of TRAF6  $\Delta$ N275 on TRAF6-mediated signal transmission were demonstrated by the ability of TRAF2  $\Delta$ N105 and TRAF6  $\Delta$ N275 to block TNF and IL-1-induced NF- $\kappa$ B activation, respectively (Fig. 5).

To further demonstrate that TRAF2 is involved in signaling from endoplasmic reticulum, we used TRAF2<sup>-/-</sup> MEF. The TRAF2<sup>-/-</sup> phenotype is characterized by sensitivity to TNF-induced cell death, almost complete reduction of JNK activation, and delayed kinetics of activation of NF- $\kappa$ B upon TNF treatment (20, 27). Treatment of TRAF2<sup>-/-</sup> MEF with tunicamycin and thapsigargin did not cause a decrease in I $\kappa$ B $\alpha$  (Fig. 6). In contrast, treatment of control MEF with the same drugs resulted in strong decrease in I $\kappa$ B $\alpha$  (Fig. 6). These results indicate that NF- $\kappa$ B is activated in endoplasmic reticulum-initiated signal transduction and suggest that TRAF2 is involved in this pathway.

### Discussion

In this paper we show that an alteration in endoplasmic reticulum homeostasis causes retention of Tg in this organelle and activation of SAPKs and NF- $\kappa$ B signal transmission pathways. Most importantly, we show that NF- $\kappa$ B activation involves, at least partially, the adaptor protein TRAF2.

Alterations in the endoplasmic reticulum homeostasis cause misfolded proteins to accumulate in the endoplasmic reticulum lumen. These retained proteins, which are eventually degraded, trigger a complex chain of events termed the UPR (1). Although the final effects of the UPR are well known, the involved signal transmission pathways are less understood and actively studied over the past several years. It has been recently shown in pancreatic acinar epithelial AR42J cells and in 293T cells that an endoplasmic reticulum stress causes activation of the SAPK pathway and that this involves TRAF2 (11). TRAF2 is a member of the TRAF family

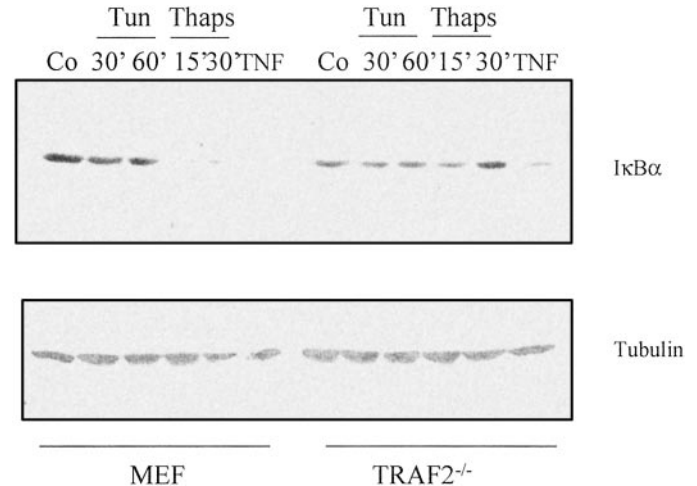


FIG. 6. In mouse embryonic fibroblasts TRAF2<sup>-/-</sup> thapsigargin and tunicamycin were unable to activate NF- $\kappa$ B. MEF and MEF TRAF2<sup>-/-</sup> cells were treated with thapsigargin (Thaps; 5  $\mu$ M) and tunicamycin (Tun; 10  $\mu$ g/ml) for the indicated periods of time. Cell extracts were Western blotted with anti-I $\kappa$ B $\alpha$  antibodies. The lower panel shows a Western blot antitubulin as a control for protein loading.

of adapter molecules that link members of the TNF receptor superfamily, IL-1 receptors, and Toll receptors to NF- $\kappa$ B and SAPK/JNK (16). In particular, TRAF2 appears to be central to signaling via TNF receptors I and II. On the other hand, the pathway originating from the endoplasmic reticulum that leads to NF- $\kappa$ B involves, in sequence, a Ca<sup>2+</sup> loss from the endoplasmic reticulum lumen, an increased production of reactive oxygen intermediates, and activation of NF- $\kappa$ B (10). Our results suggest the existence of a common mechanism coupling endoplasmic reticulum stress to SAPKs and NF- $\kappa$ B activation, in that both activation pathways use TRAF2. Notably, the time required to activate NF- $\kappa$ B and SAPK was essentially the same, 1–2 h, which is considerably shorter than the time required to up-regulate immunoglobulin heavy chain binding protein mRNA in FRTL-5 cells after treatments with thapsigargin and tunicamycin (6 h; data not shown). Moreover, our data strengthened the idea that endogenous stress signals initiated in the endoplasmic reticulum proceed by a pathway similar to that initiated by plasma membrane receptors in response to extracellular signals. In fact, it is well known that the signal transmission pathway originating from TNF receptors I and II activates both SAPKs and NF- $\kappa$ B via TRAF2. However, our results are compatible with the fact that in response to an endoplasmic reticulum stress, NF- $\kappa$ B could also be activated by other signal transmission mechanisms, for instance that described by Pahl and Bauerle (10). If this is indeed the case, the similarity of the pathways originating from TNF receptors and IRE1 is further corroborated. In fact, TRAF2 is critically important in TNF-initiated activation of SAPK/JNK. This has been confirmed by the failure of TNF to activate this signaling path in cells of mice lacking TRAF2 or expressing a dominant negative form of TRAF2 (20, 27). However, NF- $\kappa$ B activation is only partially affected in the same cells. It was suggested that other TRAF proteins, such as TRAF5, might have compensated for the lack of TRAF2 (20). The latter hypothesis is

supported by the lack of NF- $\kappa$ B activation after TNF stimulation in MEF derived from mice lacking both TRAF2 and TRAF5 (28). It is also possible, however, that an independent mechanism exists by which the TNF receptor may activate NF- $\kappa$ B.

Accumulation of cargo proteins in the endoplasmic reticulum occurs not only in various pharmacological manipulations, but also in a variety of diseases, such as viral infections, primary congenital hypothyroidism (29), cystic fibrosis (30), juvenile pulmonary emphysema (31), osteogenesis imperfecta (32), autosomal dominant neurohypophyseal diabetes insipidus (33), and familial hypercholesterolemia (34). In about 20% of primary congenital hypothyroidism a mutation is present in one of the genes encoding proteins essential in the biosynthesis of thyroid hormones (29). One of these proteins is Tg. Mutations of the Tg gene have been found in both animals (35–38) and humans (39–43). Among these mutations, missense mutations of the mouse gene (36), the rat gene (38), and the human gene (42, 43) cause impaired intracellular transport of Tg. In these cases there are greatly enlarged thyroids, with the exception of the *rdw/rdw* rat (38), and enlarged thyrocyte endoplasmic reticulum membranes. The enlargement of the endoplasmic reticulum is due to the expression of compensatory levels of endoplasmic reticulum chaperones (triggered by accumulation of Tg), whereas the increase in thyroid volume is caused by increased levels of TSH (42). Using this feedback mechanism, cells maintain a chaperone reserve to further binding to unfolded/misfolded proteins that enter the endoplasmic reticulum. However, less clear is the physiological role of NF- $\kappa$ B in the UPR. NF- $\kappa$ B could trigger chaperone and/or endoplasmic reticulum membrane formation to relieve the congestion of the endoplasmic reticulum. These hypotheses remain to be investigated. On the other hand, it is well known that NF- $\kappa$ B triggers an inflammatory response. This induction could play a role during viral infections where large quantities of viral proteins are produced, causing an endoplasmic reticulum overload. In fact, interferons and cytokines, induced by NF- $\kappa$ B, can act as antiviral agents. Moreover, inflammation is well documented in a subset of cystic fibrosis patients with the PiZ variant of the  $\alpha_1$ -antitrypsin that have extensive hepatic damage and early cirrhosis of the liver (44). An analogous case could be represented by the *rdw/rdw* rat, which dramatically contrasts with most human patients and animal models of congenital hypothyroid goiter. In this case a Tg mutation causing impaired intracellular transport does not exist in goiter, but, rather, in a hypoplastic thyroid gland (38). In these cases NF- $\kappa$ B could play a role in controlling endoplasmic reticulum stress-induced apoptosis in a way analogous to TNF receptor-triggered apoptosis. Our results showing that NF- $\kappa$ B activation from the endoplasmic reticulum involves the adaptor protein TRAF2, as NF- $\kappa$ B activation from TNF receptors does, further suggest this hypothesis. This possibility is currently under investigation. Indeed, the recent finding that caspase-12, an endoplasmic reticulum-resident caspase, physically and functionally interacts with TRAF2 (45) also substantiates the central role of TRAF2 as a key switch of the endoplasmic reticulum controlling the alternative adaptation/apoptosis.

In conclusion, in this study we demonstrate that an en-

doplasmic reticulum stress caused by thapsigargin and tunicamycin triggers activation of SAPK/JNK and NF- $\kappa$ B stress response pathways, very likely acting through a retention of Tg and other cargo proteins in the endoplasmic reticulum. Moreover, we provide further evidence for the central role that the adaptor molecule TRAF2 plays in the transduction of signals from the endoplasmic reticulum to the cytosol during endoplasmic reticulum stress.

### Acknowledgments

Received October 29, 2001. Accepted February 11, 2002.

Address all correspondence and requests for reprints to: Dr. Bruno Di Jeso, Laboratorio di Patologia Generale, Dipartimento di Scienze e Tecnologie Biologiche ed Ambientali, Facoltà di Scienze MFN, Strada Lecce-Monteroni, Università degli Studi di Lecce, 73100 Lecce, Italy. E-mail: bdijeso@ilenic.unile.it.

This work was supported in part by a grant from Associazione Italiana Ricerca sul Cancro (to A.L.) and Ministero della Università e Ricerca Scientifica Grant 2001065217 (to S.F.).

### References

1. Kaufman RJ 1999 Stress signaling from the lumen of the endoplasmic reticulum: coordination of gene transcriptional and translational controls. *Genes Dev* 13:1211–1233
2. Zinszner H, Kuroda M, Wang X, Batchvarova N, Lightfoot RT, Remotti H, Stevens JL, Ron D 1998 CHOP is implicated in programmed cell death in response to impaired function of the endoplasmic reticulum. *Genes Dev* 12:982–995
3. Brostrom CO, Brostrom MA 1998 Regulation of translational initiation during cellular responses to stress. *Prog Nucleic Acid Res Mol Biol* 58:79–125
4. Kyriakis JM, Banerjee P, Nikolakaki E, Dai T, Rubie EA, Ahmad MF, Avruch J, Woodgett J 1994 The stress-activated protein kinase subfamily of c-Jun kinases. *Nature* 369:156–160
5. Pahl HL, Baeuerle PA 1997 The ER-overload response: activation of NF- $\kappa$ B. *Trends Biochem Sci* 22:63–67
6. Pahl HL, Baeuerle PA 1995 A novel signal transduction pathway from the endoplasmic reticulum to the nucleus is mediated by transcription factor NF- $\kappa$ B. *EMBO J* 14:2580–2588
7. Wang X-Z, Harding HP, Zhang Y, Jolicoeur EM, Kuroda M, Ron D 1998 Cloning of mammalian Ire1 reveals diversity in the ER stress responses. *EMBO J* 17:5708–5717
8. Tirasophon W, Welihinda AA, Kaufman RJ 1998 A stress response pathway from the endoplasmic reticulum to the nucleus requires a novel bifunctional protein kinase/endoribonuclease (Ire1p) in mammalian cells. *Genes Dev* 12:1812–1824
9. Harding HP, Zhang Y, Ron D 1999 Protein translation and folding are coupled by an endoplasmic-reticulum-resident kinase. *Nature* 397:271–274
10. Pahl HL, Baeuerle PA 1996 Activation of NF- $\kappa$ B by ER stress requires both  $Ca^{++}$  and reactive oxygen intermediates as messengers. *FEBS Lett* 392:129–136
11. Urano F, Wang X, Bertolotti A, Zhang Y, Chung P, Harding HP, Ron D 2000 Coupling of stress in the ER to activation of JNK protein kinases by transmembrane protein kinase IRE1. *Science* 287:664–666
12. Liu ZG, Hsu H, Goeddel DV, Karin M 1996 Dissection of TNF receptor 1 effector functions: JNK activation is not linked to apoptosis while NF- $\kappa$ B activation prevents cell death. *Cell* 87:565–576
13. Reinhard C, Shamon B, Shyamala V, Williams LT 1997 Tumor necrosis factor  $\alpha$ -induced activation of c-Jun N-terminal kinase is mediated by TRAF2. *EMBO J* 16:1080–1092
14. Shi CS, Kehrl JH 1997 Activation of stress-activated protein kinase/c-Jun N-terminal kinase, but not NF- $\kappa$ B, by the tumor necrosis factor (TNF) receptor 1 through a TNF receptor-associated factor 2- and germinal center kinase related-dependent pathway. *J Biol Chem* 272:32102–32107
15. Yuasa T, Ohno S, Kehrl JH, Kyriakis JM 1998 Tumor necrosis factor signaling to stress-activated protein kinase (SAPK)/Jun NH<sub>2</sub>-terminal kinase (JNK) and p38. Germinal center kinase couples TRAF2 to mitogen-activated protein kinase/ERK kinase 1 and SAPK while receptor interacting protein associates with a mitogen-activated protein kinase kinase upstream of MKK6 and p38. *J Biol Chem* 273:22681–22692
16. Arch RH, Gedrich RW, Thompson CB 1998 Tumor necrosis factor receptor-associated factors (TRAFs) a family of adapter proteins that regulates life and death. *Genes Dev* 12:2821–2830
17. Di Jeso B, Pereira B, Consiglio E, Formisano S, Satrustegui J, Sandoval IV 1998 Demonstration of a  $Ca^{++}$  requirement for thyroglobulin dimerization and export to the golgi complex. *Eur J Biochem* 252:583–590

18. Ambesi-Impiombato FS 1986 US patent no. 4608341
19. Di Jeso B, Liguoro D, Ferranti P, Marinaccio M, Acquaviva R, Formisano S, Consiglio E 1992 Modulation of the carbohydrate moiety of thyroglobulin by thyrotropin and calcium in Fisher rat thyroid line-5 cells. *J Biol Chem* 267:1938–1944
20. Yeh WC, Shahinian A, Speiser D, Kraunus J, Billia F, Wakeham A, de la Pompa JL, Ferrick D, Hum B, Iscove N, Ohashi P, Rothe M, Goeddel DV, Mak TW 1997 Early lethality, functional NF- $\kappa$ B activation, and increased sensitivity to TNF-induced cell death in TRAF2-deficient mice. *Immunity* 7:715–725
21. Mullin BR, Levinson RE, Friedman A, Henson DE, Winand R, Kohn LD 1977 Delayed hypersensitivity in Graves' disease and exophthalmos: identification of thyroglobulin in normal human orbital muscle. *Endocrinology* 100:351–366
22. Leonardi A, Ellinger-Ziegelbauer H, Franzoso G, Brown K, Siebenlist U 2000 Physical and functional interaction of filamin (actin-binding protein-280) and tumor necrosis factor receptor-associated factor 2. *J Biol Chem* 275:271–278
23. Kornfeld R, Kornfeld S 1985 Assembly of asparagine-linked oligosaccharides. *Annu Rev Biochem* 54:631–664
24. Siebenlist U, Franzoso G, Brown K 1994 Structure, regulation and function of NF- $\kappa$ B. *Annu Rev Cell Biol* 10:405–455
25. Karin M, Ben-Neriah Y 2000 Phosphorylation meets ubiquitination: the control of NF- $\kappa$ B activity. *Annu Rev Immunol* 18:621–663
26. Verma IM, Stevenson JK, Schwarz EM, Van Antwerp D, Miyamoto S 1995 Rel/NF- $\kappa$ B/I $\kappa$ B family: intimate tales of association and dissociation. *Genes Dev* 9:2723–2735
27. Lee SY, Reichlin A, Santana A, Sokol KA, Nussenzweig MC, Choi Y 1997 TRAF2 is essential for JNK but not NF- $\kappa$ B activation and regulates lymphocyte proliferation and survival. *Immunity* 7:703–713
28. Tada K, Okazaki T, Sakon S, Kobara T, Kurosawa K, Yamaoka S, Hashimoto H, Mak TW, Yagita H, Okumura K, Yeh WC, Nakano H 2001 Critical roles of TRAF2 and TRAF5 in tumor necrosis factor-induced NF- $\kappa$ B activation and protection from cell death. *J Biol Chem* 276:36530–36534
29. De Vijlder JJM, Vulmsa T 1996 Hereditary metabolic disorders causing hypothyroidism. In: Braveman LE, Utiger RD, eds. *Werner's & Ingbar's the thyroid*. Philadelphia: Lippincott; 749–755
30. Lukacs G, Mohamed N, Kartner N, Chang X, Riordan J, Grinstein S 1994 Conformational maturation of CFRT but not its mutant counterpart ( $\Delta$ F508) occurs in the endoplasmic reticulum and requires ATP. *EMBO J* 13:6076–6086
31. Sifer RN, Finegold MJ, Woo SL 1992 Molecular biology and genetics of  $\alpha$ 1-antitrypsin deficiency. *Semin Liver Dis* 12:301–310
32. Bonadio J, Byers PH 1985 Subtle structural alteration in the chain of type I procollagen produce osteogenesis imperfecta type II. *Nature* 316:363–366
33. Beuret N, Rutishauser J, Bider MD, Spiess M 1999 Mechanism of endoplasmic reticulum retention of mutant vasopressin precursor caused by a signal peptide truncation associated with diabetes insipidus. *J Biol Chem* 274:18965–18972
34. Pathak RK, Merkle RK, Cummings RD, Goldstein JL, Brown MS, Anderson RG 1988 Immunocytochemical localization of mutant low density lipoprotein receptors that fail to reach the Golgi complex. *J Cell Biol* 106:1831–1841
35. Ricketts MH, Simons MJ, Parma J, Mercken L, Dong Q, Vassart G 1987 A nonsense mutation causes hereditary goitre in the Afrikaner cattle and unmasks alternative splicing of thyroglobulin transcripts. *Proc Natl Acad Sci USA* 84:3181–3184
36. Veenboer GJM, deVijlder JJM 1993 Molecular basis of the thyroglobulin synthesis defect in Dutch goats. *Endocrinology* 132:377–381
37. Kim PS, Hossain SA, Park YN, Lee I, Yoo SE, Arvan P 1998 A single amino acid change in the acetylcholinesterase-like domain of thyroglobulin causes congenital goiter with hypothyroidism in the *cog/cog* mouse: a model of human endoplasmic reticulum storage diseases. *Proc Natl Acad Sci USA* 95:9909–9913
38. Kim PS, Ding M, Menon S, Jung CG, Cheng JM, Miyamoto T, Li B, Furudate S, Agui T 2000 A missense mutation G2320R in the thyroglobulin gene causes non-goitrous congenital primary hypothyroidism in the WIC-rdw rat. *Mol Endocrinol* 14:1944–1953
39. Ieiri T, Cochaux P, Targovnik HM, Suzuki M, Shimoda S, Perret J, Vassart GA 1991 3' splice site mutation in the thyroglobulin gene responsible for congenital goiter with hypothyroidism. *J Clin Invest* 88:1901–1905
40. Targovnik HM, Medeiros-Neto G, Varela V, Cochaux P, Wajchenberg BL, Vassart G 1993 A nonsense mutation causes human hereditary congenital goiter with preferential production of a 171-nucleotide-deleted thyroglobulin ribonucleic acid messenger. *J Clin Endocrinol Metab* 77:210–215
41. van de Graaf SA, Ris-Stalpers C, Veenboer GJ, Cammenga M, Santos C, Targovnik HM, de Vijlder JJ, Medeiros-Neto G 1999 A premature stop codon in thyroglobulin messenger RNA results in familial goiter and moderate hypothyroidism. *J Clin Endocrinol Metab* 84:2537–2542
42. Medeiros-Neto G, Kim PS, Yoo SE, Vono J, Targovnik HM, Camargo R, Hossain SA, Arvan P 1996 Congenital hypothyroid goiter with deficient thyroglobulin. Identification of an endoplasmic reticulum storage disease with induction of molecular chaperones. *J Clin Invest* 98:2838–2844
43. Hishinuma A, Takamatsu J, Ohyama Y, Yokozawa T, Kanno Y, Kuma K, Yoshida S, Matsuura N, Ieiri T 1999 Two novel cysteine substitutions (C1263R and C1995S) of thyroglobulin cause a defect in intracellular transport of thyroglobulin in patients with congenital goiter and the variant type of adenomatous goiter. *J Clin Endocrinol Metab* 84:1438–1444
44. Qu D, Teckman JH, Perlmutter DH 1997  $\alpha$ 1-Antitrypsin deficiency associated liver disease. *J Gastroenterol Hepatol* 12:404–416
45. Yoneda T, Imaizumi K, Oono K, Yui D, Gomi F, Katayama T, Tohyama MM 2001 Activation of caspase-12, an endoplasmic reticulum (ER) resident caspase, through tumor necrosis factor receptor-associated factor 2-dependent mechanism in response to the endoplasmic reticulum stress. *J Biol Chem* 276:13935–13940



ACADEMIC  
PRESS

Available online at [www.sciencedirect.com](http://www.sciencedirect.com)

SCIENCE @ DIRECT®

Biochemical and Biophysical Research Communications 309 (2003) 84–90

BBRC

[www.elsevier.com/locate/ybbrc](http://www.elsevier.com/locate/ybbrc)

## Role of the adaptor protein CIKS in the activation of the IKK complex

Claudio Mauro,<sup>a</sup> Pasquale Vito,<sup>b</sup> Stefano Mellone,<sup>c</sup> Francesco Pacifico,<sup>c</sup> Alain Chariot,<sup>d</sup>  
Silvestro Formisano,<sup>a</sup> and Antonio Leonardi<sup>a,\*</sup>

<sup>a</sup> *Dipartimento di Biologia e Patologia Cellulare e Molecolare, 'Federico II' University of Naples, Via Pansini 5, Naples 80131, Italy*

<sup>b</sup> *Dipartimento di Scienze Biologiche e Ambientali, Università degli Studi del Sannio, Benevento, Italy*

<sup>c</sup> *Istituto di Endocrinologia e Oncologia Sperimentale, CNR, Naples, Italy*

<sup>d</sup> *Laboratory of Medical Chemistry and Human Genetics, Center for Cellular and Molecular Therapy, C.H.U. Sart-Tilman, 4000 Liège, Belgium*

Received 29 July 2003

### Abstract

Nuclear factor  $\kappa$ B (NF- $\kappa$ B) plays a pivotal role in numerous cellular processes, including stress response, inflammation, and protection from apoptosis. Therefore, the activity of NF- $\kappa$ B needs to be tightly regulated. We have previously identified a novel gene, named CIKS (connection to I $\kappa$ B-kinase and SAPK), able to bind the regulatory sub-unit NEMO/IKK $\gamma$  and to activate NF- $\kappa$ B. Here, we demonstrate that CIKS forms homo-oligomers, interacts with NEMO/IKK $\gamma$ , and is recruited to the IKK-complex upon cell stimulation. In addition, we identified the regions of CIKS responsible for these functions. We found that the ability of CIKS to oligomerize, and to be recruited to the IKK-complex is not sufficient to activate the NF- $\kappa$ B. In fact, a deletion mutant of CIKS able to oligomerize, to interact with NEMO/IKK $\gamma$ , and to be recruited to the IKK-complex does not activate NF- $\kappa$ B, suggesting that CIKS needs a second level of regulation to efficiently activate NF- $\kappa$ B.

© 2003 Elsevier Inc. All rights reserved.

**Keywords:** NF- $\kappa$ B; CIKS/Act1; NEMO/IKK $\gamma$ ; Signal transduction

The NF- $\kappa$ B proteins are an evolutionary conserved family of transcription factors that regulate the expression of a variety of cellular genes involved in control of apoptosis, immune and inflammatory responses [1,2]. In most cell types NF- $\kappa$ B is sequestered in the cytoplasm, bound to inhibitors, collectively called I $\kappa$ Bs [3]. Various stimuli, including cytokines, pathogens, and pathogen-related factors, lead to phosphorylation of I $\kappa$ B proteins on specific serine residues (Ser 32 and 36 for I $\kappa$ B $\alpha$ ). This phosphorylation marks I $\kappa$ Bs for ubiquitination by the SCF E3 ligase and subsequent degradation through a proteasome-dependent pathway [4]. The I $\kappa$ B inhibitors are phosphorylated by kinases residing in a large molecular weight complex (700–900 kDa) called the I $\kappa$ B kinase-complex (IKK-complex). IKK-complexes are composed of two catalytic sub-units, IKK $\alpha$  and  $\beta$  [5–9], and a regulatory sub-unit called NEMO/IKK $\gamma$  [10,11]. In addition to the I $\kappa$ B proteins, it has been recently

demonstrated that IKKs phosphorylate and regulate the processing of the precursors of p50 and p52 sub-units, respectively, p105/NF- $\kappa$ B1 and p100/NF- $\kappa$ B2 [12–14]. Beside these functions, IKKs may also modulate the transcriptional activity of NF- $\kappa$ B proteins, phosphorylating the transactivation domain of RelA [15].

NEMO/IKK $\gamma$  was originally identified in a genetic complementation assay, as a factor able to restore NF- $\kappa$ B activation in cells unresponsive to a variety of stimuli that normally induce the NF- $\kappa$ B pathway [10]. NEMO/IKK $\gamma$  was also identified in biochemical studies as a component of the high molecular weight IKK-complex [11]. NEMO/IKK $\gamma$  contains a leucine zipper and two coiled-coil domains. These motifs are important for its oligomerization, which is critical for activating the IKK kinase activity [16] and for recruitment of upstream signalling mediators. Different proteins have been demonstrated to interact with NEMO/IKK $\gamma$ . These include a kinase known as RIP [17], the cellular protein A20 [17], the viral transactivator tax [18–20], the cellular protein CIKS [21], and the adaptor protein TANK [22].

\* Corresponding author. Fax: +39-081-770-1016.

E-mail address: [leonardi@unina.it](mailto:leonardi@unina.it) (A. Leonardi).

Thus NEMO/IKK $\gamma$  can interact with a variety of different regulatory proteins that are important in regulating the activation of the NF- $\kappa$ B pathway in response to different stimuli. Despite all these evidences the functions and the mechanisms of NEMO/IKK $\gamma$  activation remain to be determined. Particularly, it is still unclear how the IKKs are activated following different stimuli. It has been proposed that oligomerization of NEMO/IKK $\gamma$  is sufficient to activate the kinase activity of the complex. For example, in response to TNF stimulation, RIP may trigger oligomerization of the IKK-complex through oligomerization of NEMO/IKK $\gamma$  [16]. However, other mechanisms may exist to activate the kinase activity of the IKK-complex, such as direct phosphorylation of the IKK $\alpha/\beta$  by other kinases.

Previously, we reported on the identification of a NEMO/IKK $\gamma$ -interacting protein identified in a yeast two-hybrid screen using NEMO/IKK $\gamma$  as bait, which we called CIKS [21] (a.k.a. Act-1) [23]. CIKS does not have any known enzymatic activity and contains a helix–loop–helix motif at the amino terminus and a coiled–coil at the carboxyl terminus. Forced expression of CIKS activates NF- $\kappa$ B and JNK/SAPK pathways, suggesting that CIKS may act as an adaptor protein, linking upstream signalling pathways to the NF- $\kappa$ B and JNK/SAPK pathways. Recently, Qian et al. [24] reported that CIKS may be involved in CD40 signalling, at least in epithelial cells. Kanamori et al. [25] reported a potential involvement of CIKS in the IL-1/Toll pathway, by virtue of its ability to interact with TRAF6.

In this study, we used CIKS as a model to investigate the molecular mechanism by which the IKK-complex is activated. Particularly, we demonstrated that CIKS forms oligomers, interacts with NEMO/IKK $\gamma$ , and is recruited to the IKK-complex after cell stimulation. In addition we identified the regions of CIKS responsible for these functions. However, a deletion mutant of CIKS able to oligomerize, to interact with NEMO/IKK $\gamma$ , and to be recruited to the IKK-complex does not activate NF- $\kappa$ B, suggesting that CIKS needs a second level of regulation to efficiently activate NF- $\kappa$ B.

## Materials and methods

**Cell culture and biological reagents.** HeLa, HEK293 were maintained in Dulbecco's modified Eagle's medium supplemented with 10% fetal calf serum, 1% (w/v) penicillin/streptomycin, and 1% glutamine.

We used two anti-CIKS polyclonal antibodies: one was generated in rabbits and was directed against a recombinant peptide encompassing amino acids 190–382 of human CIKS; the other was from Santa Cruz Biotechnologies. The mouse monoclonal IgM to human CD40 (clone 14G7) was from Caltag. Anti-FLAG and anti-FLAG agarose gel were from Sigma. All other antibodies were from Santa Cruz Biotechnologies.

Full-length NEMO/IKK $\gamma$  and full-length CIKS have been previously described [21]. The HA-CIKS  $\Delta$ C300 (aa 1–274), HA-CIKS  $\Delta$ N300 (aa 300–574), and HA-CIKS  $\Delta$ N87 (aa 87–574) were generated

by PCR. For yeast experiments CIKS full-length and different CIKS deletion mutants were cloned in-frame with the Gal4 DNA binding domain of the vector pGBKT7 (Clontech) or with the Gal4 activation domain of the vector pGADT7 (Clontech).

**Transfection, immunoprecipitation, and luciferase assays.** LipofectAMINE-mediated transfections were performed according to the manufacturer's instructions (Life Technologies). For immunoprecipitation of transfected proteins, HeLa cells ( $2 \times 10^6$ ) or HEK293 ( $3 \times 10^6$ ) were transiently transfected and 24 h after transfection cells were lysed in Triton X-100 lysis buffer [20 mM Hepes, pH 7.4, 150 mM NaCl, 10% glycerol, 1% Triton X-100, 1 mM Na<sub>3</sub>VO<sub>4</sub>, 10 mM  $\beta$ -glycerophosphate, 5 mM NaF, and "Complete Protease Inhibitor" mixture (Roche Molecular Biochemicals)]. After an additional 15 min on ice, cell extracts were centrifuged for 20 min at 14,000 rpm at 4°C and supernatants were immunoprecipitated by using anti-HA or anti-FLAG antibodies bound to agarose beads. The immunoprecipitates were washed five times with Triton X-100 lysis buffer and subjected to SDS-PAGE.

For immunoprecipitation of column fractions, fractions were incubated overnight with 10  $\mu$ l of anti-FLAG antibodies bound to agarose beads. The immunoprecipitates were washed five times with Triton X-100 lysis buffer and subjected to SDS-PAGE.

For luciferase assay, HeLa ( $2 \times 10^5$ ) or HEK293 ( $4 \times 10^5$ ) were seeded in 6-well (35 mm) plates. After 12 h cells were transfected with 0.5  $\mu$ g of Ig- $\kappa$ B-luciferase reporter plasmid and various amounts of each expression plasmid. Total amount of transfected DNA was kept constant by supplementing empty expression plasmid as needed. Cell extracts were prepared 24 h after transfection and reporter gene activity was determined via the luciferase assay system (Promega). Expression of the pRSV- $\beta$ Gal vector (0.2  $\mu$ g) was used to normalize transfection efficiencies.

**Gel filtration of cellular extract.** HeLa cells were lysed in Triton X-100 lysis buffer. Lysates were incubated for 15 min on ice and clarified by centrifugation at 14,000 rpm for 15 min, 4°C. Supernatants were collected and recentrifuged for 1 h at 100,000g at 4°C. One milligram of the S-100 extracts (0.5 ml) was loaded onto a Superdex S200 HR (Amersham-Pharmacia Biotech). Proteins were eluted from the column at the flow rate of 0.3 ml/min. Fractions (0.4 ml) were precipitated with 10% trichloroacetic acid, resuspended in Laemmli's buffer, and analyzed by SDS-PAGE followed by Western blotting for IKK $\alpha$ , IKK $\beta$ , NEMO/IKK $\gamma$ , and CIKS using appropriate antibodies.

**Kinase assay.** For IKK kinase assay, endogenous IKK $\beta$  was immunoprecipitated from the fractions eluted from the column by using anti-IKK $\beta$  antibodies and the kinase activity was assayed by using GST-I $\kappa$ B (aa 1–54) as substrate.

## Results

### CIKS forms oligomers

We have previously identified a novel protein we called CIKS by using NEMO/IKK $\gamma$  as bait in a yeast two-hybrid screening [21] (a.k.a. Act1) [23]. The activities of CIKS loosely resemble those of TRAF proteins. In fact, similar to TRAF2, 5 or 6, overexpression of CIKS activates SAPK/JNK and IKK kinases [21,26–30]. The capacity of TRAFs to activate downstream pathways appears to be linked to the ability of these proteins to oligomerize [30]. In order to investigate if a similar molecular mechanism was involved in the ability of CIKS to activate NF- $\kappa$ B, we examined, in yeast, if CIKS was able to form oligomers. Yeast strain AH109

was transformed with various deletion mutants of CIKS fused to the GAL4DNA-BD in the presence of full-length CIKS fused to the GAL4AD (Fig. 1A). The ability of the two fusion proteins to interact was judged by growth of the yeast strain AH109 on selective media. It was possible to detect an interaction between CIKS-DNABD and CIKS-AD, suggesting that CIKS was able

to oligomerize, at least in yeast. While any deletion at the amino terminus of CIKS did not affect its ability to oligomerize, deletion of the carboxyl-terminus coiled-coil domain disrupted the interaction.

We confirmed the results obtained in yeast, in transient transfection experiments. HeLa cells were transfected with FLAG-tagged CIKS together with HA-tagged CIKS or HA-tagged deletion mutants of CIKS, lacking the amino- or the carboxyl-terminus (CIKS  $\Delta$ N300 and CIKS  $\Delta$ C300). Cell extracts were immunoprecipitated by using anti-FLAG antibodies and the co-immunoprecipitated proteins were visualized by Western blot with anti-HA-antibodies (Fig. 1B, upper panel). Full-length HA-CIKS and HA-CIKS  $\Delta$ N300 were co-immunoprecipitated with FLAG-CIKS (Fig. 1B upper panel, lanes 5 and 6) while HA-CIKS  $\Delta$ C300 was not (Fig. 1B upper panel, lane 7), despite the higher level of expression in HeLa cells. We obtained similar results also in HEK293 cells (data not shown). These data strongly suggest that CIKS is able to form homo-oligomers and that this ability resides in the C-terminal region.

#### CIKS is recruited to the IKK-complex

We previously demonstrated that CIKS interacts with NEMO/IKK $\gamma$  and when overexpressed activates the transcription factor NF- $\kappa$ B via IKKs [21]. Given the ability of CIKS to interact with NEMO/IKK $\gamma$  and to activate NF- $\kappa$ B, we investigated if CIKS was recruited to the IKK-complex. We reasoned that if forced expression of CIKS mimics the active form of the protein then, when overexpressed, CIKS might be recruited to the IKK-complex. To this purpose, HeLa cells were transiently transfected with an expression vector encoding FLAG-tagged CIKS and cellular extract was loaded onto a Superdex S200 HR Fast Protein Liquid Chromatography column. Fractions eluted from the column were analyzed for the presence of specific components of the IKK-complex and CIKS, using Western blot analysis (Fig. 2). The majority of endogenous IKK $\alpha$ , IKK $\beta$ , and NEMO/IKK $\gamma$  were eluted in a peak centered around a volume of 9 ml (relative molecular mass higher than 660,000 Da), confirming that the IKK-complex is preconstituted in unstimulated cells. Analysis of chromatographic distribution of transfected CIKS showed that this protein was eluted in the same fractions containing the components of the IKK-complex. In addition, immunoprecipitating transfected CIKS from these high molecular weight fractions, it was possible to detect endogenous NEMO/IKK $\gamma$  co-immunoprecipitating with transfected CIKS. To further demonstrate that the interaction of CIKS with the IKK-complex correlates with the functional activation of the complex, we immunoprecipitated endogenous IKK $\beta$  from the high molecular weight fractions and assayed its ability

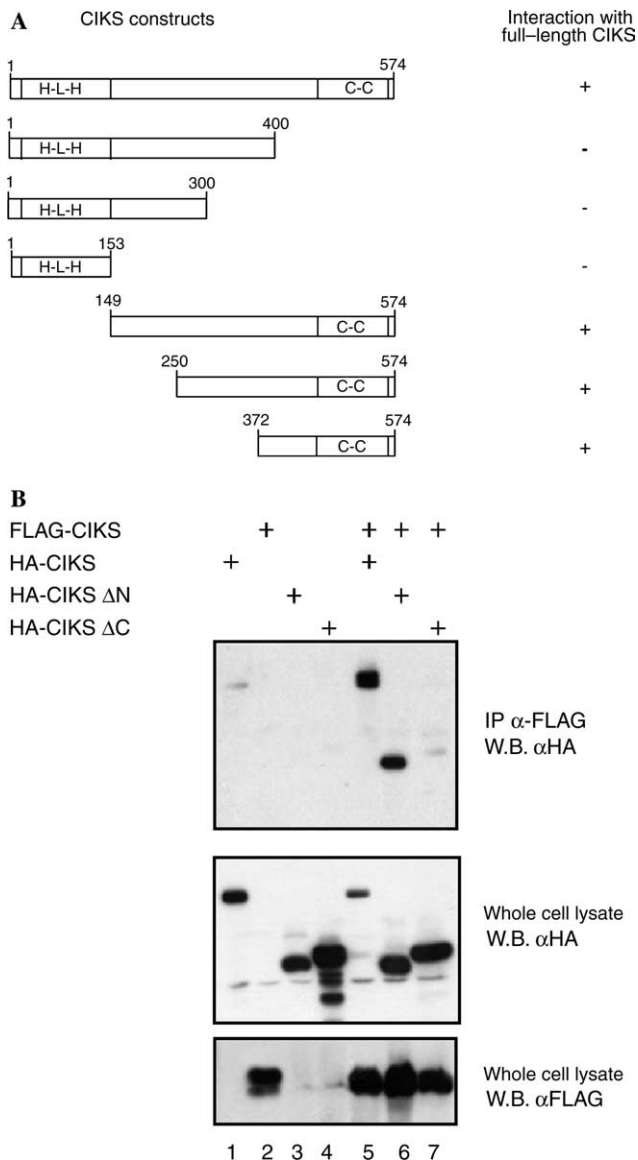


Fig. 1. Mapping the oligomerization domain of CIKS. (A) Yeast-two hybrid experiment. The CIKS constructs cloned in-frame with the GAL4 DNA binding domain of the vector pGBKT7 are schematically illustrated. Plus and minus signs indicate growth or absence of growth of the transformed yeast on medium lacking tryptophan, leucine, histidine, and adenine in the presence of 15 mM of 3-aminotriazole. (B) Co-immunoprecipitation experiment. HeLa cells were transfected with the indicated expression vector. Total extracts were immunoprecipitated with anti-FLAG antibodies followed by Western blot analyses with anti-HA antibodies (top panel). The presence of the different constructs in the whole cell lysate is demonstrated by Western blot in the middle and bottom panels.

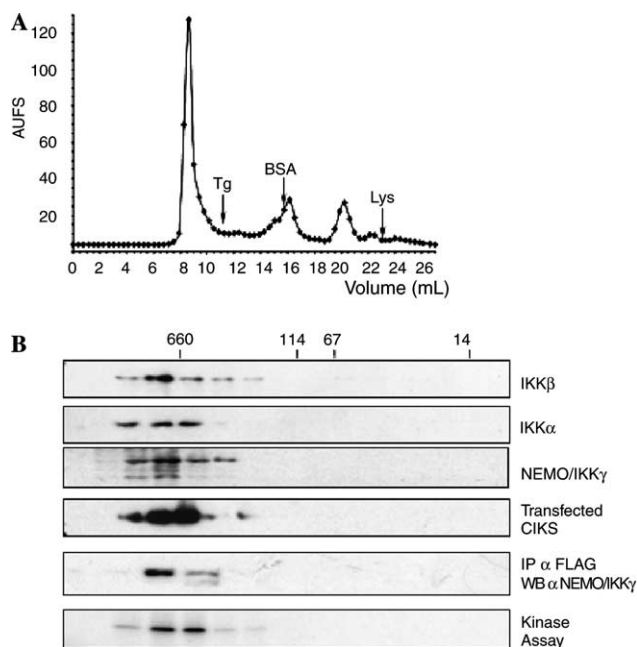


Fig. 2. Chromatographic distribution of CIKS in transfected cells. HeLa cells were transfected with an expression vector encoding FLAG-tagged CIKS. Cell extracts (S-100) were loaded onto a Superdex S200 FPLC column. (A) Elution profile of the column. Position of the molecular weight standards used to calibrate the column is indicated by arrows. Tg: thyroglobulin, MW 660,000Da; BSA: bovine serum albumin, MW 67,000Da; and Lys: lysozyme, MW 14,000. (B) Fractions isolated from the Superdex S-200 column were subjected to either Western blot or immunoprecipitation or kinase assay. For immunoprecipitation, fractions were incubated with anti-FLAG monoclonal antibodies (clone M2 from Sigma) bound to agarose beads. For kinase assay, fractions were incubated with anti-IKK $\beta$  antibodies (Santa Cruz #7607). Molecular weight markers are indicated at the top of the figure.

to phosphorylate GST-I $\kappa$ B $\alpha$ . It was possible to isolate a specific I $\kappa$ B kinase activity in high molecular weight fractions from CIKS transfected cells. These data demonstrated that transfected CIKS was recruited to the IKK-complex, via its ability to interact with NEMO/IKK $\gamma$  and triggered activation of the kinase activity of the complex.

We then analyzed the chromatographic distribution of endogenous CIKS in untransfected cells (Fig. 3). Most of the protein was eluted in a peak centered around a volume of 15 ml, corresponding to a molecular mass of about 70,000 Da, very similar to its predicted molecular weight of 64,000 Da. Recently, it has been reported that CIKS may function as an adaptor molecule in CD40-mediated pathways in epithelial cells [24]. In order to investigate if also the functionally active form of endogenous CIKS was recruited to the IKK-complex, we analyzed the chromatographic distribution of endogenous CIKS in HeLa cells after CD40 triggering. To this purpose HeLa cells were treated with a stimulating anti-CD40 antibody for thirty minutes. After stimulation, cells were washed and the lysate was

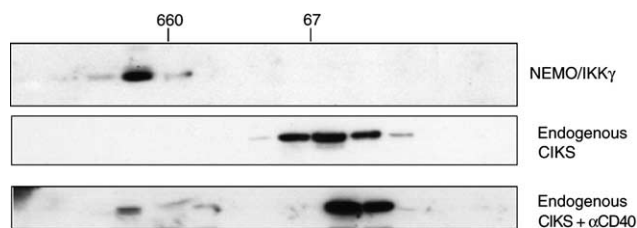


Fig. 3. Chromatographic distribution of endogenous CIKS. HeLa cells were either treated with a stimulating anti-CD40 monoclonal antibody (clone 14G7 from Caltag) for 30 min or left unstimulated. Cytoplasmic extracts (S100) were prepared and subjected to chromatography on a Superdex S-200 column. Fractions derived from the column were subjected to Western blot by using anti-NEMO/IKK $\gamma$  (Santa Cruz #8330) or anti-CIKS (Santa Cruz #11444 or rabbit polyclonal raised against a recombinant CIKS fragment) antibodies.

loaded onto a Superdex S200 HR Fast Protein Liquid Chromatography column. Part of endogenous CIKS was still eluted in a peak corresponding to a molecular mass of 70,000 Da. However, a fraction of CIKS moved to the high molecular weight fractions and was coeluted with components of the IKK-complex (Fig. 3), suggesting that following triggering of CD40, at least part of endogenous CIKS was recruited to the IKK-complex. These results suggested that endogenous CIKS was retained in the cytoplasm in a monomeric form in unstimulated cells, while after stimulation it was recruited to the IKK-complex.

#### *Both the N-terminal and the C-terminal regions of CIKS are required for interaction with NEMO/IKK $\gamma$*

We next investigated which region of CIKS was necessary for the interaction with NEMO/IKK $\gamma$ . HeLa cells were transfected with an expression vector encoding FLAG-tagged NEMO/IKK $\gamma$  in the presence of different HA-tagged CIKS deletion mutants. Cell extracts were immunoprecipitated by using anti-FLAG antibodies and the co-immunoprecipitated proteins were visualized by Western blot with anti-HA antibodies (Fig. 4). Full-length CIKS and the deletion mutant CIKS  $\Delta$ N87 were co-immunoprecipitated with FLAG-CIKS (Fig. 4 upper panel, lanes 7 and 10). Neither the  $\Delta$ N300 nor the  $\Delta$ C300 mutants interacted with NEMO/IKK $\gamma$ , thus suggesting that the central region of CIKS was involved in the interaction with NEMO/IKK $\gamma$ .

#### *CIKS oligomerization, recruitment to the IKK-complex, and interaction with NEMO/IKK $\gamma$ are not sufficient to activate the IKK-complex*

One of the proposed mechanisms for activation of the IKK-complex is that forced oligomerization of NEMO/IKK $\gamma$ , IKK $\alpha$ , and IKK $\beta$  can induce IKK and NF- $\kappa$ B activation [16]. Given the ability of CIKS to form oligomers, to be recruited to the IKK-complex and to

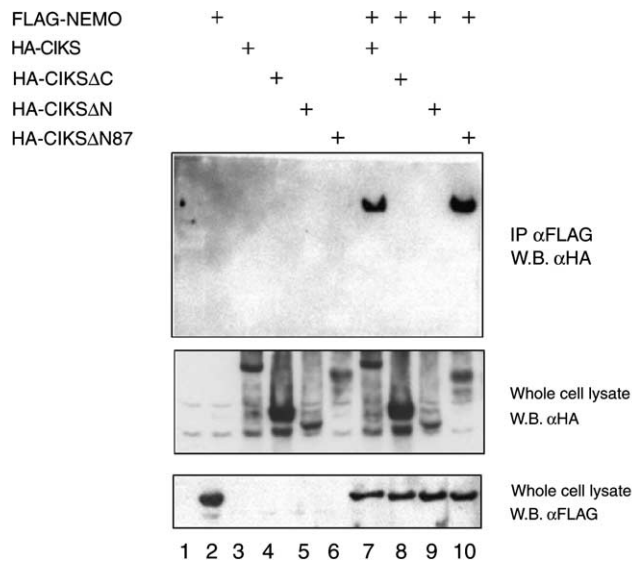


Fig. 4. Mapping the NEMO/IKK $\gamma$  interaction site on CIKS. HeLa cells were transfected with the indicated expression vectors. Total extracts were immunoprecipitated with anti-FLAG antibodies followed by Western blot analyses with anti-HA antibodies (top panel). The presence of the different constructs in the whole cell lysate is demonstrated by Western blot in the middle and bottom panels.

interact with NEMO/IKK $\gamma$ , we investigated which of these properties was necessary to activate NF- $\kappa$ B. HeLa cells were transfected with an Ig- $\kappa$ B luciferase reporter plasmid in presence of CIKS full-length or different deletion mutants of CIKS (Fig. 5A). Full-length CIKS

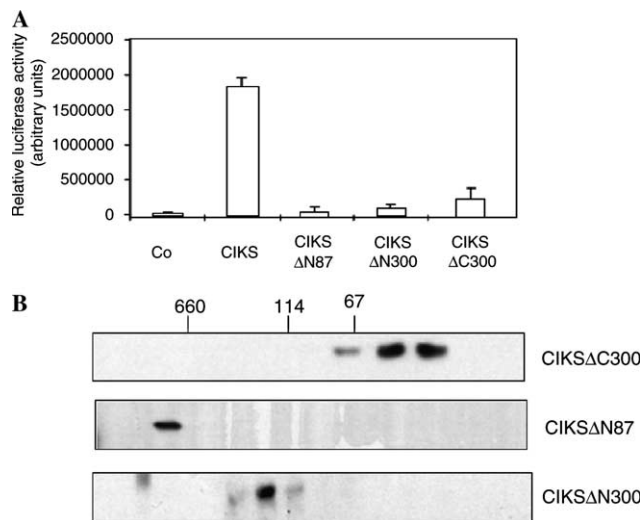


Fig. 5. (A) NF- $\kappa$ B activity of different CIKS constructs. Relative luciferase activity observed in HeLa cells transfected in triplicate with 0.5  $\mu$ g of Ig- $\kappa$ B luciferase reporter plasmid, with CIKS and different CIKS deletion mutants. Values shown (in arbitrary units) represent means ( $\pm$ SD) of three independent experiments, normalized for  $\beta$ -galactosidase activity of a cotransfected RSV- $\beta$ -galactosidase plasmid. (B) Chromatographic distribution of CIKS deletion mutants in transfected cells. HeLa cells were transfected with expression vectors encoding different FLAG-tagged CIKS deletion mutants. Fractions isolated from a Superdex S-200 column were subjected to Western blot analysis by using anti-FLAG antibodies.

was able to strongly activate a  $\kappa$ B-driven luciferase reporter plasmid, while the N-terminal deletion mutants  $\Delta$ N87 and  $\Delta$ N300 and the C-terminal deletion mutants  $\Delta$ C300 did not. The incapacity of the  $\Delta$ N300 and  $\Delta$ C300 mutants to activate NF- $\kappa$ B might be explained by the inability of these mutants to form oligomers and to interact with NEMO/IKK $\gamma$ . Interestingly, the  $\Delta$ N87 deletion mutant that forms oligomers and interacts with NEMO/IKK $\gamma$  does not activate NF- $\kappa$ B. The amount of each transfected plasmid was normalized given the different expression levels of these constructs (see Fig. 1B and data not shown).

Next we investigated the chromatographic distribution of these CIKS mutants. HeLa cells were transfected with the  $\Delta$ N87,  $\Delta$ N300, and  $\Delta$ C300 deletion mutants. Cell extracts (S100) were loaded onto a Superdex S200 HR Fast Protein Liquid Chromatography column and fractions eluted from the column were analyzed by Western blot by using anti-FLAG antibodies (Fig. 5B). The C-terminal deletion mutant  $\Delta$ C300 was eluted in a peak corresponding to a molecular mass of about 30,000 Da. The N-terminus deletion mutants  $\Delta$ N87 and  $\Delta$ N300 were eluted in peaks corresponding to molecular masses higher than 660,000 Da and of about 120,000 Da, respectively. The chromatographic distribution of these mutants reflected their ability to form oligomers and to interact with NEMO/IKK $\gamma$ . In fact, the  $\Delta$ C300 mutant that was not able to oligomerize and to interact with NEMO/IKK $\gamma$  was eluted at a volume corresponding to a molecular mass similar to its predicted molecular weight. In contrast, the  $\Delta$ N87 mutant, still able to interact with NEMO/IKK $\gamma$  and to oligomerize, was co-eluted with components of the IKK-complex. The  $\Delta$ N300 mutant that retained the ability to oligomerize but not to interact with NEMO/IKK $\gamma$  was eluted at a volume intermediate between the other two mutants.

Taken together these results suggest that the ability of CIKS to form oligomers and to be recruited to the IKK-complex resides in different regions of the protein and that both activities are necessary but not sufficient to correctly activate NF- $\kappa$ B.

## Discussion

In the present paper, we reported a functional characterization of the adaptor protein CIKS. We demonstrated that CIKS was able to form oligomers and once overexpressed was recruited to the IKK-complex through interaction with NEMO/IKK $\gamma$ . In addition, we demonstrated that both transfected CIKS and endogenous CIKS after CD40 triggering were recruited to the IKK-complex. The ability of CIKS to form oligomers resided in the C-terminal region, while the ability to interact with NEMO/IKK $\gamma$  was mediated by the central region of the protein. Both the capacities

to oligomerize and to interact with NEMO/IKK $\gamma$  were necessary to activate NF- $\kappa$ B. In fact, deletions affecting one of these functions abolished the ability of CIKS to activate NF- $\kappa$ B. However, these functions were not sufficient for a correct activation of NF- $\kappa$ B. In fact a small N-terminus deletion mutant ( $\Delta$ N87) still able to interact with NEMO/IKK $\gamma$  and to form oligomers did not activate NF- $\kappa$ B. Our data suggest that in addition to oligomerization and interaction with NEMO/IKK $\gamma$ , CIKS needs a second level of regulation to efficiently activate NF- $\kappa$ B.

CIKS has been proposed to interact with TRAF3 and by virtue of this interaction has been proposed to be involved in the CD40 signalling. Quian et al. [24] proposed a role for CIKS in the CD40 pathway. Based on this model CIKS is recruited to CD40 after receptor triggering. Our data extend this model, demonstrating that after CD40 triggering, CIKS connects the receptor and the IKK-complex, through its interaction with NEMO/IKK $\gamma$ , mediating the activation of NF- $\kappa$ B. It remains to be determined whether the IKK-complex is recruited to the cytoplasmic domain of the receptor or, after interaction with CD40, CIKS dissociates from the receptor to interact with NEMO/IKK $\gamma$ .

The functions of CIKS resemble those of TRAF proteins. These are adaptor molecules that mediate NF- $\kappa$ B activation by different receptors, such as members of the TNF and IL-1/Toll receptor family. Activation of NF- $\kappa$ B following TNF-receptor engagement is known to be initiated recruiting different adaptor molecules like TRADD, RIP, and TRAF on the trimerized cytoplasmic domain of the TNF receptor [31]. RIP and TRAF, in turn, transiently recruit and activate the IKK complex, via NEMO/IKK $\gamma$  [17,32]. However, it is not yet clear how the IKK-complex is activated. Recently, it has been demonstrated that the enforced oligomerization of NEMO/IKK $\gamma$  or any component of the IKK-complex is sufficient to activate the kinase activity of the complex. By virtue of its ability to form oligomers and to interact with NEMO/IKK $\gamma$  after CD40 triggering, CIKS may function in a similar way to activate the IKK-complex. However, while the ability of CIKS to oligomerize and to be recruited to the complex is both necessary to activate NF- $\kappa$ B, these are not sufficient. In fact, a small deletion of the N-terminal domain of CIKS (CIKS  $\Delta$ N87), that leaves unaltered the ability of CIKS to interact with NEMO/IKK $\gamma$ , to be recruited to the IKK-complex and to form oligomers, abolished its ability to activate NF- $\kappa$ B. It is possible that the  $\Delta$ N87 mutant is incapable of inducing conformational changes important for the activation of the kinase activity of the IKK-complex. However, it is tempting to speculate that the N-terminus of CIKS is interacting with some other adaptor molecule(s) or some kinase(s) that are, in turn, responsible for the activation of the IKK-complex. This hypothesis is currently under investigation. It has been

reported previously that CIKS interacts with the protein kinase TAK1 [24] but the exact role of this kinase in CD40-mediated NF- $\kappa$ B activation needs to be further addressed. In addition, the importance of other MAP3 kinase kinase kinase such as NIK, MEKK1, and MEKK3 in the activation of the IKKs is still controversial.

In summary, our data provide evidences about the role of the adaptor protein CIKS in the activation of the IKK-complex. After CD40 triggering CIKS is recruited to the IKK-complex, through its ability to interact with NEMO/IKK $\gamma$  and to form oligomers. However, these abilities are not sufficient to activate NF- $\kappa$ B, suggesting that CIKS needs a second level of regulation to efficiently activate NF- $\kappa$ B.

### Acknowledgments

The authors thank R. Acquaviva for assistance with the FPLC and helpful discussion. This work was supported by grants from AIRC (Associazione Italiana Ricerca sul Cancro) to A.L. and Ministero della Universita' e Ricerca Scientifica Grant 2001065217 to S.F.

### References

- [1] S. Ghosh, M. Karin, Missing pieces in the NF-kappaB puzzle, *Cell* (2002) S81–96.
- [2] N. Silverman, T. Maniatis, NF-kappaB signaling pathways in mammalian and insect innate immunity, *Genes Dev.* 15 (2001) 2321–2342.
- [3] I. Verma, J.K. Stevenson, E.M. Schwarz, D. Van Antwerp, S. Miyamoto, Rel/NF-kappa B/I kappa B family: intimate tales of association and dissociation, *Genes Dev.* 9 (1995) 2723–2735.
- [4] M. Karin, Y. Ben-Neriah, Phosphorylation meets ubiquitination: the control of NF-[kappa]B activity, *Annu. Rev. Immunol.* 18 (2000) 621–663.
- [5] J.A. Di Donato, M. Hayakawa, D.M. Rothwarf, E. Zandi, M. Karin, A cytokine-responsive IkappaB kinase that activates the transcription factor NF-kappaB, *Nature* 388 (1997) 548–554.
- [6] F. Mercurio, H. Zhu, B.W. Murray, A. Shevchenko, B.L. Bennett, Y. Li, D.B. Young, M. Barbosa, M. Mann, A. Manning, A. Rao, IKK-1, IKK-2: cytokine-activated IkappaB kinases essential for NF-kappaB activation, *Science* 278 (1997) 860–866.
- [7] C.H. Regnier, H.Y. Song, X. Gao, D.V. Goeddel, Z. Cao, M. Rothe, Identification and characterization of an IkappaB kinase, *Cell* 90 (1997) 373–383.
- [8] J.D. Woronicz, X. Gao, Z. Cao, M. Rothe, D.V. Goeddel, IkappaB kinase-beta: NF-kappaB activation and complex formation with IkappaB kinase-alpha and NIK, *Science* 278 (1997) 866–869.
- [9] E. Zandi, D.M. Rothwarf, M. Delhase, M. Hayakawa, M. Karin, The IkappaB kinase complex (IKK) contains two kinase subunits, IKKalpha, IKKbeta, necessary for IkappaB phosphorylation, NF-kappaB activation, *Cell* 91 (1997) 243–252.
- [10] S. Yamaoka, G. Courtois, C. Bessia, S.T. Whiteside, R. Weil, F. Agou, H.E. Kirk, R.Y. Kai, A. Israel, Complementation cloning of NEMO, a component of the IkappaB kinase complex essential for NF-kappaB activation, *Cell* 93 (1998) 1231–1240.
- [11] D.M. Rothwarf, E. Zandi, G. Natoli, N. Karin, IKK-gamma is an essential regulatory subunit of the IkappaB kinase complex, *Nature* 395 (1998) 297–300.

- [12] V. Heissmeyer, D. Krappmann, E.N. Hatada, C. Scheidereit, Shared pathways of IkappaB kinase-induced SCF(betaTrCP)-mediated ubiquitination and degradation for the NF-kappaB precursor p105, *IkappaBalpha*, *Mol. Cell. Biol.* 4 (2001) 1024–1035.
- [13] A. Salmeron, J. Janzen, Y. Soneji, N. Bump, J. Kamens, H. Allen, S.C. Ley, Direct phosphorylation of NF-kappaB1 p105 by the IkappaB kinase complex on serine 927 is essential for signal-induced p105 proteolysis, *J. Biol. Chem.* 276 (2001) 22215–22222.
- [14] U. Senftleben, Y. Cao, G. Xiao, F.R. Greten, G. Krahn, G. Bonizzi, Y. Chen, Y. Hu, A. Fong, S.C. Sun, M. Karin, Activation by IKKalpha of a second, *Science* 293 (2001) 1495–1499.
- [15] H. Sakurai, H. Chiba, H. Miyoshi, T. Sugita, W. Toriumi, IkappaB kinases phosphorylate NF-kappaB p65 subunit on serine 536 in the transactivation domain, *J. Biol. Chem.* 274 (1999) 30353–30356.
- [16] J.L. Poyet, S.M. Srinivasula, J.H. Lin, T. Fernandez-Alnemri, S. Yamaoka, P.N. Tsichlis, E.S. Alnemri, Activation of the Ikappa B kinases by RIP via IKKgamma/NEMO-mediated oligomerization, *J. Biol. Chem.* 275 (2000) 37966–37977.
- [17] S.Q. Zhang, A. Kovalenko, G. Cantarella, D. Wallach, Recruitment of the IKK signalosome to the p55 TNF receptor: RIP, A20 bind to NEMO (IKKgamma) upon receptor stimulation, *Immunity* 12 (2000) 301–311.
- [18] Z.L. Chu, Y.A. Shin, J.M. Yang, J.A. Di Donato, D.W. Ballard, IKKgamma mediates the interaction of cellular IkappaB kinases with the tax transforming protein of human T cell leukemia virus type 1, *J. Biol. Chem.* 274 (1999) 15297–15300.
- [19] E.W. Harhaj, S.C. Sun, IKKgamma serves as a docking subunit of the IkappaB kinase (IKK) and mediates interaction of IKK with the human T-cell leukemia virus Tax protein, *J. Biol. Chem.* 274 (1999) 22911–22914.
- [20] D.Y. Jin, V. Giordano, K.V. Kibler, H. Nakano, K.T. Jeang, Role of adapter function in oncoprotein-mediated activation of NF-kappaB. Human T-cell leukemia virus type I Tax interacts directly with IkappaB kinase gamma, *J. Biol. Chem.* 274 (1999) 17402–17405.
- [21] A. Leonardi, A. Chariot, E. Claudio, K. Cunningham, U. Siebenlist, CIKS, a connection to Ikappa B kinase and stress-activated protein kinase, *Proc. Natl. Acad. Sci. USA* 97 (2000) 10494–10499.
- [22] A. Chariot, A. Leonardi, J. Muller, M. Bonif, K. Brown, U. Siebenlist, Association of the adaptor TANK with the I kappa B kinase (IKK) regulator NEMO connects IKK complexes with IKK epsilon, TBK1 kinases, *J. Biol. Chem.* 277 (2002) 37029–37036.
- [23] X. Li, M. Commane, H. Nie, X. Hua, M. Chatterjee-Kishore, D. Wald, M. Haag, G.R. Stark, Act1 an NF-kappa B-activating protein, *Proc. Natl. Acad. Sci. USA* 97 (2000) 10489–10493.
- [24] Y. Qian, Z. Zhao, Z. Jiang, X. Li, Role of NF kappa B activator Act1 in CD40-mediated signaling in epithelial cells, *Proc. Natl. Acad. Sci. USA* 99 (2002) 9386–9391.
- [25] M. Kanamori, C. Kai, Y. Hayashizaki, H. Suzuki, NF-kappaB activator Act1 associates with IL-1/Toll pathway adaptor molecule TRAF6, *FEBS Lett.* 532 (2002) 241–246.
- [26] T.K. Ishida, T. Tojo, T. Aoki, N. Kobayashi, T. Ohishi, T. Watanabe, T. Yamamoto, J. Inoue, TRAF5 a novel tumor necrosis factor receptor-associated factor family protein, mediates CD40 signaling, *Proc. Natl. Acad. Sci. USA* 93 (1996) 9437–9442.
- [27] H. Nakano, H. Oshima, W. Chung, L. Williams-Abbott, C.F. Ware, H. Yagita, K. Okumura, TRAF5 an activator of NF-kappaB and putative signal transducer for the lymphotoxin-beta receptor, *J. Biol. Chem.* 271 (1996) 14661–14664.
- [28] C. Reinhard, B. Shamoony, V. Shyamala, L.T. Williams, Tumor necrosis factor alpha-induced activation of c-jun N-terminal kinase is mediated by TRAF2, *EMBO J.* 16 (1997) 1080–1092.
- [29] H.Y. Song, C.H. Regnier, C.J. Kirschning, D.V. Goeddel, M. Rothe, Tumor necrosis factor (TNF)-mediated kinase cascades: bifurcation of nuclear factor-kappaB and c-jun N-terminal kinase (JNK/SAPK) pathways at TNF receptor-associated factor 2, *Proc. Natl. Acad. Sci. USA* 94 (1997) 9792–9796.
- [30] V. Baud, Z.G. Liu, B. Bennett, N. Suzuki, Y. Xia, M. Karin, Signaling by proinflammatory cytokines: oligomerization of TRAF2, TRAF6 is sufficient for JNK, IKK activation and target gene induction via an amino-terminal effector domain, *Genes Dev.* 13 (1999) 1297–1308.
- [31] G. Chen, D.V. Goeddel, TNF-R1 signaling: a beautiful pathway, *Science* 296 (2002) 1634–1635.
- [32] A. Devin, A. Cook, Y. Lin, Y. Rodriguez, M. Kelliher, Z. Liu, The distinct roles of TRAF2, RIP in IKK activation by TNF-R1: TRAF2 recruits IKK to TNF-R1 while RIP mediates IKK activation, *Immunity* 12 (2000) 419–429.

G. Spagnuolo<sup>1\*</sup>, C. Mauro<sup>2</sup>,  
A. Leonardi<sup>2</sup>, M. Santillo<sup>3</sup>,  
R. Paternò<sup>4</sup>, H. Schweikl<sup>5</sup>,  
E.V. Avvedimento<sup>2</sup>, and S. Rengo<sup>1</sup>

<sup>1</sup>Department of Oral and Maxillofacial Sciences, <sup>2</sup>Department of Cellular and Molecular Biology and Pathology, <sup>3</sup>Department of Neuroscience, Unit of Physiology, and <sup>4</sup>Department of Clinical and Experimental Medicine, University of Naples "Federico II", via S. Pansini 5, 80131-Naples, Italy; and <sup>5</sup>Department of Operative Dentistry and Periodontology, University of Regensburg, 93042-Regensburg, Germany; \*corresponding author, gspagnuo@unina.it

*J Dent Res* 83(11):837-842, 2004

## ABSTRACT

The cytotoxicity of dental monomers has been widely investigated, but the underlying mechanisms have not been elucidated. We studied the molecular mechanisms involved in cell death induced by HEMA. In human primary fibroblasts, HEMA induced a dose-dependent apoptosis that was confirmed by the activation of caspases-8, -9, and -3. We found an increase of reactive oxygen species (ROS) and NF- $\kappa$ B activation after HEMA exposure. Blocking of ROS production by antioxidants had no direct influence on apoptosis caused by HEMA, but inhibition of NF- $\kappa$ B increased the fraction of apoptotic cells. Accordingly, mouse embryonic fibroblasts (MEF) from p65<sup>-/-</sup> mice were more susceptible to HEMA-induced apoptosis than were wild-type controls. Our results indicate that exposure to HEMA triggers apoptosis and that this mechanism is not directly dependent upon redox signaling. Nevertheless, ROS induction by HEMA activates NF- $\kappa$ B, which exerts a protective role in counteracting apoptosis.

**KEY WORDS:** NF- $\kappa$ B, HEMA, apoptosis, ROS, human fibroblasts.

# NF- $\kappa$ B Protection against Apoptosis Induced by HEMA

## INTRODUCTION

Studies on the degradation of dental resin composites have confirmed the release of substances like 2-hydroxyethyl methacrylate (HEMA) and triethyleneglycol dimethacrylate (TEGDMA) from resin composites and bonding agents. This release is highly dependent on the degree of polymerization of the system, which is never complete (Geurtsen, 2000).

HEMA is frequently used in dental bonding resins as a wetting agent. It competes with water for penetration and infiltration into dentin, and it copolymerizes with other monomers of resin composites (Peutzfeldt, 1997). HEMA has been shown to diffuse rapidly across dentin toward the pulp, and this may cause pulp irritation (Bouillaguet *et al.*, 1996).

Biological parameters such as cellular proliferation, vitality and cell death, mitochondrial activity, and protein or nucleic acid synthesis have been used as indicators of cellular responses to resin components (Hanks *et al.*, 1991; Kostoryz *et al.*, 2001; Schweikl *et al.*, 2001; Noda *et al.*, 2002). So far, few studies have assessed the type of cell death caused by dental monomers (Janke *et al.*, 2003; Engelmann *et al.* 2004; Spagnuolo *et al.*, 2004). Two modes of cell death have been described: apoptosis and necrosis. Apoptosis is an active and physiological mode of cell death, which permits the organism to eliminate unwanted or sub-lethally damaged cells without triggering inflammatory reactions. In contrast, necrosis generally sets off a tissue inflammation associated with clinical symptoms (Majno and Joris, 1995).

The execution of apoptosis is mediated by caspases, a family of cysteine proteases that plays a central role in the disassembly of the cell (Villa *et al.*, 1997). Caspase-9 is the initiator caspase of the mitochondrial pathway of apoptosis, while caspase-8 is an initiator caspase of death-receptor-induced apoptosis (Thornberry and Lazebnik, 1998). Reactive oxygen species (ROS)—including hydrogen peroxide, superoxide anion, and the hydroxyl radical—are involved in apoptosis. ROS may induce apoptosis directly or act as intracellular messengers induced by various kinds of stimuli (Mates and Sanchez-Jimenez, 2000).

Numerous studies suggest that ROS serve as common intracellular mediators of I $\kappa$ B degradation and subsequent NF- $\kappa$ B activation (Bauerle and Henkel, 1994). The NF- $\kappa$ B family of proteins is an inducible transcription factor that regulates the expression of genes involved in disparate processes such as immunity and inflammation, growth, development, cell-death regulation, and protection from apoptosis (Karin and Ben-Neriah, 2000). NF- $\kappa$ B is known to be one of the major pro-survival factors in many cells (Beg and Baltimore, 1996). In mammalian cells, there are 5 NF- $\kappa$ B proteins: p50, p52, p65 (RelA), RelB, and c-Rel. NF- $\kappa$ B is composed of homodimers and heterodimers of these proteins, typically p65:p50, which are held in the cytoplasm by the inhibitory I $\kappa$ B proteins. Several I $\kappa$ B proteins have been identified, including I $\kappa$ B $\alpha$ , I $\kappa$ B $\beta$ , I $\kappa$ B $\gamma$ , and I $\kappa$ B $\epsilon$  proteins, of which I $\kappa$ B $\alpha$  and I $\kappa$ B $\beta$  have been the best-studied (Karin

and Ben-Neriah, 2000). Activation of NF- $\kappa$ B is most often mediated by I $\kappa$ B degradation, which permits NF- $\kappa$ B to enter the nucleus (Karin, 1999).

Recent studies were focused on the type of cell death caused by dental materials and monomers (Cimpan *et al.*, 2000; Janke *et al.*, 2003; Spagnuolo *et al.*, 2004) and on a possible link between an increase in ROS levels and the toxicity of monomers (Stanislawski *et al.*, 2003). So far, there are no similar data available on HEMA toxicity. We hypothesized that HEMA causes an increase in the production of ROS, leading to apoptosis. We found that HEMA induced apoptosis and increased ROS levels in human primary skin fibroblasts. Unexpectedly, HEMA-induced apoptosis was not reduced but was enhanced by an anti-oxidant. Since several anti-oxidants are NF- $\kappa$ B inhibitors (Brennan and O'Neill, 1995), and considering that NF- $\kappa$ B is a pro-survival factor involved in protection from apoptosis, we further investigated the hypothesis that HEMA induces NF- $\kappa$ B activation by increasing ROS, speculating that HEMA-induced apoptosis is counteracted by NF- $\kappa$ B activation.

## MATERIALS & METHODS

### Cell Culture and Treatments

Human skin fibroblasts were obtained from punch biopsies taken from the forearms of healthy normal volunteers. The informed consent and protocol were reviewed and approved by the Institutional Review Board (University of Napoli "Federico II"). Primary explant cultures were established in 25-cm<sup>2</sup> culture flasks in Dulbecco's Modified Essential Medium (DMEM) containing 1000 mg/L glucose, 10% FBS, 2 mM glutamine, penicillin (100 U/mL), and streptomycin (100  $\mu$ g/mL). Monolayer cultures were maintained at 37°C in 5% CO<sub>2</sub>. All reagents were purchased from Invitrogen (Carlsbad, CA, USA). Fibroblasts between the 4th and the 10th subpassages were used in all experiments. Mouse embryonic fibroblasts (MEF) derived from wild-type mice and p65 knock-out mice (p65<sup>-/-</sup>) (gift from Dr. G. Franzoso) were cultured in the same way as human primary fibroblasts (De Smaele *et al.*, 2001).

For each experiment, HEMA (Sigma, St. Louis, MO, USA) was dissolved in dimethylsulfoxide (DMSO) (1 M stock solution) and then diluted in culture medium. Cells cultured in the presence of 0.3% DMSO alone served as the control in all experiments. A 10- $\mu$ M quantity of pyrrolidine dithiocarbamate (PDTC; Sigma), a low-molecular-weight thiol compound, was used as an anti-oxidant (Schreck *et al.*, 1992).

### Detection of Apoptosis

Cells were exposed to different concentrations of HEMA (0-10 mM) for 24 hrs at 37°C, harvested by centrifugation, and washed once with phosphate-buffered saline (PBS). Then, 1x 10<sup>5</sup>-10<sup>6</sup> cells were suspended in 500  $\mu$ L of binding buffer. Untreated and treated cells were stained with annexin V-FITC and propidium iodide (PI) (MBL Medical & Biological Laboratories Co., Ltd., Nagoya, Japan), and incubated at room temperature for 15 min before being analyzed by flow cytometry (FACScan, Becton-Dickinson, San Jose, CA, USA). Apoptotic cells (annexin V<sup>+</sup>) and necrotic cells (both PI<sup>+</sup>/annexin V<sup>+</sup> or PI<sup>+</sup> alone) were detected and quantified as a percentage of the entire population (Vermees *et al.*, 1995). Analysis of the data was performed by means of the WinMDI 2.8 program.

### Measurement of Intracellular ROS

Generation of reactive oxygen species was measured with the use of an oxidation-sensitive fluorescent probe, 2',7'-dichlorofluorescein diacetate (DCFH-DA; Molecular Probe, Inc., Eugene, OR, USA), whose oxidized form (2',7'-dichlorofluorescein, DCF) is highly fluorescent (Myhre *et al.*, 2003). Cells from routine cell cultures were harvested by centrifugation, washed twice with PBS, and suspended in 1 mL PBS. The cells were then loaded with 10  $\mu$ M DCFH-DA and incubated at 37°C for 15 min. After the addition of HEMA (from 0 to 10 mM), cells were incubated at 37°C for various times (from 0 to 60 min). We used a FACScan flow cytometer to measure ROS generation by the fluorescence intensity (FL-1, 530 nm) of 10,000 cells. Mean fluorescence intensity was obtained by histogram statistics with use of the WinMDI 2.8 program.

### SDS-PAGE and Western Blotting

Human skin fibroblasts were grown until 70-80% confluent and exposed to 0-10 mM HEMA for different time periods. Cytosolic extracts were then prepared with the use of a lysis buffer (20 mM HEPES, 1% Triton X-100, 150 mM NaCl, 10% glycerol), supplemented with protease inhibitors (Boehringer Mannheim, Mannheim, Germany) and phosphatase inhibitors (1 mM NaF, 1 mM Na<sub>3</sub>VO<sub>4</sub>). Equivalent amounts of proteins (40  $\mu$ g) were resolved on a 10% SDS-PAGE. Proteins were transferred to an Immobilon-P membrane (Millipore, Bedford, MA, USA). The membranes were blocked with 10% non-fat dry milk in TBS/Tween-20 and probed with rabbit polyclonal anti-caspases antibodies (-8, -9, and -3) and anti-I $\kappa$ B $\alpha$  (Santa Cruz Biotechnology Inc., Santa Cruz, CA, USA). The secondary antibody was a horseradish-peroxidase-linked anti-rabbit IgG (Amersham Biosciences, Little Chalfont, Buckinghamshire, England). Signals were detected by the ECL system (Amersham Biosciences, Little Chalfont, Buckinghamshire, England).

### EMSA (Electromobility shift assay)

Cells were treated with 10 mM HEMA for various time periods, and total cell extracts were prepared by the use of a detergent lysis buffer (50 mM Tris, pH 7.4, 250 mM NaCl, 0.5% Nonidet P-40, 50 mM NaF, 1 mM Na<sub>3</sub>VO<sub>4</sub> and complete protease inhibitor mixture [Roche]). Cells were harvested by centrifugation, washed once in cold PBS, and then re-suspended in lysis buffer (30  $\mu$ L 5 x 10<sup>6</sup> cells). The cell lysate was incubated on ice for 30 min and then centrifuged for 10 min at 10,000 x g at 4°C. The protein content of the supernatant was determined, and equal amounts of proteins (5  $\mu$ g) were added to a reaction mixture containing 20  $\mu$ g BSA, 2  $\mu$ g poly (di-dC), 10  $\mu$ L binding buffer (20 mM HEPES, pH 7.5, 10 mM MgCl<sub>2</sub>, 20% glycerol, 100 mM KCl, 0.2 mM EDTA, 0.5 mM dithiothreitol), and 100,000 cpm of a <sup>32</sup>P-labeled - $\kappa$ B oligonucleotide in a final volume of 20  $\mu$ L. For competition assay, a 100-ng quantity of non-radioactive - $\kappa$ B oligonucleotide was added to the reaction mixture. Samples were incubated at room temperature for 30 min and then run on a 4% acrylamide gel.

### Statistical Analysis

The statistical analyses of the data were performed by *t* tests or one-way ANOVA, followed by the Bonferroni procedure for multiple comparisons. The level of significance was set at *p* < 0.05.

## RESULTS

### Induction of Apoptosis and Caspases Activation by HEMA

In the concentration range of 4-10 mM HEMA, the fraction of

apoptotic cells increased linearly, reaching a level of 30.5% of cells at a concentration of 10 mM HEMA. In contrast, the fraction of necrotic cells did not significantly increase (Fig. 1A) (*n* = 4).

Various caspases were activated during HEMA-induced apoptosis. Caspase-3 was activated in a concentration-dependent manner after 24 hrs of treatment with HEMA (Fig. 1B). Caspase-3 activation started 6 hrs after treatment with 10 mM HEMA cells (Fig. 1C). Moreover, the processing of procaspases-9 and -8 appeared to be complete, as shown by the disappearance of the precursor forms (Fig. 1D).

**HEMA Induces ROS and NF-κB Activation**

HEMA increased ROS levels in a dose-dependent manner; treatment of cell culture with 10 mM HEMA produced a two-fold increase in fluorescence units compared with untreated controls (Fig. 2A) (*n* = 5). The time-course of ROS showed that ROS were produced immediately after HEMA treatment at all concentrations used. The increase of ROS in untreated cell cultures indicated high metabolic activity (Fig. 2B) (*n* = 5).

We treated the cells with 10 mM HEMA for 30, 60, and 180 min, and monitored the level of the NF-κB inhibitory subunit IκBα.

The levels of IκBα in cell lysates were decreased 180 min after exposure to 10 mM HEMA (Fig. 3A). In addition, IκBα degradation was dose-dependent (Fig. 3B). To assess the DNA binding of NF-κB, we performed an EMSA on total cell extracts. A 10-mM quantity of HEMA caused DNA binding after 180 min (Fig. 3C). The specificity of the protein-DNA complex was confirmed by a competition assay performed by a non-radioactive -κB oligonucleotide (Fig. 3C).

**NF-κB Counteracts HEMA-induced Apoptosis**

Since HEMA induced elevated ROS levels, we determined whether ROS mediates HEMA toxicity. To this end, we investigated the anti-oxidant effects of PDTC on HEMA-induced apoptosis. PDTC is a small thiol compound, which displays potent anti-oxidant activity (Schreck *et al.*, 1991). PDTC significantly blocked basal and HEMA-induced ROS (Fig. 4A). Paradoxically, PDTC alone did not affect basal apoptosis but significantly increased HEMA-induced apoptosis, notwithstanding the reduction of ROS (Fig. 4B). To identify the signals influenced by HEMA and PDTC, we treated cells with HEMA in the absence and in the presence of PDTC for 180 min and then determined IκBα degradation and

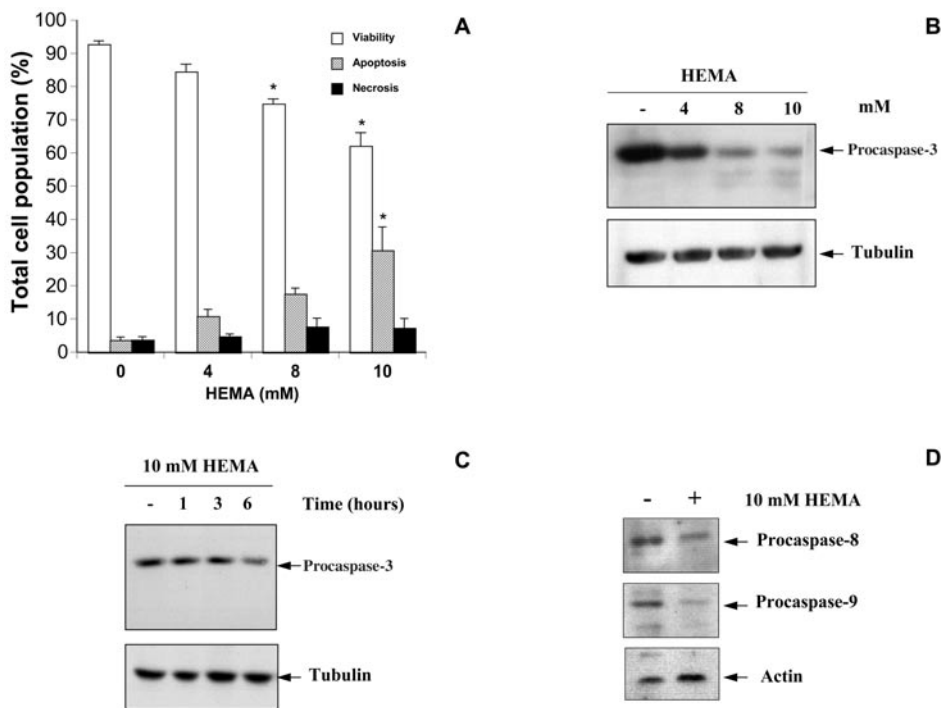


**Figure 1.** HEMA-induced apoptosis and caspases activation. (A) Dose-dependent induction of apoptosis. Cells were treated with various concentrations of HEMA for 24 hrs, and apoptotic and necrotic cells were stained with annexin V-FITC or PI, respectively. Cells were then detected and quantified by flow cytometry as a percentage of the entire population (see MATERIALS & METHODS). Results represent the means ± SEM of 4 independent experiments in duplicate (*n* = 4). \* Significantly different from the untreated control group (one-way ANOVA followed by Bonferroni *post hoc* test, *p* < 0.05). (B) Dose-dependent caspase-3 activation. Cytosolic extracts from cells treated with 0-10 mM HEMA for 24 hrs were analyzed by Western blotting with anti-caspase-3 antibodies. (C) Time-dependence of caspase-3 activation. The cells were treated with 10 mM HEMA for the indicated periods of time, and cytosolic extracts were analyzed by Western blotting with anti-caspase-3 antibodies. (D) Caspase-8 and -9 activation. Cytosolic extracts from cells treated with 10 mM HEMA for 24 hrs were analyzed by Western blotting with anti-caspase-8 and -9 antibodies. The amounts of cell lysate were normalized with the use of polyclonal anti-actin or tubulin antibodies. Each Western blot is representative of at least 2 independent experiments.

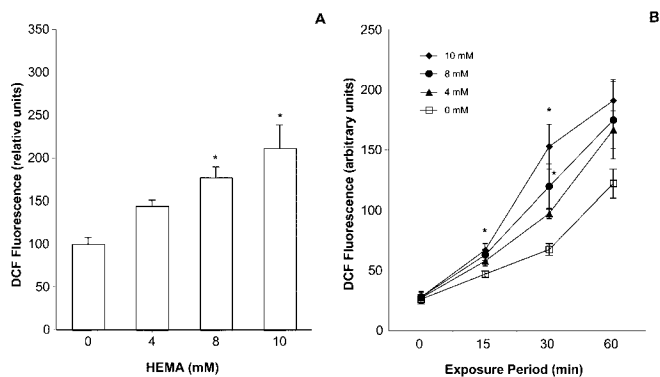


**Figure 2.** Generation of ROS by HEMA in human fibroblasts. Suspended cells were incubated with 10 μM DCFH-DA for 15 min at 37°C. (A) The indicated concentrations of HEMA were added to the cells and incubated for 30 min at 37°C. (B) From 0 to 10 mM HEMA was added to the cells and incubated for 15, 30, and 60 min at 37°C. DCF fluorescence was measured by means of a flow cytometer with an FL-1 filter. Results represent the means ± SEM (*n* = 5). \*Values are significantly different from untreated controls (one-way ANOVA followed by the Bonferroni *post hoc* test, *p* < 0.05).

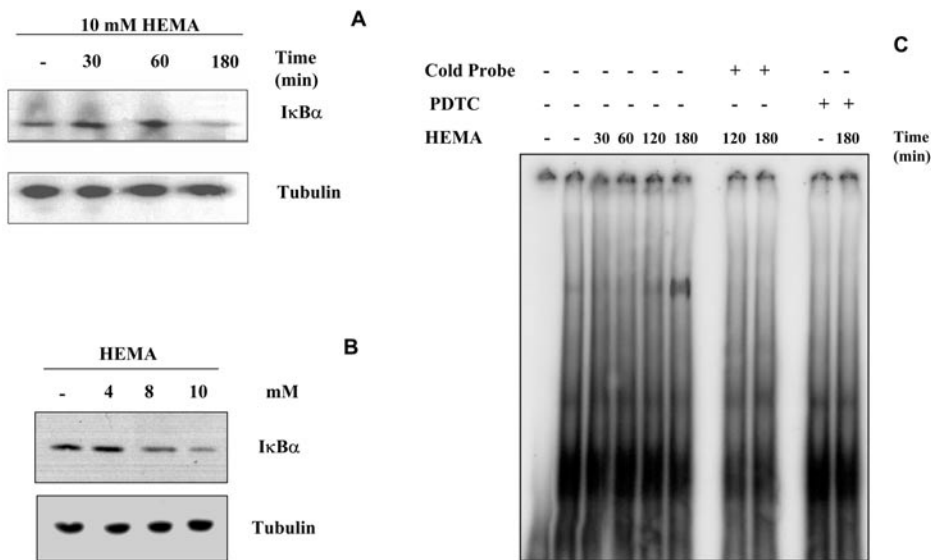


**Figure 3.** HEMA induces IκBα degradation and DNA binding of NF-κB. **(A)** The cells were treated with 10 mM HEMA for the indicated periods of time and **(B)** with 0-10 mM HEMA for 180 min. Cytosolic extracts were analyzed by Western blotting with anti-IκBα antibodies. The lower panel shows a Western blot anti-tubulin as control for protein loading. Experiments were performed 3 times, and a representative result is shown. **(C)** EMSA from cells treated with 10 mM HEMA for the indicated period of time with or without PDTC. Total cell extracts were prepared and analyzed by EMSA with a <sup>32</sup>P-labeled oligonucleotide probe containing a NF-κB-binding site. The middle portion of the autoradiograph shows the same cell extracts incubated with a 50-fold molar excess of unlabeled (cold) NF-κB oligonucleotide.

DNA binding of NF-κB. PDTC completely blocked the binding and IκBα degradation induced by 10 mM HEMA (Figs. 3C, 4C). Reduction of active NF-κB resulted in an amplification of apoptosis (Fig. 4B) ( $n = 3$ ). To investigate this hypothesis, we used MEF from p65<sup>-/-</sup> mice. MEF wild-type and p65<sup>-/-</sup> cells were treated with a sub-lethal concentration of 8 mM HEMA. Interestingly, p65<sup>-/-</sup> fibroblasts showed a significant increase ( $n = 3$ ) of apoptosis (three-fold) and necrosis (two-fold) compared with that in wild-type cells (Fig. 4D).

## DISCUSSION

In the present study, it was shown that HEMA elicited activation of apoptotic pathways in primary human fibroblasts. To elucidate the cell responses associated with HEMA-induced apoptosis, we investigated the roles of several components of apoptotic cell death mechanisms. We found evidence that HEMA caused cell death predominantly due to apoptosis rather than necrosis. This finding was confirmed quantitatively by flow cytometry and supported by caspases activation. HEMA induced processing of the initiator procaspases-8 and -9, and the common downstream effector procaspase-3. Apoptosis was dose- and time-dependent.

ROS are involved in apoptosis as well as in cell survival (Mates and Sanchez-Jimenez, 2000). Here, elevated levels of ROS were observed immediately after HEMA treatment. The amounts of ROS due to treatment with HEMA may be underestimated related to *in vivo* situations, since the solvent

DMSO has previously been reported to have ROS scavenger activity (Zegura *et al.*, 2004). ROS generation was completely reduced by a free radical scavenger such as PDTC. However, reduction of ROS generation by PDTC did not prevent HEMA-induced apoptosis. This strongly suggested that ROS do not directly mediate HEMA-induced toxicity.

Many studies have suggested that ROS serve as intracellular mediators of IκB degradation and subsequent NF-κB activation (Bauerle and Henkel, 1994). NF-κB has been implicated as a key regulatory molecule that may function to mediate a cellular survival response (Beg and Baltimore, 1996). In our experimental system, IκBα was degraded after 3 hrs of HEMA treatment. This delayed timing of IκB degradation and DNA binding of NF-κB suggests that HEMA did not directly induce NF-κB. It is likely that HEMA caused cell damage which, in turn, could be responsible for NF-κB activation.

The fact that PDTC can independently inhibit NF-κB activation has been used in support of a general model in which NF-κB activation is governed by oxidative stress (Schreck *et al.*, 1991, 1992; Moellering *et al.*, 1999). Evidence is emerging, however, that the major mode of the inhibitory action of PDTC may not be restricted to its anti-oxidant activity (Brennan and O'Neill, 1995). We have shown that inhibition of IκB degradation and DNA binding of NF-κB by PDTC significantly increased HEMA-induced apoptosis in human fibroblasts. This suggests that NF-κB may be important for protection from HEMA-induced apoptosis. The role played by NF-κB was further confirmed by the evidence that MEF from p65<sup>-/-</sup> mice are more susceptible to HEMA-induced apoptosis.

It has been shown that HEMA diffuses through dentin, and the risk of cytotoxic effects in pulp cells might be increased (Bouillaguet *et al.*, 1996). Noda *et al.* (2002) estimated that HEMA leaching from dentin adhesives might reach concentrations up to 1.5-8 mM in the pulp. This concentration is within the range of our study. If used in a direct pulp-capping procedure, then this concentration is clearly higher than those used here. The balance of the apoptotic-necrosis response induced by HEMA may have time-concentration dependence. Therefore, if the HEMA concentration is high, then apoptosis would never occur. If low, then apoptosis could be more prominent. This might be a critical feature in pulp-capping (direct or indirect), where high-acute or low-chronic amounts of HEMA are exposed to pulpal cells.

In summary, we demonstrated that HEMA induces cell death through an apoptotic pathway in primary human

fibroblasts, involving activation of caspase-8, -9, and -3. The HEMA-induced apoptosis is not directly dependent on the generation of ROS, because reduction of ROS by antioxidants had no effect on apoptosis. Moreover, we provided experimental evidence that NF- $\kappa$ B plays a major role in protecting cells from apoptosis induced by HEMA.

## ACKNOWLEDGMENT

This project was supported by the Medical School of the University of Naples "Federico II", by MIUR (Italian Ministry of University and Research) and by AIRC (Associazione Italiana Ricerca sul Cancro).

## REFERENCES

- Baeuerle PA, Henkel T (1994). Function and activation of NF- $\kappa$ B in the immune system. *Annu Rev Immunol* 12:141-179.
- Beg AA, Baltimore D (1996). An essential role for NF- $\kappa$ B in preventing TNF- $\alpha$ -induced cell death. *Science* 274:782-784.
- Bouillaguet S, Wataha JC, Hanks CT, Ciucchi B, Holz J (1996). In vitro cytotoxicity and dentin permeability of HEMA. *J Endod* 22:244-248.
- Brennan P, O'Neill LA (1995). Effects of oxidants and antioxidants on nuclear factor kappa B activation in three different cell lines: evidence against a universal hypothesis involving oxygen radicals. *Biochim Biophys Acta* 1260:167-175.
- Cimpan MR, Cressey LL, Skaug N, Halstensen A, Lie SA, Gjertsen BT, et al. (2000). Patterns of cell death induced by eluates from denture base acrylic resins in U-937 human monoblastoid cells. *Eur J Oral Sci* 108:59-69.
- De Smaele E, Zazzeroni F, Papa S, Nguyen DU, Jin R, Jones J, et al. (2001). Induction of gadd45beta by NF-kappaB downregulates pro-apoptotic JNK signalling. *Nature* 414:308-313.
- Engelmann J, Janke V, Volk J, Leyhausen G, von Neuhoff N, Schlegelberger B, et al. (2004). Effects of BisGMA on glutathione metabolism and apoptosis in human gingival fibroblasts in vitro. *Biomaterials* 25:4573-4580.
- Geurtsen W (2000). Biocompatibility of resin-modified filling materials. *Crit Rev Oral Biol Med* 11:333-355.
- Hanks CT, Strawn SE, Wataha JC, Craig RG (1991). Cytotoxic effects of resin components on cultured mammalian fibroblasts. *J Dent Res* 70:1450-1455.
- Janke V, von Neuhoff N, Schlegelberger B, Leyhausen G, Geurtsen W (2003). TEGDMA causes apoptosis in primary human gingival fibroblasts. *J Dent Res* 82:814-818.
- Karin M (1999). How NF- $\kappa$ B is activated: the role of the I $\kappa$ B kinase (IKK) complex. *Oncogene* 18:6867-6874.
- Karin M, Ben-Neriah Y (2000). Phosphorylation meets ubiquitination: the control of NF-kappaB activity. *Annu Rev Immunol* 18:621-663.
- Kostoryz EL, Tong PY, Strautman AF, Glaros AG, Eick JD, Yourtee DM (2001). Effects of dental resin on TNF- $\alpha$ -induced ICAM-1 expression in endothelial cells. *J Dent Res* 80:1789-1792.
- Majno G, Joris I (1995). Apoptosis, oncosis, and necrosis. An overview of cell death. *Am J Pathol* 146:3-15.
- Mates JM, Sanchez-Jimenez FM (2000). Role of reactive oxygen species in apoptosis: implications for cancer therapy. *Int J Biochem Cell Biol* 32:157-170.
- Moellering D, McAndrew J, Jo H, Darley-Usmar VM (1999). Effects of pyrrolidine dithiocarbamate on endothelial cells: protection against oxidative stress. *Free Radic Biol Med* 26:1138-1145.
- Myhre O, Andersen JM, Aarnes H, Fonnum F (2003). Evaluation of the probes 2',7'-dichlorofluorescein diacetate, luminol, and lucigenin as indicators of reactive species formation. *Biochem Pharmacol* 65:1575-1582.
- Noda M, Wataha JC, Kaga M, Lockwood PE, Volkmann KR, Sano H (2002). Components of dental adhesives modulate heat shock

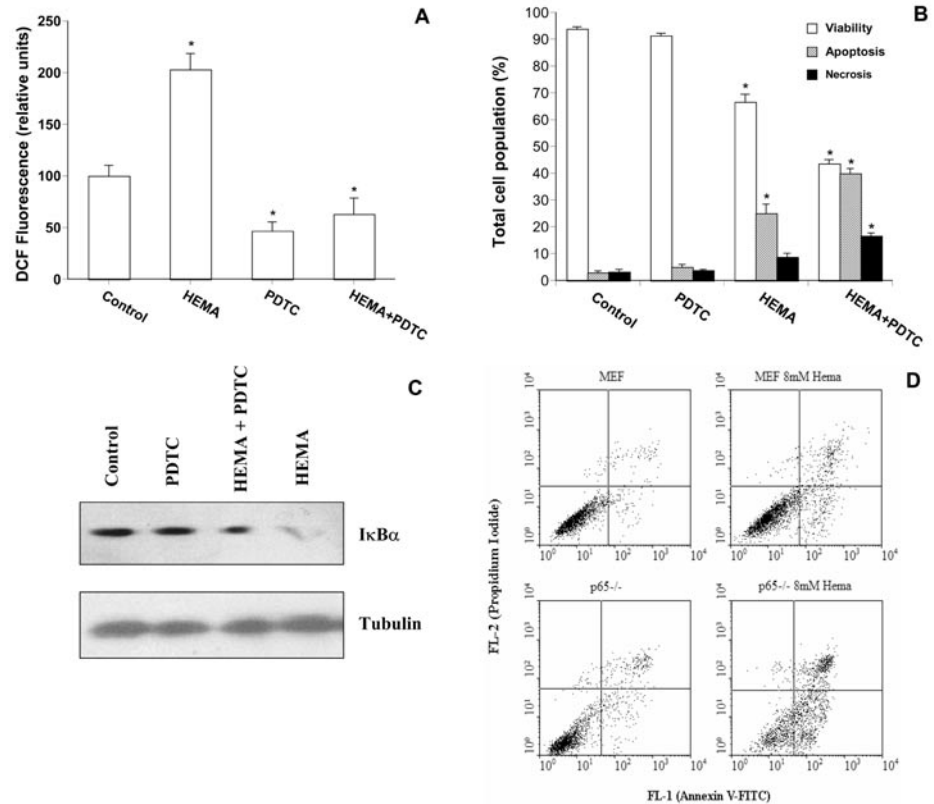


**Figure 4.** Effects of PDTc on ROS production, apoptosis, and I $\kappa$ B $\alpha$  degradation induced by HEMA. Cells were pre-treated with 10  $\mu$ M PDTc for 30 min. (A) The cells were loaded with DCFH-DA and further treated with 10 mM HEMA and PDTc for 30 min. DCF fluorescence was analyzed by flow cytometry. Results represent the means  $\pm$  SEM ( $n = 4$ ). (B) Apoptotic and necrotic cells were detected after 10 mM HEMA and PDTc treatments for 24 hrs. Results represent means  $\pm$  SEM ( $n = 3$ ). \*Values are significantly different from untreated controls (one-way ANOVA, followed by the Bonferroni *post hoc* test,  $p < 0.05$ ). (C) I $\kappa$ B $\alpha$  degradation was evaluated after 10 mM HEMA and PDTc treatment for 180 min. Western blot is representative of 2 independent experiments. (D) HEMA-induced apoptosis in MEF wild-type vs. p65<sup>-/-</sup> cells. MEF and p65<sup>-/-</sup> cells were treated with 8 mM HEMA for 24 hrs. Apoptotic (lower right quadrant) and necrotic (left and right upper quadrants) cells were then detected by flow cytometry. The dot plot is representative of 3 independent experiments.

- protein 72 expression in heat-stressed THP-1 human monocytes at sublethal concentrations. *J Dent Res* 81:265-269.
- Peutzfeldt A (1997). Resin composites in dentistry: the monomer systems. *Eur J Oral Sci* 105:97-116.
- Schreck R, Rieber P, Baeuerle PA (1991). Reactive oxygen intermediates as apparently widely used messengers in the activation of the NF- $\kappa$ B transcription factor and HIV-1. *EMBO J* 10:2247-2258.
- Schreck R, Meier B, Männel DN, Dröge W, Baeuerle PA (1992). Dithiocarbamates as potent inhibitors of nuclear factor- $\kappa$ B activation in intact cells. *J Exp Med* 175:1181-1194.
- Schweikl H, Schmalz G, Spruss T (2001). The induction of micronuclei *in vitro* by unpolymerized resin monomers. *J Dent Res* 80:1615-1620.
- Spagnuolo G, Galler K, Schmalz G, Cosentino C, Rengo S, Schweikl H (2004). Inhibition of phosphatidylinositol 3-kinase amplifies TEGDMA-induced apoptosis in primary human pulp cells. *J Dent Res* 83:703-707.
- Stanislawski L, Lefeuvre M, Bourd K, Soheili-Majd E, Goldberg M, Perianin A (2003). TEGDMA-induced toxicity in human fibroblasts is associated with early and drastic glutathione depletion with subsequent production of oxygen reactive species. *J Biomed Mater Res* 66(A):476-482.
- Thornberry NA, Lazebnik Y (1998). Caspases: enemies within. *Science* 281:1312-1316.
- Vermes I, Haanen C, Steffens-Nakken H, Reutelingsperger C (1995). A novel assay for apoptosis. Flow cytometric detection of phosphatidylserine expression on early apoptotic cells using fluorescein labelled annexin V. *J Immunol Methods* 184:39-51.
- Villa P, Kaufmann SH, Earnshaw WC (1997). Caspases and caspase inhibitors. *Trends Biochem Sci* 22:388-392.
- Zegura B, Lah TT, Filipic M (2004). The role of reactive oxygen species in microcystin-LR-induced DNA damage. *Toxicology* 200(1):59-68.

## Oncogenic and Anti-apoptotic Activity of NF- $\kappa$ B in Human Thyroid Carcinomas\*

Received for publication, March 30, 2004, and in revised form, September 23, 2004  
Published, JBC Papers in Press, October 8, 2004, DOI 10.1074/jbc.M403492200

Francesco Pacifico<sup>‡§</sup>, Claudio Mauro<sup>§¶</sup>, Ciro Barone<sup>¶</sup>, Elvira Crescenzi<sup>¶</sup>, Stefano Mellone<sup>‡</sup>, Mario Monaco<sup>||</sup>, Gennaro Chiappetta<sup>||</sup>, Giuseppe Terrazzano<sup>¶</sup>, Domenico Liguoro<sup>‡</sup>, Pasquale Vito<sup>\*\*</sup>, Eduardo Consiglio<sup>¶¶</sup>, Silvestro Formisano<sup>¶</sup>, and Antonio Leonardi<sup>¶¶¶</sup>

From the <sup>‡</sup>Istituto di Endocrinologia ed Oncologia Sperimentale, CNR, the <sup>¶</sup>Dipartimento di Biologia e Patologia Cellulare e Molecolare, "Federico II," University of Naples, via S. Pansini, 5, <sup>||</sup>Istituto Nazionale Tumori "Fondazione G. Pascale," via M. Semmola, 80131 Naples, and the <sup>\*\*</sup>Dipartimento di Scienze Biologiche ed Ambientali, Facoltà di Scienze MM. FF. NN., Università degli Studi del Sannio, via Port'Arso, 11, 82100 Benevento, Italy

Thyroid cancer includes three types of carcinomas classified as differentiated thyroid carcinomas (DTC), medullary thyroid carcinomas, and undifferentiated carcinomas (UTC). DTC and medullary thyroid carcinomas generally have a good prognosis, but UTC are usually fatal. Consequently, there is a need for new effective therapeutic modalities to improve the survival of UTC patients. Here we show that NF- $\kappa$ B is activated in human thyroid neoplasms, particularly in undifferentiated carcinomas. Thyroid cell lines, reproducing *in vitro* the different thyroid neoplasias, also show basal NF- $\kappa$ B activity and resistance to drug-induced apoptosis, which correlates with the level of NF- $\kappa$ B activation. Activation of NF- $\kappa$ B in the DTC cell line NPA renders these cells resistant to drug-induced apoptosis. Stable expression of a super-repressor form of I $\kappa$ B $\alpha$  (I $\kappa$ B $\alpha$ M) in the UTC cell line FRO results in enhanced sensitivity to drug-induced apoptosis, to the loss of the ability of these cells to form colonies in soft agar, and to induce tumor growth in nude mice. In addition, we show that FRO cells display a very low JNK activity that is restored in FRO-I $\kappa$ B $\alpha$ M clones. Moreover, inhibition of JNK activity renders FRO-I $\kappa$ B $\alpha$ M clones resistant to apoptosis induced by chemotherapeutic agents. Our results indicate that NF- $\kappa$ B plays a pivotal role in thyroid carcinogenesis, being required for tumor growth and for resistance to drug-induced apoptosis, the latter function very likely through the inhibition of JNK activity. Furthermore, the strong constitutive NF- $\kappa$ B activity in human anaplastic thyroid carcinomas, besides representing a novel diagnostic tool, makes NF- $\kappa$ B a target for the development of novel therapeutic strategies.

Thyroid carcinomas are one of the most common neoplasias of the endocrine system (1). Four types of thyroid cancer comprise more than 98% of all thyroid tumors: papillary thyroid carcinoma, follicular thyroid carcinoma, both of which may be summarized as differentiated thyroid carcinoma, medullary

thyroid carcinoma (MTC),<sup>1</sup> and undifferentiated anaplastic thyroid carcinoma (ATC) (2). Papillary thyroid carcinoma, follicular thyroid carcinoma, and ATC are derived from the thyroid follicular epithelial cells, whereas MTC is derived from the parafollicular C cells (3). Papillary thyroid carcinoma is the most common malignant thyroid neoplasm in countries with sufficient iodine diets and comprises up to 80% of all thyroid malignancies. Follicular thyroid carcinoma is more common in regions with insufficient iodine diets and represents ~10–20% of all thyroid malignancies. The overall 5–10 year survival rate of patients with papillary thyroid carcinoma is about 80–95%, whereas that of patients with follicular thyroid carcinoma is about 70–95% (3). The incidence of MTC is not well known because epidemiologic studies are rare. Generally, it is believed that MTC comprises about 5–10% of all thyroid malignancies (2–4). ATC is one of the most aggressive human malignancies, with a very poor prognosis. Although rare, accounting for up to 10% of clinically recognized thyroid cancers, the overall median survival is limited to months (2, 3, 5). Surgery, radiotherapy, and chemotherapy, based primarily on doxorubicin and cisplatin treatment, do not meaningfully improve survival of ATC patients (5, 6). Consequently, there is a need for new therapeutic tools for the treatment of these tumors.

The NF- $\kappa$ B family of transcription factors regulates the expression of a wide spectrum of genes involved in inflammation, immune response, cellular stress, cancer, and apoptosis (7–9). In most cell types, NF- $\kappa$ B is present in a latent form in the cytoplasm and bound to NF- $\kappa$ B inhibitory proteins collectively termed I $\kappa$ Bs (10). A wide variety of extracellular signals, such as pro-inflammatory cytokines, bacterial and viral infections, oxidative stress, etc., initiate signaling cascade that culminates in the phosphorylation and subsequent degradation of I $\kappa$ Bs, through a proteasome-dependent pathway (11, 12). Degradation of I $\kappa$ B frees NF- $\kappa$ B to enter the nucleus and to activate transcription of target genes (11). I $\kappa$ B phosphorylation is mediated by a large complex referred to as the I $\kappa$ B kinase complex (IKK complex), composed of two catalytic subunits, IKK $\alpha$  and IKK $\beta$  (13) as well as a regulatory protein, named NEMO/IKK $\gamma$  (14, 15).

\* This work was supported by grants from Associazione Italiana Ricerca sul Cancro, MIUR-FIRB RBNE0155LB, and Centro di Competenza GEAR. The costs of publication of this article were defrayed in part by the payment of page charges. This article must therefore be hereby marked "advertisement" in accordance with 18 U.S.C. Section 1734 solely to indicate this fact.

§ Both authors contributed equally to this work.

¶¶ To whom correspondence should be addressed: Dept. di Biologia e Patologia Cellulare e Molecolare, Federico II University of Naples, Via S. Pansini 5, 80131, Naples, Italy. Tel.: 39-081-7463606; Fax: 39-081-7701016; E-mail: leonardi@umina.it.

<sup>1</sup> The abbreviations used are: MTC, medullary thyroid carcinoma; NF- $\kappa$ B, nuclear factor- $\kappa$ B; IKK, I $\kappa$ B kinase; JNK, c-Jun NH<sub>2</sub>-terminal kinase; MAPK, mitogen-activated protein kinase; DTC, differentiated thyroid carcinomas; UTC, undifferentiated carcinomas; ATC, anaplastic thyroid carcinoma; EMSA, electromobility shift assay; Ab, antibody; PBS, phosphate-buffered saline; XIAP, X-linked inhibitor of apoptosis; CFSE, 5,6-carboxyfluorescein diacetate succinimidyl ester; GADD, growth arrest and DNA damage; TNF, tumor necrosis factor; MTS, 3-(4,5-dimethylthiazol-2-yl)-5-(3-carboxymethoxyphenyl)-2-(4-sulfophenyl)-2H-tetrazolium, inner salt.

Numerous studies have indicated that NF- $\kappa$ B activation can block cell-death pathways (16). NF- $\kappa$ B-inducible anti-apoptotic factors include those that inhibit caspase function, such as cellular inhibitor of apoptosis (17), X-linked inhibitor of apoptosis (XIAP) (18), and Fas-associated death domain-like interleukin 1 $\beta$ -converting enzyme (19), those that inhibit NF- $\kappa$ B signaling after TNF receptor stimulation, such as TNF receptor-associated factors (20), those that preserve function of mitochondria, such as Bcl-XL (21), and those that block JNK function, such as XIAP and growth arrest and DNA damage (GADD)45 $\beta$  (22). Because it has been proposed that suppression of apoptosis is associated with oncogenic potential, and given the ability of NF- $\kappa$ B inhibitors to increase susceptibility to apoptosis in transformed cells (23), one role for NF- $\kappa$ B activation could be to suppress transformation-associated apoptosis. The NF- $\kappa$ B signal transduction pathway is misregulated in a variety of human cancers, especially ones of lymphoid origin, due either to genetic changes (such as chromosomal rearrangements, amplifications, and mutations) or to chronic activation of the pathway by epigenetic mechanisms (24). Basal activation of the NF- $\kappa$ B pathway can contribute to the oncogenic state in several ways: by driving proliferation (25), by enhancing cell survival (26), by promoting angiogenesis, or by metastasis (27). Because the development of a highly malignant tumor requires several changes in cellular metabolism, including ones affecting apoptosis, it is not surprising that the NF- $\kappa$ B signal transduction pathway, which influences various aspects of cellular physiology, has emerged as playing a major role in many human cancers.

c-Jun NH<sub>2</sub>-terminal protein kinase (JNK), also known as stress-activated protein kinase (28), is a member of the mitogen-activated protein kinase superfamily (29), having three isoforms, JNK1, JNK2, and JNK3, with splicing variants (30).

Several lines of evidence suggest that JNK signaling is involved in stress-induced apoptosis via the mitochondrial pathway (30, 31), even though some studies have indicated that JNK may also contribute to cell survival (30). From different experimental evidence, it seems clear that the duration of JNK activation affects its role in apoptosis: *i.e.* prolonged but not transient JNK activation promotes TNF- $\alpha$ -induced apoptosis (32, 33). However, it has also been demonstrated that prolonged JNK activation alone may not be sufficient to induce apoptosis (33). Thus, the dual role of JNK in both apoptotic and antiapoptotic signaling pathways suggests that the function of JNK is complex and that the physiological response most likely reflects a balance between the ability of JNK to signal both apoptosis and cell survival. It has long been speculated that the role of the JNK pathway in apoptosis is affected by other signaling pathways. This has been recently demonstrated by two different groups (32, 33) in two independent ways. Both of them showed that NF- $\kappa$ B is able to inhibit TNF- $\alpha$ -induced apoptosis by negatively regulating activation of the JNK pathway. They also demonstrated that the negative regulation of JNK activity exerted by NF- $\kappa$ B is mediated by two genes, GADD45 $\beta$  (32) and XIAP (33), both of them under the transcriptional control of NF- $\kappa$ B.

Very little is known about the role that NF- $\kappa$ B plays in thyroid physiology. There is little evidence that NF- $\kappa$ B may be important in RET-mediated carcinogenesis and that may be involved in maintaining the transformed phenotype of thyroid cell lines (34, 35). However, the role that NF- $\kappa$ B plays "*in vivo*" in human thyroid neoplasia has not been fully investigated. Here we show that NF- $\kappa$ B is aberrantly expressed in primary human thyroid carcinomas, and we provide evidence that NF- $\kappa$ B is required for maintaining the transformed phenotype of UTC cells.

TABLE I  
NF- $\kappa$ B nuclear localization in normal and pathological human thyroid tissues

The percentage of cells with nuclear staining for NF- $\kappa$ B was scored from 0 to 3: 0, no positive cells; 1+, <10% of positive cells; 2+, 11–50% of positive cells; 3+, 76–100% of positive cells.

Histological type of thyroid samples	No. positive cases/no. total cases analyzed by immunohistochemistry	NF- $\kappa$ B staining score
Normal thyroid	0/4	0
Papillary carcinoma	6/6	1+
Follicular carcinoma	5/5	2+
Anaplastic carcinoma	4/4	3+

#### EXPERIMENTAL PROCEDURES

**Cell Lines**—NPA is a cell line derived from human papillary thyroid carcinoma (36); FRO is a cell line derived from human anaplastic thyroid carcinoma (37); and WRO is a cell line derived from human follicular thyroid carcinoma (38). They were grown in Dulbecco's modified Eagle's medium (Sigma) supplemented with 10% fetal bovine serum (Sigma). FRO cells were transfected with the empty expression vector pcDNA3.1-FLAG (Invitrogen) (FRO Neo cells) or with the expression vector pcDNA3.1-FLAG vector encoding a mutant form (S32A/S36A) of I $\kappa$ B $\alpha$  (FRO I $\kappa$ B $\alpha$ M cells) (a kindly gift of Dr. G. Franzoso) (32). NPA cells were transfected with the empty expression vector pcDNA3.1-FLAG (Invitrogen) (NPA Neo cells) or with the expression vector pcDNA3.1-FLAG vector encoding human IKK $\beta$  (39) (NPA IKK $\beta$  cells). The stable transfected clones were selected and maintained

FIG. 1. Immunohistochemical analysis of NF- $\kappa$ B activity in normal thyroid and anaplastic human thyroid carcinomas. Localization of RelA (p65) *in situ* was determined by immunohistochemistry in sections from normal thyroid tissue (A) and three different anaplastic thyroid carcinomas (B–D).

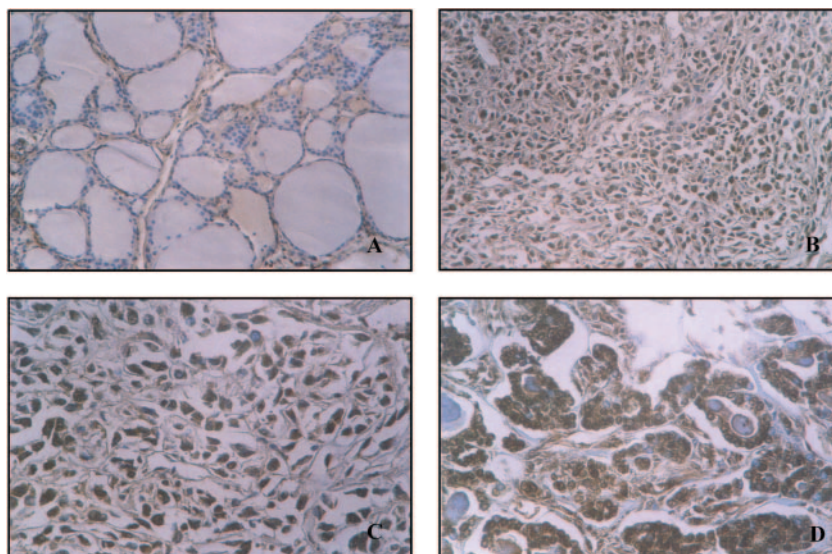


**FIG. 2. NF- $\kappa$ B activity in human thyroid carcinoma cell lines.** *A*, EMSA on total cell extracts from human thyroid carcinoma cell lines WRO, FRO, and NPA in the presence of a  $^{32}$ P-labeled NF- $\kappa$ B oligonucleotide alone (*lanes -*) or with a 50-fold molar excess of an analogous unlabeled oligonucleotide (*lanes +*) as competitor. *B*, reporter gene assay on human thyroid carcinoma cell lines WRO, FRO, and NPA cell lines. A plasmid, containing NF- $\kappa$ B-binding sites of immunoglobulin promoter region (Ig- $\kappa$ B) upstream to a promoterless luciferase reporter gene (Ig- $\kappa$ B-Luc), was transfected in thyroid carcinoma cell lines, and luciferase activity was measured 24 h later. Values shown (in arbitrary units) represent the means ( $\pm$ S.D.) of three independent experiments, normalized for  $\beta$ -galactosidase activity of a cotransfected Rous sarcoma virus- $\beta$ -galactosidase plasmid.

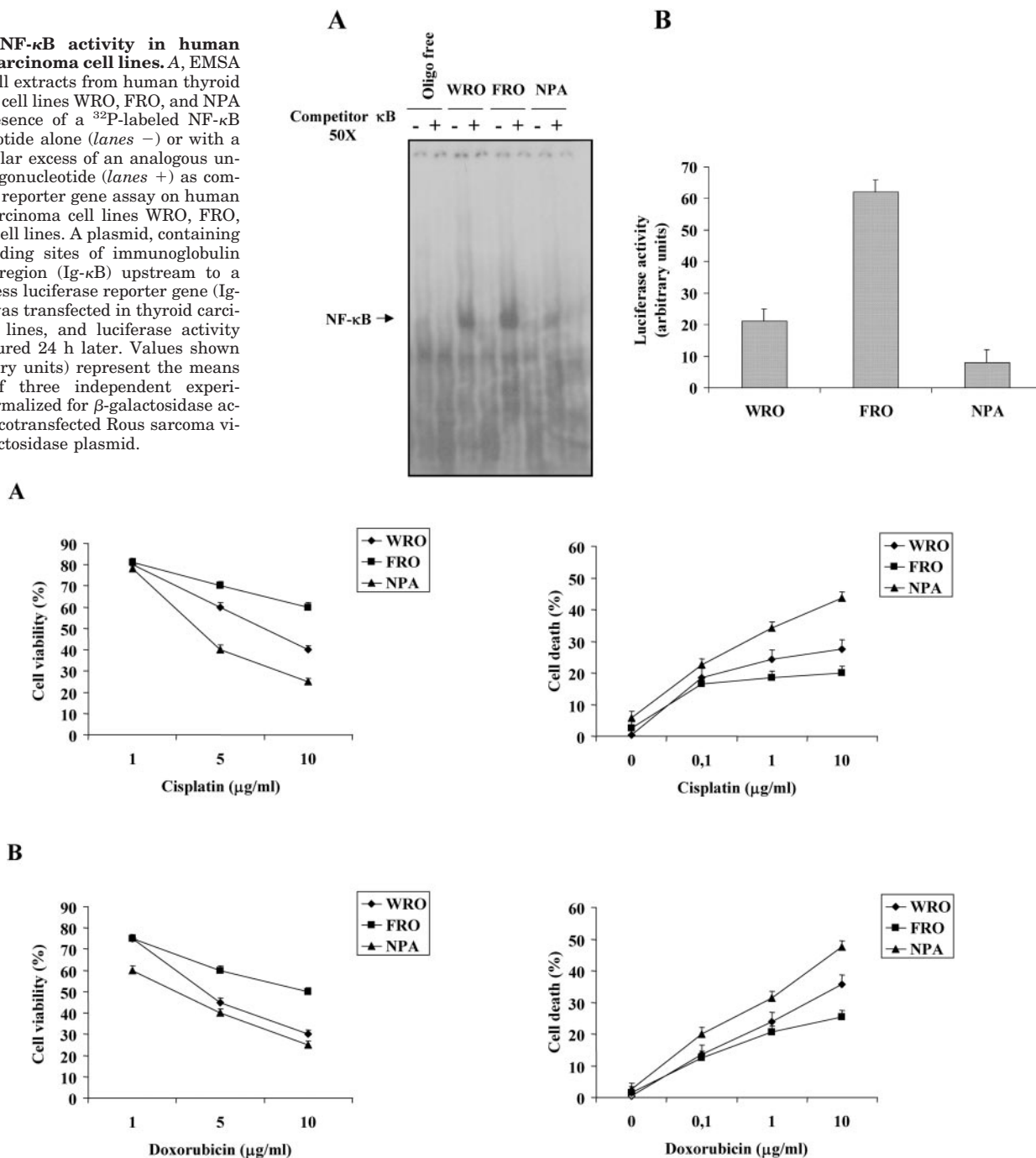


**FIG. 3. Cytotoxic effects of chemotherapeutic drugs on human thyroid carcinoma cell lines.**  $1 \times 10^3$  cells/well were seeded in 96-well culture plates and incubated for 48 h at 37 °C with different concentrations of cisplatin (*A*) or doxorubicin (*B*). Cell survival was examined by using MTS and an electron coupling reagent (phenazine methosulfate), according to the manufacturer's instructions (Promega, Madison, WI). Cell death was assessed by staining of exposed phosphatidylserine on cell membranes with fluorescein isothiocyanate-conjugated annexin V (Pharmingen). Samples were analyzed by flow cytometry using a FACSCalibur (Beckman Instruments, Fullerton, CA), equipped with ModFit Software. Results were mean  $\pm$  S.D. of at least three separate experiments.

in the presence of geneticin (200  $\mu$ g/ml).

**Immunohistochemical Analysis**—Specimens from normal and pathological human thyroid were isolated, rinsed with PBS, fixed in 4% buffered neutral formalin, and embedded in paraffin. 5–6- $\mu$ m-thick paraffin sections were then deparaffinized and placed in a solution of absolute methanol and 0.3% hydrogen peroxide for 30 min and then washed in PBS before immunoperoxidase staining. Slides were then incubated overnight at 4 °C in a humidified chamber with antibody anti-p65 diluted 1:100 in PBS and subsequently incubated, first with biotinylated goat anti-rabbit IgG for 20 min (Vectostain ABC kits, Vector Laboratories) and then with pre-mixed reagent ABC (Vector Laboratories) for 20 min. The antibody anti-p65 used was a rabbit polyclonal antibody from Santa Cruz Biotechnology (SC 7151). The

same results were obtained by using a mouse monoclonal anti-nuclear localization signal from Roche Applied Science. The immunostaining was performed by incubating slides in diaminobenzidine (Dako) solution containing 0.06 mM diaminobenzidine and 2 mM hydrogen peroxide in 0.05% PBS (pH 7.6) for 5 min, and after chromogen development, slides were washed, dehydrated with alcohol and xylene, and mounted with coverslips using a permanent mounting medium (Permount).

**Electromobility Shift Assays**—To analyze NF- $\kappa$ B DNA binding activity, total cell extracts were prepared using a detergent lysis buffer (50 mM Tris (pH 7.4), 250 mM NaCl, 50 mM NaF, 1 mM  $\text{Na}_3\text{VO}_4$ , 0.5% Nonidet P-40, 0.5 mM dithiothreitol, and Complete protease inhibitor mixture (Roche Applied Science)). Cells were harvested by centrifugation, washed once in cold PBS, and resuspended in detergent lysis

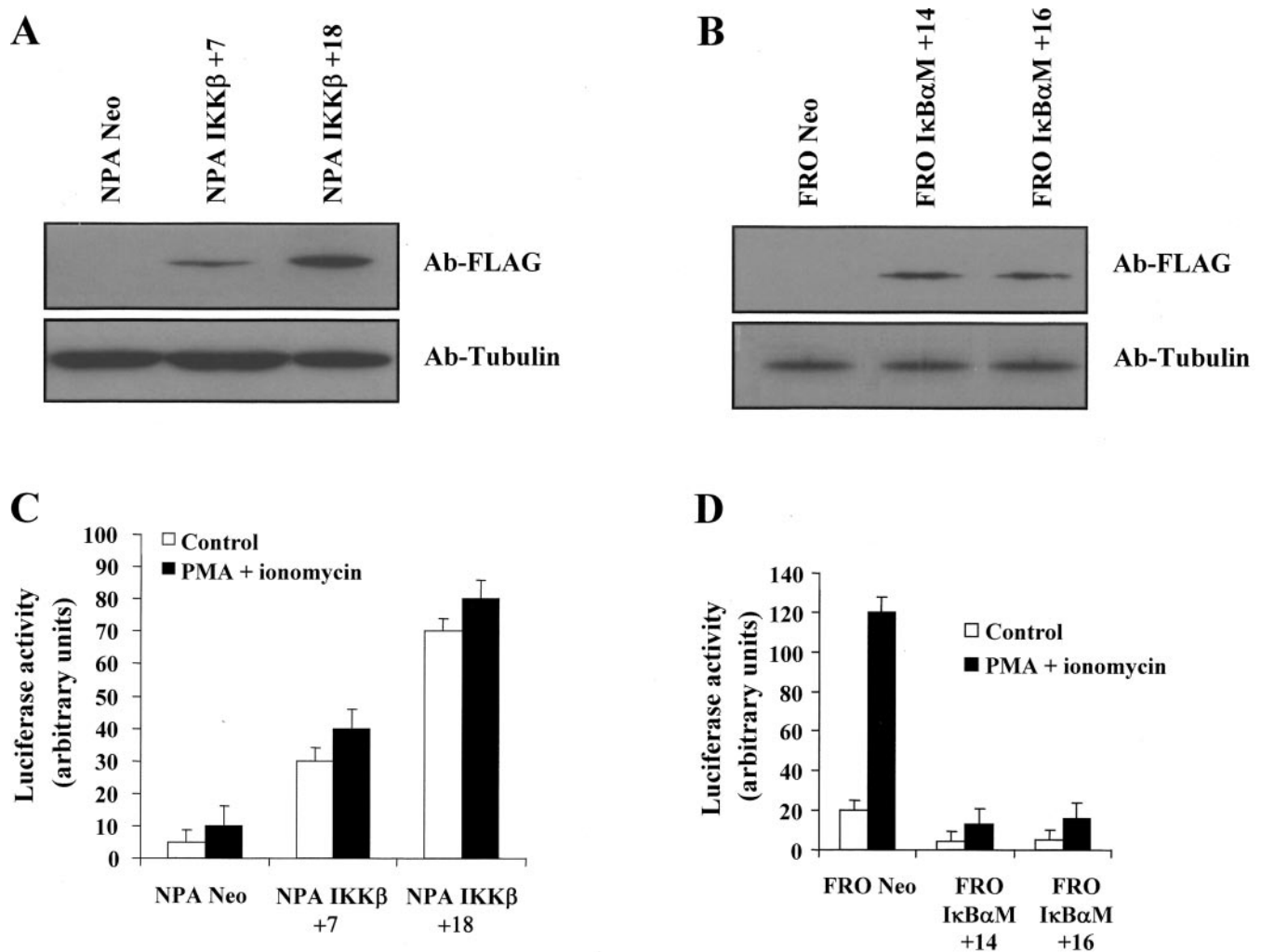


**FIG. 4. Characterization of NPA IKK $\beta$  and FRO I $\kappa$ B $\alpha$ M clones.** NPA cells were transfected with the empty vector pcDNA3.1-FLAG (Invitrogen) (NPA Neo cells) or with the pcDNA3.1-FLAG vector containing the full-length cDNA encoding human IKK $\beta$  (NPA IKK $\beta$  cells). FRO cells were transfected with the empty vector pcDNA3.1FLAG (Invitrogen) (FRO Neo cells) or with the pcDNA3.1FLAG vector containing the mutant form (S32A/S36A) of I $\kappa$ B $\alpha$  super-repressor (FRO I $\kappa$ B $\alpha$ M cells). The stable transfectants, selected and maintained in the presence of geneticin (200  $\mu$ g/ml), were characterized for their ability to express FLAG-tagged IKK $\beta$  (A) or I $\kappa$ B $\alpha$ M (B) proteins by Western blot analysis with the Ab-FLAG (F 7425) polyclonal antibody (Sigma), and to respond to phorbol 12-myristate-13-acetate (PMA) plus ionomycin treatment (C and D) by luciferase assay.

buffer (30  $\mu$ l/5  $\times$  10<sup>6</sup> cells). The cell lysate was incubated on ice for 30 min and then centrifuged for 5 min at 10,000  $\times$  g at 4  $^{\circ}$ C. The protein content of the supernatant was determined, and equal amounts of protein (10  $\mu$ g) were added to a reaction mixture containing 20  $\mu$ g of bovine serum albumin, 2  $\mu$ g of poly(dI-dC), 10  $\mu$ l of binding buffer (20 mM HEPES (pH 7.9), 10 mM MgCl<sub>2</sub>, 20% glycerol, 100 mM KCl, 0.2 mM EDTA, 0.5 mM dithiothreitol, and 0.5 mM phenylmethylsulfonyl fluoride), and 100,000 cpm of a <sup>32</sup>P-labeled oligonucleotide, containing specific binding sites for NF- $\kappa$ B, in a final volume of 20  $\mu$ l. Samples were incubated at room temperature for 30 min and run on a 4% acrylamide gel.

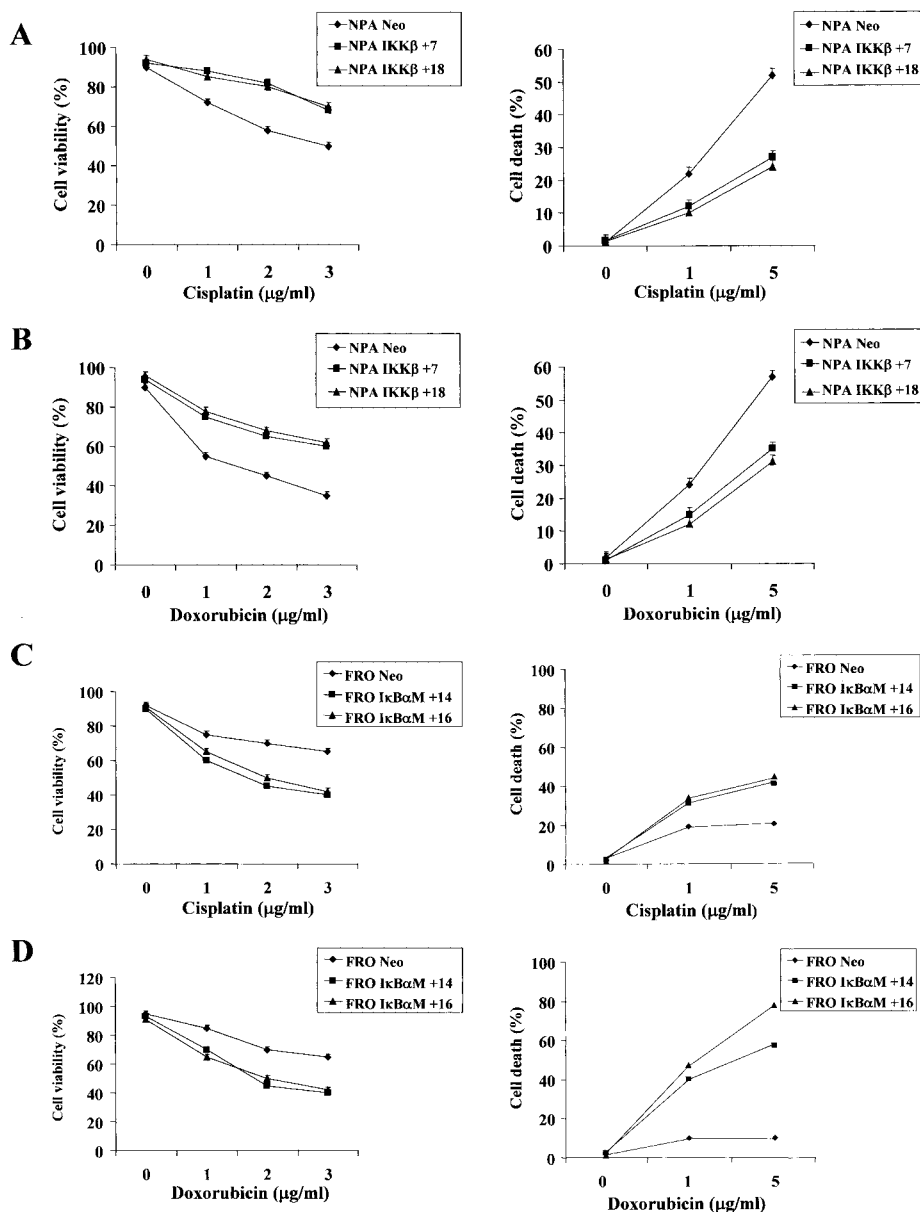
To analyze AP-1 DNA binding activity, nuclear extracts were prepared as follows: cells were harvested by centrifugation, washed once in cold PBS, and resuspended in buffer A (10 mM HEPES (pH 7.9), 10 mM KCl, 1.5 mM MgCl<sub>2</sub>, and 0.1 mM EGTA). The cells were then centrifuged for 5 min at 1,000  $\times$  g and resuspended in cold buffer C (20 mM HEPES (pH 7.9), 400 mM NaCl, 1.5 mM MgCl<sub>2</sub>, 0.1 mM EGTA, and 25% glycerol). The cell resuspension was subjected to strong shaking for 30 min at 4  $^{\circ}$ C and then centrifuged for 15 min at 1,000  $\times$  g. The protein content of the supernatant was determined, and equal amounts of protein (10  $\mu$ g) were added to a reaction mixture containing 20  $\mu$ g of bovine serum albumin, 2  $\mu$ g of poly(dI-dC), 10  $\mu$ l of binding buffer (20 mM HEPES (pH 7.9), 10 mM MgCl<sub>2</sub>, 20% glycerol, 100 mM KCl, 0.2 mM EDTA, 0.5 mM dithiothreitol, and 0.5 mM phenylmethylsulfonyl fluoride), and 100,000 cpm of wild-type or mutant <sup>32</sup>P-labeled AP-1 oligonucleotides, in a final volume of 20  $\mu$ l. Samples were incubated at room temperature for 30 min and run on a 4% acrylamide gel.

**Luciferase Assays**—4  $\times$  10<sup>5</sup> cells/well were seeded in a 6-well plate. After 12 h, cells were transfected with 0.5  $\mu$ g of the I $\kappa$ B-luciferase reporter gene plasmid. Cell extracts were prepared 24 h after transfection, and reporter gene activity was determined by the luciferase system (Promega). A pRSV- $\beta$ -galactosidase vector (0.2  $\mu$ g) was used to normalize for transfection efficiencies. Cells were stimulated with phorbol 12-myristate-13-acetate (400 ng/ml) plus ionomycin (2  $\mu$ M) for 3 h before lysis.

**In Vitro and in Vivo Tumorigenicity Assays**—To analyze the ability of the various FRO clones to form colonies in soft agar, 1  $\times$  10<sup>4</sup> cells were seeded in 60-mm dishes onto 0.3% Noble Agar (Difco) on top of a 0.6% bottom layer. Colonies larger than 50 cells were scored after 2 weeks incubation at 37  $^{\circ}$ C (40).

To analyze the ability of the various FRO clones to induce tumor growth in nude mice, 2  $\times$  10<sup>7</sup> cells were injected subcutaneously on a flank of each 6-week-old nude mouse (Charles River Breeding Laboratories, Lecco, Italy). Thirty days later, mice were killed, and tumors were excised. Tumors weight was determined, and their diameters were measured with calipers. Tumors volumes were calculated by the formula:  $a^2 \times b \times 0.4$ , where  $a$  is the smallest diameter, and  $b$  is the diameter perpendicular to  $a$ . No mouse showed signs of wasting or other visible indications of toxicity. The mice were maintained at the Dipartimento di Biologia e Patologia Cellulare e Molecolare animal facility and housed in barrier facilities on a 12-h light-dark cycle with food and water available *ad libitum*. The animal experiments described here were conducted in accordance with accepted standards of animal care and in accordance with the Italian regulations for the welfare of ani-

**FIG. 5. Cytotoxic effects of chemotherapeutic drugs on parental and transfected thyroid carcinoma cells.**  $1 \times 10^3$  cells/well were seeded in 96-well culture plates and incubated for 48 h at 37 °C with different concentrations of cisplatin or doxorubicin. Cell survival was examined by using MTS and an electron coupling reagent (phenazine methosulfate), according to manufacturer's instructions (Promega, Madison, WI). Cell death was assessed by staining of exposed phosphatidylserine on cell membranes with fluorescein isothiocyanate-conjugated annexin V (Pharmingen). Samples were analyzed by flow cytometry using a FACSCalibur (Beckman Instruments, Fullerton, CA), equipped with ModFit Software. A representative experiment out of three is shown. **A and B**, NPA Neo cells and NPA IKK $\beta$  clones; **C and D**, FRO Neo cells and FRO I $\kappa$ B $\alpha$ M clones.



mals used in studies of experimental neoplasia, and the study was approved by our institutional committee on animal care.

**Cytotoxic Treatments and Measurements of Apoptosis**— $1 \times 10^3$  cells/well were seeded in 96-well culture plates and incubated for 48 h at 37 °C with different concentrations of cisplatin or doxorubicin and, where indicated, with/without 10  $\mu$ M JNK inhibitor SP600125 (BioMol Research Laboratories Inc., Plymouth Meeting, PA). Cell survival was examined by using 3-(4,5-dimethylthiazol-2-yl)-5-(3-carboxymethoxyphenyl)-2-(4-sulfophenyl)-2H-tetrazolium, inner salt (MTS), and an electron coupling reagent (phenazine methosulfate), according to the manufacturer's instructions (Promega, Madison, WI). Cell death was assessed by staining of exposed phosphatidylserine on cell membranes with fluorescein isothiocyanate-conjugated annexin V (Pharmingen) or by propidium iodide staining according to Nicoletti *et al.* (41). Samples were analyzed by flow cytometry using a FACSCalibur (Beckman Instruments, Fullerton, CA), equipped with ModFit Software. Results were mean  $\pm$  S.D. of at least three separate experiments.

**Western Blot Analysis**—Subconfluent monolayers of parental and transfected FRO cells were washed three times with PBS and then lysed in a buffer containing 20 mM HEPES (pH 7.5), 150 mM NaCl, 10% glycerol, 1% Triton X-100, and a mixture of protease inhibitors (Sigma). An aliquot of the cell lysates was used to evaluate the protein content by colorimetric assay (Bio-Rad). Total proteins from cell lysates (50  $\mu$ g) were analyzed by 10% SDS-PAGE. After electroblotting of gels onto polyvinylidene difluoride sheets (Millipore, Bedford, MA), filters were

blocked for 1 h at room temperature with 10% non-fat dry milk in TBST buffer (10 mM Tris-HCl (pH 8.0), 0.1% Tween 20, 150 mM NaCl). The filters were then incubated in the same buffer for 14–16 h at 4 °C with 1:2000 dilution of the Ab-FLAG (F 7425) polyclonal antibody (Sigma). After TBST washing, blots were incubated for 1 h at room temperature with anti-rabbit horseradish peroxidase-conjugated antibodies (Amersham Biosciences) diluted 1:5000 in TBST buffer and then revealed by ECL (Amersham Biosciences).

A similar procedure was achieved to analyze phospho-JNK and total JNK levels on lysates from parental and transfected FRO cells after treatment with 10  $\mu$ g/ml anisomycin (Sigma) at different time intervals. In this case, the monoclonal Ab-pJNK1/2 (9255) (Cell Signaling Technology Inc., Beverly, MA) recognizing phosphorylated JNK or the polyclonal Ab-JNK1/2 (9252) (Cell Signaling Technology Inc.) recognizing total JNK were used at 1:1000 dilution. After TBST washing, blots were incubated for 1 h at room temperature with secondary antibodies horseradish peroxidase-conjugated (Amersham Biosciences), diluted 1:5000 in TBST buffer, and then revealed by ECL (Amersham Biosciences).

**$^3$ H/Thymidine DNA Incorporation**— $5 \times 10^4$  cells/well were seeded in 12-well culture plates and incubated for 4 h at 37 °C with 0.5  $\mu$ Ci/well of [ $^3$ H]thymidine (Amersham Biosciences). After three washings with cold PBS, cells were incubated for 10 min at 4 °C with 0.5 ml of 20% trichloroacetic acid. The trichloroacetic acid was removed, and cells were lysed with gentle shaking for 30 min at 37 °C in the presence of 1 N NaOH (0.5 ml/well). An aliquot of lysates (0.1 ml) was used to

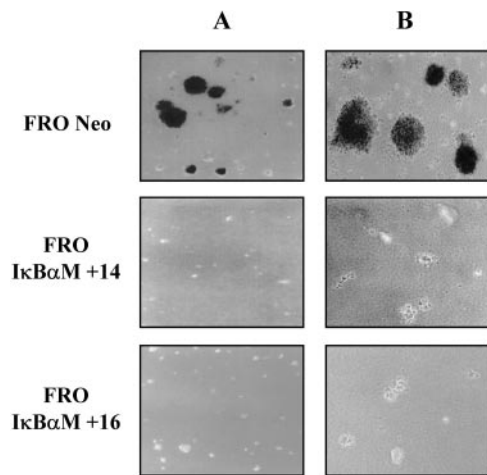


**FIG. 6. *In vitro* oncogenic potential of FRO Neo cells and FRO I $\kappa$ B $\alpha$ M clones.**  $1 \times 10^4$  cells were seeded in 60-mm dishes onto 0.3% Noble Agar (Difco) on top of a 0.6% bottom layer. Colonies larger than 50 cells were scored after 2 weeks of incubation at 37 °C. FRO Neo cells = >50 colonies/plate; FRO I $\kappa$ B $\alpha$ M +14 cells = 0 colonies/plate; FRO I $\kappa$ B $\alpha$ M +16 =  $\leq 5$  colonies/plate. A,  $\times 100$  magnification. B,  $\times 200$  magnification.

evaluate the protein content by colorimetric assay (Bio-Rad), whereas the remnant was analyzed at the  $\beta$ -counter (Beckman Instruments) after adding an equal volume (0.4 ml) of 1 N HCl to neutralize the samples. Results were the means  $\pm$  S.D. of two separate experiments.

**CFSE Cell Proliferation Assay**—The analysis of cell proliferation was performed by labeling cells with CFSE (Molecular Probes, Eugene, OR) as originally described (42). Flow cytometry and data analysis were performed by using a two laser equipped FACSCalibur apparatus and the Cellquest analysis software (BD Biosciences), as described (43).

## RESULTS

**Basal NF- $\kappa$ B Activity in Human Thyroid Carcinomas**—To determine the activation state of NF- $\kappa$ B in primary thyroid cancer tissues, human specimens from normal thyroid, papillary, follicular and anaplastic thyroid carcinomas were collected and stained with anti-p65 (RelA) antibodies. The results of these experiments are summarized in Table I. No nuclear staining for RelA was detected in normal thyroid follicular cells (Fig. 1A), whereas few nuclei from papillary carcinoma cells were positive for RelA. Follicular carcinoma cells showed  $\sim 50\%$  of their nuclei stained for NF- $\kappa$ B, whereas anaplastic carcinoma cells showed almost 100% of their nuclei strongly positive for NF- $\kappa$ B (Fig. 1, B–D, and Table I). Most interestingly, the increased nuclear localization of NF- $\kappa$ B correlates with the increased malignant phenotype of thyroid carcinomas, suggesting that sustained activation of NF- $\kappa$ B confers an advantage for clonal selectivity. These results indicate that the nuclear localization of p65 is a characteristic of human anaplastic thyroid carcinomas and suggest a role of NF- $\kappa$ B in human thyroid carcinomas.

**NF- $\kappa$ B Transcriptional Activity in Human Thyroid Transformed Cells**—The high levels of basal NF- $\kappa$ B activity in human thyroid carcinomas prompted us to investigate the role of NF- $\kappa$ B in thyroid neoplastic transformation. To this aim, we used three different cell lines that resembled the features of thyroid tumors. These cell lines are as follows: WRO (38), derived from a human follicular thyroid carcinoma, FRO (37), derived from a human anaplastic thyroid carcinoma, and NPA (36), derived from a human papillary thyroid carcinoma.

In these cells we analyzed by EMSA the nuclear localization of NF- $\kappa$ B and, by reporter assay, its transcriptional activity. As shown in Fig. 2A, FRO cells showed the highest NF- $\kappa$ B DNA binding activity, whereas it was barely detectable in NPA cells (Fig. 2A). The specificity of the protein-DNA complex was con-

**TABLE II**  
*In vivo* tumor growth induced by FRO Neo cells and FRO I $\kappa$ B $\alpha$ M clones

$2 \times 10^7$  cells were injected subcutaneously on a flank of each 6-week-old nude mouse (Charles River Breeding Laboratories, Lecco, Italy). Thirty days later, mice were killed, and tumors were excised. Tumor weight was determined, and their diameters were measured with calipers. Tumor volumes were calculated by the formula:  $a^2 \times b \times 0.4$ , where  $a$  is the smallest diameter, and  $b$  is the diameter perpendicular to  $a$ .

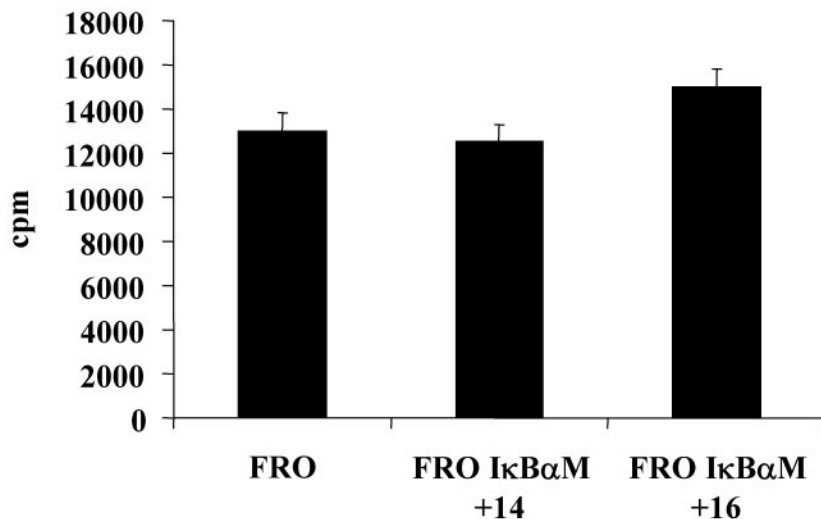
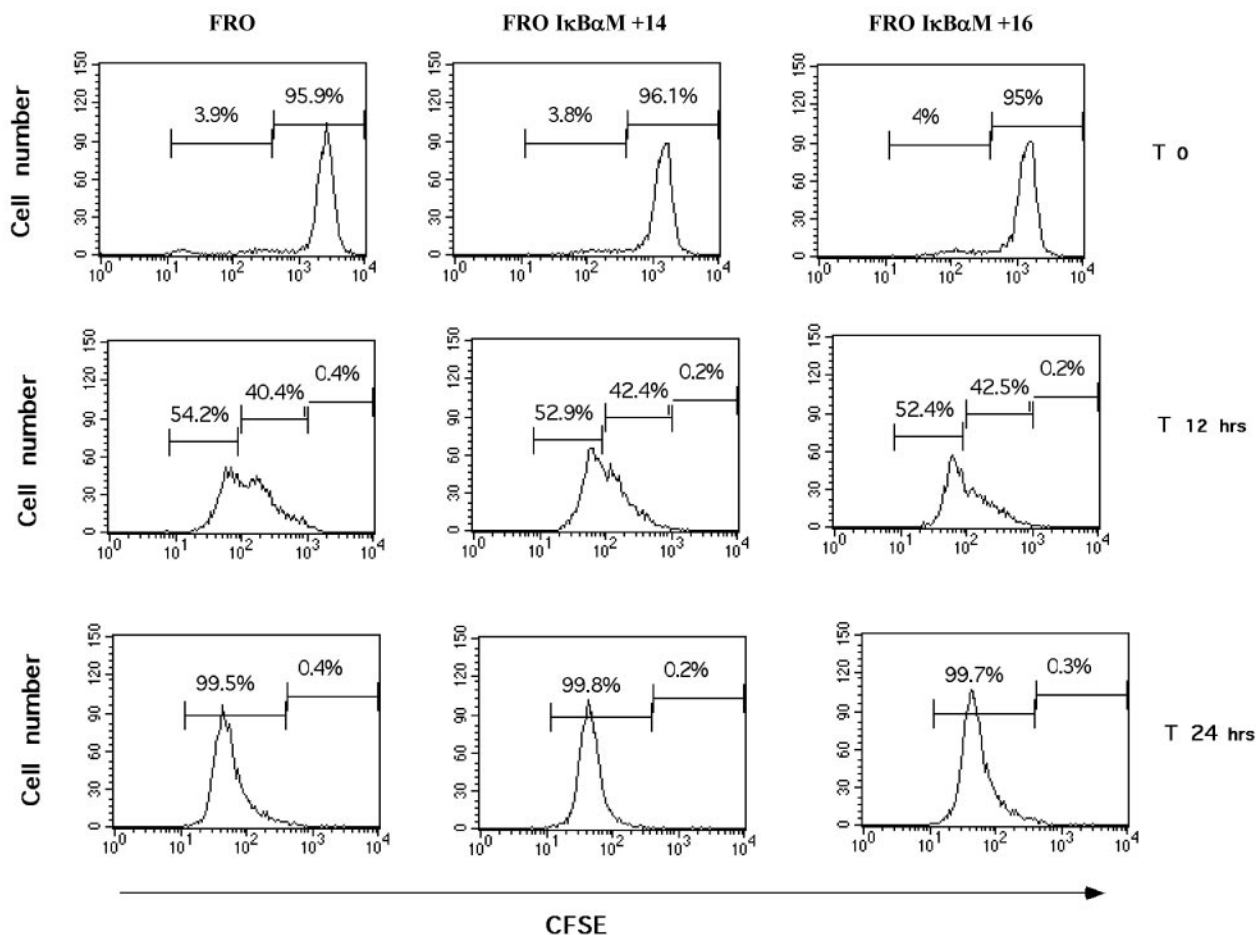
Cell type	Tumor incidence	Tumor volume average	Tumor weight average
		$cm^3$	$g$
Parental cells			
FRO Neo	6/6	$1.48 \pm 0.4$	$0.146 \pm 0.04$
Transfected cells			
FRO I $\kappa$ B $\alpha$ M +14	0/6		
FRO I $\kappa$ B $\alpha$ M +16	2/6	$0.27 \pm 0.06$	$0.029 \pm 0.002$

firmed by a competition assay with nonradioactive  $\kappa$ B oligonucleotide. To demonstrate that the nuclear NF- $\kappa$ B was transcriptionally active, we performed reporter gene assays in all three cell lines. Consistent with EMSA experiments, FRO cells showed the highest NF- $\kappa$ B transcriptional activity, whereas NPA cells showed an almost undetectable activity (Fig. 2B). Taken together, these data indicate that NF- $\kappa$ B was transcriptionally activated in thyroid carcinoma cell lines, particularly in the human anaplastic thyroid cell line FRO.

**NF- $\kappa$ B Activity Is Essential to Confer Resistance to Drug-induced Apoptosis in Thyroid Carcinoma Cell Lines**—In order to determine a correlation between NF- $\kappa$ B activity and cell sensitivity to drug-induced apoptosis, we tested the ability of cisplatin and doxorubicin in promoting cell death in WRO, FRO, and NPA cells. As shown in Fig. 3, A and B, both drugs induced cell death in all three cell lines, at an extent that correlated with the levels of basal NF- $\kappa$ B activity. To test whether NF- $\kappa$ B activation protects neoplastic thyroid cells from apoptosis induced by chemotherapeutic drugs, we stably transfected NPA cells with an expression vector encoding IKK $\beta$ , to induce constitutive NF- $\kappa$ B activity, and FRO cells with a super-repressor form of I $\kappa$ B $\alpha$  (I $\kappa$ B $\alpha$ M), to suppress basal NF- $\kappa$ B activity. Two NPA clones, NPA IKK $\beta$  +7 and NPA IKK $\beta$  +18, as well as two FRO clones, FRO I $\kappa$ B $\alpha$ M +14 and FRO I $\kappa$ B $\alpha$ M +16, were used in our study. They expressed different levels of IKK $\beta$  (Fig. 4A) or I $\kappa$ B $\alpha$ M (Fig. 4B) and were differentially able to activate NF- $\kappa$ B (Fig. 4, C and D). In fact, although the constitutive IKK $\beta$  expression strongly increased basal NF- $\kappa$ B activity in NPA clones (Fig. 4C), the presence of I $\kappa$ B $\alpha$ M in FRO clones led to a decrease of both basal and phorbol 12-myristate-13-acetate/ionomycin-induced NF- $\kappa$ B activity (Fig. 4D).

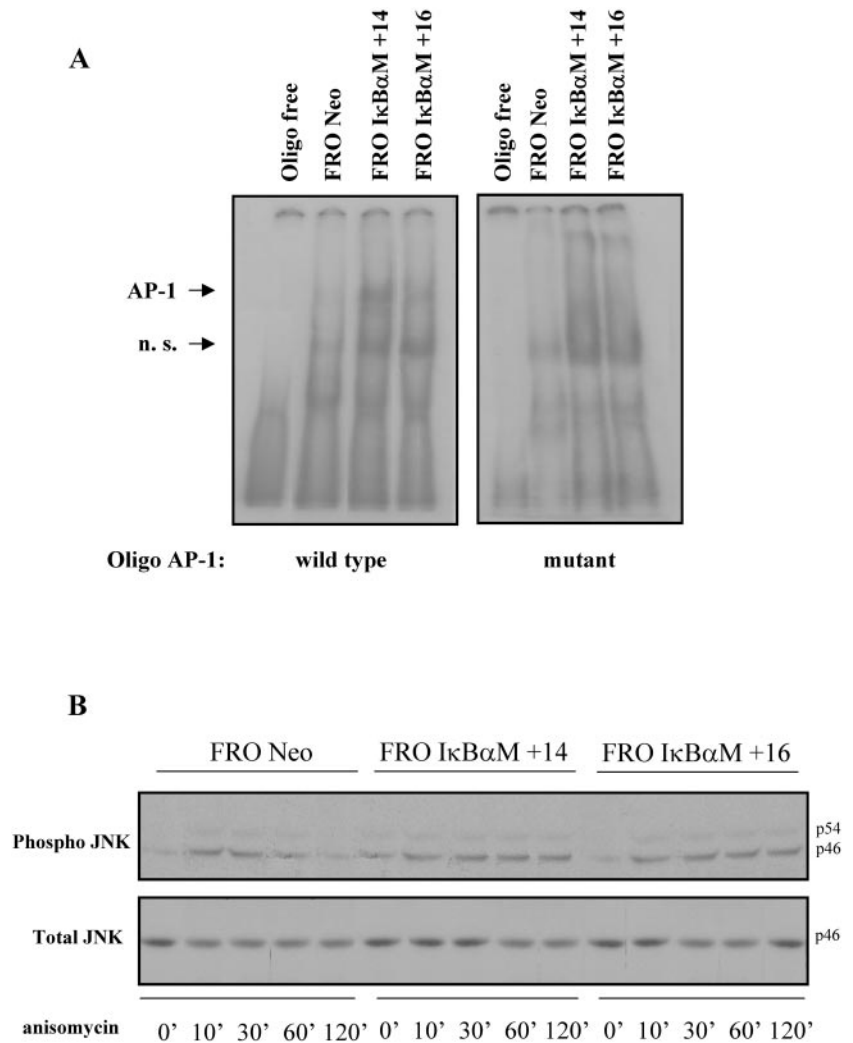
Stably transfected and mock-transfected cells were then treated with increasing amounts of cisplatin (Fig. 5, A and C) or doxorubicin (Fig. 5, B and D) for 48 h, and the cell survival and cell death were measured. Although NPA Neo cells were sensitive to cell death induced by chemotherapeutic drugs, NPA IKK $\beta$  clones became resistant to apoptosis induced by either cisplatin (Fig. 5A) or doxorubicin (Fig. 5B). On the other hand, FRO Neo cells were still resistant to drug-induced cell death, whereas FRO I $\kappa$ B $\alpha$ M clones underwent apoptosis after treatment even at low dosage of either cisplatin (Fig. 5C) or doxorubicin (Fig. 5D). These results indicate that NF- $\kappa$ B activity is required and sufficient to confer resistance to drug-induced apoptosis of neoplastic thyroid cells.

**Inhibition of FRO Cells Transforming Potential by NF- $\kappa$ B Inactivation**—We next investigated if in addition to its role in protecting cells from apoptosis, NF- $\kappa$ B was also involved in other oncogenic properties of thyroid carcinoma cells. There-

**A****B**

**FIG. 7. Analysis of cell proliferation rate in FRO Neo cells and FRO I $\kappa$ B $\alpha$ M clones.** A,  $5 \times 10^4$  cells/well were seeded in 12-well culture plates and incubated for 4 h at 37 °C with 0.5  $\mu$ Ci/well of [<sup>3</sup>H]thymidine (Amersham Biosciences). After three washings with cold PBS, cells were incubated for 10 min at 4 °C with 0.5 ml of 20% trichloroacetic acid. Trichloroacetic acid was then removed, and cells were lysed with gentle shaking for 30 min at 37 °C in the presence of 1 N NaOH (0.5 ml/well). An aliquot of lysates (0.1 ml) was used to evaluate the protein content by colorimetric assay (Bio-Rad), whereas the remnant was analyzed at the  $\beta$ -counter (Beckman Coulter) after adding an equal volume (0.4 ml) of 1 N HCl to neutralize the samples. Results were the mean  $\pm$  S.D. of three separate experiments. B, FRO Neo cells and FRO I $\kappa$ B $\alpha$ M clones were collected and analyzed after 0, 12, and 24 h after CFSE labeling, as indicated. *x* axes indicate the CFSE fluorescence log intensity, whereas *y* axes refer to cell number count. Data are representative of one of two independent experiments.

**FIG. 8. JNK activity in FRO Neo cells and FRO I $\kappa$ B $\alpha$ M clones.** *A*, EMSA on nuclear extracts from human thyroid carcinoma cell lines FRO Neo, FRO I $\kappa$ B $\alpha$ M +14, and +16 in the presence of a  $^{32}$ P-labeled wild-type AP-1 oligonucleotide (*left panel*) or in the presence of a  $^{32}$ P-labeled mutant AP-1 oligonucleotide (*right panel*). *n. s.* = nonspecific. *B*,  $5 \times 10^5$  cells/well were seeded in 6-well culture plates and incubated for different time intervals at 37 °C with 10  $\mu$ g/ml anisomycin (Sigma). Cell lysates were analyzed by Western blot assays with the monoclonal Ab-pJNK1/2 (9255) (Cell Signaling Technology Inc.) raised against phosphorylated JNK (*upper panel*) or with the polyclonal Ab-JNK1/2 (9252) (Cell Signaling Technology, Inc.) raised against total JNK (*lower panel*).



fore, we analyzed *in vitro* and *in vivo* the transforming potential of FRO Neo and FRO I $\kappa$ B $\alpha$ M cells. The *in vitro* assay was performed by analyzing the ability of transformed cells to form colonies on soft agar. As shown in Fig. 6, whereas parental FRO cells (FRO Neo) gave rise to numerous and large colonies in soft agar (*upper panels*), FRO I $\kappa$ B $\alpha$ M +14 and FRO I $\kappa$ B $\alpha$ M +16 clones lost this property (*middle and lower panels*). These results were also confirmed by *in vivo* assays. Table II shows that injection in nude mice of FRO Neo cells induced tumor formation in 6 out of 6 nude mice. Injection of FRO I $\kappa$ B $\alpha$ M +14 and FRO I $\kappa$ B $\alpha$ M +16 cells induced tumor formation in 0 out of 6 and 2 out of 6 mice, respectively. In addition, the two tumors developed from FRO I $\kappa$ B $\alpha$ M +16 cells were about 5-fold smaller than that formed after injection of parental cells (Table II). Thus, inhibition of NF- $\kappa$ B activity in FRO cells led to a strong decrease of their transforming potential, suggesting a role for this transcription factor in thyroid carcinogenesis.

**The Inhibition of NF- $\kappa$ B Activity in FRO Cells Did Not Affect Their Proliferative State**—The imbalance between proliferation and apoptosis is one of the critical cellular events that lead to oncogenesis. Because NF- $\kappa$ B controls transcription of genes involved in the regulation of apoptosis and cell proliferation, the inhibition of NF- $\kappa$ B activity in FRO cells could affect both proliferation and apoptosis. To test for this, we analyzed the proliferation rate of parental and transfected FRO cells by [ $^3$ H]thymidine DNA incorporation and by CFSE assay (Fig. 7). No significant differences in the rate of [ $^3$ H]thymidine DNA

incorporation were appreciable between FRO Neo cells and FRO I $\kappa$ B $\alpha$ M clones (Fig. 7A), and a very similar doubling time was detected after 12 and 24 h of CFSE treatment (Fig. 7B), indicating that NF- $\kappa$ B activation is not required to control proliferation of FRO cells.

**The Anti-apoptotic Activity of NF- $\kappa$ B Was Mediated by Down-regulation of JNK Activity**—NF- $\kappa$ B is crucial to oncogenesis and to chemoresistance in cancer, controlling activation of pro-survival genes and down-regulation of pro-apoptotic genes (16). For example, it has been shown recently that NF- $\kappa$ B inhibits TNF- $\alpha$ -induced apoptosis by repressing the JNK pathway (32, 33). Therefore, we investigated if inhibition of NF- $\kappa$ B activity in FRO I $\kappa$ B $\alpha$ M clones affects JNK activation. To this aim, we first analyzed transcriptional activity of AP-1, a target of JNK activity, by EMSA on nuclear extracts from FRO Neo cells and FRO I $\kappa$ B $\alpha$ M clones (Fig. 8A). As shown in the Fig. 8, AP-1 DNA binding activity, almost undetectable in FRO Neo cells, was partially restored in FRO I $\kappa$ B $\alpha$ M clones (Fig. 8A, *left panel*). Next, we investigated JNK activity in FRO Neo cells and FRO I $\kappa$ B $\alpha$ M clones by analyzing its phosphorylation status following anisomycin stimulation (Fig. 8B, *upper panel*). As shown in Fig. 8, anisomycin induced JNK phosphorylation as early as 10 min of treatment in all cell lines, but, while the pJNK level in FRO Neo cells decreased with time, it remained sustained in FRO I $\kappa$ B $\alpha$ M clones. Anisomycin treatment had no effect on JNK expression, as assessed by Western blot analysis.

These data suggest that the basal NF- $\kappa$ B activation repressed JNK activity in FRO cells, and suggested that the

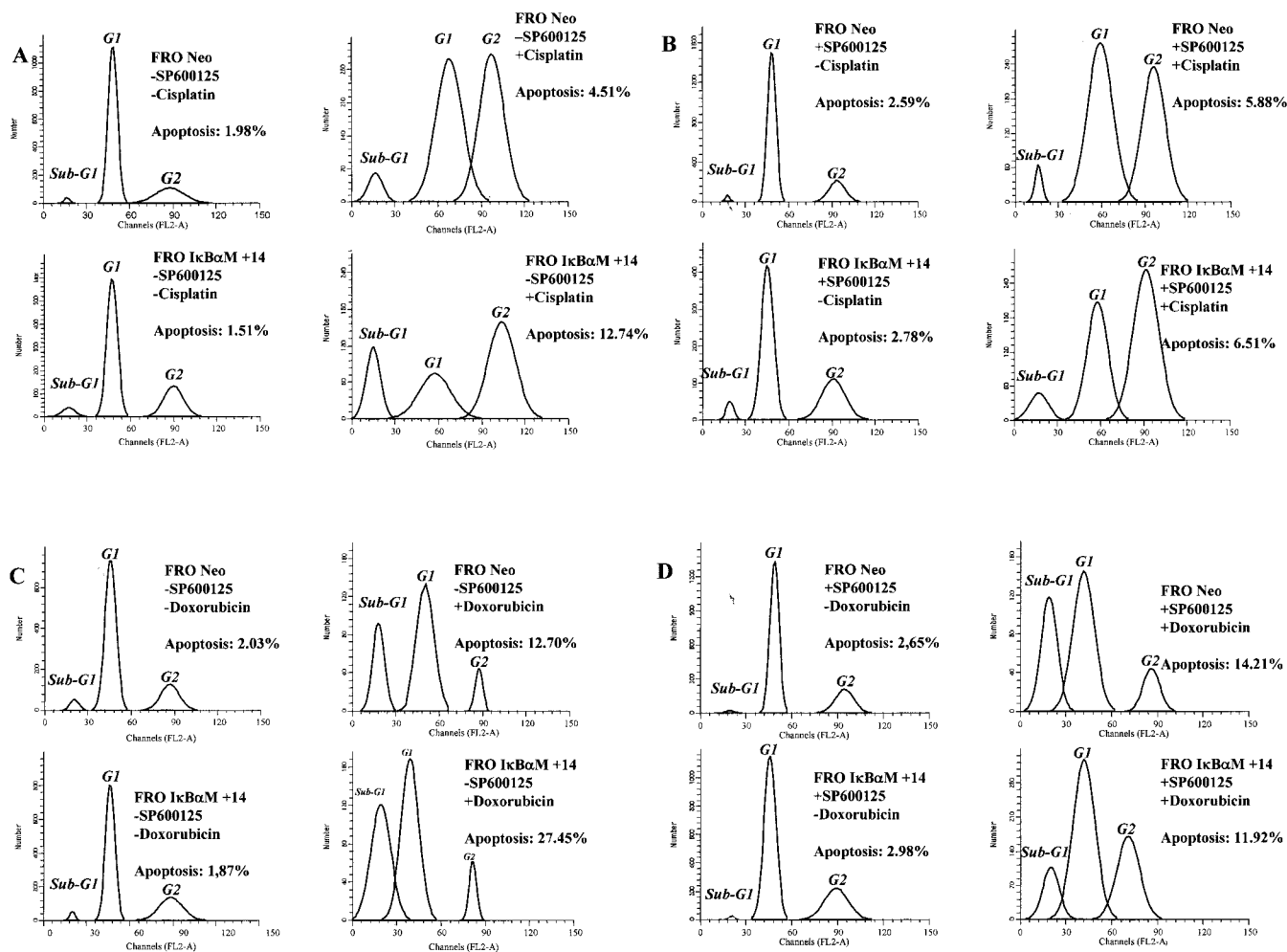


FIG. 9. Inhibition of JNK activity restored cell death resistance in FRO I $\kappa$ B $\alpha$ M clones.  $1 \times 10^5$  cells/well were seeded in 6-well culture plates and incubated for 48 h at 37 °C with 5  $\mu$ g/ml cisplatin (A and B) or doxorubicin (C and D) in the presence of 10  $\mu$ M JNK inhibitor SP600125. Cell death was assessed by propidium iodide staining according to Nicoletti *et al.* (41). Samples were analyzed by flow cytometry using a FACSCalibur (Beckman Coulter, Fullerton, CA), equipped with ModFit Software. A representative experiment out of two is shown.

sensitivity of FRO I $\kappa$ B $\alpha$ M clones to apoptosis induced by chemotherapeutic agents could be due to restoration of JNK activity. To investigate this hypothesis, we analyzed the apoptosis rate in FRO Neo and FRO I $\kappa$ B $\alpha$ M +14 cells after treatment with 5  $\mu$ g/ml cisplatin or doxorubicin in the presence of 10  $\mu$ M SP600125, a specific inhibitor of JNK activity (44). Cell death was assessed by propidium iodide staining and was represented by the fraction of cells in sub-G<sub>1</sub> phase (Fig. 9). The inhibition of JNK activity by SP600125 rendered FRO I $\kappa$ B $\alpha$ M resistant to apoptosis induced by cisplatin (Fig. 9B) or doxorubicin (Fig. 9D). These results suggest that NF- $\kappa$ B inhibits chemotherapeutic drug-induced apoptosis of FRO cells by, at least partially, negatively regulating JNK signaling.

#### DISCUSSION

In the present paper, we show that the transcription factor NF- $\kappa$ B plays an important role in thyroid cancer. Its activity was constitutively elevated in primary human thyroid carcinomas and was correlated with malignant phenotype. In particular, anaplastic thyroid carcinoma cells displayed almost 100% of their nuclei positively stained for NF- $\kappa$ B. Activated NF- $\kappa$ B was also detected in an *in vitro* model of human thyroid cancer that resembles the *in vivo* differentiated and undifferentiated thyroid tumors. In these cell lines we demonstrate that persistent NF- $\kappa$ B activity was progressively detected in papillary thyroid carcinoma cells (NPA) to follicular carcinoma cells (WRO) until reach-

ing the highest levels in anaplastic carcinoma cells (FRO), suggesting that sustained activation of NF- $\kappa$ B confers an advantage for clonal selectivity. An interesting question is how thyroid cancer cells acquired a basal NF- $\kappa$ B activity. By using Western blot analysis, we detected low levels of I $\kappa$ B $\alpha$  protein in FRO cells (data not shown). Given that transcription of the I $\kappa$ B $\alpha$  gene is strongly up-regulated by NF- $\kappa$ B, the low level of I $\kappa$ B $\alpha$  protein suggests a high turnover of the protein. One may speculate that thyroid cells may have acquired defects in components that regulate I $\kappa$ B $\alpha$  phosphorylation, ubiquitination, and degradation, thus resulting in basal NF- $\kappa$ B activity. Another possibility is that thyroid cells produce an autocrine factor that chronically activates the NF- $\kappa$ B pathway. The latter hypothesis is supported by the recent evidence that at least some differentiated thyroid carcinomas secrete growth factors and chemotactic factors potentially responsible for NF- $\kappa$ B up-regulation (45). In addition, it has been demonstrated recently that CXC chemokine receptor 4 is highly expressed in a human thyroid cell line (46) and that the ability of breast cancer cells to migrate and form metastasis depends on the NF- $\kappa$ B-mediated CXC chemokine receptor 4 expression (47).

NF- $\kappa$ B inhibition in FRO cells strongly enhanced the sensitivity of these cells to undergo apoptosis induced by cisplatin or doxorubicin treatment, and caused a dramatic decrease of their transforming potential. These *in vitro* functions of NF- $\kappa$ B were consistent with its role in tumor growth *in vivo*; FRO I $\kappa$ B $\alpha$ M

cells failed to form tumors in nude mice. The increased susceptibility to apoptosis of FRO I $\kappa$ B $\alpha$ M and the evidence that constitutive activation of the NF- $\kappa$ B pathway rendered NPA cells resistant to drug-induced apoptosis confirms and extends the idea that one of the roles played by NF- $\kappa$ B in neoplastic transformation is protection from apoptosis.

Even though escape from apoptosis may play an important role in the development of cancer, deregulation of this process, alone, may not fully explain the inability of FRO I $\kappa$ B $\alpha$ M to grow in soft agar and to form tumors in nude mice. Given that NF- $\kappa$ B controls expression of genes involved in different cell functions such as proliferation (cyclin D1 and *myc*), apoptosis, and drug resistance (MDR1), it is very possible that a combination of different factors are responsible for the loss of the transforming potential of these cells. However, stable transfected FRO I $\kappa$ B $\alpha$ M +14 and +16 did not show gross differences in proliferation rate compared with the mock-transfected counterpart, indicating that NF- $\kappa$ B is not playing a central role in controlling proliferation of neoplastic cells, at least in our experimental system.

Our data also suggest that the anti-apoptotic function of NF- $\kappa$ B was mediated by the inhibition of JNK signaling. In fact, JNK activity was restored in FRO I $\kappa$ B $\alpha$ M cells, where its duration was prolonged after treatment with anisomycin. In addition, incubation of FRO I $\kappa$ B $\alpha$ M cells with the specific JNK inhibitor SP600125 restored their resistance to chemotherapeutic drug-induced apoptosis. The role of JNK in programmed cell death is debated. Recently, it has been shown that NF- $\kappa$ B is able to inhibit TNF- $\alpha$ -induced apoptosis by negatively regulating activation of the JNK pathway (32, 33). This effect is mediated by two genes, GADD45 $\beta$  and XIAP, both of them under the transcriptional control of NF- $\kappa$ B. In our experimental system GADD45 $\beta$  expression paralleled the levels of NF- $\kappa$ B activity in thyroid carcinoma cells and decreased in FRO I $\kappa$ B $\alpha$ M clones (data not shown), suggesting that this gene might mediate the anti-apoptotic role of NF- $\kappa$ B in thyroid cancer. Taken together, the data presented in this paper clearly substantiate the fundamental role of NF- $\kappa$ B in thyroid oncogenesis and could open new perspectives for diagnosis and therapy of human ATC.

**Acknowledgments**—We thank G. Franzoso for providing the pCDNA3I $\kappa$ B $\alpha$ M expression vector and M. Santoro and D. Salvatore for critical reading of the manuscript.

#### REFERENCES

- Figge, J. (1999) in *Thyroid Cancer: A Comprehensive Guide to Clinical Management* (Wartofsky, L., ed) pp. 515–535, Humana Press, Inc., Totowa, NJ
- Sherman, S. I. (2003) *The Lancet* **361**, 501–511
- Gimm, O. (2001) *Cancer Lett.* **163**, 143–156
- Ball, D. W., Baylin, S. B., and de Bustros, A. C. (1996) in *The Thyroid* (Werner, S. C., and Ingbars, D. H., eds) pp. 1166–1184, 7th Ed., Lippincott-Raven, Philadelphia
- McIver, B., Hay, I. D., Giuffrida, D. F., Dvorak, C. E., Grant, C. S., Thompson, G. B., van Heerden, J. A., and Goellner, J. R. (2001) *Surgery* **130**, 1028–1034
- Tennvall, J., Lundell, G., Hallquist, A., Wahlberg, P., Wallin, G., and Tibblin, S. (1994) *Cancer (Phila.)* **74**, 1348–1354
- Ghosh, S., May, M. J., and Kopp, E. B. (1998) *Annu. Rev. Immunol.* **16**, 225–260
- Tak, P. P., and Firestein, G. S. (2001) *J. Clin. Investig.* **107**, 7–11
- Karin, M., and Ben-Neriah, Y. (2000) *Annu. Rev. Immunol.* **18**, 621–663
- Verma, I. M., Stevenson, J. K., Schwarz, E. M., Van Antwerp, D., and Miyamoto, S. (1995) *Genes Dev.* **9**, 2723–2735
- Pahl, H. L. (1999) *Oncogene* **18**, 6853–6866
- Brown, K., Gerstberger, S., Carlson, L., Franzoso, G., and Siebenlist, U. (1995) *Science* **267**, 1485–1488
- Karin, M. (1999) *Oncogene* **18**, 6867–6874
- Yamaoka, S., Courtois, G., Bessia, C., Whiteside, S. T., Weil, R., Agou, F., Kirk, H. E., Kay, R. J., and Israel, A. (1998) *Cell* **93**, 1231–1240
- Rothwarf, D. M., Zandi, E., Natoli, G., and Karin, M. (1998) *Nature* **395**, 297–300
- Baldwin, A. (2001) *J. Clin. Investig.* **107**, 241–246
- Deveraux, Q. L., Roy, N., Stennicke, H. R., Van Arsdale, T., Zhou, Q., Srinivasula, S. M., Alnemri, E. S., Salvesen, G. S., and Reed, J. C. (1998) *EMBO J.* **17**, 2215–2223
- Liston, P., Roy, N., Tamai, K., Lefebvre, C., Baird, S., Cherton-Horvat, G., Farahani, R., McLean, M., Ikeda, J. E., MacKenzie, A., and Korneluk, R. G. (1996) *Nature* **379**, 349–353
- Muzio, M., Chinnayan, A. M., Kischkel, F. C., O'Rourke, K., Shevchenko, A., Ni, J., Scaffidi, C., Bretz, J. D., Zhang, M., Gentz, R., Mann, M., Krammer, P. H., Peter, M. E., and Dixit, V. M. (1996) *Cell* **85**, 817–827
- Wang, C. Y., Mayo, M. W., Korneluk, R. G., Goeddel, D. V., and Baldwin, A. S., Jr. (1998) *Science* **281**, 1680–1683
- Boise, L. H., Gonzalez-Garcia, M., Postema, C. E., Ding, L., Lindsten, T., Turka, L. A., Mao, X., Nunez, G., and Thompson, C. B. (1993) *Cell* **74**, 597–608
- Takekawa, M., and Saito, H. (1998) *Cell* **95**, 521–530
- Orlowski, R. Z., and Baldwin, A. S., Jr. (2002) *Trends Mol. Med.* **8**, 385–389
- Gilmore, T., Gapuzan, M. E., Kalaitzidis, D., and Starczynowski, D. (2002) *Cancer Lett.* **181**, 1–9
- Bargou, R. C., Emmerich, F., Krappmann, D., Bommert, K., Mapara, M. Y., Arnold, W., Royer, H. D., Grinstein, E., Greiner, A., Scheidereit, C., and Dörkin, B. (1997) *J. Clin. Investig.* **100**, 2961–2969
- Duffey, D. C., Chen, Z., Dong, G., Ondrey, F. G., Wolf, J. S., Brown, K., Siebenlist, U., and Van Waes, C. (1999) *Cancer Res.* **59**, 3468–3474
- Huang, S., Pettaway, C. A., Uehara, H., Bucana, C. D., and Fidler, I. J. (2001) *Oncogene* **20**, 4188–4197
- Kyriakis, J. M., Banerjee, P., Nikolakaki, E., Dai, T., Rubie, E. A., Ahmad, M. F., Avruch, J., and Woodgett, J. R. (1994) *Nature* **369**, 156–160
- Hibi, M., Lin, A., Smeal, T., Minden, A., and Karin, M. (1993) *Genes Dev.* **7**, 2135–2148
- Davis, R. J. (2000) *Cell* **103**, 239–252
- Tournier, C., Hess, P., Yang, D. D., Xu, J., Turner, T. K., Nimmual, A., Bar-Sagi, D., Jones, S. N., Flavell, R. A., and Davis, R. J. (2000) *Science* **288**, 870–874
- De Smaele, E., Zazzeroni, F., Papa, S., Nguyen, D. U., Jin, R., Jones, J., Cong, R., and Franzoso, G. (2001) *Nature* **414**, 308–313
- Tang, G., Minemoto, Y., Dibling, B., Purcell, N. H., Li, Z., Karin, M., and Lin, A. (2001) *Nature* **414**, 313–317
- Pang, X. P., Hershman, J. M., Chung, M., and Pekary, A. E. (1989) *Endocrinology* **125**, 1783–1788
- Visconti, R., Cerutti, J., Battista, S., Fedele, M., Trapasso, F., Zeki, K., Miano, M. P., de Nigris, F., Casalino, L., Curcio, F., Santoro, M., and Fusco, A. (1997) *Oncogene* **15**, 1987–1994
- Ludwig, L., Kessler, H., Wagner, M., Hoang-vu, C., Dralle, H., Adler, G., Böhm, B. O., and Schmid, R. M. (2001) *Cancer Res.* **61**, 4526–4535
- Fagin, J. A., Matsuo, K., Karmakar, A., Chen, D. L., Tang, S. H., and Koeffler, H. P. (1993) *J. Clin. Investig.* **91**, 179–184
- Estour, B., Van Herle, A. J., Juillard, G. J., Totanes, T. L., Sparkes, R. S., Giuliano, A. E., and Klandorf, H. (1989) *Virchows Arch. B Cell Pathol. Incl. Mol. Pathol.* **57**, 167–174
- Leonardi, A., Chariot, A., Claudio, E., Cunningham, K., and Siebenlist, U. (2000) *Proc. Natl. Acad. Sci. U. S. A.* **97**, 10494–10499
- Macpherson, I., and Montagnier, I. (1964) *Virology* **23**, 291–294
- Nicoletti, I., Migliorati, G., Pagliarini, M. C., Grignani, F., and Riccardi, C. (1991) *J. Immunol. Methods* **139**, 271–279
- Lyons, A. B. (1999) *Immunol. Cell Biol.* **77**, 516–518
- Lanier, L. L., and Recktenwald, D. J. (1991) *Methods Companion Methods Enzymol.* **2**, 192–195
- Bennett, B. L., Sasaki, D. T., Murray, B. W., O'Leary, E. C., Sakata, S. T., Xu, W., Leisten, J. C., Motiwala, A., Pierce, S., Satoh, Y., Bhagwat, S. S., Manning, A. M., and Anderson, D. W. (2001) *Proc. Natl. Acad. Sci. U. S. A.* **98**, 13681–13686
- Russell, J. P., Shinohara, S., Melillo, R. M., Castellone, M. D., Santoro, M., and Rothstein, J. L. (2003) *Oncogene* **22**, 4569–4577
- Hwang, J. H., Hwang, J. H., Chung, H. K., Kim, D. W., Hwang, E. S., Suh, J. M., Kim, H., You, K. H., Kwon, O. Y., Ro, H. K., Jo, D. Y., and Shong, M. (2003) *J. Clin. Endocrinol. Metab.* **88**, 408–416
- Helbig, G., Christopherson, K. W., II, Bhat-Nakshatri, P., Kumar, S., Kishimoto, H., Miller, K. D., Broxmeyer, H. E., and Nakshatri, H. (2003) *J. Biol. Chem.* **278**, 21631–21638

# Central Role of the Scaffold Protein Tumor Necrosis Factor Receptor-associated Factor 2 in Regulating Endoplasmic Reticulum Stress-induced Apoptosis<sup>\*S</sup>

Received for publication, February 25, 2005, and in revised form, October 17, 2005. Published, JBC Papers in Press, November 18, 2005, DOI 10.1074/jbc.M502181200

Claudio Mauro<sup>†1</sup>, Elvira Crescenzi<sup>†1</sup>, Roberta De Mattia<sup>‡</sup>, Francesco Pacifico<sup>§</sup>, Stefano Mellone<sup>§</sup>, Salvatore Salzano<sup>§</sup>, Cristiana de Luca<sup>‡</sup>, Luciano D'Adamio<sup>¶||</sup>, Giuseppe Palumbo<sup>‡</sup>, Silvestro Formisano<sup>‡</sup>, Pasquale Vito<sup>\*\*</sup>, and Antonio Leonardi<sup>‡2</sup>

From the Dipartimento di <sup>†</sup>Biologia e Patologia Cellulare e Molecolare and <sup>||</sup>Biochimica e Biotecnologie Mediche, Università degli Studi di Napoli "Federico II," Via Pansini 5, 80131 Naples, Italy, the <sup>§</sup>Istituto di Endocrinologia e Oncologia Sperimentale, CNR, Via Pansini 5, 80131 Naples, Italy, <sup>\*\*</sup>Dipartimento di Scienze Biologiche e Ambientali, Università degli Studi del Sannio, Via Port'Arsa 11, 82100 Benevento, Italy, and the <sup>¶</sup>Department of Microbiology and Immunology, Albert Einstein College of Medicine, Bronx, New York 10461

The endoplasmic reticulum represents the quality control site of the cell for folding and assembly of cargo proteins. A variety of conditions can alter the ability of the endoplasmic reticulum (ER) to properly fold proteins, thus resulting in ER stress. Cells respond to ER stress by activating different signal transduction pathways leading to increased transcription of chaperone genes, decreased protein synthesis, and eventually to apoptosis. In the present paper we analyzed the role that the adaptor protein tumor necrosis factor-receptor associated factor 2 (TRAF2) plays in regulating cellular responses to apoptotic stimuli from the endoplasmic reticulum. Mouse embryonic fibroblasts derived from TRAF2<sup>-/-</sup> mice were more susceptible to apoptosis induced by ER stress than the wild type counterpart. This increased susceptibility to ER stress-induced apoptosis was because of an increased accumulation of reactive oxygen species following ER stress, and was abolished by the use of antioxidant. In addition, we demonstrated that the NF- $\kappa$ B pathway protects cells from ER stress-induced apoptosis, controlling ROS accumulation. Our results underscore the involvement of TRAF2 in regulating ER stress responses and the role of NF- $\kappa$ B in protecting cells from ER stress-induced apoptosis.

In eukaryotic cells, proteins must be correctly folded and assembled before to transit to intracellular organelles and the cell surface (1, 2). A number of cellular stress conditions can interfere with protein folding, leading to accumulation of unfolded or misfolded proteins in the endoplasmic reticulum (ER)<sup>3</sup> lumen. The ER has evolved specific signaling pathway to deal with the potential danger represented by the misfolded proteins. This adaptive response is named unfolded protein response (3). Activation of unfolded protein response results in attenuation of

protein synthesis, and up-regulation of genes encoding chaperones that facilitate the protein folding process in the ER. Thus, unfolded protein response reduces accumulation and aggregation of misfolded proteins, giving the cell the possibility of correcting the environment inside the ER (3, 4). However, if the damage is too strong and homeostasis cannot be restored, the mammalian unfolded protein response initiates apoptosis. In mammalian cells, three transmembrane proteins Ire1 $\alpha$  (5), Ire1 $\beta$  (6), and PERK (7) act as ER stress sensor proteins and play important roles in transducing the stress signals initiated by the accumulation of misfolded proteins from the ER to the cytoplasm and nucleus. Ire1s and PERK are kept in an inactive state through association of their N-terminal lumen domain with the chaperone BiP. Following accumulation of misfolded proteins in the lumen of the ER, BiP dissociates to bind the misfolded proteins and Ire1s and PERK undergo oligomerization and transphosphorylation within their cytoplasmic kinase domains (8, 9).

Other stress response pathways are activated following ER stress, such as the JNK/SAPK and NF- $\kappa$ B pathways (10, 11). Activation of these pathways following ER stress is mediated by the physical and functional interaction of Ire1 $\alpha$  and TRAF2 (10). The central role played by TRAF2 in mediating cellular response to ER stress has been proposed based upon the observation that ectopic expression of a dominant negative mutant of TRAF2 lacking the N terminus Ring finger domain, blocks ER stress-induced NF- $\kappa$ B and JNK/SAPK activation, and that mouse embryonic fibroblast derived from TRAF2 knock-out mice failed to activate NF- $\kappa$ B following ER stress (10, 11). TRAF2 was initially identified as a TNF receptor 2 interacting protein (13). Interestingly, TRAF2-deficient MEFs are very sensitive to cell death induced by TNF and other members of the TNF receptor family (14, 15). At least part of the anti-apoptotic effect of TRAF2 can be explained by its function as a mediator of NF- $\kappa$ B activation, thus leading to NF- $\kappa$ B-dependent expression of anti-apoptotic genes. The anti-apoptotic activity of NF- $\kappa$ B also involves inhibition of the JNK cascade via at least two distinct mechanisms: through GADD45- $\beta$ -mediated blockade of MKK7 and interference with ROS production (16, 17). It is well known that ROS or oxidative stress plays an important role in various physiological and pathological processes such as aging, inflammation, and neurodegenerative diseases (18–20). Recently, it has been demonstrated that accumulation of misfolded protein within the lumen of the ER causes accumulation of ROS and cell death (21). However, it is currently unknown whether some of the key molecules involved in ER stress response, such as TRAF2, are involved in modulation of ROS and induction of apoptosis. Here we use MEFs derived from TRAF2 knock-out mice to study the role of TRAF2

<sup>\*</sup> This work was supported by grants from the Associazione Italiana Ricerca sul Cancro, MIUR-FIRB RBNE0155LB, and Centro di Competenza GEAR. The costs of publication of this article were defrayed in part by the payment of page charges. This article must therefore be hereby marked "advertisement" in accordance with 18 U.S.C. Section 1734 solely to indicate this fact.

<sup>S</sup> The on-line version of this article (available at <http://www.jbc.org>) contains Figs. A and B.

<sup>1</sup> Both authors contributed equally to this work.

<sup>2</sup> To whom correspondence should be addressed. Tel.: 39-0817463606; E-mail: [leonardi@unina.it](mailto:leonardi@unina.it).

<sup>3</sup> The abbreviations used are: ER, endoplasmic reticulum; NF- $\kappa$ B, nuclear factor- $\kappa$ B; MEF, mouse embryonic fibroblast; TRAF, tumor necrosis factor receptor-associated factor; ROS, reactive oxygen species; JNK, c-Jun N-terminal kinase; SAPK, stress-activated protein kinase; TNF, tumor necrosis factor; WT, wild type; H<sub>2</sub>DCFDA, dichlorodihydrofluorescein diacetate; MTS, 3-(4,5-dimethylthiazol-2-yl)-5-(3-carboxymethoxyphenyl)-2-(4-sulfophenyl)-2H-tetrazolium; FL, full-length; NAC, N-acetyl-L-cysteine.

## TRAF2 Regulates ER Stress-induced Apoptosis

in the regulation of pro-survival or pro-apoptotic pathways following ER stress.

### EXPERIMENTAL PROCEDURES

**Cell Culture and Biological Reagents**—Wild type (WT) and TRAF2<sup>-/-</sup> murine embryonic fibroblasts (MEFs) were provided by Drs. T. W. Mak and W. C. Yeh (14). WT and JNK1/2<sup>-/-</sup> and WT and p65<sup>-/-</sup> MEFs were provided by Dr. R. Davis and Dr. G. Franzoso, respectively (22, 23). Cells were cultured in Dulbecco's modified Eagle's medium (Invitrogen) supplemented with 10% fetal calf serum, 100 units/ml penicillin, and 100  $\mu$ g/ml streptomycin. Thapsigargin was from Calbiochem and used at 5–50 nM; tunicamycin was purchased from Roche and used at 50–150 ng/ml. Dichlorodihydrofluorescein diacetate (H<sub>2</sub>DCFDA) (Calbiochem) was dissolved in Me<sub>2</sub>SO and used at 5  $\mu$ M; L-NAC was dissolved in sterile water and used at 5 mM. Anti-TRAF2, anti-I $\kappa$ B $\alpha$ , and anti-JNK antibodies were purchased from Santa Cruz Biotechnology. The TRAF2 full-length expression vector was previously described (24).

**Western Blot Analysis**—Subconfluent monolayer of murine embryonic fibroblasts were washed with phosphate-buffered saline and then lysed in a lysis buffer containing 20 mM HEPES, pH 7.5, 150 mM NaCl, 10% glycerol, 1% Triton X-100, supplemented with a mixture of protease inhibitors (Roche). Equal amounts of total proteins (50  $\mu$ g) were resolved by SDS-polyacrylamide gels. Separated proteins were transferred to polyvinylidene difluoride membranes (Millipore, Bedford, MA) at 4 °C for Western blot analysis. Filters were blocked for 1 h at room temperature with 10% nonfat dry milk in TBS-T buffer (10 mM Tris-HCl, pH 8, 150 mM NaCl, 0.1% Tween 20). Then, filters were probed with specific antibodies in the same buffer for 14–16 h at 4 °C. After TBS-T washing to remove excess primary antibodies, the blots were incubated in horseradish peroxidase-coupled secondary antibody for 1 h followed by enhanced chemiluminescence detection of the proteins with Hyper-film ECL detection (Amersham Biosciences).

**Luciferase Assay**—For luciferase assay, WT, TRAF2<sup>-/-</sup>, and TRAF2FL MEFs (4  $\times$  10<sup>5</sup> cells per well) were seeded in 6-well (35 mm) plates. After 12 h cells were transfected with 0.5  $\mu$ g of Ig- $\kappa$ B-LUC reporter gene plasmid using Lipofectamine. Cells were stimulated with thapsigargin or tunicamycin for 8 h, and reporter gene activity was determined by the luciferase assay system (Promega). A pRSV- $\beta$ -galactosidase vector (0.2  $\mu$ g) was used to normalize for transfection efficiencies.

**Retroviral Infection**—Full-length hemagglutinin-tagged TRAF2 was subcloned into the retroviral expression vector pBMN by standard cloning techniques. pBMN vector was then transfected in a packaging cell line using Lipofectamine. 48 h after transfection, the viral supernatants were supplemented with Polybrene (9 mg/ml) and filtered through a 0.45- $\mu$ m filter. TRAF2<sup>-/-</sup> fibroblasts (1  $\times$  10<sup>6</sup>) were incubated with viral supernatants for 48 h. The expression of exogenous protein was assayed by Western blot analysis on total cell extracts using anti-TRAF2 antibodies.

**ER Stress Induction and Measurements of Apoptosis**—5  $\times$  10<sup>3</sup> cells/well were seeded in 96-well culture plates and incubated for 24 or 48 h at 37 °C with different concentrations of thapsigargin or tunicamycin. Cell survival was examined using 3-(4,5-dimethylthiazol-2-yl)-5-(3-carboxymethoxyphenyl)-2-(4-sulfophenyl)-2H-tetrazolium, inner salt (MTS) and an electron coupling reagent (phenazine methosulfate), according to the manufacturer's instructions (Promega). Cell death was assessed by staining the exposed phosphatidylserine on cell membranes with fluorescein isothiocyanate-conjugated annexin V (BD Pharmingen), or propidium iodide staining according to Nicoletti *et al.* (25). Samples were analyzed by flow cytometry using a FACScalibur (Beck-

man Coulter, Fullerton, CA), equipped with ModFit Software. Results were mean  $\pm$  S.D. of at least three separate experiments.

**Measurement of ROS Production**—Reactive oxygen species were detected with H<sub>2</sub>DCFDA (Calbiochem). H<sub>2</sub>DCFDA diffuses into the cells where it is converted into a non-fluorescent derivative (H<sub>2</sub>DCF) by endogenous esterases. H<sub>2</sub>DCF is oxidized to green fluorescent DCF in the presence of intracellular ROS. Cells were routinely treated with either tunicamycin or thapsigargin for 24 or 48 h, washed, and incubated at 37 °C for 30 min in the presence of H<sub>2</sub>DCFDA in serum-free medium. Me<sub>2</sub>SO-treated cells were used as controls. After incubation, cells were washed twice with phosphate-buffered saline, resuspended in phosphate-buffered saline, and analyzed by flow cytometry using a FACScan Cell Scanner (BD Biosciences).

**Kinase Assay**—JNK immunoprecipitates were used for the immune complex kinase assay that was performed at 30 °C for 10 min with 2  $\mu$ g of substrate, 10  $\mu$ Ci of [ $\gamma$ -<sup>32</sup>P]ATP in a total of 20  $\mu$ l of kinase buffer (20 mM HEPES, pH 7.4, 10 mM MgCl<sub>2</sub>, 25 mM  $\beta$ -glycerophosphate, 50  $\mu$ M Na<sub>3</sub>VO<sub>4</sub>, and 50  $\mu$ M dithiothreitol). The substrate was glutathione S-transferase-c-Jun (amino acids 1–79). The reaction was terminated by boiling in SDS sample buffer, and the products were resolved by 12% SDS-PAGE. Phosphorylated proteins were detected by autoradiography.

### RESULTS

**Increased Susceptibility of TRAF2<sup>-/-</sup> MEFs to ER Stress-induced Apoptosis**—TRAF2 is a scaffold protein that transduces signals from membrane receptors and the ER membrane (10–12). To assess the role of TRAF2 in apoptosis induced by ER stress, we treated MEFs derived from TRAF2<sup>-/-</sup> mice and WT MEFs with increasing concentrations of thapsigargin and tunicamycin. Both drugs induce ER stress by inhibiting ER-resident Ca<sup>2+</sup>-ATPase, and N-glycosylation, respectively. After a 48-h treatment, some morphological changes were observed. In particular, WT MEFs showed an extended shape, typical of cellular stress response, whereas TRAF2<sup>-/-</sup> MEFs appeared detached and shrunken (Fig. 1A). Because these morphological changes were reminiscent of apoptosis, we performed annexin V staining on WT and TRAF2<sup>-/-</sup> MEFs. As shown in Fig. 1B, treatment with thapsigargin or tunicamycin caused a dramatic increase in apoptosis in TRAF2<sup>-/-</sup> MEFs but not in WT MEFs. The higher sensitivity to apoptosis observed in TRAF2<sup>-/-</sup> MEFs was not because of an intrinsic defect of these cells, given that reintroduction of TRAF2 (TRAF2FL) completely rescued cell viability (Fig. 1, C–E). TRAF2<sup>-/-</sup> MEFs showed the same susceptibility as WT MEFs to serum starvation- and doxorubicin-induced cell death (Fig. 1F). These results suggest a specific role for TRAF2 in modulating survival signals from the ER.

**ROS Mediate Increased Apoptosis in TRAF2<sup>-/-</sup> MEFs**—ER stress has recently been shown to promote oxidative stress and apoptosis (21). Hence, to have some insight on the molecular mechanism determining the increased susceptibility to ER stress-induced apoptosis, we compared ROS production in WT and TRAF2<sup>-/-</sup> MEFs. As shown in Fig. 2, treatment with thapsigargin or tunicamycin caused an increase in ROS production in TRAF2<sup>-/-</sup> MEFs but not in WT. Reconstitution of these cells with TRAF2 (TRAF2FL) blocked ROS accumulation following treatment with thapsigargin and tunicamycin (Fig. 2, A and B). To investigate whether the increased production of ROS was responsible for the susceptibility of TRAF2<sup>-/-</sup> MEFs to ER stress-induced apoptosis, TRAF2<sup>-/-</sup> MEFs were treated with thapsigargin or tunicamycin in the presence of different antioxidants and 48 h later cell viability was measured by MTS assay and the ROS level by flow cytometry. As shown in Fig. 3, NAC abolished ROS accumulation and protected these cells from

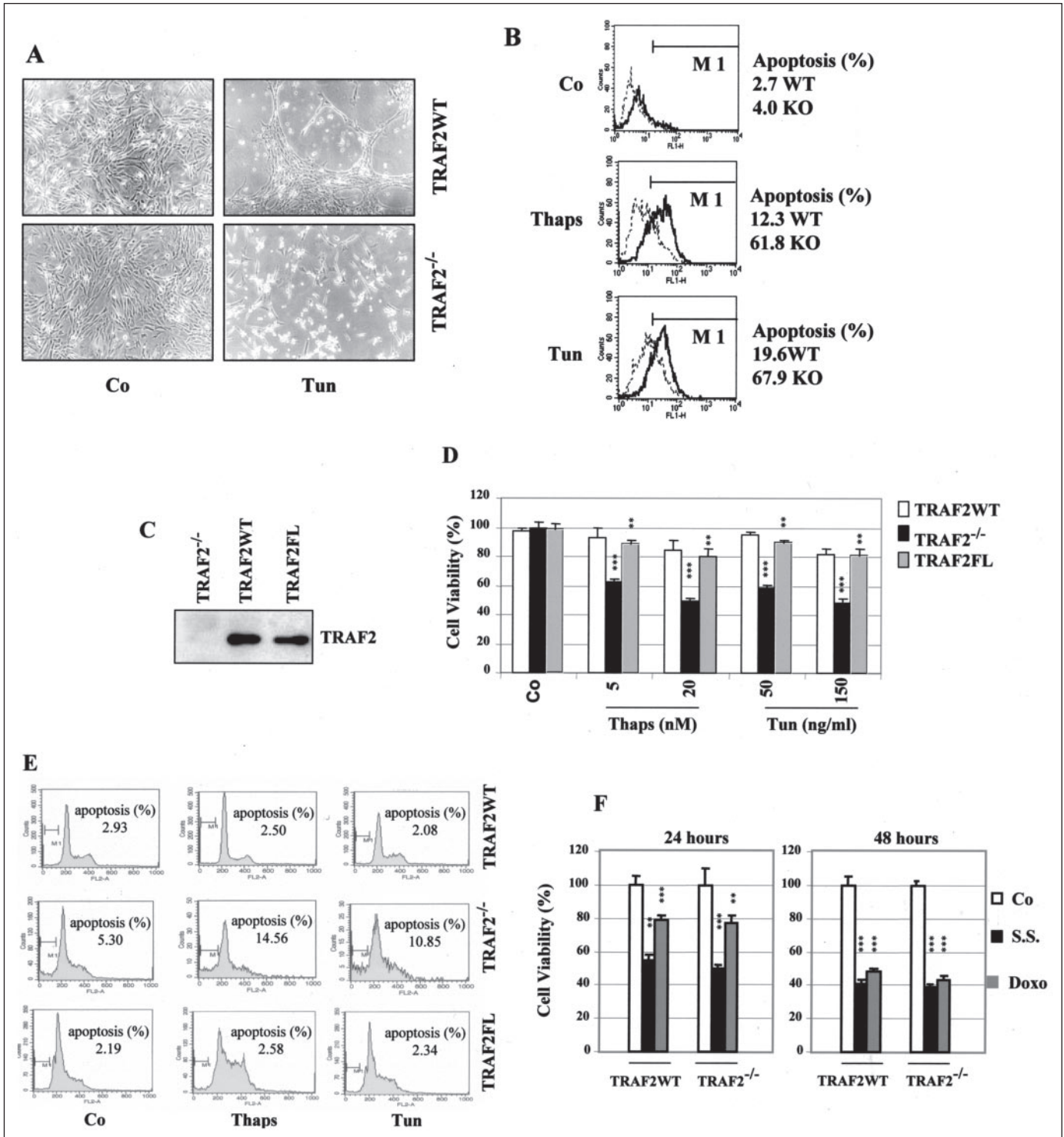
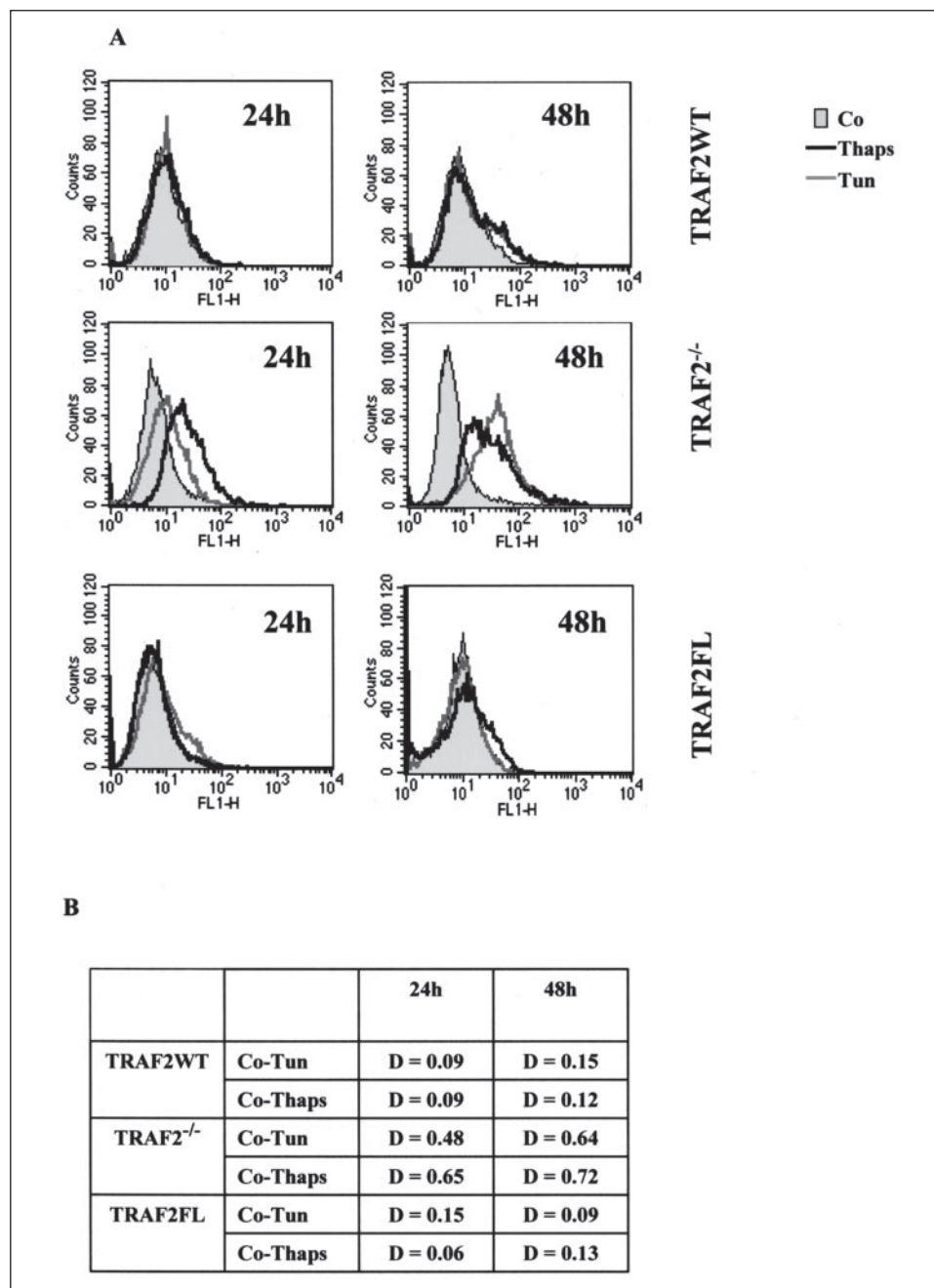


FIGURE 1. ER stress causes apoptosis in TRAF2<sup>-/-</sup> MEFs. *A*, WT and TRAF2<sup>-/-</sup> MEFs were treated with 100 ng/ml tunicamycin or vehicle for 48 h. Cell death was examined by morphological changes under a phase-contrast microscope. *B*, WT and TRAF2<sup>-/-</sup> MEFs were treated with 5 nM thapsigargin or 50 ng/ml tunicamycin for 48 h. Apoptosis was assessed by flow cytometry after staining with fluorescein isothiocyanate-conjugated annexin V. Percentage of the apoptotic cell is indicated. *C*, restoration of TRAF2 protein expression. TRAF2<sup>-/-</sup> MEFs were infected with an expression vector encoding full-length TRAF2. Expression of the TRAF2 protein was assessed by Western blot in WT, TRAF2<sup>-/-</sup>, and TRAF2-reconstituted cells (TRAF2FL). *D*, restoration of TRAF2 protein expression rescues TRAF2<sup>-/-</sup> cells from ER stress-induced apoptosis. WT, TRAF2<sup>-/-</sup>, and TRAF2FL MEFs were treated with Me<sub>2</sub>SO (Co), tunicamycin (Tun), or thapsigargin (Thaps) for 48 h. Cell viability was assessed by MTS assay. Data are mean ± S.D. from five independent experiments. Statistical analysis was by unpaired Student's *t* test: \*\*, *p* < 0.002; \*\*\*, *p* < 0.0001. *E*, restoration of TRAF2 protein expression rescues TRAF2<sup>-/-</sup> cells from endoplasmic reticulum stress-induced apoptosis. TRAF2<sup>-/-</sup>, WT, and TRAF2FL MEFs were treated with Me<sub>2</sub>SO (Co), 20 nM thapsigargin, or 150 ng/ml tunicamycin for 48 h and analyzed by flow cytometry. Percentage of sub-G<sub>0</sub> cells is indicated. *F*, TRAF2<sup>-/-</sup> and WT MEFs were serum starved for 24 and 48 h, or treated with 0.2 μM doxorubicin for 24 and 48 h, and cell viability was assessed by MTS assay. Data are mean ± S.D. from three independent experiments. Statistical analysis was by the unpaired Student's *t* test: \*\*, *p* < 0.002; \*\*\*, *p* < 0.0001. KO, knock-out.

**FIGURE 2. Susceptibility of TRAF2<sup>-/-</sup> MEFs to endoplasmic reticulum-dependent oxidative stress.** A, WT, TRAF2<sup>-/-</sup>, and TRAF2FL MEFs were treated with Me<sub>2</sub>SO (Co), 20 nM thapsigargin (Thaps), or 150 ng/ml tunicamycin (Tun) for 24 or 48 h. Cells were labeled with 5 μM H<sub>2</sub>DCFDA and analyzed by flow cytometry. B, Kolmogorov-Smirnov statistical analysis of flow cytometric data were used according to Cell Quest Software (BD Biosciences Immunocytometry Systems). D values by Kolmogorov-Smirnov analysis (*p* ≤ 0.001) are shown.



apoptosis. Similar results were obtained by using dithiothreitol as antioxidant (data not shown). Interestingly, also the small percentage of WT MEFs and reconstituted TRAF2<sup>-/-</sup> MEFs undergoing apoptosis following treatment with tunicamycin and thapsigargin were almost completely protected by both antioxidants (Fig. 3 and data not shown). These results demonstrated that susceptibility of TRAF2<sup>-/-</sup> MEFs to ER stress-induced apoptosis was because of increased accumulation of ROS. It is worth noting that in TRAF2<sup>-/-</sup> cells, higher levels of ROS and apoptosis were detected, even in the absence of ER stressing agents (Fig. 1, B and E, and data not shown).

**TRAF2-mediated NF-κB Activation Protects Cells from ER Stress-induced Apoptosis**—Given the central role played by TRAF2 to correctly signal activation of NF-κB and JNK from ER, we investigated which of these pathways control ROS accumulation and protect cells from ER stress-induced apoptosis. MEFs derived from p65 knock-out

and JNK1/2 double knock-out mice were treated with thapsigargin or tunicamycin in the presence or absence of NAC. As shown in Fig. 4A, p65<sup>-/-</sup> MEFs showed very high levels of ROS following treatment with thapsigargin and tunicamycin. As expected, treatment with NAC decreased ROS accumulation by about 40%. In contrast, JNK1/2<sup>-/-</sup> MEFs showed an accumulation of ROS similar to WT MEFs (Fig. 4A). Statistical analysis is reported in Fig. 4B. We next investigated the susceptibility of p65<sup>-/-</sup> and JNK1/2<sup>-/-</sup> MEFs to apoptosis induced by thapsigargin or tunicamycin in the presence or absence of NAC. As shown in Fig. 4C, p65<sup>-/-</sup> MEFs were highly susceptible to apoptosis compared with WT MEF and treatment with NAC significantly increased cell viability. JNK1/2<sup>-/-</sup> MEFs did not show susceptibility to ER stress-induced cell death, as compared with WT MEFs. These results suggest that NF-κB protects cells from ER stress-induced apoptosis by controlling ROS accumulation.

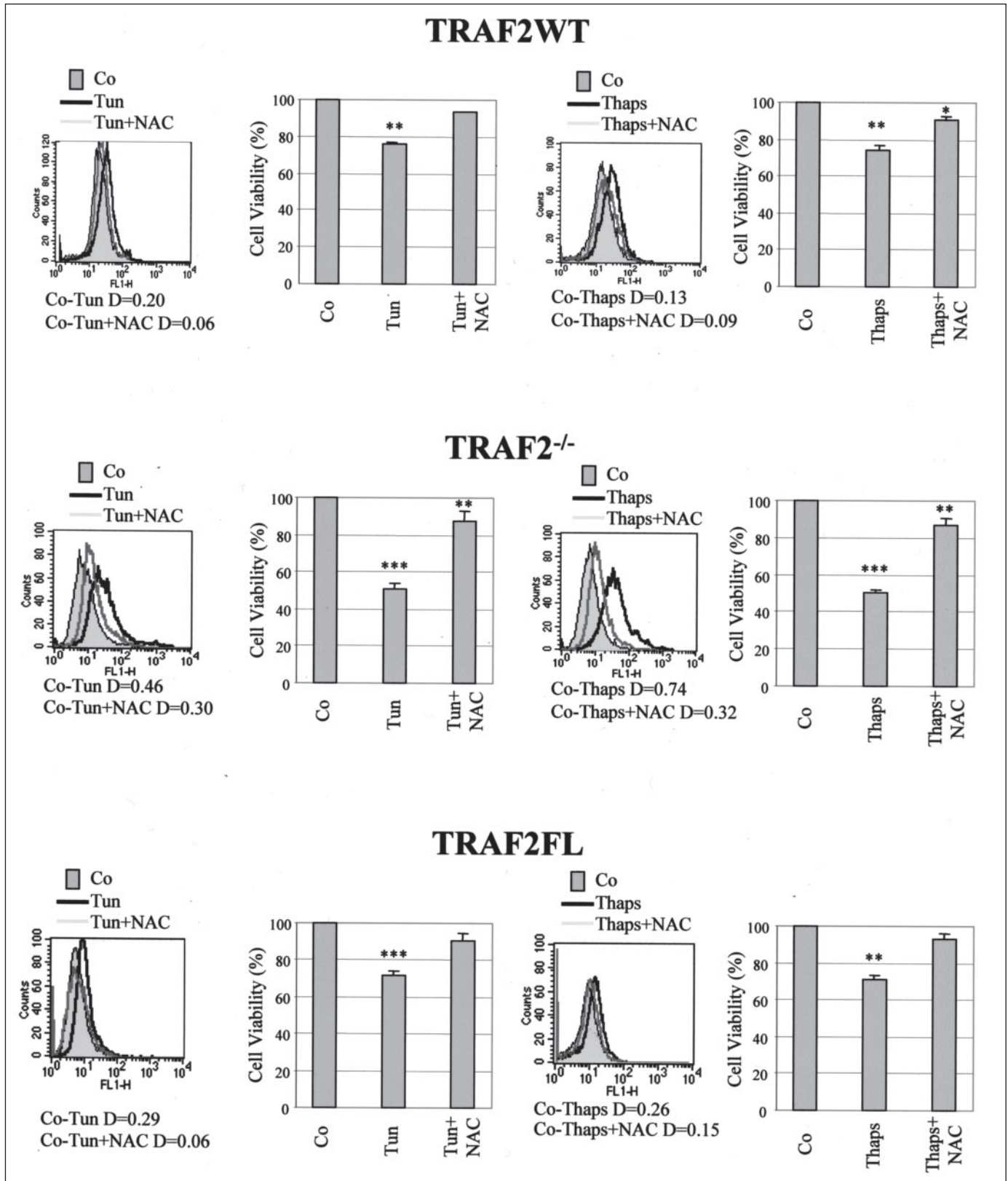


FIGURE 3. ROS production correlates with endoplasmic reticulum stress-induced apoptosis. WT, TRAF2<sup>-/-</sup>, and TRAF2FL MEFs were treated with Me<sub>2</sub>SO (Co), 150 ng/ml tunicamycin (Tun), or 20 nM thapsigargin (Thaps) for 48 h, in the presence or absence of antioxidants (NAC or dithiothreitol). ROS production was assessed by flow cytometry after labeling with H<sub>2</sub>DCFDA. Cell viability was evaluated by MTS assay. Data are mean ± S.D. from three independent experiments. Statistical analysis was by the unpaired Student's *t* test: \*, *p* < 0.02; \*\*, *p* < 0.002; \*\*\*, *p* < 0.0001.

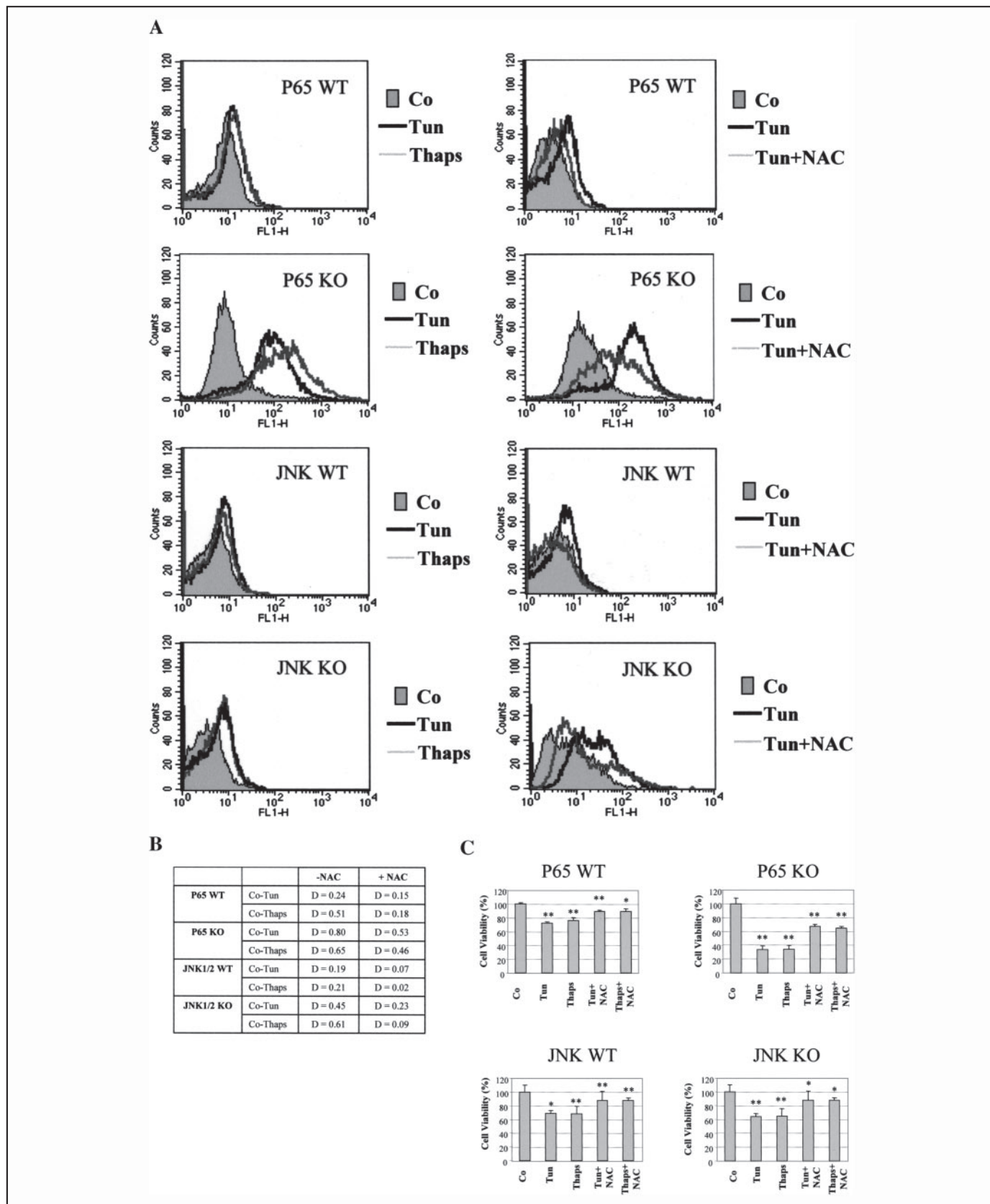
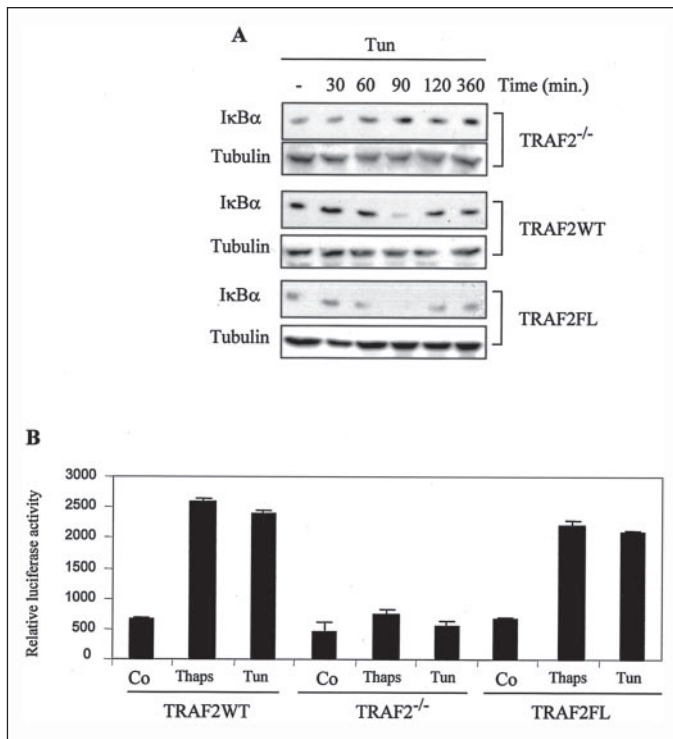


FIGURE 4. Differential susceptibility of p65<sup>-/-</sup> and JNK1/2<sup>-/-</sup> MEFs to endoplasmic reticulum-dependent oxidative stress. *A*, JNK1/2<sup>-/-</sup> and p65<sup>-/-</sup> MEFs were treated with Me<sub>2</sub>SO (Co), 20 nM thapsigargin (*Thaps*), or 150 ng/ml tunicamycin (*Tun*) for 24 h, in the presence or absence of 5 mM NAC. ROS production was assessed by flow cytometry after labeling with H<sub>2</sub>DCFDA. *B*, Kolmogorov-Smirnov statistical analysis of flow cytometric data were used according to Cell Quest Software (BD Biosciences). *D* values by Kolmogorov-Smirnov analysis ( $p \leq 0.001$ ) are shown. *C*, p65<sup>-/-</sup> and JNK1/2<sup>-/-</sup> MEFs were treated with Me<sub>2</sub>SO (Co), thapsigargin (*Thaps*), or tunicamycin (*Tun*) for 24 h, in the presence or absence of 5 mM dithiothreitol. Cell viability was evaluated by MTS assay. Data are mean  $\pm$  S.D. from three independent experiments. Statistical analysis was by the unpaired Student's *t* test: \*,  $p < 0.02$ ; \*\*,  $p < 0.002$ . KO, knock-out.



**FIGURE 5. Defective activation of the NF- $\kappa$ B pathway in TRAF2<sup>-/-</sup> MEFs after endoplasmic reticulum stress.** A, WT, TRAF2<sup>-/-</sup>, and reconstituted TRAF2FL MEFs were treated with tunicamycin (Tun) (150 ng/ml), and expression of the I $\kappa$ B $\alpha$  protein was analyzed by Western blot. Filters were stripped and reprobed with anti- $\alpha$ -tubulin antibodies, as loading control. B, relative luciferase activity observed in WT, TRAF2<sup>-/-</sup>, and TRAF2FL MEFs transfected in triplicate with 0.5  $\mu$ g of the Ig- $\kappa$ B-luciferase reporter plasmid, stimulated with thapsigargin or tunicamycin, as indicated. Values shown (in arbitrary units) represent the mean ( $\pm$  S.D.) of two independent experiments, normalized for  $\beta$ -galactosidase activity of a cotransfected Rous sarcoma virus- $\beta$ -galactosidase plasmid.

To have further insight on the cross-talk between the NF- $\kappa$ B and the JNK pathways after ER stress, we evaluated activation of both pathways in WT, TRAF2<sup>-/-</sup>, and reconstituted TRAF2FL MEFs. Treatment with tunicamycin caused activation of NF- $\kappa$ B in WT and TRAF2FL MEFs, as demonstrated by the disappearance of the inhibitory subunit I $\kappa$ B $\alpha$  (Fig. 5A) and by the increased activity of a  $\kappa$ B-driven luciferase reporter gene (Fig. 5B). In the absence of TRAF2 it was not possible to detect activation of NF- $\kappa$ B. The observed activation of NF- $\kappa$ B was functional as demonstrated by the reappearance of the inhibitory subunit I $\kappa$ B $\alpha$ , a known early target gene of NF- $\kappa$ B (Fig. 5A).

Activation of JNK in WT and TRAF2FL MEFs stimulated with tunicamycin was detected 90 min after stimulation and decreased thereafter. Treatment with antioxidant did not affect JNK activation (Fig. 6). In contrast, in TRAF2<sup>-/-</sup> MEFs, activation of JNK was detectable only 6 h after stimulation and remained sustained for up to 12 h. This sustained activation of JNK was almost completely suppressed by NAC (Fig. 6). This result confirms that TRAF2 was necessary to activate JNK after ER stress, and suggests that the increased level of ROS detected in the absence of TRAF2 may mediate the sustained activation of JNK. This is in agreement with previous reports showing that after TNF stimulation the early activation of JNK depends on TRAF2 and that the sustained activation of JNK depends on ROS (26). Altogether these results suggested that following ER stress, the TRAF2-mediated activation of NF- $\kappa$ B was responsible for protection from apoptosis by decreasing ROS levels and controlling sustained JNK activation.

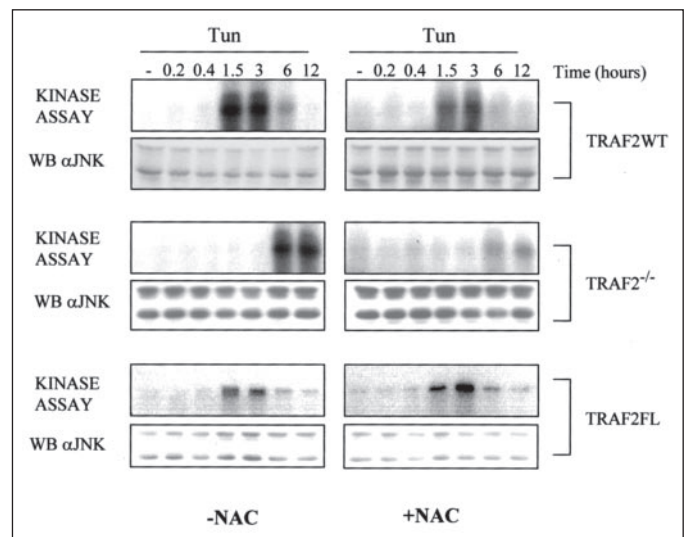


**FIGURE 6. Sustained activation of the JNK pathway in TRAF2<sup>-/-</sup> MEFs after endoplasmic reticulum stress.** WT, TRAF2<sup>-/-</sup>, and TRAF2FL MEFs were treated with tunicamycin (150 ng/ml) for the indicated periods of time in the presence or absence of the antioxidant NAC, and activity of endogenous JNK was assessed by kinase assay using glutathione S-transferase-c-Jun as substrate. Lower panel shows a Western blot for total JNK. WB, Western blot.

**DISCUSSION**

The endoplasmic reticulum is the principal site for protein synthesis and folding, and also serves as a cellular storage site for calcium. Agents that interfere with protein folding or export lead to ER stress and eventually cell death. Although initiation of apoptosis induced by death receptors and mitochondria is well studied, the mechanism by which ER stress triggers apoptosis is still not clear. In the present paper, we present evidence supporting a central role played by TRAF2 in regulation of pro-apoptotic and anti-apoptotic pathways initiated at the ER. We demonstrate that TRAF2<sup>-/-</sup> MEFs have increased susceptibility to ER stress-induced apoptosis. This increased susceptibility to ER stress-induced apoptosis was because of accumulation of ROS following ER stress, and was abolished by the use of antioxidants, such as NAC. In addition, we demonstrated that NF- $\kappa$ B was protecting cells from ER stress-induced apoptosis by controlling ROS accumulation.

TRAF2 has been demonstrated to be involved in signaling from endoplasmic reticulum being able to interact with Ire1 (10), one of the ER transmembrane proteins involved in initiating signals from the ER. TRAF2 mediates activation of both the JNK/SAPK and the NF- $\kappa$ B pathways following ER stress (10, 11). This scenario is reminiscent of TNF signaling, in which TRAF2 mediates simultaneous activation of the NF- $\kappa$ B survival pathway and pro-apoptotic JNK pathway, and the fate of the cell would be determined by interplay between these opposing signals. NF- $\kappa$ B exerts its anti-apoptotic activity by inhibiting caspase function (28–30), preserving function of mitochondria (31), and down-regulating JNK activity (23, 32). The latter function is mediated by at least two different mechanisms: by blocking activation of MKK7 via GADD45 $\beta$  (16) and decreasing ROS accumulation via the ferritin heavy chain (17). The importance of ROS in regulating sustained activation of JNK following TNF receptor triggering has been recently investigated in a NF- $\kappa$ B null cell model (26). Based on this study, TRAF-mediated NF- $\kappa$ B activation suppresses the TNF-induced ROS accumulation that, in turn, induces prolonged JNK activation and cell death. Our result supports this model and suggests that a similar mechanism may also operate for the ER. In fact, induction of ER stress causes activation of both NF- $\kappa$ B and JNK. In the absence of TRAF2 or p65, the NF- $\kappa$ B

## TRAF2 Regulates ER Stress-induced Apoptosis

pathway is not activated, and the late, ROS-dependent JNK activity is not counteracted, leading to cell death.

How does ROS affect JNK activation? ROS may affect JNK activation by at least two different mechanisms: by oxidizing and inhibiting mitogen-activated protein kinase phosphatase (33) and activating the protein ASK1 (34). This kinase may be activated via ROS and TRAF2 and has been demonstrated to be essential for inducing cell death after ER stress, at least in neuronal cells (34, 35). It may be possible that after ER stress and in the absence of a functional NF- $\kappa$ B activation, ASK1 is activated by the increased level of ROS and mediates sustained JNK activation and cell death.

Whereas it is clear from our results that the presence of a functional NF- $\kappa$ B is necessary for survival, counteracting increased induction of ROS following ER stress, the mechanism by which NF- $\kappa$ B exerts this function is not fully understood. It has been recently demonstrated that NF- $\kappa$ B up-regulates expression of ferritin heavy chain, an enzyme involved in iron metabolism and suppression of ROS accumulation (17). However, it is possible that in addition to up-regulation of genes involved in disposal of the ROS, NF- $\kappa$ B may also control transcription of genes that suppress production of ROS.

Our results confirm the central role played by TRAF2 in regulating activation of NF- $\kappa$ B following ER stress, and also sheds light on the functional significance of this activation. Recently, it has been demonstrated that in addition to the TRAF2-mediated NF- $\kappa$ B activation, another mechanism leading to activation of NF- $\kappa$ B following ER stress might exist. Based on this model, following ER stress, phosphorylation of eukaryotic initiation factor 2 represses synthesis of the inhibitory subunit I $\kappa$ B $\alpha$ , leading to activation of NF- $\kappa$ B (36). The two models of activation of NF- $\kappa$ B following ER stress, the TRAF2-mediated and the eukaryotic initiation factor 2-mediated, are not mutually exclusive. It is possible that both mechanisms contribute to activate NF- $\kappa$ B upon ER stress. However, whereas the biological significance of the link between eukaryotic initiation factor 2 phosphorylation and NF- $\kappa$ B activation is not fully understood, the functional significance of TRAF2-mediated NF- $\kappa$ B activation seems to be clear, at least in our experimental system. In fact, cells lacking TRAF2 or functional NF- $\kappa$ B undergo massive cell death after ER stress.

In conclusion, in the present study we provide evidence, for the first time, that the adaptor protein TRAF2 plays a central role in regulating signaling from the ER and that the activation of NF- $\kappa$ B, mediated by TRAF2, protects cells from ER stress-induced apoptosis. Therefore TRAF2 and NF- $\kappa$ B may be potential targets to control ER stress-induced apoptosis.

*Acknowledgment*—We thank Dr. Kostas Pantopoulos (McGill University, Canada) for helpful advice on ROS detection.

### REFERENCES

1. Berridge, M. J. (1995) *Biochem. J.* **312**, 1–11
2. Sambrook, J. F. (1990) *Cell* **61**, 197–199
3. Kaufman, R. J. (1999) *Genes Dev.* **13**, 1211–1233
4. Sitia, R., and Braakman, I. (2003) *Nature* **426**, 891–894
5. Tirasophon, W., Welihinda, A. A., and Kaufman, R. J. (1998) *Genes Dev.* **12**, 1812–1824
6. Wang, X. Z., Harding, H. P., Zhang, Y., Jolicoeur, E. M., Kuroda, M., and Ron, D. (1998) *EMBO J.* **17**, 5708–5717
7. Shi, Y., Vattem, K. M., Sood, R., An, J., Liang, J., Stramm, L., and Wek, R. C. (1998) *Mol. Cell. Biol.* **18**, 7499–7509
8. Bertolotti, A., Zhang, Y., Hendershot, L. M., Harding, H. P., and Ron, D. (2000) *Nat. Cell. Biol.* **2**, 326–332
9. Breckenridge, D. G., Germain, M., Mathai, J. P., Nguyen, M., and Shore, G. C. (2003) *Oncogene* **22**, 8608–8618
10. Urano, F., Wang, X. Z., Bertolotti, A., Zhang, Y., Chung, P., Harding, H. P., and Ron, D. (2000) *Science* **287**, 664–666
11. Leonardi, A., Vito, P., Mauro, C., Pacifico, F., Ulianich, L., Consiglio, E., Formisano, S., and Di Jeso, B. (2002) *Endocrinology* **143**, 2169–2177
12. Chung, J. Y., Park, Y. C., Ye, H., and Wu, H. (2002) *J. Cell Sci.* **115**, 679–688
13. Rothe, M., Wong, S. C., Henzel, W. J., and Goeddel, D. V. (1994) *Cell* **78**, 681–692
14. Yeh, W. C., Shahinian, A., Speiser, D., Kraunus, J., Billia, F., Wakeham, A., de la Pompa, J. L., Ferrick, D., Hum, B., Iscove, N., Ohashi, P., Rothe, M., Goeddel, D. V., and Mak, T. W. (1997) *Immunity* **7**, 715–725
15. Lee, S. Y., Reichlin, A., Santana, A., Sokol, K. A., Nussenzweig, M. C., and Choi, Y. (1997) *Immunity* **7**, 703–713
16. Papa, S., Zazzeroni, F., Bubici, C., Jayawardena, S., Alvarez, K., Matsuda, S., Nguyen, D. U., Pham, C. G., Nelsbach, A. H., Melis, T., De Smaele, E., Tang, W. J., D'Adamo, L., and Franzoso, G. (2004) *Nat. Cell. Biol.* **6**, 146–153
17. Pham, C. G., Bubici, C., Zazzeroni, F., Papa, S., Jones, J., Alvarez, K., Jayawardena, S., De Smaele, E., Cong, R., Beaumont, C., Torti, F. M., Torti, S. V., and Franzoso, G. (2004) *Cell* **119**, 529–542
18. Bray, T. M. (1999) *Proc. Soc. Exp. Biol. Med.* **222**, 195
19. Forsberg, L., deFaire, U., and Morgenstern, R. (2001) *Arch. Biochem. Biophys.* **389**, 84–93
20. Finkel, T. (2003) *Curr. Opin. Cell Biol.* **15**, 247–254
21. Haynes, C. M., Titus, E. A., and Cooper, A. A. (2004) *Mol. Cell* **15**, 767–776
22. Tournier, C., Hess, P., Yang, D. D., Xu, J., Turner, T. K., Nimmual, A., Bar-Sagi, D., Jones, S. N., Flavell, R. A., and Davis, R. J. (2000) *Science* **288**, 870–874
23. De Smaele, E., Zazzeroni, F., Papa, S., Nguyen, D. U., Jin, R., Jones, J., Cong, R., and Franzoso, G. (2001) *Nature* **414**, 308–313
24. Leonardi, A., Ellinger-Ziegelbauer, H., Franzoso, G., Brown, K., and Siebenlist, U. (2000) *J. Biol. Chem.* **275**, 271–278
25. Nicoletti, I., Migliorati, G., Pagliacci, M. C., Grignani, F., and Riccardi, C. (1991) *J. Immunol. Methods* **139**, 271–279
26. Sakon, S., Xue, X., Takekawa, M., Sasazuki, T., Okazaki, T., Kojima, Y., Piao, J. H., Yagita, H., Okumura, K., Doi, T., and Nakano, H. (2003) *EMBO J.* **22**, 3898–3909
27. Deleted in proof
28. Deveraux, Q. L., Roy, N., Stennicke, H. R., Van Arsdale, T., Zhou, Q., Srinivasula, S. M., Alnemri, E. S., Salvesen, G. S., and Reed, J. C. (1998) *EMBO J.* **17**, 2215–2223
29. Liston, P., Roy, N., Tamai, K., Lefebvre, C., Baird, S., Cherton-Horvat, G., Farahani, R., McLean, M., Ikeda, J. E., MacKenzie, A., and Korneluk, R. G. (1996) *Nature* **379**, 349–353
30. Muzio, M., Chinnaiyan, A. M., Kischkel, F. C., O'Rourke, K., Shevchenko, A., Ni, J., Scaffidi, C., Bretz, J. D., Zhang, M., Gentz, R., Mann, M., Krammer, P. H., Peter, M. E., and Dixit, V. M. (1996) *Cell* **85**, 817–827
31. Boise, L. H., Gonzalez-Garcia, M., Postema, C. E., Ding, L., Lindsten, T., Turka, L. A., Mao, X., Nunez, G., and Thompson, C. B. (1993) *Cell* **74**, 597–608
32. Tang, G., Minemoto, Y., Dibling, B., Purcell, N. H., Li, Z., Karin, M., and Lin, A. (2001) *Nature* **414**, 313–317
33. Kamata, H., Honda, S., Maeda, S., Chang, L., Hirata, H., and Karin, M. (2005) *Cell* **120**, 649–661
34. Tobiume, K., Matsuzawa, A., Takahashi, T., Nishitoh, H., Morita, K., Takeda, K., Minora, O., Miyazono, K., Noda, T., and Ichijo, H. (2001) *EMBO Rept.* **2**, 222–228
35. Nishitoh, H., Matsuzawa, A., Tobiume, K., Saegusa, K., Takeda, K., Inoue, K., Kikuzaka, A., and Ichijo, H. (2002) *Genes Dev.* **16**, 1345–1355
36. Deng, J., Lu, D. L., Zhang, Y., Scheuner, D., Kaufman, R. J., Sonenberg, N., Harding, H. P., and Ron, D. (2004) *Mol. Cell. Biol.* **24**, 10161–10168

# ABIN-1 Binds to NEMO/IKK $\gamma$ and Co-operates with A20 in Inhibiting NF- $\kappa$ B\*<sup>[S]</sup>

Received for publication, February 16, 2006, and in revised form, April 26, 2006 Published, JBC Papers in Press, May 9, 2006, DOI 10.1074/jbc.M601502200

Claudio Mauro<sup>†1</sup>, Francesco Pacifico<sup>§1</sup>, Alfonso Lavorgna<sup>‡</sup>, Stefano Mellone<sup>§</sup>, Alessio Iannetti<sup>‡</sup>, Renato Acquaviva<sup>‡</sup>, Silvestro Formisano<sup>‡</sup>, Pasquale Vito<sup>¶</sup>, and Antonio Leonardi<sup>‡2</sup>

From the <sup>†</sup>Dipartimento di Biologia e Patologia Cellulare e Molecolare, "Federico II," University of Naples, via S. Pansini, 5, 80131 Naples, the <sup>§</sup>Istituto di Endocrinologia ed Oncologia Sperimentale, CNR, via S. Pansini, 5, 80131 Naples, and the <sup>¶</sup>Dipartimento di Scienze Biologiche ed Ambientali, Università degli Studi del Sannio, via Port'Arso, 11, 82100 Benevento, Italy

Nuclear factor  $\kappa$ B (NF- $\kappa$ B) plays a pivotal role in inflammation, immunity, stress responses, and protection from apoptosis. Canonical activation of NF- $\kappa$ B is dependent on the phosphorylation of the inhibitory subunit I $\kappa$ B $\alpha$  that is mediated by a multimeric, high molecular weight complex, called I $\kappa$ B kinase (IKK) complex. This is composed of two catalytic subunits, IKK $\alpha$  and IKK $\beta$ , and a regulatory subunit, NEMO/IKK $\gamma$ . The latter protein is essential for the activation of IKKs and NF- $\kappa$ B, but its mechanism of action is not well understood. Here we identified ABIN-1 (A20 binding inhibitor of NF- $\kappa$ B) as a NEMO/IKK $\gamma$ -interacting protein. ABIN-1 has been previously identified as an A20-binding protein and it has been proposed to mediate the NF- $\kappa$ B inhibiting effects of A20. We find that both ABIN-1 and A20 inhibit NF- $\kappa$ B at the level of the IKK complex and that A20 inhibits activation of NF- $\kappa$ B by de-ubiquitination of NEMO/IKK $\gamma$ . Importantly, small interfering RNA targeting ABIN-1 abrogates A20-dependent de-ubiquitination of NEMO/IKK $\gamma$  and RNA interference of A20 impairs the ability of ABIN-1 to inhibit NF- $\kappa$ B activation. Altogether our data indicate that ABIN-1 physically links A20 to NEMO/IKK $\gamma$  and facilitates A20-mediated de-ubiquitination of NEMO/IKK $\gamma$ , thus resulting in inhibition of NF- $\kappa$ B.

NF- $\kappa$ B is a ubiquitously expressed family of transcription factors that controls the expression of numerous genes involved in immune and inflammatory responses (1). NF- $\kappa$ B also plays an important role during cellular stress responses, due to its anti-apoptotic and proliferation-promoting functions (2). Aberrant activation of NF- $\kappa$ B is a major hallmark of several inflammatory diseases such as arthritis (3, 4), and a variety of human cancers (5, 6). In resting cells, NF- $\kappa$ B is sequestered in the cytoplasm in an inactive form by members of the inhibitory family of I $\kappa$ B proteins (1). Various stimuli including pathogens, pathogen-related factors, and cytokines lead to phosphorylation of the inhibitory subunit I $\kappa$ B $\alpha$  on specific serine residues (Ser<sup>32</sup> and Ser<sup>36</sup>) (7) catalyzed by two I $\kappa$ B kinases (IKKs),<sup>3</sup> namely IKK $\alpha$  and IKK $\beta$  (8–12). This step marks

the I $\kappa$ B protein for ubiquitination and subsequent degradation through a proteasome-dependent pathway (1). The active NF- $\kappa$ B is then free for translocation to the nucleus, where it binds the  $\kappa$ B sequences present in the promoters of responsive genes.

IKK $\alpha$  and IKK $\beta$  reside in a larger kinase complex (700–900 kDa), called the I $\kappa$ B kinase complex (IKK complex), that also contains the essential regulatory subunit NEMO (also known as IKK $\gamma$ ) (13, 14). Genetic studies suggest that NEMO/IKK $\gamma$  is absolutely required for the activation of IKKs and NF- $\kappa$ B in response to different stimuli (13, 15). NEMO/IKK $\gamma$  contains several coiled-coil domains, a leucine zipper, and a C-terminal zinc finger domain. These motifs are required for the correct assembly of the IKK complex (13) and recruitment of upstream signaling mediators (16). Numerous proteins have been demonstrated to interact with NEMO/IKK $\gamma$ , as the kinase RIP and the inhibitor of NF- $\kappa$ B A20 (17), the viral trans-activator TAX (18–20), and the adaptor proteins CIKS/Act-1, TANK, and CARMA (21–23). Therefore, NEMO/IKK $\gamma$  represents the point where most NF- $\kappa$ B signaling pathways converge. Despite this information, the molecular mechanism regulating IKK complex function is not fully understood.

Ubiquitin conjugation has been most prominently associated with protein degradation through a proteasome-dependent pathway, but it is becoming increasingly evident that ubiquitination plays a key role in the signal transduction pathway leading to activation of NF- $\kappa$ B (24, 25). Recent reports show that lysine 63-linked ubiquitination of NEMO/IKK $\gamma$  is an important step for the activation of IKKs and NF- $\kappa$ B following various stimuli, such as TNF, lipopolysaccharide, and antigen receptor (26–28). In contrast, the tumor suppressor CYLD is reported as a negative regulator of NF- $\kappa$ B by specific de-ubiquitination of NF- $\kappa$ B signaling molecules, such as TRAF2, TRAF6, and NEMO/IKK $\gamma$  (29). Also A20 functions as an inhibitor of the NF- $\kappa$ B pathway by removing Lys<sup>63</sup>-linked ubiquitin chains from RIP, an essential mediator of the proximal TNF-Receptor-1 signaling complex. Then A20 targets RIP for Lys<sup>48</sup>-linked polyubiquitination and proteasomal degradation (30). Furthermore, A20 terminates Toll-like receptor-induced NF- $\kappa$ B signaling, by cleaving ubiquitin chains from TRAF6 (27). The central role played by A20 in terminating NF- $\kappa$ B activation is further demonstrated by the fact that A20<sup>-/-</sup> mice develop severe inflammation and cachexia, are hypersensitive to both lipopolysaccharide and TNF, and die prematurely (27, 31). Here we used NEMO/IKK $\gamma$  as bait in yeast two-hybrid screening, and identified ABIN-1 (A20 binding inhibitor of NF- $\kappa$ B) as a NEMO/IKK $\gamma$ -interacting protein.

## EXPERIMENTAL PROCEDURES

**Cell Culture and Biological Reagents**—HEK293 cells were maintained in Dulbecco's modified Eagle's medium (Invitrogen) supplemented with 10% fetal calf serum, 100 units/ml penicillin, 100 mg/ml streptomycin, and 1% glutamine.

\* This work was supported by grants from the Associazione Italiana Ricerca sul Cancro (AIRC), MIUR-PRIN 2005051307, European Molecular Imaging Laboratory Network Grant LSHC-2004-503569, and Fondazione Italiana Sclerosi Multipla (2003/R66). The costs of publication of this article were defrayed in part by the payment of page charges. This article must therefore be hereby marked "advertisement" in accordance with 18 U.S.C. Section 1734 solely to indicate this fact.

This work is dedicated to the memory of Prof. Serafino Zappacosta.

<sup>[S]</sup> The on-line version of this article (available at <http://www.jbc.org>) contains supplemental Fig. S1.

<sup>1</sup> Both authors equally contributed to this work.

<sup>2</sup> To whom correspondence should be addressed. Tel.: 39-081-7463606; Fax: 39-081-7701016; E-mail: [leonardi@unina.it](mailto:leonardi@unina.it).

<sup>3</sup> The abbreviations used are: IKK, I $\kappa$ B kinases; TNF, tumor necrosis factor; ABIN-1, A20 binding inhibitor of NF- $\kappa$ B; HA, hemagglutinin; GST, glutathione S-transferase; siRNA, small interfering RNA; CIKS, connection to I $\kappa$ B kinase and SAPK.

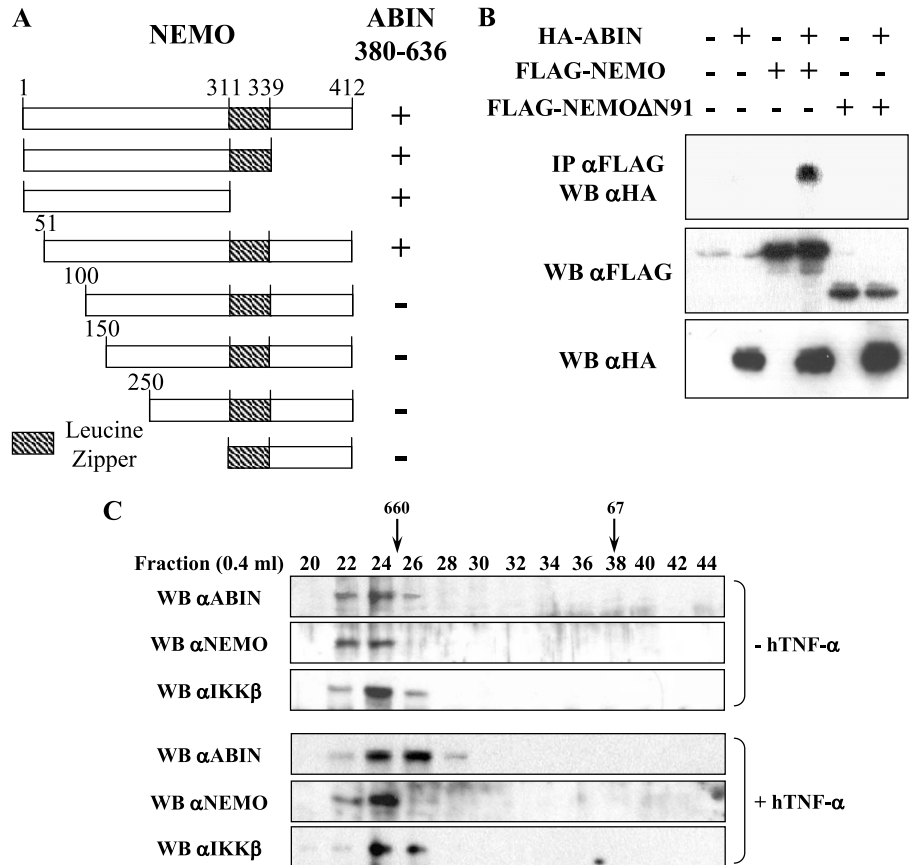


**FIGURE 1. Mapping of the ABIN-1 interaction domain on NEMO/IKK $\gamma$ .** *A*, mapping of the NEMO/IKK $\gamma$ -ABIN interaction by yeast two-hybrid experiments. The NEMO/IKK $\gamma$  constructs are schematically represented. The interaction of the NEMO/IKK $\gamma$  constructs with the clone isolated by yeast two-hybrid screening (ABIN 380–636) is indicated by the *plus sign*. *B*, *in vivo* mapping of the NEMO/IKK $\gamma$ -ABIN interaction. HEK293 cells were transfected with the indicated combinations of expression constructs encoding HA-ABIN and either FLAG-NEMO/IKK $\gamma$  or FLAG-NEMO $\Delta$ N91. Cell extracts were analyzed by immunoblotting either directly or after immunoprecipitation with anti-FLAG antibodies. *C*, chromatographic distribution of endogenous ABIN-1, NEMO/IKK $\gamma$ , and IKK $\beta$ . Cytoplasmic extracts were prepared from HEK293 treated with TNF for 120 min or left unstimulated, and subjected to chromatography on a Superdex S-200 column. Fractions were analyzed by Western blot (WB) by using the indicated antibodies. Molecular weight markers are indicated at the top of the figure.

Anti-ABIN-1 polyclonal antibodies were generated in rabbits, by using a recombinant peptide encompassing amino acids 380–636 of human ABIN-1. Other antibodies used for this study were: FLAG epitope (Sigma), A20 (BD Pharmingen), HA epitope, NEMO/IKK $\gamma$ , IKK $\beta$ , I $\kappa$ B $\alpha$ , and tubulin (Santa Cruz Biotechnologies). Human TNF- $\alpha$  (Peprotech Inc.) was used at 2,000 units/ml.

Human ABIN-1 was amplified by PCR from a human liver c-DNA library (Clontech) and cloned into pcDNA3.1-HA, -FLAG, and -His vectors (Invitrogen) for expression in mammalian cells. A20, TAX, and ubiquitin expression vectors were gifts from G. Natoli, T. K. Jeang, and G. Courtois, respectively. NEMO/IKK $\gamma$ , IKK $\beta$ , CIKS, and TRAF2 expression vectors were previously described (21, 32). All deletion mutants were prepared by conventional PCR and cloned into pcDNA3.1-HA or -FLAG vectors. Point mutants of A20 (C103S and D100A/C103S) were generated by the QuikChange Site-directed Mutagenesis kit (Stratagene), according to the manufacturer's protocol.

**Yeast Two-hybrid Screening**—The cDNA encoding the N-terminal part of mouse NEMO/IKK $\gamma$  (amino acids 1–311) was cloned in-frame into the GAL-4 DNA-binding domain vector pGBKT7 (Clontech). The resulting plasmid pGBKT7-NEMO/IKK $\gamma$  was used as bait in a yeast two-hybrid screen of a human liver cDNA library (Clontech) in *Saccharomyces cerevisiae* strain AH109. The NEMO/IKK $\gamma$  deletion mutants for two-hybrid mapping were made by conventional PCR and cloned into the pGBKT7 vector.

**Gel Filtration of Cellular Extracts**—Gel filtration procedures were performed as previously described (42). Fractions were analyzed by Western blotting for ABIN-1, NEMO/IKK $\gamma$ , and IKK $\beta$ .

**In Vitro Translation and GST Pull-down Assays**—*In vitro* transcription and translation were carried out with 1  $\mu$ g of ABIN-1 constructs according to the TNT Quick Coupled Transcription/Translation System protocol (Promega) in the presence of [<sup>35</sup>S]methionine.

GST-NEMO/IKK $\gamma$  fusion protein was produced and purified as described (33). GST pull-down assays were performed by incubating an aliquot of GST-NEMO/IKK $\gamma$  bound to glutathione-Sepharose beads (Amersham Biosciences) together with 10  $\mu$ l of *in vitro* translated ABIN-1 protein in phosphate-buffered saline, 1% Triton X-100 buffer (including Complete Protease Inhibitor mixture (Roche)) for 2 h at 4  $^{\circ}$ C. Beads were then washed five times with the same buffer, resuspended in Laemmli buffer, and run on a SDS-polyacrylamide gel before autoradiography.

**Transfection, Immunoprecipitation, and Luciferase Assay**—Lipofectamine-mediated transfections were performed according to the manufacturer's instructions (Invitrogen). All transfections included supplemental empty vector to ensure that the total amount of transfected DNA was kept constant in each dish culture.

For immunoprecipitation of transfected proteins, HEK293 cells ( $3 \times 10^6$ ) were transiently transfected and 24 h after transfection cells were lysed in Triton X-100 lysis buffer (20 mM Hepes, pH 7.4, 150 mM NaCl, 10% glycerol, 1% Triton X-100, and Complete Protease Inhibitor mixture). After an additional 15 min on ice, cell extracts were centrifuged for 10 min at  $14,000 \times g$  at 4  $^{\circ}$ C and supernatants were incubated for 4 h at 4  $^{\circ}$ C with anti-FLAG antibodies bound to agarose beads (M2, Sigma). The immunoprecipitates were washed five times with Triton X-100 lysis buffer and subjected to SDS-PAGE.

For luciferase assay, HEK293 cells ( $4 \times 10^5$ ) were seeded in 6-well plates. After 12 h cells were transfected with 0.5  $\mu$ g of Ig- $\kappa$ B-luciferase reporter plasmid and various combinations of expression plasmids. 24 h after transfection, cells were stimulated with TNF- $\alpha$  for 3 h or left untreated. Cell extracts were prepared and reporter gene activity was determined via the luciferase assay system (Promega). Expression of the pRSV- $\beta$ -galactosidase vector (0.2  $\mu$ g) was used to normalize transfection efficiencies.

**FIGURE 2. Mapping of the NEMO/IKK $\gamma$  and the A20 binding domains on ABIN-1.** A and B, GST pull-down assays: GST-NEMO/IKK $\gamma$  was incubated with *in vitro* translated full-length (FL) or deletion mutants of ABIN. Aliquots of *in vitro* translated constructs and GST-NEMO/IKK $\gamma$  stained by Coomassie Blue are shown. C, co-immunoprecipitation of FLAG-A20 with HA-ABIN or ABIN $\Delta$ 407–431. HEK293 cells were transfected with FLAG-A20 and either HA-ABIN or ABIN $\Delta$ 407–431. Cell extracts were immunoprecipitated with anti-FLAG antibodies (A20) followed by Western blot (WB) anti-HA (ABIN). The presence of –HA and –FLAG proteins in total extracts is shown.

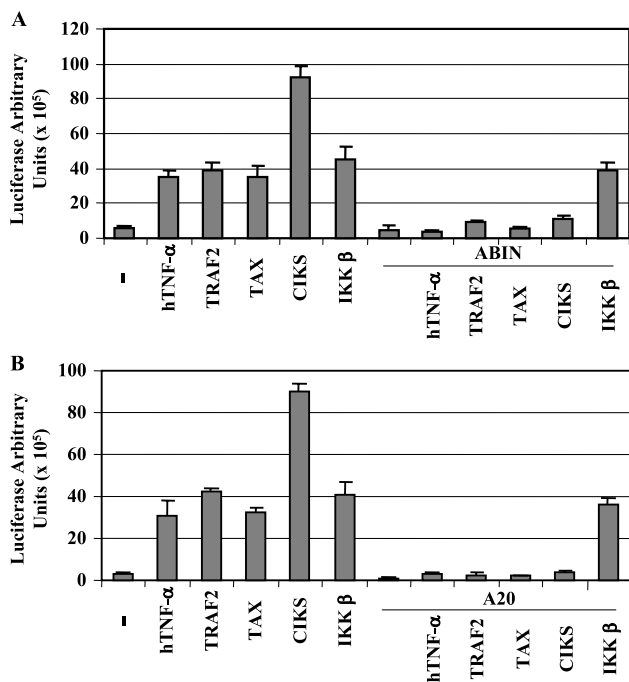
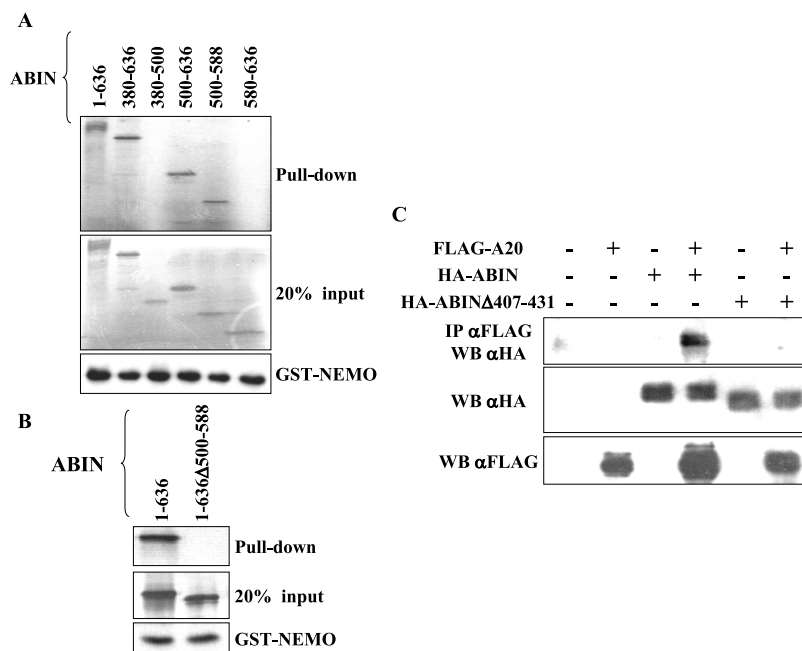


**FIGURE 3. ABIN-1 and A20 are inhibitors of NF- $\kappa$ B.** A and B, ABIN-1 and A20 inhibit NF- $\kappa$ B at level of the IKK complex. Relative reporter activity was evaluated in HEK293 cells co-transfected with the Ig- $\kappa$ B-luciferase plasmid and the indicated expression vectors. 24 h after transfection cells were stimulated with TNF- $\alpha$  for 3 h or left untreated, as indicated. Values shown in arbitrary units represent the mean  $\pm$  S.D. of three experiments done in triplicate, normalized for  $\beta$ -galactosidase expression of a co-transfected pRSV- $\beta$ -galactosidase plasmid.

**In Vivo Ubiquitination and De-ubiquitination Assays**— HEK293 cells ( $3 \times 10^6$ ) were co-transfected with expression vectors containing epitope-tagged ubiquitin (1 mg) and NEMO/IKK $\gamma$  (200 ng), plus various constructs encoding A20 or ABIN-1 proteins. 24 h after transfection, cell lysates were prepared as above and analyzed for polyubiquitination of NEMO/IKK $\gamma$  either by Western blot anti-NEMO/IKK $\gamma$  (-FLAG) on total extracts or by immunoprecipitating FLAG-NEMO/IKK $\gamma$  with anti-FLAG beads followed by Western blot anti-HA-ubiquitin.

**ABIN-1 Small Interfering RNA (siRNA) Expression Vectors**— To knockdown ABIN-1 expression, we designed double-stranded oligonucleotides containing sequences derived from the human ABIN-1 open reading frame (nucleotides 1136–1156 and 1685–1705) in forward and reverse orientations separated by a 7-base pair spacer region (caagaga) to allow the formation of the hairpin structure in the expressed siRNAs; ABINi-370: sense strand, 5'-aattcGAGGAGACCGACAAGGAGCAGcaagagaCTGCTCCTTGTCCGGTCTCCTCtttttc; antisense strand, 5'-tcgag-aaaaGAGGAGACCGACAAGGAGCAGtctcttgCTGCTCCTTGTCCG-TTCTCCTCg; ABINi-560: sense strand, 5'-aattcCCACACCATGGCTT-CGAGGACcaagagaGTCCTCGAAGCCATGGTGTGGtttttc; antisense strand, 5'-tcgagaaaaCCACACCATGGCTTTCGAGGACTctcttgGTCCT-CGAAGCCATGGTGTGGg. The resulting double-stranded oligonucleotides were cloned into the pcRNAi vector that we derived from the pcDNA3.1 vector (Invitrogen) by replacing the viral promoter cassette with the H1 gene promoter that is specifically recognized by RNA polymerase III. The plasmids used to knockdown A20 expression (pU6-A20i and the pU6) were a kind gift of Dr. S. Yamaoka and have been previously described (43).

**RESULTS**

**ABIN-1 Binds to NEMO/IKK $\gamma$** —The regulatory subunit of the IKK complex, NEMO/IKK $\gamma$ , has an essential role in NF- $\kappa$ B activation. To gain insights into how NEMO/IKK $\gamma$  modulates the activation of NF- $\kappa$ B, we screened a human liver cDNA library for NEMO/IKK $\gamma$  interacting proteins, via the yeast two-hybrid system. 25 clones were identified that expressed NEMO/IKK $\gamma$ -interacting proteins, including IKK $\alpha$  and CARMA (23). Three clones encoded for overlapping fragments of ABIN-1, a protein previously identified as an A20-binding protein that mimics the NF- $\kappa$ B inhibiting effects of A20 (34).

To define the region of NEMO/IKK $\gamma$  that interacts with ABIN-1, we tested various deletion mutants of NEMO/IKK $\gamma$  for binding to the ABIN-1 fragment (amino acids 380–636) in yeast. Data shown in Fig. 1A indicate that the region between amino acids 50 and 100 of NEMO/IKK $\gamma$  is required for interaction with ABIN-1. The binding was confirmed in mammalian cells (Fig. 1B). HA-ABIN-1 was transiently co-expressed in HEK293 cells together with FLAG-NEMO/IKK $\gamma$  or a NEMO/IKK $\gamma$  mutant lacking the first 91 amino acids (FLAG-

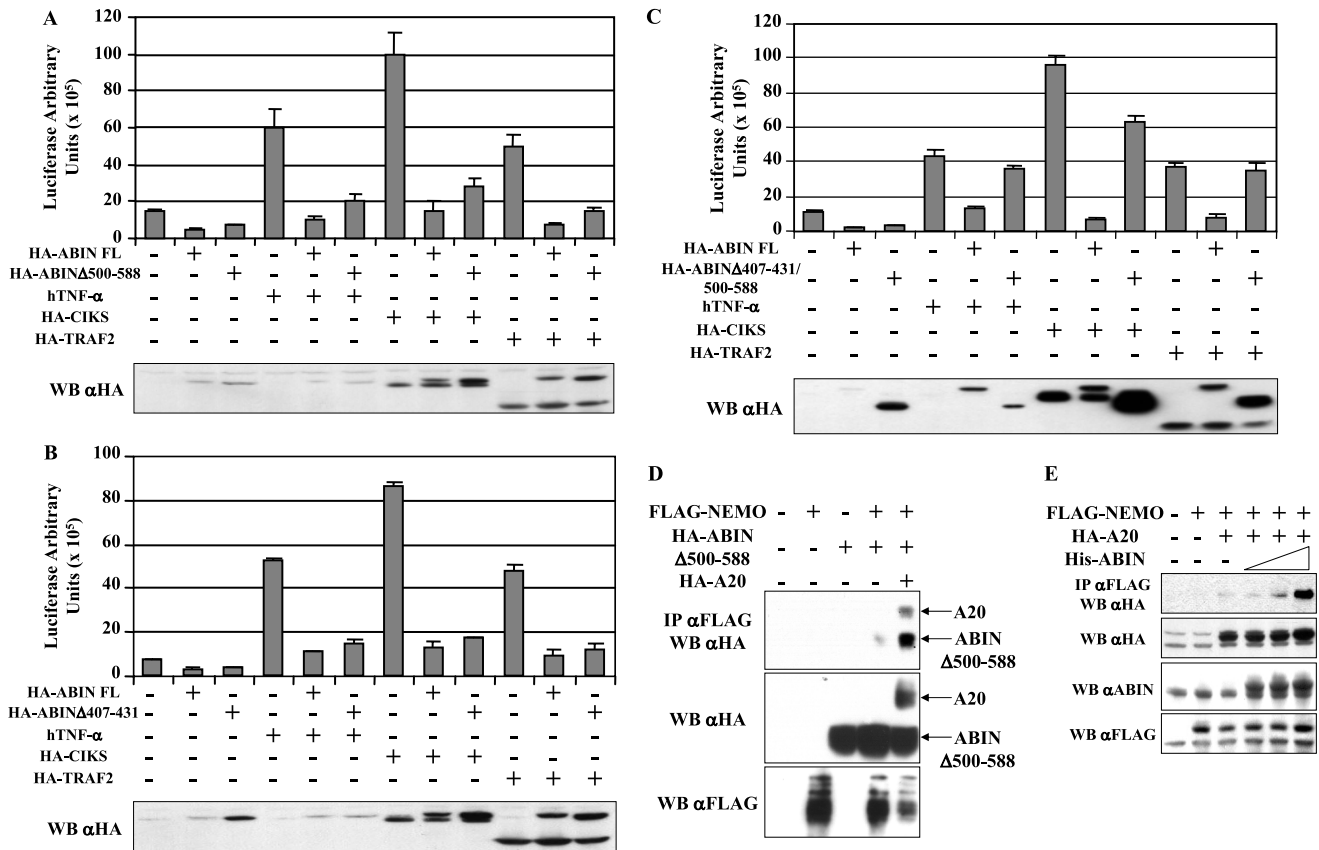


**FIGURE 4. ABIN-1 interacts with NEMO/IKK $\gamma$  and A20 to inhibit NF- $\kappa$ B activity.** A–C, the deletion mutant of ABIN-1 lacking both NEMO/IKK $\gamma$ - and A20-binding domains (ABIN $\Delta$ 407–431/ $\Delta$ 500–588) does not block NF- $\kappa$ B activation (C), in contrast to ABIN $\Delta$ 500–588 (A) and ABIN $\Delta$ 407–431 (B). HEK293 cells were co-transfected with the Ig- $\kappa$ B-luciferase reporter plasmid and the indicated combinations of expression plasmids. 24 h after transfection cells were stimulated with TNF- $\alpha$  for 3 h or left untreated, as indicated. Analysis was done as in Fig. 3. Lower panels in A–C show relative expression levels of each of the transfected proteins. D, ABIN-1 forms a complex with NEMO/IKK $\gamma$  and A20. HEK293 cells were transfected with constructs encoding NEMO/IKK $\gamma$ , A20, and a deletion mutant of ABIN lacking the NEMO/IKK $\gamma$ -binding domain (ABIN $\Delta$ 500–588). Cell extracts were immunoprecipitated with anti-FLAG antibodies (NEMO/IKK $\gamma$ ) and Western blotted (WB) anti-HA to reveal the co-precipitation of A20 and ABIN $\Delta$ 500–588. The presence of –HA and –FLAG proteins in total extracts is shown. E, ABIN-1 promotes association of A20 with NEMO/IKK $\gamma$ . HEK293 cells were transiently transfected with constructs encoding FLAG-NEMO/IKK $\gamma$ , HA-A20, and an increasing amount of His-ABIN. Cell extracts were immunoprecipitated with anti-FLAG antibodies (NEMO/IKK $\gamma$ ) and Western blotted anti-HA to reveal the co-precipitation of A20. The presence of ABIN, NEMO/IKK $\gamma$ , and A20 in the whole cell lysate is shown.

NEMO $\Delta$ N91). Immunoprecipitates of FLAG-NEMO/IKK $\gamma$  contained HA-ABIN-1 only if both proteins were co-expressed (Fig. 1B, compare lanes 3 and 4). In agreement with the data obtained in yeast, ABIN-1 did not co-immunoprecipitate with NEMO $\Delta$ N91 (lane 6, Fig. 1B). We were unable to detect the association between endogenous NEMO/IKK $\gamma$  and ABIN-1, probably because of the transient nature of the association and/or the high stringent conditions we used to perform co-immunoprecipitation experiments. However, gel filtration experiments showed that endogenous ABIN-1 was eluted from the column in the same fractions containing endogenous NEMO/IKK $\gamma$  and other components of IKK complex (Fig. 1C).

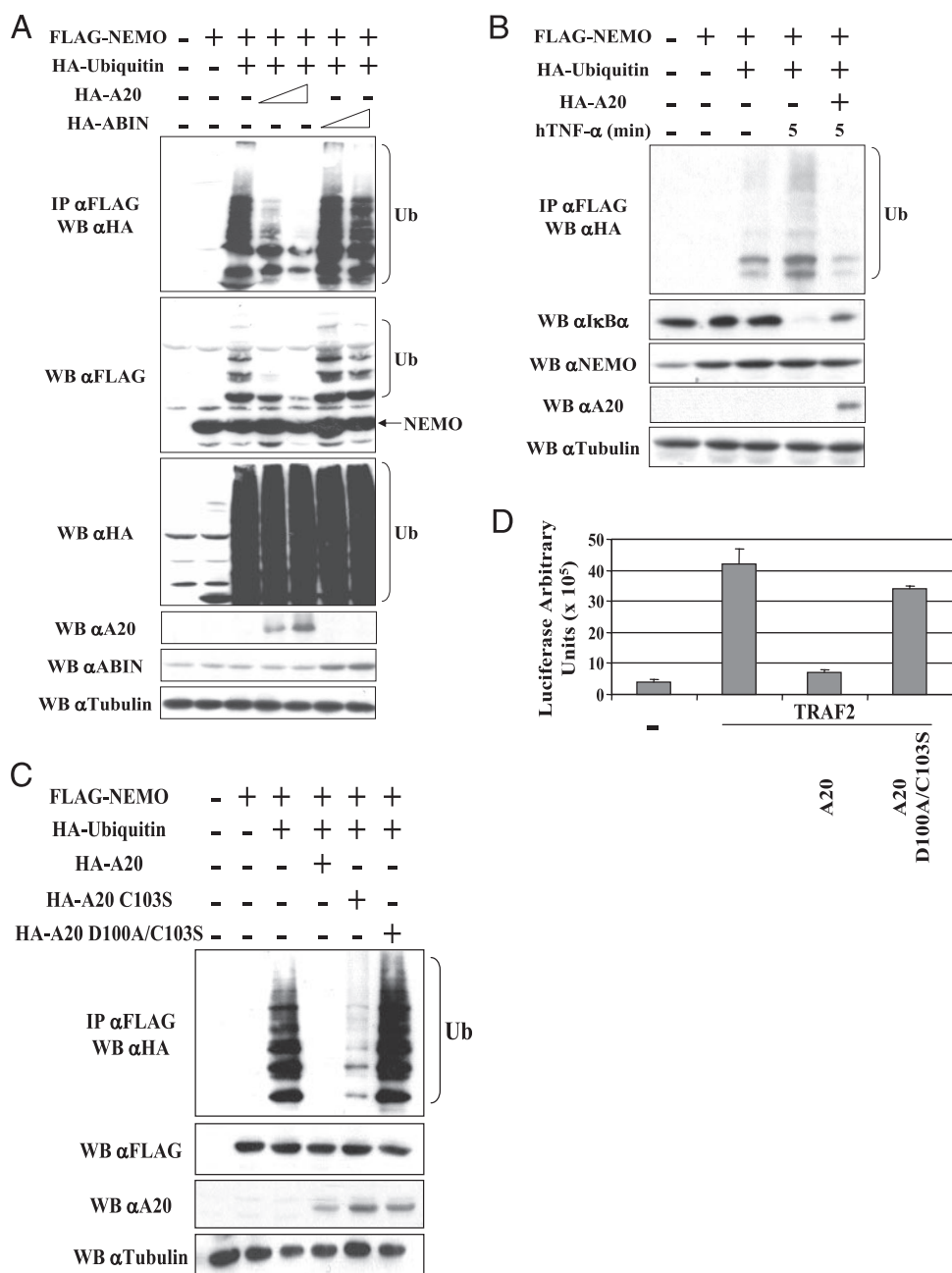
**Mapping of the NEMO/IKK $\gamma$  and the A20 Binding Domains on ABIN-1**—To define the domain of ABIN-1 required for its interaction with NEMO/IKK $\gamma$ , we performed pull-down assays by using recombinant GST-NEMO/IKK $\gamma$  and *in vitro* translated [<sup>35</sup>S]ABIN-1 (Fig. 2A). ABIN-1 binds to GST-NEMO/IKK $\gamma$ , indicating a direct interaction between the two proteins. Furthermore, amino acids 500–588 of ABIN-1 represent the minimal region that binds to NEMO/IKK $\gamma$  (Fig. 2A, upper panel). To confirm that the region between amino acids 500 and 588 of ABIN-1 was responsible for interaction with NEMO/IKK $\gamma$ , we generated an internal deletion mutant of ABIN-1 ( $\Delta$ 500–588) and evaluated its ability to interact with NEMO/IKK $\gamma$ . As expected, the internal deletion of 89 amino acids from ABIN-1 abolished the interaction with NEMO/IKK $\gamma$  (Fig. 2B). Because ABIN-1 was identified as an

A20-interacting protein (35), we confirmed that the region between amino acids 407 and 431 of ABIN-1 is responsible for interaction with A20 (Fig. 2C).

**Both ABIN-1 and A20 Inhibit NF- $\kappa$ B at the Level of the IKK Complex by Associating with NEMO/IKK $\gamma$** —Both ABIN-1 and A20 are inhibitors of NF- $\kappa$ B. It has been proposed that they interfere with a RIP and TRAF2-mediated transactivation signal (34). The identification of the interaction between ABIN-1 and NEMO/IKK $\gamma$  prompted us to investigate if ABIN-1 was involved in controlling NF- $\kappa$ B activation not only upstream but also at the level of the IKK complex. To this aim, we performed reporter assays by transfecting HEK293 cells with the Ig- $\kappa$ B-luciferase plasmid in the presence of ABIN-1 and various activators of NF- $\kappa$ B. ABIN-1 efficiently inhibited TNF- $\alpha$  and TRAF2-dependent activation of NF- $\kappa$ B (Fig. 3A). ABIN-1 also blocked NF- $\kappa$ B activation induced by proteins acting at the level of the IKK complex, such as CIKS and TAX (18–21). In contrast, ABIN-1 was not able to inhibit the IKK $\beta$ -mediated activation of NF- $\kappa$ B (Fig. 3A). Similarly, A20 inhibits NF- $\kappa$ B activation mediated by TNF- $\alpha$  or ectopic expression of TRAF2, CIKS, and TAX but not IKK $\beta$  (Fig. 3B). These results indicate that both ABIN-1 and A20 interfere with activation of NF- $\kappa$ B at the level of the IKK complex, suggesting that the association of ABIN-1 with NEMO/IKK $\gamma$  could play an important role in the inhibition of NF- $\kappa$ B.

Because ABIN-1 interacts with both NEMO/IKK $\gamma$  and A20, we tested whether the NEMO/IKK $\gamma$ - and A20-binding domains of ABIN-1 were required for inhibition of NF- $\kappa$ B. ABIN-1 deletion mutants lacking

**FIGURE 5. A20 inhibits NF- $\kappa$ B by de-ubiquitinating NEMO/IKK $\gamma$ .** *A*, A20 but not ABIN-1 de-ubiquitinates NEMO/IKK $\gamma$ . HEK293 cells were transfected with FLAG-NEMO/IKK $\gamma$  and HA-ubiquitin, plus increasing amounts of either HA-A20 or HA-ABIN. Cell extracts were immunoprecipitated with anti-FLAG antibodies (NEMO/IKK $\gamma$ ) followed by Western blot analysis with anti-HA antibodies to reveal the polyubiquitinated forms of NEMO/IKK $\gamma$ . Western blot analyses with anti-FLAG, -HA, -A20, -ABIN, and -tubulin antibodies were performed on total extracts. *B*, A20 blocks the ubiquitination of NEMO/IKK $\gamma$  and the degradation of I $\kappa$ B $\alpha$  induced by TNF- $\alpha$ . HEK293 cells were transfected with FLAG-NEMO/IKK $\gamma$ , HA-ubiquitin, and HA-A20. 24 h after transfection cells were stimulated with TNF- $\alpha$  for 5 min or left untreated, as indicated. Cell extracts were immunoprecipitated with anti-FLAG antibodies (NEMO/IKK $\gamma$ ) and Western blotted with anti-NEMO/IKK $\gamma$ , -I $\kappa$ B $\alpha$ , -A20, and -tubulin are shown. *C*, a catalytically inactive form of A20 (D100A/C103S) does not de-ubiquitinate NEMO/IKK $\gamma$ . Conditions were similar to those in *A*, except for the plasmids encoding HA-A20 C103S, or D100A/C103S. *D*, A20 D100A/C103S does not inhibit NF- $\kappa$ B activation dependent on TRAF2 in contrast to wild type A20. Reporter assay was performed by co-transfection of the Ig- $\kappa$ B-luciferase plasmid with combinations of TRAF2, plus A20-WT, or -D100A/C103S. Values shown in arbitrary units represent the mean  $\pm$  S.D. of three experiments done in triplicate, normalized for  $\beta$ -galactosidase expression of a co-transfected pRSV- $\beta$ -galactosidase plasmid.



either the NEMO/IKK $\gamma$  binding domain (ABIN $\Delta$ 500–588) or the A20 binding domain (ABIN $\Delta$ 407–431) were still able to inhibit the activity of a NF- $\kappa$ B-driven luciferase reporter following different stimuli (Fig. 4, *A* and *B*). In contrast, a mutant of ABIN-1 in which both the NEMO/IKK $\gamma$ - and the A20-binding domains were deleted (ABIN $\Delta$ 407–431/ $\Delta$ 500–588) lost the ability to block activation of NF- $\kappa$ B (Fig. 4*C*). These data were consistent with the hypothesis that ABIN-1 forms a complex with both NEMO/IKK $\gamma$  and A20. To address this hypothesis, we immunoprecipitated FLAG-NEMO/IKK $\gamma$  and monitored the co-precipitation of the ABIN-1 mutant lacking the NEMO/IKK $\gamma$ -binding domain (HA-ABIN $\Delta$ 500–588) either in the presence or absence of A20 (Fig. 4*D*). ABIN $\Delta$ 500–588 co-immunoprecipitated with NEMO/IKK $\gamma$  only in the presence of A20 (Fig. 4*D*). To further support the idea that ABIN-1 promotes association of A20 with NEMO/IKK $\gamma$ , we transfected A20 and NEMO/IKK $\gamma$  in the presence of an increasing amount of over-expressed ABIN-1. As expected, the amount of A20 co-immunoprecipi-

tating with NEMO/IKK $\gamma$  increased in the presence of ABIN-1 (Fig. 4*E*). Taken together, these data indicated that ABIN-1 interferes with activation of NF- $\kappa$ B at the level of the IKK complex, and support the idea that ABIN-1 promotes association of A20 with NEMO/IKK $\gamma$ .

**A20 Inhibits NF- $\kappa$ B by De-ubiquitinating NEMO/IKK $\gamma$** —To explore the mechanism by which the interactions of both A20 and ABIN-1 with NEMO/IKK $\gamma$  down-regulate NF- $\kappa$ B signaling, we assessed the effect of either A20 or ABIN-1 on NEMO/IKK $\gamma$  ubiquitination. Transfection of FLAG-NEMO/IKK $\gamma$  in the presence of HA-ubiquitin results in the polyubiquitination of NEMO/IKK $\gamma$  (Fig. 5*A*, lane 3). Co-transfection of A20 and NEMO/IKK $\gamma$  resulted in a dose-dependent disappearance of the ubiquitinated forms of NEMO/IKK $\gamma$  (Fig. 5*A*, lanes 4 and 5). In contrast, co-transfection of ABIN-1 did not affect NEMO/IKK $\gamma$  ubiquitination (Fig. 5*A*, lanes 6 and 7). We did not observe reduction in the overall level of ubiquitinated cellular proteins in the presence of A20, indicating that A20 does not have a global de-ubiquitinating activity in

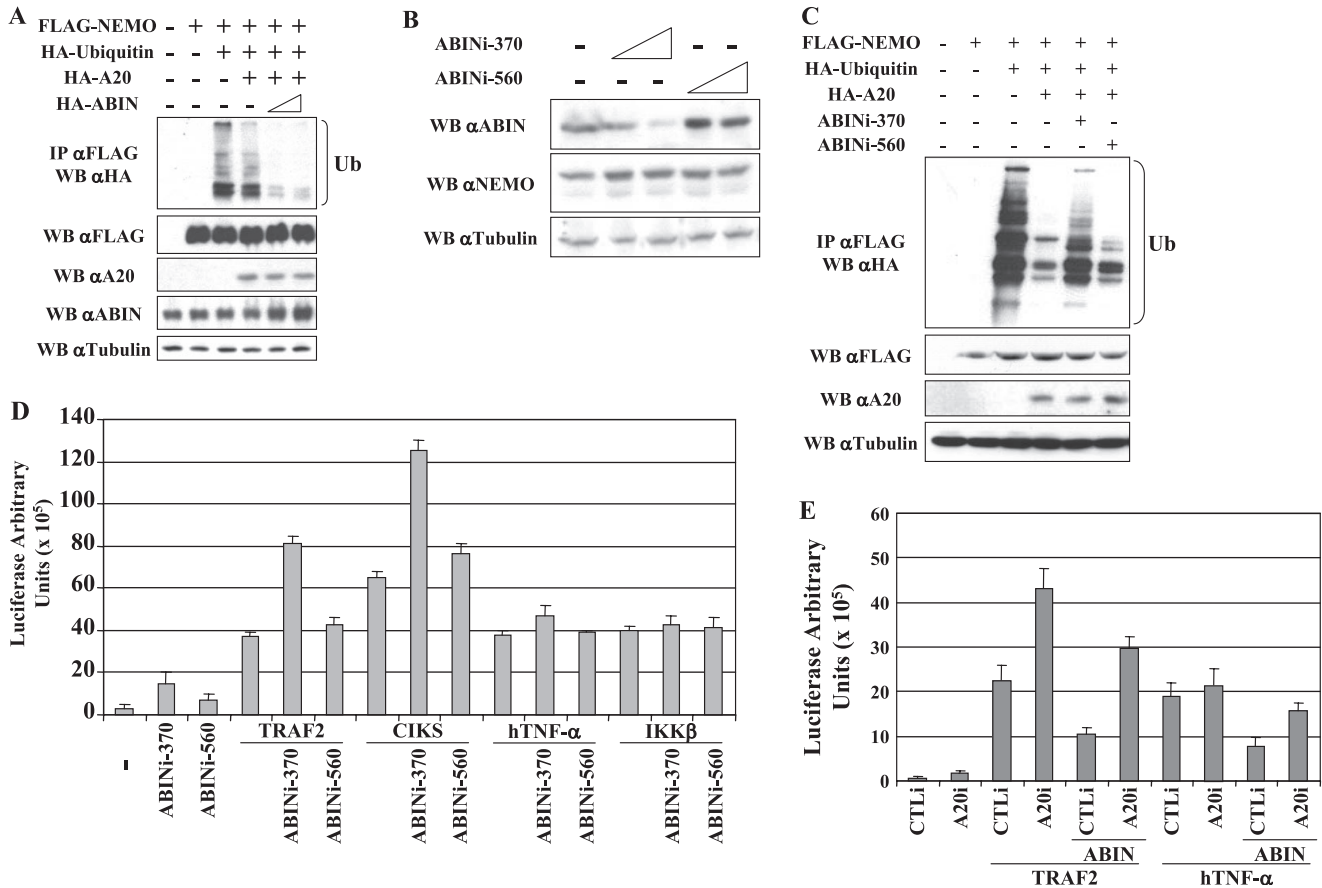


**FIGURE 6. ABIN-1 participates to the A20-dependent de-ubiquitination of NEMO/IKK $\gamma$ .** A, ABIN-1 increases the effects of A20 on NEMO/IKK $\gamma$  ubiquitination. HEK293 cells were transfected with FLAG-NEMO/IKK $\gamma$ , HA-ubiquitin, suboptimal amounts of HA-A20, and increasing amounts of HA-ABIN. Cell extracts were immunoprecipitated with anti-FLAG antibodies (NEMO/IKK $\gamma$ ) and analyzed by Western blot for anti-HA. Western blots of anti-FLAG, -A20, -ABIN, and -tubulin are shown. B, RNA interference of ABIN-1. HEK293 cells were transiently transfected with siRNAs targeting ABIN (ABINi-370 or -560). ABIN expression was analyzed by immunoblotting with antibodies against ABIN. Equivalency of protein loading is shown in the tubulin and NEMO/IKK $\gamma$  blots. C, ABIN-1 siRNAs impairs the A20-dependent de-ubiquitination of NEMO/IKK $\gamma$ . HEK293 cells were co-transfected with FLAG-NEMO/IKK $\gamma$ , HA-ubiquitin, and -A20, plus either ABINi-370 or -560. Cell extracts were immunoprecipitated with anti-FLAG antibodies and Western blotted with anti-HA. Western blots of anti-FLAG, -A20, and -tubulin were performed on total extracts. D, ABIN-1 siRNAs increase NF- $\kappa$ B activation by TRAF2 and CIKS. HEK293 cells were co-transfected with TRAF2, CIKS, or IKK $\beta$ , plus Ig- $\kappa$ B-luciferase reporter and either ABINi-370 or -560. 24 h after transfection cells were stimulated with TNF for 3 h or left untreated. Analysis was done as in Fig. 5D. E, RNA interference of A20 impairs the ABIN-1-mediated inhibition of NF- $\kappa$ B. Relative reporter activity was evaluated in HEK293 cells co-transfected with the Ig- $\kappa$ B-luciferase reporter, TRAF2, and either A20i or CTLi plasmids. 24 h after transfection cells were stimulated with TNF- $\alpha$  for 3 h or left untreated, as indicated. Analysis of luciferase activity was done as above.

cultured cells (Fig. 5A). Importantly, A20 also blocks I $\kappa$ B $\alpha$  degradation and NEMO/IKK $\gamma$  ubiquitination induced by TNF- $\alpha$  (Fig. 5B). To demonstrate that the de-ubiquitinating activity of A20 was required for the observed reduction in NEMO/IKK $\gamma$  ubiquitination, we generated two mutants in the OTU domain of A20, which is the domain responsible for the de-ubiquitinating activity of A20 (36). We replaced the cysteine residue of the DXXC motif with serine (C103S), and both the aspartic acid and the cysteine residues (D100A/C103S) with alanine and serine, respectively. The mutation C103S affected the ability of A20 to de-ubiquitinate NEMO/IKK $\gamma$  compared with wild type A20, whereas the double mutant D100A/C103S resulted in the complete loss of the de-ubiquitinating activity of A20 on NEMO/IKK $\gamma$  (Fig. 5C). As expected, the D100A/C103S mutant was not able to block the NF- $\kappa$ B activity induced by different stimuli, such as TRAF2 (Fig. 5D and data not shown).

These findings strongly suggest that NEMO/IKK $\gamma$  is a target of the de-ubiquitinating activity of A20 and confirmed that the ubiquitination of NEMO/IKK $\gamma$  is a crucial step in the mechanisms of NF- $\kappa$ B activation.

*ABIN-1 Mediates the De-ubiquitinating Activity of A20 on NEMO/IKK $\gamma$* —Next, we explored whether ABIN-1 was involved in the A20-dependent de-ubiquitination of NEMO/IKK $\gamma$ . To this purpose, we transfected HEK293 cells with a suboptimal amount of A20 and an

increasing amount of ABIN-1 and checked for NEMO/IKK $\gamma$  ubiquitination. We found that ABIN-1 increases the ability of A20 to de-ubiquitinate NEMO/IKK $\gamma$  (Fig. 6A). To demonstrate a role for ABIN-1 in the A20-mediated de-ubiquitination of NEMO/IKK $\gamma$ , we generated siRNA constructs targeting ABIN-1 (ABINi-370 and i-560). Fig. 6B shows that the construct i-370 knocked-down ABIN-1 expression, whereas the i-560 construct did not. Then, we evaluated whether interference of ABIN-1 impairs the de-ubiquitinating activity of A20 on NEMO/IKK $\gamma$ . We co-transfected HEK293 cells with FLAG-NEMO/IKK $\gamma$  and HA-ubiquitin and assessed the de-ubiquitinating activity of A20 alone or in the presence of either i-370 or i-560 constructs. The A20-dependent de-ubiquitination of NEMO/IKK $\gamma$  decreased only in the presence of the i-370 construct (Fig. 6C). The i-370 construct led to a 2-fold increase of both basal and induced (TRAF2 and CIKS) NF- $\kappa$ B activity compared with the empty vector or the i-560 construct, which we used as controls (Fig. 6D). Accordingly with the data shown in Fig. 3A, interference of ABIN-1 did not influence the activation of the NF- $\kappa$ B-dependent transfected IKK $\beta$ . Also in this case, NF- $\kappa$ B activity correlated with the levels of NEMO/IKK $\gamma$  ubiquitination. In fact, transfected i-370 increased the ubiquitination of NEMO/IKK $\gamma$  with respect to both empty vector and i-560 (data not shown). From these experiments, we concluded that reduced levels of the ABIN-1 protein affect the ability of

## ABIN-1 Binds to NEMO/IKK $\gamma$

A20 to de-ubiquitinate NEMO/IKK $\gamma$  and, consequently the A20-mediated inhibition of NF- $\kappa$ B. To further support the functional interplay between ABIN-1 and A20, we knocked-down A20 (43) and evaluated the ability of ABIN-1 to interfere with NF- $\kappa$ B activation. As shown in Fig. 6E, ABIN-1 requires A20 to efficiently block NF- $\kappa$ B activation induced by TNF and TRAF2.

### DISCUSSION

In the present study, we have performed experiments in yeast, *in vitro* and in transfected cells demonstrating that ABIN-1 physically associates with NEMO/IKK $\gamma$ . The functional consequence of this interaction is that overexpression of ABIN-1 blocks not only activation of NF- $\kappa$ B upstream of the IKK complex, but also NF- $\kappa$ B activation mediated by proteins directly contacting the IKK complex, such as CIKS and TAX. Indeed, activation of NF- $\kappa$ B mediated by overexpression of IKK $\beta$ , which may be considered functionally downstream of NEMO/IKK $\gamma$ , is not affected by ABIN-1. ABIN-1 has been identified as an A20-binding protein and its overexpression mimics the inhibitory effect of A20, suggesting that ABIN-1, at least partially, mediates the inhibitory function of A20. A20 is a TNF- $\alpha$  responsive gene that inhibits NF- $\kappa$ B-dependent gene transcription in response to TNF- $\alpha$  and other stimuli (37–39). Given that A20 expression itself is regulated by NF- $\kappa$ B, it is possible that A20 and ABIN-1 participate in a negative feedback regulation of NF- $\kappa$ B activation (40, 41). However, the mechanism by which ABIN-1 participates in this process is not clear. We provide evidence that ABIN-1 and A20 co-operate to promote de-ubiquitination of NEMO/IKK $\gamma$ , which results in functional inactivation of NF- $\kappa$ B. In fact, recent studies have indicated ubiquitination as a key event in the regulation of NF- $\kappa$ B activation. For example, A20 modifies the ubiquitination profile of RIP in a two-step model, by removing the Lys<sup>63</sup>-linked ubiquitin chain and by the subsequent ligation of the Lys<sup>48</sup>-linked ubiquitin chain (30). Similarly, A20 inhibits Toll-like receptor signaling by removing the Lys<sup>63</sup>-linked ubiquitin chain from TRAF6 (27). In this context our data demonstrate that NEMO/IKK $\gamma$  is an additional target of the de-ubiquitinating activity of A20. Currently, it is not clear if A20 directly de-ubiquitinates NEMO/IKK $\gamma$ , or it affects the activity of other protein(s) regulating NEMO/IKK $\gamma$  ubiquitination. However, we have now shown that in cells knocked-down for ABIN-1, we observed a decrease in the ability of A20 to de-ubiquitinate NEMO/IKK $\gamma$ , and that in cells knocked-down for A20, the inhibitory function of ABIN-1 is impaired. Altogether our data strongly suggest that ABIN-1 functionally connects A20 and NEMO/IKK $\gamma$ .

In summary, we have identified a previously not reported association between ABIN-1 and NEMO/IKK $\gamma$  and we provide evidence that ABIN-1 co-operates with A20 in inhibiting NF- $\kappa$ B at the level of the IKK complex. In addition, we propose that this association could target A20 on NEMO/IKK $\gamma$  and interfere with NEMO/IKK $\gamma$  ubiquitination, to negatively regulate NF- $\kappa$ B activation.

### REFERENCES

- Hayden, M. S., and Ghosh, S. (2004) *Genes Dev.* **18**, 2195–2224
- Karin, M., and Lin, A. (2002) *Nat. Immunol.* **3**, 221–227
- Walsh, N. C., Crotti, T. N., Goldring, S. R., and Gravallesse, E. M. (2005) *Immunol. Rev.* **208**, 228–251
- Orange, J. S., Levy, O., and Geha, R. S. (2005) *Immunol. Rev.* **203**, 21–37
- Clevers, H. (2004) *Cell* **118**, 671–674
- Karin, M., and Greten, F. R. (2005) *Nat. Rev. Immunol.* **5**, 749–759

- Brown, K., Gerstberger, S., Carlson, L., Franzoso, G., and Siebenlist, U. (1995) *Science* **267**, 1485–1488
- Di Donato, J. A., Hayakawa, M., Rothwarf, D. M., Zandi, E., and Karin, M. (1997) *Nature* **388**, 548–554
- Mercurio, F., Zhu, H., Murray, B. W., Shevchenko, A., Bennet, B. L., Li, J., Young, D. B., Barbosa, M., Mann, M., Manning, A., and Rao, A. (1997) *Science* **278**, 860–866
- Woronicz, J. D., Gao, X., Cao, Z., Rothe, M., and Goeddel, D. V. (1997) *Science* **278**, 866–869
- Regnier, C. H., Song, H. Y., Gao, X., Goeddel, D. V., Cao, Z., and Rothe, M. (1997) *Cell* **90**, 373–383
- Zandi, E., Rothwarf, D. M., Delhase, M., Hayakawa, M., and Karin, M. (1997) *Cell* **91**, 243–252
- Yamaoka, S., Courtois, G., Bessia, C., Whiteside, S. T., Weil, R., Agou, F., Kirk, H. E., Kai, R. Y., and Israel, A. (1998) *Cell* **93**, 1231–1240
- Rothwarf, D. M., Zandi, E., Natoli, G., and Karin, M. (1998) *Nature* **395**, 297–300
- Schmidt-Suppran, M., Bloch, W., Courtois, G., Addicks, K., Israel, A., Rajewsky, K., and Pasparakis, M. (2000) *Mol. Cell* **5**, 981–992
- Israel, A. (2000) *Trends Cell Biol.* **10**, 129–133
- Zhang, S. Q., Kovalenko, A., Cantarella, G., and Wallach, D. (2000) *Immunity* **12**, 301–311
- Chu, Z. L., Shin, Y. A., Yang, J. M., Di Donato, J. A., and Ballard, D. W. (1999) *J. Biol. Chem.* **274**, 15297–15300
- Harhaj, E. W., and Sun, S. C. (1999) *J. Biol. Chem.* **274**, 22911–22914
- Jin, D. Y., Giordano, V., Kibler, K. V., Nakano, H., and Jeang, K. T. (1999) *J. Biol. Chem.* **274**, 17402–17405
- Leonardi, A., Chariot, A., Claudio, E., Cunningham, K., and Siebenlist, U. (2000) *Proc. Natl. Acad. Sci. U. S. A.* **97**, 10494–10499
- Chariot, A., Leonardi, A., Muller, J., Bonif, M., Brown, K., and Siebenlist, U. (2002) *J. Biol. Chem.* **277**, 37029–37036
- Stilo, R., Liguoro, D., Di Jeso, B., Formisano, S., Consiglio, E., Leonardi, A., and Vito, P. (2004) *J. Biol. Chem.* **279**, 34323–34331
- Chen, Z. J. (2005) *Nat. Cell Biol.* **7**, 758–765
- Liu, Y. C., Penninger, J., and Karin, M. (2005) *Nat. Rev. Immunol.* **5**, 941–952
- Tang, E. D., Wang, C. Y., Xiong, Y., and Guan, K. L. (2003) *J. Biol. Chem.* **278**, 37297–37305
- Boone, D. L., Turer, E. E., Lee, E. G., Ahmad, R. C., Wheeler, M. T., Tsui, C., Hurley, P., Chien, M., Chai, S., Hitotsumatsu, O., McNally, E., Pickart, C., and Ma, A. (2004) *Nat. Immunol.* **5**, 1052–1060
- Zhou, H., Wertz, I. E., O'Rourke, K. M., Ultsch, M., Seshgiri, S., Eby, M., Xiao, W., and Dixit, V. M. (2004) *Nature* **427**, 167–171
- Kovalenko, A., Chable-Bessia, C., Cantarella, G., Israel, A., Wallach, D., and Courtois, G. (2003) *Nature* **424**, 801–805
- Wertz, I. E., O'Rourke, K. M., Zhou, H., Eby, M., Aravind, L., Seshgiri, S., Wu, P., Wlesmann, C., Baker, R., Boone, D. L., Ma, A., Koonin, E. V., and Dixit, V. M. (2004) *Nature* **430**, 694–699
- Lee, E. G., Boone, D. L., Chai, S., Libby, S. L., Chien, M., Lodolce, G. P., and Ma, A. (2000) *Science* **289**, 2350–2354
- Leonardi, A., Ellinger-Ziegelbauer, H., Franzoso, G., Brown, K., and Siebenlist, U. (2000) *J. Biol. Chem.* **275**, 271–278
- Chariot, A., Princen, F., Gielen, J., Merville, M. P., Franzoso, G., Brown, K., Siebenlist, U., and Bours, V. (1999) *J. Biol. Chem.* **274**, 5318–5325
- Heyninck, K., De Valck, D., Vanden Berghe, W., Van Crielinge, W., Contreras, R., Fierz, W., Haegeman, G., and Beyaert, R. (1999) *J. Cell Biol.* **145**, 1471–1482
- Heyninck, K., Kreike, M. M., and Beyaert, R. (2003) *FEBS Lett.* **536**, 135–140
- Evans, P. C., Smith, T. S., Lai, M. J., Williams, M. G., Burke, D. F., Heyninck, K., Kreike, M. M., Beyaert, R., Blundell, T. L., and Kilshaw, P. J. (2003) *J. Biol. Chem.* **278**, 23180–23186
- Dixit, V. M., Green, S., Sarma, V., Holzman, L. B., Wolf, F. W., O'Rourke, K., Ward, P. A., Prochownik, E. V., and Marks, R. M. (1990) *J. Biol. Chem.* **265**, 2973–2978
- Jaattela, M., Mouritzen, H., Elling, F., and Bastholm, L. (1996) *J. Immunol.* **156**, 1166–1173
- Hu, X., Lee, E., Harlan, J. M., Wong, F., and Karsan, A. (1998) *Blood* **92**, 2759–2765
- Laherty, C. D., Hu, H. M., Oipari, A. W., Wuang, F., and Dixit, V. M. (1992) *J. Biol. Chem.* **267**, 24157–24160
- Krikos, A., Laherty, C. D., and Dixit, V. M. (1992) *J. Biol. Chem.* **267**, 17971–17976
- Mauro, C., Vito, P., Mellone, S., Pacifico, F., Chariot, A., Formisano, S., and Leonardi, A. (2003) *Biochem. Biophys. Res. Commun.* **309**, 84–90
- Saitoh, T., Yamamoto, M., Miyagishi, M., Taira, K., Nakanishi, M., Fujita, T., Akira, S., Yamamoto, N., and Yamaoka, S. (2005) *J. Immunol.* **174**, 1507–1512

## Neopterin induces pro-atherothrombotic phenotype in human coronary endothelial cells

P. CIRILLO,\* M. PACILEO,\* S. DE ROSA,\* P. CALABRÒ,† A. GARGIULO,\* V. ANGRI,\*  
F. GRANATO-CORIGLIANO,\* I. FIORENTINO,‡ N. PREVETE,‡ R. DE PALMA,§ C. MAURO,¶  
A. LEONARDI¶ and M. CHIARIELLO\*

\*Division of Cardiology, University of Naples 'Federico II'; †Division of Cardiology, Second University of Naples; ‡Division of Clinical Immunology, University of Naples 'Federico II'; §Department of Clinical and Experimental Medicine, Second University of Naples; and ¶Dipartimento di Biologia e Patologia Cellulare e Molecolare Generale, University of Naples 'Federico II', Italy

**To cite this article:** Cirillo P, Pacileo M, De Rosa S, Calabrò P, Gargiulo A, Angri V, Granato-Corigliano F, Fiorentino I, Prevete N, De Palma R, Mauro C, Leonardi A, Chiariello M. Neopterin induces pro-atherothrombotic phenotype in human coronary endothelial cells. *J Thromb Haemost* 2006; 4: 2248–55.

**Summary.** *Background:* Inflammation plays a pivotal role in atherothrombosis. Recent data indicate that serum levels of neopterin, a marker of inflammation and immune modulator secreted by monocytes/macrophages, are elevated in patients with acute coronary syndromes and seem to be a prognostic marker for major cardiovascular events. The aim of the present study was to determine whether neopterin might affect the thrombotic and atherosclerotic characteristics of human coronary artery endothelial cells (HCAECs). *Methods and results:* In HCAECs, neopterin induced TF-mRNA transcription as demonstrated by real time polymerase chain reaction and expression of functionally active tissue factor (TF) as demonstrated by procoagulant activity assay, and of cellular adhesion molecules (CAMs) as demonstrated by FACS analysis, in a dose-dependent fashion. These neopterin effects were prevented by lovastatin, a HMG-CoA reductase inhibitor. Neopterin-induced TF and CAMs expression was mediated by oxygen free radicals through the activation of the transcription factor, nuclear factor-kappa B (NF- $\kappa$ B), as demonstrated by electrophoretic mobility shift assay and by suppression of CAMs and TF expression by superoxide dismutase and by NF- $\kappa$ B inhibitor, pyrrolidine-dithio-carbamate ammonium. *Conclusions:* These data indicate that neopterin exerts direct effects on HCAECs by promoting CAMs and TF expression and support the hypothesis that neopterin, besides representing a marker of inflammation, might be an effector molecule able to induce a pro-atherothrombotic phenotype in cells of the coronary circulation.

**Keywords:** adhesion molecules, atherosclerosis, inflammation, thrombosis, tissue factor.

### Introduction

Increasing evidence has assigned a central role to inflammation in both the initiation, and progression of atherosclerosis linking it to the clinical occurrence of acute coronary syndromes; in the last few years, it has been demonstrated that selected markers of inflammation might play an active role in modulating these phenomena [1–3]. In recent years, some epidemiological studies have pointed out the association existing between increased plasma levels of neopterin, a marker of inflammation released by activated macrophages, and coronary artery disease and acute coronary syndromes [4–8]. However, despite these clinical data, to date the possible pathophysiological links existing between increased plasma levels of neopterin and the occurrence of major cardiovascular events are still unknown.

Increasing evidence suggest an important role for adhesion molecules (CAMs) in the early stages and in the progression of atherosclerosis, thus triggering the development of atherosclerotic complications as acute coronary syndromes [9,10].

Tissue factor (TF) plays a pivotal role in the pathophysiology of acute coronary syndromes by triggering the formation of intracoronary thrombi following endothelial injury [11–12]. In this respect, endothelial cells, being normally exposed to the blood stream, express TF on their membrane only when activated after exposure to specific stimuli [13–14].

In the present study, we provide support *in vitro* for the hypothesis that neopterin, another marker of vascular or systemic inflammation, might play an active role in the pathophysiology of coronary events by induction of CAMs and TF, thus promoting both pro-atherosclerotic and pro-thrombotic state in human coronary endothelial cells.

Correspondence: Plinio Cirillo, Division of Cardiology, University of Naples 'Federico II', Via Sergio Pansini 5, 80131 Naples, Italy.  
Tel.: +39 081 7462216; fax: +39 081 7462229; e-mail: pccirillo@unina.it

Received 6 April 2006, accepted 4 July 2006

## Methods

The investigation conforms with the *Guide for the Care and Use of Laboratory Animals* published by the US National Institutes of Health.

Experiments were performed using human coronary artery endothelial cells (HCAECs; Cambrex Bio Science, Walkersville, MD, USA). Cells were grown in EGM 2 medium (Cambrex Bio Science) with endothelial cell growth supplement and 10% fetal serum. Cells were used at passages 2–5.

Neopterin (Sigma Chemical Co., St Louis, MO, USA) was used in all studies described. Given the concern surrounding the potential contamination of neopterin with endotoxin, we analyzed our substance and found endotoxin level to be  $< 0.125 \text{ EU mL}^{-1}$  ( $< 12.5 \text{ pg mL}^{-1}$ ) by Limulus assay (BioWhittaker, Walkersville, MD, USA). All media, and water were also tested and endotoxin level found to be  $< 0.125 \text{ EU mL}^{-1}$ .

### Effects of neopterin on TF transcription

Preliminary dose–response effects of neopterin on TF-mRNA transcription were evaluated by semi-quantitative polymerase chain reaction (PCR). Then, the effect of neopterin on TF-mRNA was investigated by real-time reverse transcription (RT) analysis as previously described [15]. HCAECs were incubated with neopterin (20 nM, concentration chosen on the basis of semi-quantitative results). Thirty minutes after the addition of neopterin, cells were washed with phosphate buffered saline (PBS) and then fresh medium (EGM 2 containing 0.1% serum) was added. Total mRNA was extracted at baseline, 30, 60, and 120 min after neopterin stimulation and TF mRNA levels were examined by RT and PCR by LightCycler (Roche Diagnostics, Basel, Switzerland). In positive control experiments, HCAECs were incubated for 30 min with lipopolysaccharide (LPS) ( $50 \mu\text{g mL}^{-1}$ ) for 30 min and then mRNA was extracted at 60 min.

### Dose–response effects of neopterin on TF activity

HCAECs were incubated with increasing concentration of neopterin (10, 20, 50, 100 nM) for 6 h. TF activity was determined by a two-step colorimetric assay, based on the ability of TF to promote generation of coagulation factor Xa, as previously described [15].

To evaluate whether neopterin-induced expression of TF resulted from de novo synthesis of this protein, in another set of experiments cells were preincubated with cycloheximide (CE) ( $10 \mu\text{g mL}^{-1}$ ), an inhibitor of protein synthesis, or with 5, 6-dichloro-1- $\beta$ -D-ribofuranosylbenzimidazole (DRB,  $10 \mu\text{g mL}^{-1}$ ), an inhibitor of DNA transcription, before adding neopterin (20 nM). Additional control experiments included cells preincubated with a mouse monoclonal antibody against human TF (American Diagnostica Inc, Greenwich, CT, USA). Moreover, in additional experiments we have investigated the effect of lovastatin on neopterin-induced TF expression.

HCAECs were cultivated in medium enriched with increasing lovastatin concentrations (0.1, 1, 5, and  $10 \mu\text{M}$ ) for 24 h, then stimulated with neopterin (20 nM) for 6 h and finally processed as above to evaluate TF activity.

As it has been documented that promotion of oxidative stress is a fundamental principle of neopterin's mode of operation [16], in another set of experiments, TF activity was evaluated as above, but in HCAECs preincubated for 30 min in the presence of the free radical scavenger superoxide dismutase (SOD;  $500 \text{ U mL}^{-1}$ ). Finally, because neopterin is able to induce nitric oxide (NO) synthase gene in vascular cells [17], it has been investigated whether NO might play a role in neopterin-induced TF activity. Thus, TF activity has been evaluated in HCAECs preincubated with non-selective NO synthase inhibitor *N*-nitro-*L*-arginine methyl ester (*L*-NAME, 0.1, 1, and  $10 \mu\text{M}$ ).

Positive control experiments included cells incubated for 6 h with LPS ( $50 \mu\text{g mL}^{-1}$ ). Six different experiments were performed for each experimental condition.

### Effects of neopterin on adhesion molecules expression

HCAECs were incubated with different doses of neopterin (10, 20, 50, and  $100 \text{ nM}$ ) or with LPS ( $50 \mu\text{g mL}^{-1}$ ) for 12 h. Cells were then detached with  $10 \text{ mmol L}^{-1}$  EDTA in PBS (without trypsin) and stained with *R*-phycoerythrin-labeled monoclonal antibodies (Pharmingen, Franklin Lakes, NJ, USA) against VCAM-1 (CD106) or ICAM-1 (CD54), or with the appropriate isotype IgG (phycoerythrin or FITC) as control. Fluorescence intensity of 9000 cells for each sample was quantified by a FACSCalibur analyzer (Becton-Dickinson, Franklin Lakes, NJ, USA). Moreover, in additional experiments we have investigated the effect of lovastatin on neopterin-induced CAMs expression. HCAECs were cultivated in medium enriched with increasing lovastatin concentrations (0.1, 1, 5, and  $10 \mu\text{M}$ ) for 24 h, then stimulated with neopterin (20 nM) for 12 h and finally processed as above to evaluate VCAM-1 and ICAM-1 expression.

Finally, as described above, CAMs expression has been evaluated in HCAECs cultivated in the presence of the free radical scavenger SOD ( $500 \text{ U mL}^{-1}$ ), and in cells preincubated with non-selective NO synthase inhibitor *L*-NAME (0.1, 1, and  $10 \mu\text{M}$ ). All experiments were performed in triplicate.

### Effects of neopterin on nuclear factor-kappa B (NF- $\kappa$ B) activation

To elucidate the intracellular mechanisms by which neopterin induced TF, ICAM-1, and VCAM-1 on endothelial cells, in another set of experiments, we tested the hypothesis that NF- $\kappa$ B might be involved in mediating this phenomenon.

The levels of NF- $\kappa$ B proteins in nuclear extracts from the cells were analyzed by electrophoretic mobility shift assay (EMSA). HCAECs starved in serum-free medium were washed and incubated with different doses of neopterin (10, 20, 50, and  $100 \text{ nM}$ ) for 30 min. Cells incubated with  $50 \mu\text{g mL}^{-1}$  of LPS

served as positive control. Moreover, to elucidate whether lovastatin could modulate NF- $\kappa$ B activity induced by neopterin, in another set of experiments HCAECs were cultivated in medium enriched with lovastatin (10  $\mu$ M) for 24 h and then stimulated with neopterin (20 nM) for 30 min. Finally, in an additional set of experiments, NF- $\kappa$ B activity was measured in cells preincubated with SOD (500 U mL<sup>-1</sup>) or in the presence of L-NAME, (1  $\mu$ M), before adding neopterin (20 nM for 30 min). Control experiments included cells preincubated with pyrrolidine dithio carbamate ammonium (PDTC, 100  $\mu$ mol L<sup>-1</sup>), an inhibitor of NF- $\kappa$ B activation, for 60 min before stimulation with neopterin as described above. Nuclear proteins from these cells were isolated as previously described [18] and were subjected to EMSA using <sup>32</sup>P-labeled NF- $\kappa$ B double-strand oligonucleotide (5'-ACTTGAGGGGACTTTCCCAGGC-3'). Nuclear proteins were incubated with oligonucleotide for 30 min, subjected to gel electrophoresis and finally autoradiographed.

In additional experiments, the protein levels of I $\kappa$ B- $\alpha$  were determined by Western blot. A total of 20  $\mu$ g of cytoplasmatic proteins was separated on a 15% SDS-PAGE and transferred to a PVDF membrane. The membrane was blocked in washing solution with 5% non-fat dried milk for 30 min at 37 °C, then it was incubated first with 1  $\mu$ g mL<sup>-1</sup> of primary antibody overnight at 4 °C and then with a peroxidase-conjugated secondary antibody for 30 min at 37 °C. The bands were detected by colorimetry. All experiments were performed in triplicate.

#### Statistical analysis

Data are presented as mean  $\pm$  SD. Differences between groups were determined by a one-way ANOVA followed by a Student's *t*-test with Bonferroni's correction. A *P*-value < 0.05 was considered statistically significant.

## Results

#### Effects of neopterin on TF transcription

TF mRNA was undetectable in unstimulated endothelial cells as expected [19]. Incubation with neopterin, caused a progressive, time-dependent, increase in TF mRNA levels, as compared to unstimulated cells. The peak of TF mRNA levels was observed after 60 min of neopterin incubation, while at 120 min, TF mRNA levels started decreasing (Fig. 1).

#### Dose-response effects of neopterin on TF expression

TF antigen was not expressed on HCAEC at baseline, and, when they were exposed to neopterin, the antigen levels evaluated by FACS analysis, increased (data not shown). Endothelial cells showed undetectable TF activity at baseline, and exposure to neopterin induced a significant increase in TF activity (Fig. 2A).

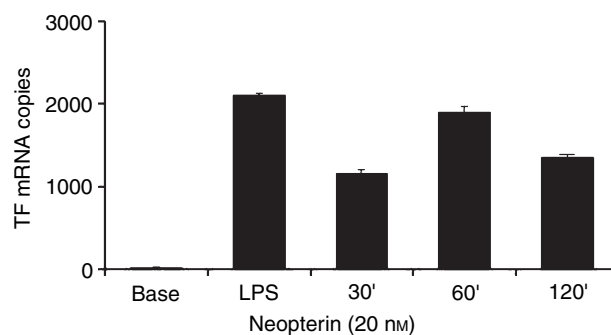


**Fig. 1.** Effects of neopterin on tissue factor (TF) transcription in human coronary artery endothelial cells (HCAECs) assessed by real time quantitative polymerase chain reaction. TF mRNA was undetectable at baseline (Base) in unstimulated HCAECs. Incubation with neopterin, caused a progressive, time-dependent, increase in TF mRNA levels, as compared to unstimulated cells. The peak of TF mRNA levels was observed after 60 min of neopterin incubation while at 120 min, TF mRNA levels started decreasing. Each bar represents the mean  $\pm$  SD of three different experiments.

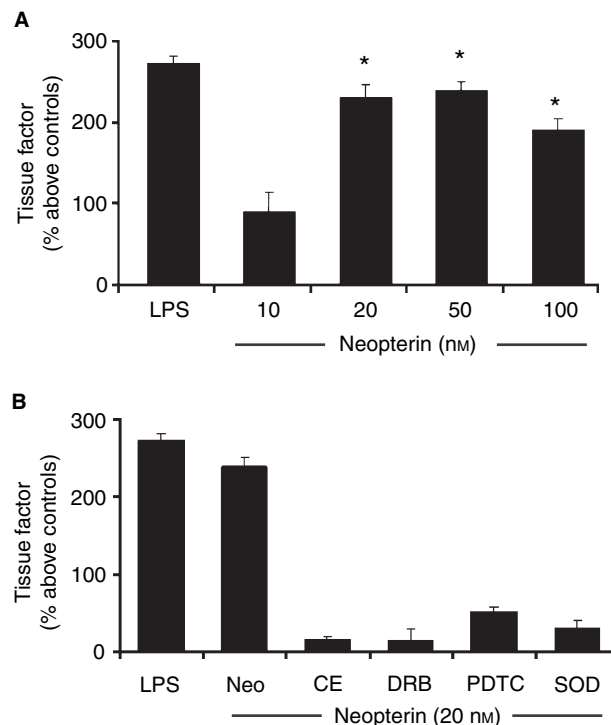


**Fig. 2.** Dose-response effects of neopterin (10, 20, 50, and 100 nM for 6 h) on tissue factor (TF) activity in human coronary artery endothelial cells (HCAECs), determined by a two-step colorimetric assay based on the ability of TF/factor (F) VIIa to promote generation of coagulation FXa. Neopterin induced a dose-response increase in TF activity (A). Control experiments performed by preincubating endothelial cells with cycloheximide or with 6-dichloro-1- $\beta$ -D-ribofuranosylbenzimidazole (B), showed that neopterin-induced TF expression required *de novo* mRNA transcription and protein synthesis. Pretreatment of endothelial cells with superoxide dismutase (SOD), an oxygen free radicals scavenger, or with pyrrolidine dithio carbamate ammonium (PDTC), an inhibitor of nuclear factor-kappa B (NF- $\kappa$ B) activation, decreased the expression of TF (B). Each bar represents the mean  $\pm$  SD of six different experiments. \* = *P* < 0.05 vs. corresponding value at baseline.

Control experiments, performed by preincubating HCAECs with a mouse monoclonal antibody directed against human TF, confirmed that the procoagulant activity measured was actually due to TF expression on cell surface after neopterin induction (data not shown).

In additional experiments, preincubation with CE, an inhibitor of protein synthesis, or with DRB, an inhibitor of DNA transcription, completely inhibited TF expression (Fig. 2B). These data suggest that neopterin is able to induce *de novo* synthesis of TF, and these new TF molecules are then expressed in an active form on the cell surface.

Moreover, different concentrations of lovastatin had similar effects in prevent significantly neopterin-induced TF expression (Fig. 3A). Interestingly, in cells preincubated with the free radical scavenger SOD, neopterin failed to induce TF expression, suggesting that these high reactive oxygen derived molecules play an important role in mediating neopterin effects (Fig. 2B). Vice versa, inhibition of NO synthesis by L-NAME did not interfere with neopterin-induced TF expression, suggesting that NO is not involved in mediating the neopterin effects on TF expression (Fig. 3A).

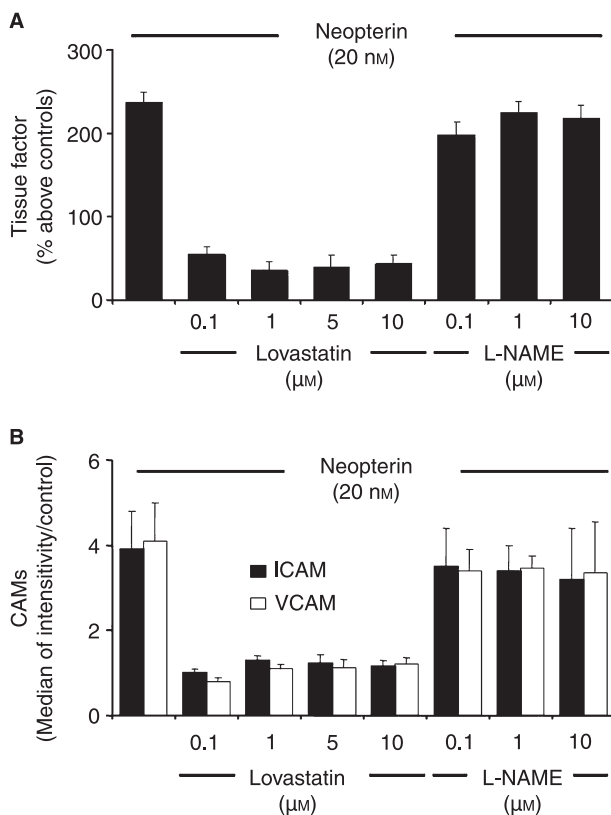


**Fig. 3.** Effects of Lovastatin and of *N*-nitro-*L*-arginine methyl ester (L-NAME) on neopterin-induced expression of tissue factor (TF) and cellular adhesion molecules (CAMs). Neopterin-induced TF expression was prevented by lovastatin at different concentrations (A). Inhibition of nitric oxide (NO) synthesis by L-NAME did not interfere with neopterin-induced TF expression (A). Similarly, lovastatin prevented neopterin-induced CAMs expression (B) and inhibition of NO synthesis by L-NAME did not interfere with neopterin-induced expression of the adhesion molecules (B).

To investigate whether lovastatin concentrations used in our experiments exerted toxic effects on HCAECs, trypan blue exclusion assays were performed at conclusion of the experiments with increasing lovastatin concentrations and demonstrated > 95% viability with no differences between control and statin-treated group (data not shown).

#### Effects of neopterin on adhesion molecules

HCAECs expressed low basal levels of ICAM-1 and VCAM-1. Incubation with neopterin induced expression of both adhesion molecules on cell surface. Conversely, pretreatment of endothelial cells with lovastatin as well as with SOD decreased the expression of ICAM-1 as well as of VCAM-1 (Figs 3B and 4). Inhibition of NO synthesis with L-NAME had no effect on neopterin-induced CAMs expression (Fig. 3B).

#### Neopterin and activation of NF- $\kappa$ B

To investigate whether expression of TF, ICAM-1 and VCAM-1 induced by neopterin involved activation of the NF- $\kappa$ B pathway, we employed EMSA on nuclear extracts

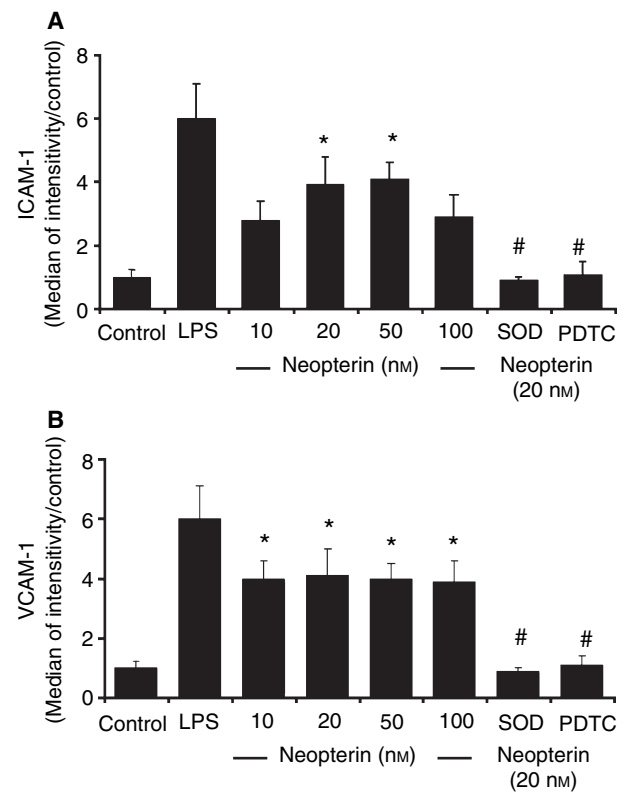


**Fig. 4.** Dose-response effects of neopterin (10, 20, 50 and 100 nM for 12 h) on adhesion molecules expression in human coronary endothelial cells, determined by FACS analysis. Neopterin induced expression of ICAM-1 and VCAM-1 on cell surface. Conversely, pretreatment of endothelial cells with superoxide dismutase (SOD) or with pyrrolidine dithio carbamate ammonium (PDTC) an inhibitor of NF- $\kappa$ B activation, decreased the expression of ICAM-1 as well as of VCAM-1. Each bar represents the mean  $\pm$  SD of six experiments. \* =  $P < 0.05$  vs. corresponding value at baseline. #  $P < 0.05$  vs. neopterin (20 and 50 nM).

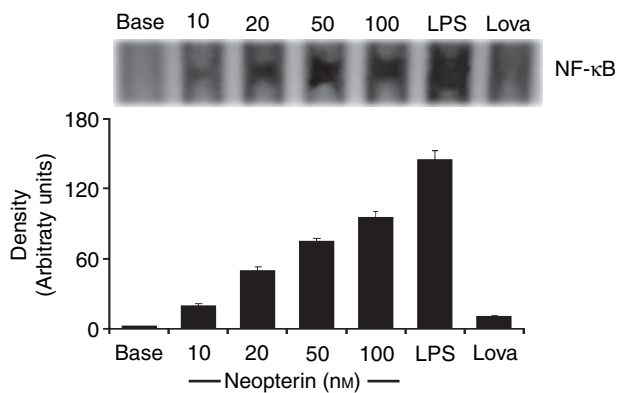


**Fig. 5.** Effects of neopterin on nuclear translocation of NF- $\kappa$ B. Nuclear extracts were prepared from untreated endothelial cells (Base) or cells treated with increasing concentrations of neopterin (10, 20, 50, and 100 nM, for 30 min) or lipopolysaccharide as a positive control. The NF- $\kappa$ B activation was determined by electrophoretic mobility shift assay. Neopterin was able to induce a distinct shifted band in stimulated cells, while no shift could be observed in unstimulated, control cells. Pre-incubation of cells with lovastatin (10  $\mu$ M) diminished NF- $\kappa$ B activation induced by neopterin (20 nM). Data are representative of three separate experiments. Top, result of a representative experiment, bottom, summary of data from three separate experiments (mean  $\pm$  SD).

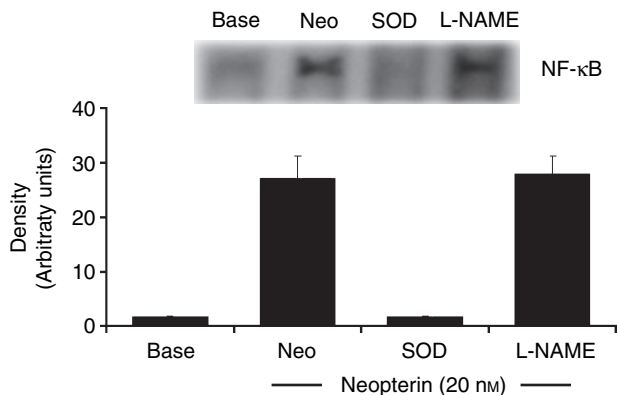


**Fig. 6.** Effects of superoxide dismutase (SOD) and of *N*-nitro-*L*-arginine methyl ester (*L*-NAME) on the activation of NF- $\kappa$ B by Neopterin. Pre-incubation of human coronary artery endothelial cells (HCAECs) with SOD prevented neopterin activation of the transcription factor NF- $\kappa$ B. Vice versa, *L*-NAME did not prevent NF- $\kappa$ B activation. Top, result of a representative experiment, bottom, summary of data from three separate experiments (mean  $\pm$  SD).

obtained from cells stimulated with it. As shown in Fig. 5, NF- $\kappa$ B was activated after incubation with the macrophage derivative substance. In fact, neopterin was able to induce a distinct shifted band in stimulated cells, while no shift could be observed in unstimulated, control cells. Preincubation of cells with lovastatin and with SOD diminished NF- $\kappa$ B activation induced by neopterin (Figs 5 and 6). Moreover, in cells incubated with the inhibitor of NO synthesis, NF- $\kappa$ B was activated anyway by neopterin stimulation (Fig. 6). Interestingly, pretreatment of cells with PDTC, significantly reduced TF activity, and CAMs expression (Figs 2B and 4).

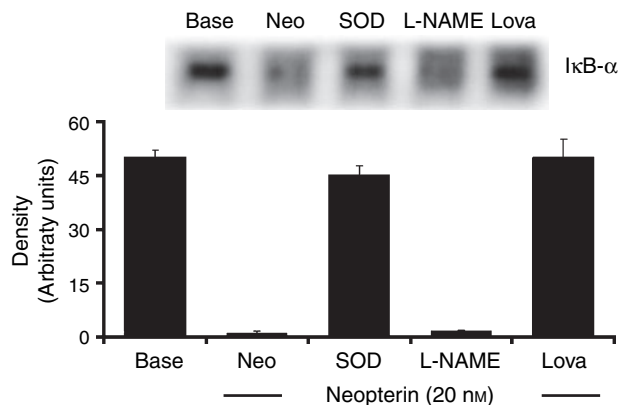


**Fig. 7.** Activation of I $\kappa$ B. Cellular extracts were prepared from untreated endothelial cells (Base) or cells treated with neopterin (Neo, 10 nM, for 30 min). In additional experiments endothelial cells were preincubated with superoxide dismutase (SOD), *N*-nitro-*L*-arginine methyl ester (*L*-NAME) or with Lovastatin (Lova) and then stimulated with Neopterin as above. Elevated levels of I $\kappa$ B were detected at baseline, in unstimulated cells (Base). Conversely, I $\kappa$ B levels decreased after neopterin stimulation and in cells preincubated with *L*-NAME. Any change in I $\kappa$ B- $\alpha$  levels were observed after cell pretreatment with SOD or with Lova. Data are representative of three separate experiments. Top, result of a representative experiment, bottom, summary of data from three separate experiments (mean  $\pm$  SD).

To investigate the correlation of NF- $\kappa$ B activation with changes of the expression of I $\kappa$ B, levels of this factor were determined by Western blot analysis. Elevated levels of I $\kappa$ B- $\alpha$  were detected at baseline, in unstimulated cells, as expected. Conversely, I $\kappa$ B- $\alpha$  levels decreased after neopterin stimulation. Similarly, I $\kappa$ B- $\alpha$  levels decreased after neopterin stimulation in cells preincubated with *L*-NAME, while any change in I $\kappa$ B- $\alpha$  levels were observed after cell pretreatment with SOD or with lovastatin, (Fig. 7). These changes in I $\kappa$ B- $\alpha$  levels were time coincided with changes of NF- $\kappa$ B levels described above.

## Discussion

The main findings of the present study are: (i) exposure of HCAECs to neopterin, a pteridine compound released by activated macrophages and known as marker of inflammation, induces expression of adhesion molecules; (ii) neopterin induces TF-mRNA transcription and *de novo* synthesis of functionally active TF; and (iii) these phenomenon appear to be regulated by oxygen free radicals through activation of NF- $\kappa$ B pathway.

Over the past few years it has become clear that inflammation plays an important pathophysiological role not only in initiating the pathogenesis of atherosclerosis, but also in developing its complications, such as the occurrence of acute coronary syndromes [1–3]. More recently, it has been reported an association between a marker of inflammation, neopterin, and coronary artery disease. In particular, Scumacher *et al.* [4] have shown that neopterin levels are increased in patients with chronic and acute coronary syndromes, while another report has demonstrated that serum levels of this substance are associated with the presence of complex vulnerable coronary

lesions in patients with unstable angina [5]. Moreover, Zouridakis *et al.* [6] have demonstrated that increased levels of serum neopterin are associated with a rapid CAD progression. Finally a recent report by Avanzas *et al.* [7] has shown that high neopterin levels are an independent predictor of major adverse coronary events in patients with CAD. Despite these growing clinical observations, the literature about neopterin and coronary artery disease is still scanty and our understanding of the possible underlying mechanisms of the pathophysiological links between increased neopterin serum levels and the occurrence of acute coronary syndromes still remains largely incomplete.

In the present study we have demonstrated, using a cell culture model, that neopterin induces TF expression in HCAECs in a dose-dependent fashion and that this phenomenon appears to be mainly related to the synthesis of new TF molecules, as CE and DRB, an inhibitor of protein synthesis and mRNA transcription, respectively, completely inhibited the neopterin effects on TF expression.

Of particular pathophysiological interest was the finding that these newly formed TF molecules were functionally active, as demonstrated by the parallel increase in TF-procoagulant activity, which was detectable on the surface of stimulated cells. This observation might have important pathophysiological consequences, considering that endothelial cells are at the interface between the vessel wall and circulating blood coagulation factors; thus, neopterin seems to be able to induce a 'procoagulant' phenotype in endothelial cells.

Moreover, we have demonstrated that neopterin causes the up-regulation of expression of CAMs such as ICAM 1 and VCAM 1 on endothelial cell surface. These CAMs are responsible of attachment and transendothelial migration of leukocytes [20], and are known to be directly involved in the pathogenesis of atherosclerosis mediating many of the stages of the disease progression [20]. In addition, serum concentration of CAMs are strongly correlated with CAD [21] and with the risk of cardiovascular events [22].

Studies dealing with the potential effects of neopterin provided evidence that promotion of oxidative stress is a fundamental principle of neopterin's mode of action [16]. In line with these previous observations, we have demonstrated that neopterin-induced TF and CAM expression in endothelial cells is mediated by oxygen free radicals and that the transcription factor NF- $\kappa$ B is the potential link in modulating these phenomena. Indeed SOD, a scavenger for oxygen-free radicals, significantly reduced NF- $\kappa$ B activation as well as TF and CAM expression. In addition, neopterin effects on TF and CAM expression were significantly reduced by PDTC, a selective NF- $\kappa$ B inhibitor.

Several lines of evidence indicate that the activation of NF- $\kappa$ B may be controlled by the redox status of cells [23]. NF- $\kappa$ B is present but inactive in the cytoplasm of many cells such as lymphocytes, monocytes, endothelial and smooth muscle cells. It seems to be activated by several stimuli during the atherosclerotic process and it is responsible of the expression of inflammatory proteins that actively participate in this

process and might lead to plaque disruption and acute coronary events [24]. In particular, activation of NF- $\kappa$ B stimulates the promoter for TF [25], for CAMs [26] as well as for NO genes [27]. Previous evidence has already suggested that neopterin induces NF- $\kappa$ B activation in smooth muscle cells, and consequently promotes NOS gene expression [17,28]. However, in the present study we have demonstrated for the first time that activation of the NF- $\kappa$ B pathway by neopterin causes expression of TF and of ICAM-1 and VCAM-1. These proteins are actively involved in the pathophysiology of atherosclerosis and its complication. Again, neopterin effects on TF and CAMs expression seem not correlated to neopterin-induced NO synthesis as NO inhibitor L-NAME did not reduce TF and CAMs levels in neopterin-stimulated HCAECs.

Considering that NF- $\kappa$ B has been demonstrated to be activated in the peripheral monocytes [29], as well as within the unstable plaques of patients with acute coronary syndromes [30], the finding observed in our study that neopterin induces TF and CAM expression via activation of NF- $\kappa$ B might explain, at least in part, why patients with CAD and elevated neopterin serum levels have a worse clinical outcome than patients with normal serum levels.

Importantly, we demonstrated that the effects of neopterin on endothelial cell activation and on expression of TF and CAMs can be prevented by HMG-CoA reductase inhibition. In particular, we wanted to study whether a lipid-lowering agent, lovastatin possessed anti-inflammatory properties independently of its lipid-lowering action, and so we have investigated its effects on neopterin-induced NF- $\kappa$ B activation. Previous reports have shown that statins exert protective effects on endothelial cells, allowing restoration of their functions [31]. Specifically, Ortego *et al.* [32] have shown that atorvastatin can reduce the expression of some chemokines and cytokines with pro-inflammatory effects in several cell types through inhibition of NF- $\kappa$ B pathway, while Lin *et al.* [33] have recently demonstrated that lovastatin reduces the effects induced by C-reactive protein in human vascular endothelial cells. In the present study, lovastatin significantly diminished NF- $\kappa$ B activation induced by neopterin, thus preventing the effects of this marker of inflammation on endothelial cells *in vitro*, avoiding their dysfunction.

#### *Potential limitations of the present study*

The present study, although *in vitro*, describes a potential new link between inflammation (as reflected by high neopterin levels) and atherothrombosis. The evidence that neopterin exerts direct effects on coronary artery endothelial cells, leading to TF and CAM expression on their surface, might explain, at least in part, why patients with increased plasma levels of neopterin have a worse clinical outcome than patients with normal neopterin levels, via a broad activation of the coronary endothelial cells ultimately increasing the risk to develop new coronary events. These findings clearly indicate a direct effect of neopterin in promoting atherothrombosis, but the clinical relevance of this pathophysiological mechanism might appear

questionable, considering that some of the experiments performed in the present study employed high neopterin concentrations. Plasma neopterin concentrations in healthy controls range between 1.0 and 9.0 nM [34], and increase to about 15.0 nM in patients with coronary artery disease [7]. Thus, this discrepancy is only apparent, as it should be emphasized that the transcription factor NF- $\kappa$ B was activated at neopterin concentrations as low as 10 nM, which are well within the range observed in patients with increased cardiovascular risk. Moreover, it should be kept in mind that plasma neopterin concentrations might only loosely reflect tissue neopterin levels and that locally, that is, within the arterial wall, neopterin might be present in amounts sufficiently high to exert relevant cellular effects. Indeed, coronary plaques of patients with acute coronary syndromes have more extensive macrophage-rich areas than those with stable angina [35]. Again, vulnerable plaques reflect increased numbers of macrophages and activated lymphocytes [36]. Thus, it is very probably that, at the site of vulnerable plaque, local neopterin concentrations are significantly higher than that measured in peripheral blood. Therefore, we might speculate that activated monocytes/macrophages in atherosclerotic lesions significantly increase local neopterin levels; thus, they induce expression of ICAM-1 and VCAM-1 on endothelial cells in coronary circulation. Increased expression of CAMs may result in increase binding of T lymphocytes, platelets and other monocytes (that, once activated, further increase local neopterin concentration), key players in the atherosclerotic process. The endothelial activation causes expression of TF, promoting an 'endothelial pro-thrombotic phenotype', and finally leading to the occurrence of acute coronary syndromes.

In conclusion, the present study, although *in vitro*, describes the close relationship between inflammation and atherothrombosis, providing for the first time support to the view that neopterin might be not only a risk marker but it may indeed be a participant and culprit in atherogenesis and thrombosis. Further studies are warranted to clarify whether these mechanisms are also important in the clinical setting.

### Acknowledgement

This study was supported in part by grant 'Programma di Ricerca Scientifica di Rilevante Interesse Nazionale' (PRIN 2004) of Ministero Università e Ricerca Scientifica.

### Addendum

P. Cirillo contributed to the conception, design and interpretation of data and drafting of the manuscript; M. Pacileo, S. De Rosa, A. Gargiulo and V. Angri contributed to tissue factor activity experiments, P. Calabrò, F. G. Corigliano, I. Fiorentino and N. Prevete contributed to FACS analysis of adhesion molecules; R. De Palma contributed to real time analysis; A. Leonardi and C. Mauro contributed to EMSA experiments; M. Chiariello contributed to the drafting and gave the final approval of the manuscript.

### Disclosure of Conflict of Interests

The authors state that they have no conflict of interest.

### References

- Ross R. The pathogenesis of atherosclerosis: a perspective for the 1990s. *Nature* 1993; **362**: 801–9.
- Libby P, Ridker PM, Maseri A. Inflammation and atherosclerosis. *Circulation* 2002; **105**: 1135–43.
- Libby P, Aikawa M. Stabilization of atherosclerotic plaques: new mechanisms and clinical targets. *Nat Med* 2002; **8**: 1257–62.
- Schumacher M, Halwachs G, Tatzber F, Fruhwald FM, Zweiker R, Watzinger N, Eber B, Wilders-Truschnig M, Esterbauer H, Klein W. Increased neopterin in patients with chronic and acute coronary syndromes. *J Am Coll Cardiol* 1997; **30**: 703–7.
- Avanzas P, Arroyo-Espliguero R, Cosin-Sales J, Aldama G, Pizzi C, Quiles J, Kaski JC. Markers of inflammation and multiple complex stenoses (pancoronary plaque vulnerability) in patients with non-ST segment elevation acute coronary syndromes. *Heart* 2004; **90**: 847–52.
- Garcia Moll X, Coccolo F, Cole D, Zourikakis E, Kaski JC. Serum neopterin and complex stenosis morphology in patients with unstable angina. *J Am Coll Cardiol* 2000; **35**: 956–62.
- Zouridakis E, Avanzas P, Arroyo-Espliguero R, Fderericks S, Kaski JC. Markers of inflammation and rapid coronary artery disease progression in patients with stable angina pectoris. *Circulation* 2004; **110**: 1747–53.
- Avanzas P, Arroyo-Espliguero R, Quiles J, Roy D, Kaski JC. Elevated serum neopterin predicts future adverse cardiac events in patients with chronic stable angina pectoris. *Eur Heart J* 2005; **26**: 457–63.
- Libby P. Coronary artery injury and the biology of atherosclerosis: inflammation, thrombosis and stabilization. *Am J Cardiol* 2000; **86**: 3J–8J.
- Price DT, Loscalzo J. Cellular adhesion molecules and atherogenesis. *Am J Med* 1999; **107**: 85–97.
- Pawashe AB, Golino P, Ambrosio G, Migliaccio F, Ragni M, Pascucci I, Chiariello M, Bach R, Garen A, Konigsberg WK. A monoclonal antibody against rabbit tissue factor inhibits thrombus formation in stenotic injured rabbit carotid arteries. *Circ Res* 1994; **74**: 56–63.
- Ragni M, Cirillo P, Pascucci I, Scognamiglio A, D'Andrea D, Eramo N, Ezekowitz MD, Pawashe AB, Chiariello M, Golino P. A monoclonal antibody against tissue factor shortens tissue-plasminogen activator lysis time and prevents reocclusion in a rabbit model of carotid artery thrombosis. *Circulation* 1996; **93**: 1913–20.
- Bierhaus A, Chen J, Liliensiek B, Nawroth PP. LPS and cytokine activated endothelium. *Semin Thromb Hemost* 2000; **26**: 571–87.
- Golino P, Ragni M, Cirillo P, Avvedimento VE, Feliciello A, Esposito N, Scognamiglio A, Trimarco B, Iaccarino G, Condorelli M, Chiariello M, Ambrosio G. Effects of tissue factor induced by oxygen free radicals on coronary flow during reperfusion. *Nat Med* 1996; **2**: 35–40.
- Cirillo P, Golino P, Calabrò P, Cali G, Ragni M, De Rosa S, Cimmino G, Pacileo M, De Palma R, Forte L, Gargiulo A, Granato Corigliano F, Angri V, Spagnuolo R, Nitsch L, Chiariello M. C-reactive protein induces tissue factor expression and promotes smooth muscle and endothelial cell proliferation. *Cardiovasc Res* 2005; **68**: 47–55.
- Oettl K, Rebnegger G. Pteridine derivatives as modulators of oxidative stress. *Current Drug Metab* 2002; **3**: 203–9.
- Schobersberger W, Hoffmann G, Grote J, Wachter H, Fuchs D. Induction of inducible nitric oxide synthase expression by neopterin in vascular smooth muscle cells. *FEBS Lett* 1995; **377**: 461–4.
- Andrews NC, Fallen DV. A rapid micropreparation technique for extraction of DNA-binding proteins from limiting numbers of mammalian cells. *Nucleic Acid Res* 1991; **19**: 2499.
- Wilcox JN, Smith KM, Schwartz S, Gordon D. Localization of tissue factor in the normal vessel wall and in the atherosclerotic plaque. *Proc Natl Acad Sci USA* 1989; **86**: 2839–43.

- 20 Adams DH, Shaw S. Leucocyte-endothelial interactions and regulation of leucocyte migration. *Lancet* 1994; **343**: 831–6.
- 21 Morisaki N, Saito I, Tamura K, Tashiro J, Masuda M, Kanzaki T, Watanabe S, Masuda Y, Saito Y. New indices of ischemic heart disease and aging: studies on the serum levels of soluble intercellular adhesion molecule-1 (ICAM.1) and soluble vascular cell adhesion molecule-1 (VCAM-1) in patients with hypercholesterolemia and ischemic heart disease. *Atherosclerosis* 1997; **131**: 43–8.
- 22 Ridkler PM, Hennekens CH, Roitman-Johnson B, Stampfer MJ, Allen J. Plasma concentration of soluble intracellular adhesion molecule 1 and risks of future myocardial infarction in apparently healthy men. *Lancet* 1998; **351**: 88–92.
- 23 Flohe L, Brigelius-Flohe R, Saliou C, Traber MG, Packer L. Redox regulation of NF-kappa B activation. *Free Radic Biol Med* 1997; **22**: 1115–26.
- 24 Barnes PJ, Karin M. Nuclear factor-kappa B: a pivotal transcription factor in chronic inflammatory disease. *N Engl J Med* 1997; **336**: 1066–71.
- 25 Mackman N. regulation of the tissue factor gene. *Thromb Haemost* 1997; **78**: 747–54.
- 26 Collins T, Read MA, Neish AS, Whitley MZ, Thanos D, Maniatis T. Transcriptional regulation of endothelial cell adhesion molecules: NF-kappa B and cytokine-inducible enhancers. *FASEB J* 1995; **9**: 899–909.
- 27 Yan Z, Sirsjo A, Bochaton-Piallat ML, Gabbiani G, Hansson GK. Augmented expression of inducible NO synthase in vascular smooth muscle cells during aging is associated with enhanced NF-kappa B activation. *Arterioscler Thromb Vasc Biol* 1999; **19**: 2854–62.
- 28 Hoffmann G, Schobersberger W, Frede S, Pelzer L, Fandrey J, Wachter H, Fuchs D, Grote J. Neopterin activates transcription factor nuclear factor-kappa B in vascular smooth muscle cells. *FEBS Lett* 1996; **391**: 181–4.
- 29 Ritchie ME. Nuclear Factor-kappa B is selectively and markedly activated in humans with unstable angina pectoris. *Circulation* 1998; **98**: 1707–13.
- 30 Wilson SH, Best PJ, Edwards WD, Holmes DR, Carlson PJ, Celer-majer DS, Lerman A. Nuclear factor-kappa B immunoreactivity is present in human coronary plaque and enhanced in patients with unstable angina pectoris. *Atherosclerosis* 2002; **160**: 147–53.
- 31 Wolfrum S, Jensen KS, Liao JK. Endothelium-dependent effects of statins. *Arterioscler Thromb Vasc Biol* 2003; **23**: 729–36.
- 32 Ortego M, Bustos C, Hernández-Presa MA, Tuñón J, Díaz C, Hernández G, Egado J. Atorvastatin reduces NF-kappa B activation and chemokines cells and mononuclear cells. *Atherosclerosis* 1999; **147**: 253–61.
- 33 Lin R, Liu J, Peng N, Yang G, Gan W, Wang W. Lovastatin reduces nuclear factor kappa B activation induced by C-reactive protein in human vascular endothelial cells. *Biol Pharm Bull* 2005; **28**: 1630–4.
- 34 Hoffmann G, Wirleitner B, Fuchs D. Potential role of immune system activation-associated production of neopterin derivatives in humans. *Inflamm Res* 2003; **52**: 313–21.
- 35 Moreno PR, Falk E, Palacios IF, Newell JB, Fuster V, Fallon JT. Macrophage infiltration in acute coronary syndromes: implication for plaque rupture. *Circulation* 1994; **90**: 775–8.
- 36 Libby P. Molecular bases of acute coronary syndromes. *Circulation* 1995; **91**: 2844–50.